A thesis entitled

Novel Polymeric Materials for Nuclear Track Detection

Submitted to

Goa University

for

the Degree of

Doctor of Philosophy

(in Chemistry)

by

Mr. Vinod K. Mandrekar

M. Sc.

Department of Chemistry

Goa University

Taleigao Plateau

Goa 403 206

India

March 2010

DECLARATION

I hereby declare that the matter embodied in this thesis entitled "Novel Polymeric Materials for Nuclear Track Detection" is the result of investigations carried out by me, in the Department of Chemistry, Goa University, Goa, India under the supervision of Dr. V. S. Nadkarni, Reader, Department of Chemistry, Goa University.

In keeping with the general practice of reporting scientific observations, due acknowledgement has been made wherever the work described is based on the findings of other investigators.

Goa University

March 2010

Mr. Vinod K. Mandrekar

(Research Scholar)

Certified that all the corrections are incorporated in the thesis.

11.10.2010.

EXAMINED BY

11 OCT 2010

CERTIFICATE

Certified that the work entitled "Novel Polymeric Materials for Nuclear Track Detection" presented in this thesis has been carried out by Mr. Vinod K. Mandrekar, under my supervision and the same has not been submitted elsewhere for the award of a degree.

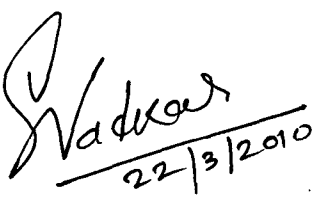

Goa University

March 2010

Dr. V. S. Nadkarni

(Research Guide)

Acknowledgment

This thesis is a result of research that has been done by me since I came to Goa University. I was fortunate to work with many peoples whose contribution in assorted ways to this research and the making of the thesis deserves a special mention. It is a pleasure to convey my gratitude to them all in my humble acknowledgment.

First and foremost, I want to thank my guide Dr. V. S. Nadkarni for his supervision, advice, and guidance from the very early stage of this research as well as giving me good experience of research throughout this work. His truly scientist intuition has made him a constant oasis of ideas and passions in science which exceptionally inspired and enriched my growth as a student, a researcher and a scientist want to be. I could never have started all of this without his prior teachings in the subject.

Many spacial thanks goes to Prof. A. V. Salkar (Head, Department of Chemistry, Goa University), Prof. S. P. Kamat (Former Head, Department of Chemistry, Goa University and my subject expert), Prof J. B. Fernandes and Prof. K. S. Rane (Former Heads of the Department of Chemistry, Goa University). I benefited from their valuable advice in research, science discussion and supervision.

I am thankful to all my teachers right from my school till my post graduation studies. I gratefully acknowledge their advice, supervision, and crucial contribution, which makes them a backbone of this research and also my future career. Their involvement with originality has triggered and nourished my intellectual maturity that I will benefit from, for a long time to come.

I am very grateful to Dr. P. S. Parameshwaran and would like to thank him for his help in getting spectral data. I would espetially like to thank, Dr. B. R. Srinivasan, for his Valuable advise. Dr. P. C.

Kalsi (Radiochemistry division, BARC) and Dr. G. Chaurasia (Radiological physics and advisory division) deserve a special vote of thanks for their active help whenever required during the course of study. I am thankful to Dr. S. G. Tilve and Dr. V. M. S. Verenkar for their help and encouragement during the course of completion of this work.

I should like to thank Dr. D. B. Arolkar(Principal, DM's College of Arts, Science and Commerce) for allowing flexible timings during my office hours. I also thank Dr. Vidya and Dr. Rajesh for their scientific discussion and support for my Thesis.

I gratefully thank the supporting staff of the chemistry department, administration block, library and USIC, especially Mr. Jayprakash Kamat for helping me to complete my research work midst of all their activities.

Collective and individual acknowledgments are also owed to my colleagues Dr. Adelete, Dr. Mahesh, Umesh, Prakash, Dr. Rupesh, Santosh, Rajesh, Rohan, Satish, Chinmaya, Dr. Chandan, Shrikant, Dr. Reshma, Prachi, Lactina, Dr. Savia, Priyanka, Dr. Sulaksha, Dr. Jose, Sneha, Kashinath, Sandesh, Hari and others at the department who stood by me in completing the thesis. Since I knew them, their presence was refreshing, helpful, and memorable.

I thank the Atomic Energy Regulatory Board (AERB) for providing fellowship to me during the course of this investigation and also for funding this work.

Where would I be without my family? My parents deserve special mention for their inseparable support and prayers. First and foremost, I thank my father Kashinath Mandrekar a source of inspiration for me, for his love and ancouragement. My Mother Mrs. Pramila is the one who sincerely raised me with her caress-

ing, caring and gentle love. Words fail me to express my appreciation to my brother Vijay Mandrekar whose dedication, love and persistent confidence in me has taken the load off my shoulder. I am indebted to him more than he knows. Special thanks to My sister Vandana and Mrs. Vijay, for providing me unflinching encouragement and support in various ways.

Last but not the least, thanks to the Almighty God for making me able to face all the tests in the life. I thank him for making my life bountiful. May your name be exalted, honored, and glorified forever.

Finally, I would like to thank one and all, who was important to the successful realization of the thesis. My apology for not being able to mention their names individually.

Mr. Vinod K. Mandrekar
Research Scholar
Department of Chemistry,
Goa University

CONTENTS

ABBREVIATIONS

AA	Allyl alcohol
ABNEC	Allyl bis-(2-nitroxy-ethyl) carbamate
ADC	Allyl diglycol carbonate
ADS	Allyl diglycol sulphite
BP	Benzoyl peroxide
CE	Chemical etching
CHPC	Cyclohexyl peroxydicarbonate
CN	Nitocellulose (cellulose nitrate)
CR-39	ADC polymer (Trademark of PPG Industries, UK)
CR-39^{PM}	CR-39 SSNTD film manufactured by Pershore Mouldings, UK
DAC	Diallyl carbonate
DAS	Diallyl sulphite
DEG	Diethylene glycol
DEAS	Diethylene glycol bis(allyl sulfonate)
DEPS	Diethylene glycol bis(n-propyl sulfonate)
DOP	Dioctyl phthalate
DP	Degree of polymerization
DTD	Dielectric track detectors
ECE	Electrochemical etching
EM	Electron microscope
IPA	Isopropyl alcohol
IPP	Isopropylperoxydicarbonate
LR 115	(Trademark) CN SSNTD film manufactured by Kodak Pathe, France
OM	Optical microscope
NADAC	N-Allyloxycarbonyloxy-diethanolamine bis(allyl carbonate)

PBCBS	Pentaerythritol bis(allyl carbonate) bis(allyl sulfonate)
PC	Polycarbonate
PET	Polyethylene terphthalate
PETAC	Pentaerythritol tetrakis(allyl carbonate)
PP	Polypropylene
PeAC	Pentanediol bis(allyl carbonate)
SR-86(10)	Copolymer of CR-39:DEAS 9:1 w/w.
SR-86(20)	Copolymer of CR-39:DEAS 8:2 w/w.
SSNTD	Solid state nuclear track detection
SSNTD's	Solid State Nuclear Track detectors
TBP	t-butyl peroxide
TBPB	t-butyl peroxy benzoate (TBPB)
TDONM	Tris-(2,4-dioxa-3-oxohept-6-en-1-yl) nitromethane

Physical Quantities:

V_b - Bulk etch rate

V_t - Track etch rate

S - Sensitivity

θc - Critical angle of etching

v - Velocity of charged particle

c - Velocity of light

b - v/c

T_g - Glass transition temperature

m - Mass of the particle

Chapter I: Introduction

1.1 Origin of radiation science:

1.1.1 Discovery of radiations: November 8th, 1895 could be considered as the birthday of radiation science. Wilhelm Conrad Roentgen who was working with the discharge tube, completely covered with a thin black cardboard in a dark room, found a faint greenish light glimmering momentarily from a table nearby.[1] The source of the light was found to be a small piece of cardboard coated with fluorescent chemical barium platinocyanide. The fluorescent effect was due to the mysterious invisible rays, the X-rays, which emanated from the part of the discharge tube where cathode rays strike.

The discovery of radioactivity is directly related to the discovery of X-rays and followed 114 days later. Upon learning that the X-rays emerged from the fluorescing glass of the Hittorf tube, W. C. Roentgen assumed that other fluorescing materials might also emit X-rays. Sealing a photographic plate in black paper, he sprinkled a layer of the uranium salt onto the paper and kept the whole thing under the sun for several hours. On developing the plate he rightly inferred that none of the sun rays penetrate the black paper to affect the photographic plates. He repeated the same experiments after placing the crystals of potassium uranyl sulphate, which fluoresces under UV light from sun rays and subsequently developed it. He observed that the silhouette of the uranium appeared black on the plate and assumed that the sunlight caused the emission of the penetrating rays and that X-rays generate automatically from fluorescing substances.[2]

Antoine Henri Becquerel repeated the experiment with care, incidentally in a cloudy weather, and observed that intense images appeared on the photographic plate. Thus, the uranium salt

emitted rays capable of penetrating black paper, whether or not it had been previously exposed to sunlight and the action took place even in darkness.[3] The uranyl salt obviously produced radiation spontaneously. This radiation, which was first called uranium rays (or Becquerel rays), was similar to X-rays in that it ionized air, as observed through the discharge of electroscope. Thus it was possible to measure the activity in a sample simply by measuring the ionization that it produced.

1.1.2 The discoveries of Marie Sklodowska Curie and Pierre Curie: In September of 1897, Marie Curie started studying the new phenomenon discovered by Becquerel. She used quantitative ionization method for measuring the intensity of radiation and decided to look for radiations emitted from a wide range of elements, compounds and even their ores. All the compounds of uranium studied were active and the extent of ionization created by a uranium sample and the intensity of its radiation emission was proportional to the amount of uranium in the compound and independent of its chemical state.

. Curies investigated the radioactivity of pitchblende and chalconite and found two new elements polonium and radium,[4] most importantly their radioactive nature. Noble prize was awarded to Becquerel for the discovery of spontaneous radioactivity in 1903 (Physics) and to the Curies for their research on the radiation phenomenon. Madam Curie was also awarded Chemistry Noble Prize, in 1911, for her discovery of the elements Radium and Polonium.

1.1.3 Effect of radiations and nuclear particles: The impact of radiation on living tissue is complicated by the type of radiation and the variety of tissues. Radiation may alter the DNA within any

cell. Cell damage and death that result from mutations in somatic cells occur only in the organism in which the mutation occurred and are therefore termed somatic or non heritable effects. Cancer is the most notable long-term somatic effect. In contrast, mutations that occur in germ cells (sperm and ova) can be transmitted to future generations and are therefore called genetic or heritable effects. Genetic effects may not appear until many generations later.

1.1.4 Detection of radiation: brief history of radiation detectors used:[5] Although animals have no known senses for detection of nuclear radiation, large radiation fields can affect animals in various ways such as disturbing the sleep of dogs or causing ants to follow a new pathway etc. Apollo astronauts observed scintillations in their eyes when their space ship crossed very intense showers of high energy cosmic rays. People who have been involved in criticality accidents experiencing high intensities of radiations have noted fluorescence in their eyes and felt a heat shock in their body. However, we are not physiologically aware of the normal radiation fields in our environment. In such low fields we must entirely rely on instruments. The ionization and/or excitation of atoms and molecules when the energies of nuclear particles are absorbed in matter are the basis for the detection of individual particles. Macroscopic collective effects, such as chemical changes and heat evolution, can also be used. The most common techniques used for detection and quantitative measurement of individual nuclear particles are

i) Gas counters: The ionization chambers are the first detectors to be used in nuclear physics for radiation detection. The detector consists of a closed vessel containing an ionization media and

electrodes at different electrical potentials. The ionization media consists of Gas or a semi conducting solids. The incident radiations ionize the gas between the electrodes producing ion pairs. The ionization produced in an ion chamber by a single nuclear particle produces too low a charge pulse to be detectable except for a-particle. Thus, an ion chamber can be designed so that the number of ion pairs formed in each event is multiplied greatly. The ions migrate to the electrodes of opposite sign, creating a current that can be amplified and measured. The GeLi detector used in multichannel analyzer is a solid ionization detector. The Gas filled ionization chambers can be operated as Ion chambers, Proportional counters and Geiger-Mueller tubes.

ii) Spark chamber: In a spark chamber, the air or a gas between plates or wire grids are kept alternately positively and negatively charged which is ionized by the incoming high-energy particles. Sparks jump along the paths of ionization and can be photographed to show particle tracks. A spark chamber can be operated quickly and selectively. The instrument can be set to record particle tracks only when a particle of the type that the researchers want to study is produced in a nuclear reaction. This advantage is important in studies of the rarer particles; spark-chamber pictures, however, lack the resolution and fine detail of bubble-chamber pictures.

iii) Scintillation counter: The scintillation counters measure radiations by analyzing the incident radiation excitations of the detector material. Charged particles moving at high speed within certain transparent solids and liquids, known as scintillating materials (phosphors) causes flashes of visible light. The emitted light is collected and measured to detect the amount of incident radiation. The gases argon, krypton, and xenon produce ultravio-

let light, and hence are used in scintillation counters. The scintillating material is placed in front of a photomultiplier tube, a type of photoelectric cell. The light flashes are converted into electrical pulses that can be amplified and recorded electronically. Various organic and inorganic substances such as plastic, zinc sulfide, sodium iodide and anthracene are used as phosphors.

iv) Other types of detector:[6] Many other types of interactions between matter and elementary particles are used in detectors. Thus, in semiconductor detectors, electron-hole pairs that elementary particles produce in a semiconductor junction momentarily increase the electric conduction across the junction. In the Cherenkov detector, a particle emits light when it passes through a non conducting medium at a velocity higher than the velocity of light in that medium. As in scintillation counters, the light flashes are then detected with photomultiplier tubes.

1) Particle track detectors: Neutral particles such as neutrons or neutrinos can be detected by nuclear reactions that occur when they collide with nuclei of certain atoms. Slow neutrons produce easily detectable alpha particles when they collide with boron nuclei in borontrifluoride. Neutrinos, which barely interact with matter, are detected in huge tanks containing perchloroethylene (C_2CI_4, a dry-cleaning fluid). The neutrinos that collide with chlorine nuclei produce radioactive argon nuclei. The perchloroethylene tank is flushed at regular intervals, and the newly formed argon atoms, present in minute amounts, are counted. Neutrino detectors may also take the form of scintillation counters, the tanks in this case being filled with an organic liquid that emits light flashes when traversed by electrically charged particles produced by the interaction of neutrinos with the liquid's molecules.

The detectors now being developed for use with the storage rings and colliding particle beams of the most recent generation of accelerators are bubble-chamber types known as time-projection chambers. They can measure three-dimensionally the tracks produced by particles from colliding beams, with supplementary detectors to record other particles resulting from the high-power collisions. The most striking evidence for the existence of atoms comes from the observation of tracks formed by nuclear particles in cloud chambers, in solids and in photographic emulsions. The tracks reveal individual nuclear reactions and radioactive decay processes. From a detailed study of such tracks, the mass, charge and energy of the particle can be determined. The tracks formed can be directly observed by the naked eye in cloud and bubble chambers, but the tracks remain only for a short time before they fade. For a permanent record we must use photography. On the other hand, in solid state nuclear track detectors (SSNTD's), of which the photographic emulsion is the most common variant, the tracks have a much longer lifetime during which they can be made permanent and visible by a suitable chemical treatment. Because of the much higher density of the absorber, the tracks are also much shorter and often therefore not visible for the naked eye. Thus, the microscope is an essential tool for studying tracks in solids. We look at each of these techniques in brief, in the segment below.

2) Cloud chamber: Charles Thomson Rees Wilson (1869-1959) invented the cloud chamber. The cloud chamber consists of a vessel several centimeters or more in diameter, with a glass window on one side and a movable piston on the other. The piston can be dropped rapidly to expand the volume of the chamber. The cham-

ber is usually filled with dust-free air saturated with water vapor. Dropping the piston causes the gas to expand rapidly and causes its temperature to fall. The air is now supersaturated with water vapor, but the excess vapor cannot condense unless ions are present. Charged nuclear or atomic particles produce such ions. Any such particle passing through the chamber leave behind them a trail of ionized particles upon which the excess water vapor will condense, thus making visible the course of the charged particle. These tracks can be photographed and the photographs then analyzed to provide information on the characteristics of the particles. Because the paths of electrically charged particles are bent or deflected by a magnetic field, and the amount of deflection depends on the energy of the particles, a cloud chamber is often operated within a magnetic field.

3) Bubble chamber: The bubble chamber was invented in 1952 by the American physicist Donald A. Glaser. A bubble chamber is a vessel filled with a superheated transparent liquid used to detect electrically charged particles moving through it. The liquid is momentarily superheated to a temperature just above its boiling point. The liquid will not boil unless some impurity or disturbance is introduced. High-energy particles provide such a disturbance. Tiny bubbles form along the tracks as these particles pass through the liquid. If a photograph is taken just after the particles have crossed the chamber, these bubbles will make visible the paths of the particles. Like the cloud chamber, a bubble chamber placed between the poles of a magnet can be used to measure the energies of the particles. Many bubble chambers are equipped with superconducting magnets instead of conventional magnets.

4) Nuclear emulsions and silver halide crystals: In a photographic

nuclear emulsion, Ag^+ atoms are converted to Ag atoms by a charged particle. These silver atoms can link together to form complexes. When a developer is added to these films the complexes can catalyze the reduction of whole AgBr grain to metallic silver. All the undeveloped grains are washed away by the fixer. Thus, a particle track is imaged as a black array of silver grains. The particle can be identified on the measurements of track width and length, degree of scattering of charged particles while traversing the emulsion. The δ ray density can be utilized to determine the charge and energy of the particle.

Silver halide single crystals are also used to determine the charge particle tracks. The crystals are more or less analogous to nuclear emulsions in their mode of action. Table 1.1 enlists some of the remarkable achievements, made due to photographic materials in the first half of the 20th Century.

Year	Achievement
1896	Discovery of radioactivity with the help of photo graphic plate
1911	First traces of charged particles from developed emulsion grains
1925	First proton tracks were observed
1932	Proton recoil tracks produced by neutron
1939	Uranium fragment collision, uranium decay and registration of with Z = 6-8.
1947	First tracks consisting of several grains, recorded in photographic emulsion by electrons with low energy
1947	First registered tracks of mesons
1950	Nuclear emulsions sensitive to relativistic electrons

Table 1.1: Important discoveries during the first half of 20th century due to photographic materials.

1.2 Solid state nuclear track detection (SSNTD):[6] Solid State Nuclear Track detectors (SSNTDs) are essentially materials that are permanently damaged by energetic particles in such a way, that the particle tracks can be developed by subsequent development process, observed microscopically and retained permanently. The development of SSNTD began in the year 1958, when D.A.Young at AERE, Harwell observed number of shallow etch pits in LiF crystal.[7] The name "etch tracks" was coined later for these shallow etch pits. D.A.Young observed these latent tracks in LiF crystal placed in contact (1 mm) with a uranium foil (U_3O_8) and irradiated with slow neutrons. The slow neutrons lead to fission of the uranium nuclei followed by emission of fission fragments. These fission fragments traversed the LiF crystals and damaged the internal arrangements of atoms in the crystal structure, making these regions more chemically active than the surrounding undamaged region.

When the LiF crystal was treated with concentrated HF (1 part) in glacial acetic acid (1 part) saturated with FeF_3 for time intervals of 45 - 60 minutes at 12 °C, the tracks were observable under an optical microscope. Fine channels are thus produced which accurately delineate the particle path and shows as a dark needle shaped tracks in a transparent detector under an optical microscope. E. C. H. Silk and R. S. Barnes unaware of the findings of Young, independently observed with the transmission electron microscope damaged regions in mica which marked the paths of heavy charged particles such as those from fission fragments or cosmic rays.[8]

R. L. Fleischer, P. B. Price and R. M. Walker working at General Electric Research Laboratory conducted extensive research in

the investigation of this method and pioneered the track etching technique.[9] The main types of SSNTD's (or DTD, for dielectric track detector) studied were crystals, glasses, and plastics. Because the density of these materials is much higher, nuclear particles can spend all their kinetic energy in these detectors, allowing identification of the particle. Since SSNTD's retain the particle path, it can be used to record these reactions over a long time period. These advantages have made SSNTD's very valuable in the fields of cosmic ray physics, radiochemistry, and earth sciences.

One of the most commonly used nuclear track detectors is the CR-39™ detector, which was discovered by Cartwright *et al* and is based on poly(allyl diglycol carbonate).[10] Another most commonly used nuclear track material is cellulose nitrate(CN). The most well-known detector in this group is being sold under the commercial name LR 115. Other kinds of detectors are also in use, such as the Makrofol 52 D[11] detector which is based on poly-carbonate. Some natural materials that show the track effect, such as apatite, mica, olivine, etc. are used for fission or fossil track studies.

The extensive application of particular track detector depends on the ability of a particular track detector towards different particles of varied energy. Though there are very few materials that can compete the sensitivity of CR-39™ track detector, efforts are on to devise new materials which can exceed the sensitivity of CR-39™. The SR-86 polymer has sensitivity higher than that of CR-39™ track detector but has a low shelf life.

1.2.1 Track formation in SSNTD's: The solid-state nuclear track detector works on the principle that a heavy charged particle causes extensive ionization of the material when it passes through a

medium.[7,12,13] SSNTD's are insulating solids both naturally occurring and man-made which includes inorganic crystals, glasses and plastics. Heavily ionizing particles passing through insulating media leave narrow trail of damage of approximately 30-100 Å, i.e. 3 - 10 nm. This is called a latent track as it is not visible to the naked eyes. It is possible to view the latent tracks under an electron microscope. Charge particle tracks consist of atomic displacements of atoms formed, either by colliding with atoms ejecting them from their proper positions or by ionizing process.

An alpha particle traversing a cellulose nitrate track detector with energy of 6 MeV creates about 150,000 of ion pairs. However, the range of a 6 MeV alpha particle in this material is only about 40 μm and will ionize almost all bonds close to its path. Free radicals and other chemical species are thus formed due to the primary ionization along the path of the alpha particle. Thus, a zone enriched with free radicals and other chemical species is then created and is called a latent track. Under certain conditions the resulting radiation-damaged regions may be nearly continuous along the particle trajectories and can be developed to a convenient size for viewing under an optical microscope.

The detector containing these latent tracks is now treated with etchants such as aq. NaOH or hydrofluoric acid. The chemical reactions will take place at an accelerated rates at these active sites. The rate of chemical etching is high at the damaged site i.e. tracks (V_t) rather than at the surface i.e. bulk (V_b) of the detector material. This leads to a track which can be observed under an optical microscope. Etchable tracks may be found in almost any type of electrically insulating materials whether crystalline, glassy or polymeric. However, polymeric materials are preferred due to

their high sensitivity towards charged particle track detection. The detailed SSNTD process can be schematically observed in Figure 1.1.[12]

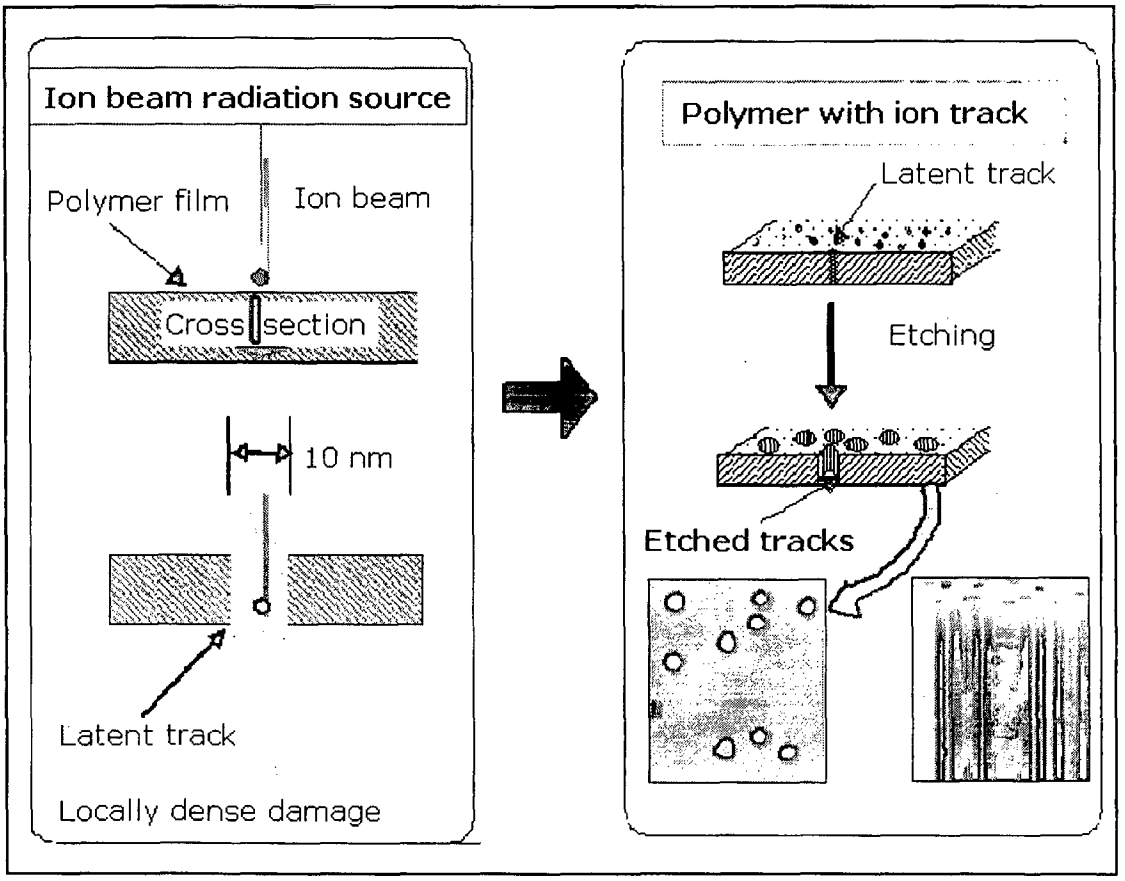

Figure 1.1: The technique of solid state nuclear track detection.

1.2.2 Characteristics of nuclear tracks:[13] The latent track of charged particle have following characteristics

i) The tracks mainly consists of damaged region along the path of the projectile due to displaced atoms.

ii) The particle tracks are reactive centers towards chemical reagents due to presence of unstable centers along the trajectory.

iii) The particle tracks are stable and can be viewed when required.

iv) The track region is atomically continuous along the path with a diameter of less than 10 nm.

v) The length of the damaged trail is equal to the range of the particle in the material under study.

Materials having electrical resistivity value, greater than 2000 Ωcm store the tracks. Cellulose nitrates or different polycarbonates which have long chain polymeric backbone are most convenient for this application. The effect is also seen in some amorphous materials like glasses, etc. Metals and good semiconductors do not store tracks as the process of recombination of the unstable nuclei occurs rapidly and the latent tracks are not stable. Materials with high degree of electrical resistance can retain the tracks with maximum efficiency. Table 1.2 gives electrical resistivity values and track forming abilities of some common materials.[13]

	Materials	Resistivity (Ωcm)
Track forming	Alkali halides, silicate minerals, Insulating glasses,Polymers	10^{6}-10^{20}
	Poor insulators; MoS_2	3000-25,000
	Semiconductors: V_2O_5 glass	2000-20,000
Non track forming materials	Ge, Si	10-2000
	Metals: Al, Cu, Au, Pt, W, Zn	10^{-6}-10^{-4}

Table 1.2: Resistivity of different materials.

Polymers like CR-39™(PADC), nitrocellulose(LR-115), Bisphenol-A polycarbonate (Macrofol) are most commonly used as

track detectors. Various inorganic materials (glasses and minerals) e.g. apatite, mica, olivine etc. are also used for track detection. Table 1.3 gives a brief idea of detection threshold of different track detectors.[14]

The basic processes after charged particle loses its energy are the ionization and excitation of atoms/molecules of the material. The exact nature of these changes taking place on the damaged sites depends on charge and velocity of the particle, on the chemical structure of the detector material and also on the environmental conditions like temperature and pressure.

Detector	Detection Threshold	Remarks
Inorganic	15 MeV/mg.cm^2	
Lexan, Makrofol	4 MeV/mg.cm^2	
Cellulose Nitrate	1 MeV/mg.cm^2	
CR-39	< 0.05 MeV/mg.cm^2	~ 100 times more sensitive than lexan
SR-86		Three times more sensitive than CR-39 for alphas and high energy heavy ions.

Table 1.3: Detection threshold of different solid state nuclear track detectors.

1.2.3 Special features of solid state nuclear track detectors:

The SSNTDs, mainly the polymers, are more advantageous as com-

pared to conventional track detection methods. The merits of the technique are,

i) They are very simple to use, durable and rugged. They are also cost effective and could be used in different sizes as per the requirements.

ii) The detectors can be used in presence of large amount of background radiations.

iii) The tracks are stored over a large period of time under normal temperature and pressure and can be analyzed even after long time.

iv) The small size allows them to be used in remote and difficult locations where other techniques become ineffective.

v) Some of the naturally occurring materials can also act as SSNTD's. The prominent among them are minerals, crystals and even the surface materials of the celestial bodies. Thus, natural records of geological and cosmological events can be revealed from these materials.

1.2.4 Bulk etch rate (V_b):[6] The bulk etch rate V_b is the rate at which the undamaged surface of the detector is being removed during chemical etching. Due to the chemical reaction between the etchant and the detector material, some molecules of the detectors are removed. The final effect is the removal of the material from the detector surface. During etching, the material is removed layer by layer and the thickness of the detector becomes smaller and smaller. The bulk etch rate is probably the most frequently measured parameter concerning track detectors.

1.2.5 Track etch rate (V_t):[6] The rate at which the latent track is etched is called track etch rate in other words it is the rate of detector etching along the track of particle. The track etching

process involves attack of the etchant along the track. Track etch rate depends on the amount of damage located in the trace core region. The track etch rate should be always more than the bulk etch rate for efficient track viewing under optical microscope.

1.2.6 Critical angle of incidence (θ_c): The surface of some detectors dissolve at a finite rate of etching, tracks incident at a very shallow angle in these detectors will not be detectable. There exists a critical angle of etching (θ_c) for each detector material. Table 1.4 gives the θ_c values for some of the detector materials.[13] From the θ_c values given above, it may be seen that plastics, are certainly going to be more efficient, owing to its lower value of θ_c. At any angle below θ_c, no etchable track will be observed after chemical etching as the surface would dissolve at a faster rate than the track material was etched out.[15]

Materials	θ_c (°)
Minerals	0-7
Glasses	
soda, borosilicate, flint etc.	20-70
Phosphate glass	1-5
Silica glass	13-19
Plastics	
Nitrocellulose	>2
Lexan	2.5
Makrofol	3

Table 1.4: θc values different track detectors for full energy fission fragments.

Thus, if a track a meets the surface at an angle less than θc

no track can be formed. One should therefore be cognizant in using these plastics, that particles incident at very small angles will not be detected. In most glasses the angle is so large that they are unsuitable for most applications as solid state nuclear track detectors.[16]

1.2.7 Geometry of track development:[17] During irradiation of the track detector by charged nuclear particles, latent ion tracks are formed along the path of the ions. After irradiation, the material is subject to chemical etching to reveal preferentially the latent ion tracks. Figure 1.2 shows the track etch geometry of the material. The incident angle is normal with respect to the diameter surface and V_t is constant.

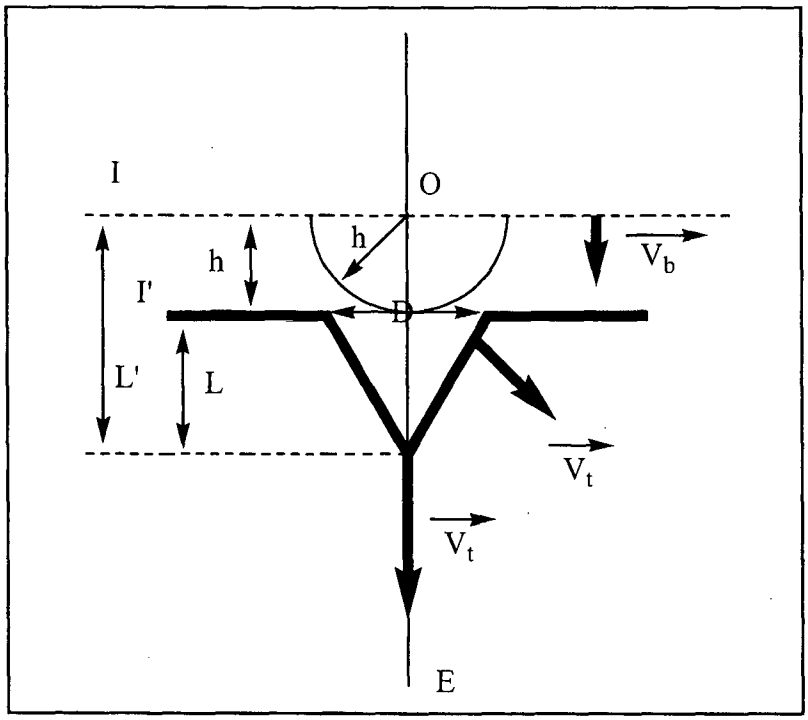

Figure 1.2: Geometry of track development.

The simplest case of track development refers to that when the incident particle enters a detector under normal incidence with respect to the detector surface as shown in Figure 1.2. In this

figure, I is the initial detector surface, I' is the surface after the etching, V_t is the etch rate along the particle trajectory (track etch rate), V_b is the etch rate of the undamaged regions of the detector (bulk etch rate), O is the entrance point and E is the end point of a particle in the detector material, and OE = R is the particle range in the detector material. The distance between I and I' is equal to h, i.e., the thickness of the layer removed by etching, L' is the total distance traveled by the etching solution along the particle track, and L is the track depth. D is the diameter of the etched track.

During this chemical stage of processing, the size and shape of the etched ion track is determined. The most influential experimental parameter is the ratio between the track etch rate and the bulk etch rate, the so-called track etch ratio. Track development is governed by the ratio $V = V_t/V_b$ and track formation is not possible if V is smaller than or equal to 1. In other words, the condition $V > 1$ must be fulfilled to form a track. The quality of the etching process depends on the energy deposition density of the ion along its path, on the radiation sensitivity of the material, on the storage conditions of the ion-irradiated material before etching, and on the etchant.

As mentioned earlier, the etching progresses in all directions with the rate V_b except along the particle path where the etching goes with the rate V_t. In three dimensions, the track is a cone with the developing angle d, which is obtained by rotation of the track wall around the particle path. During etching, the track wall moves parallel to itself. Depending upon the angle of incidence (normal or oblique to detector surface) track geometry can change.

1.2.8 Criteria for track formation: The primary condition for track development is that the, bulk etch rate must be lower than the track etch rate for efficient track development. The validity of this condition has been examined by many theories put forth by different track detector workers. A track formation must define a parameter X, having a precise and definite limit X_c, below which a non-etchability limit occurs. Many reports are available discussing these criteria. Some of them are listed as follows

i) Total energy loss rate criteria:[18] The charge particle track is formed in a detector material if rate of energy loss by the charged particle is above the critical value which is characteristic of the material under study. In other words, the rate of energy loss per unit length d_E/d_X by the bombarding particle must exceed a critical value, $(d_E/d_X)_c$. The criterion was very successful for particle velocities over a narrow region. As the δ electrons scatter away from the site of latent track, the energy is deposited along the path on the sides of latent track thus making the total energy loss rate criteria a failure when applied to relativistic particles.

ii) The primary ionization criterion (PI):[19] When a charged particle enters a detector material, intense ionization takes place and the particle is stripped off of its electrons. If the primary ionization takes place at a higher rate than its critical value, etchable track will be formed. But, the criterion does not take into account the δ rays and their ionizations. Moreover, in crystals the radial extent of unetched tracks is of the order of few angstroms, so the primary process should predominate over the secondary ones, but it may not be the case in polymers.

iii) The restricted energy loss (REL) criteria:[20] The charged particle upon entering the detector loses its energy due to distant

collisions with the electrons of the stopping material and this is called restricted energy loss. Latent track formation takes place only if REL of the particle exceeds a critical value characteristic of the detector material. REL includes both the energies of primary ionizations as well as higher order ionizations. The criterion works well when the incident particle energy is greater than nearly 3.5 MeV/nucleon.

iv) Radius restricted energy loss (RREL) criteria:[21] All the events of energy deposition occurring within a radius 'r' of the traversing particle are accounted in the RREL criteria. This criterion emphasizes the track region and tries to consider only that part of energy of δ rays, which actually gets deposited in the core region irrespective of the energy of the δ rays.

v) The delta-ray criterion by Katz and Kobetich:[22] This criterion postulates that for a etchable track to form the secondary electrons should deposit critical energy at a critical distance. This approach is in contrast to that of the total energy loss and the primary ionization criterion. To calculate the spatial energy distribution the δ ray energy spectra and the range energy relation in the vicinity of the particle track were combined. The criterion fails as it neglects the contributions of the primary excitations.

iv) The δ-ray criterion by Monin:[23] This approach is similar to that of Katz and Kobetich. This criterion does not assume any critical radius initially as the dose deposited within the cylindrical area is calculated. A traversing particle is thus assumed to produces an etchable track when the absorbed dose exceeds the specific value within a cylinder of certain radius.

1.2.9 Mechanism of track formation:[6] The track formation mechanism in solids depends largely on the type of materials used and

can be classified into inorganic crystals and organic polymers. Organic polymers can record particles at energy loss rates less than 4×10^7 $MeVm^2g^{-1}$ which enables to detect proton recoil tracks. However, inorganic detector materials cannot detect particles with energy loss rates less than 15×10^7 $MeVm^2g^{-1}$. Thus, the damage mechanism for the two materials would be different. The different mechanisms proposed are as follows

i) Thermal spike model:[24] The thermal spike mechanism can be used to explain track formation in inorganic insulating materials. When an energetic nuclear particle traverses a detector material it produces an intense heat in localized region of the crystal lattice. The localized heat raises the region to a higher temperature level and subsequently cools via heat conduction. These processes damage the lattice structure of the material by various atomic processes. This model explains the track formation in insulating materials and inability of metals to reveal tracks. Metals can dissipate the heat formed very rapidly due to the presence of large number of electrons in the conduction band which gives δ rays by electron-electron collision. In insulators, the electrons can interact with the various modes of vibrations and the excitation is communicated to the lattice more conveniently.

ii) The ion-explosion spike model:[13] The ion-explosion spike model is the widely accepted mechanism for track formation in inorganic materials. Figure 1.3 shows different stages of track formation. The damage process involving five stages can be described as follows.

Stage 1: Electron stripping of the charged particle

In this stage a nuclear particle enters a detector material and loses some or almost all of its electrons due to interactions

with the electrons of the detector material. For example 280 MeV ^{56}Fe particle when enters mica detector it loses all its electrons on entering the material and proceeds as Fe^{26+}, the iron nucleus.

Stage 2: penetration at velocity too great to leave etchable track

No etchable track occurs on initial impact as the damage is not continuous enough to provide a preferential etch path. Unless the damage is continuous atomically the track will not be continuous in the detector material.[25] At least one atom must be ionized per atomic plane traversed by the nuclei.[26]

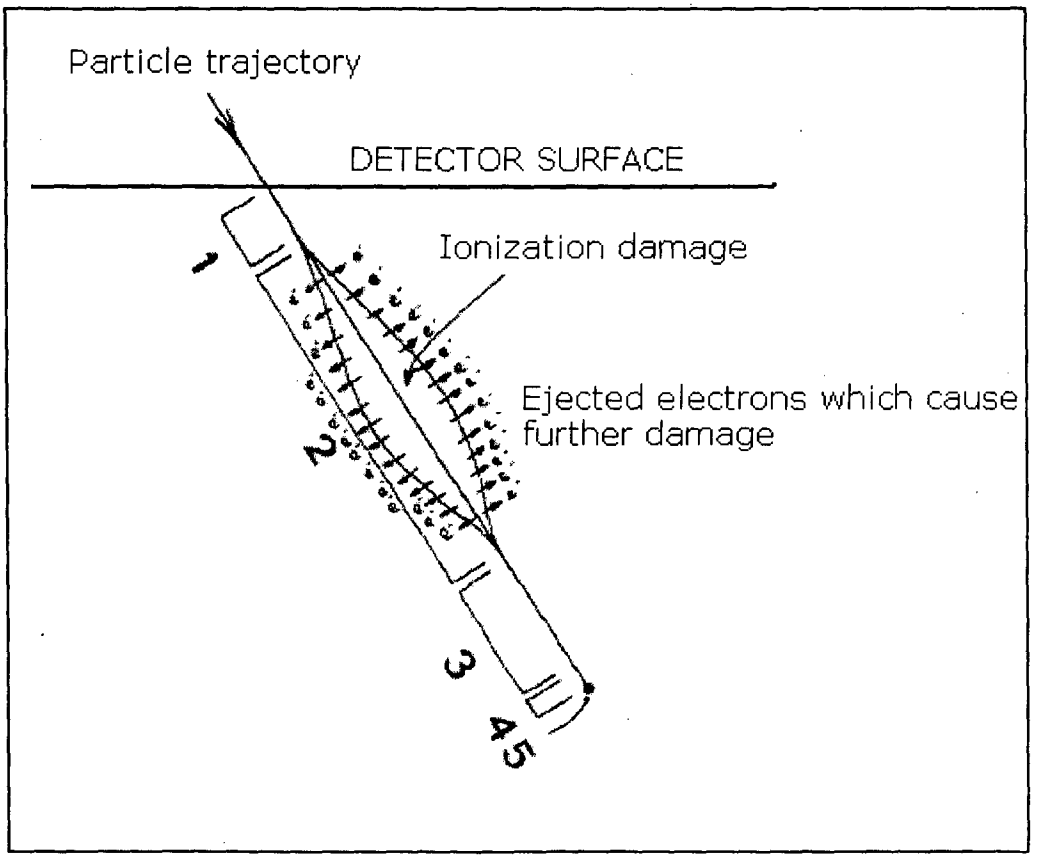

Figure 1.3: Track formation in detector material.[13]

Stage 3: Actual damage region

At this stage the particle is moving slowly enough to provide sufficient damage density along its path. The highly charged nucleus collides with atoms imparting energy to them. The electrons are

excited and get ejected from the atoms and penetrate the surrounding material. They are known as δ rays or bremsstrahlung electrons.[26] The atoms which have lost electrons, grouped as they are down the path, will recoil from each other as a result of coulombic repulsion. It is this linear concentration of damage due to the "ion explosion" which forms the etchable track. When the penetrating particle has slowed and regained electrons to the extent that it is no longer potent to create the damage density necessary for track etchability Stage 3 terminates. Figure 1.4 shows detailed ion explosion mechanism

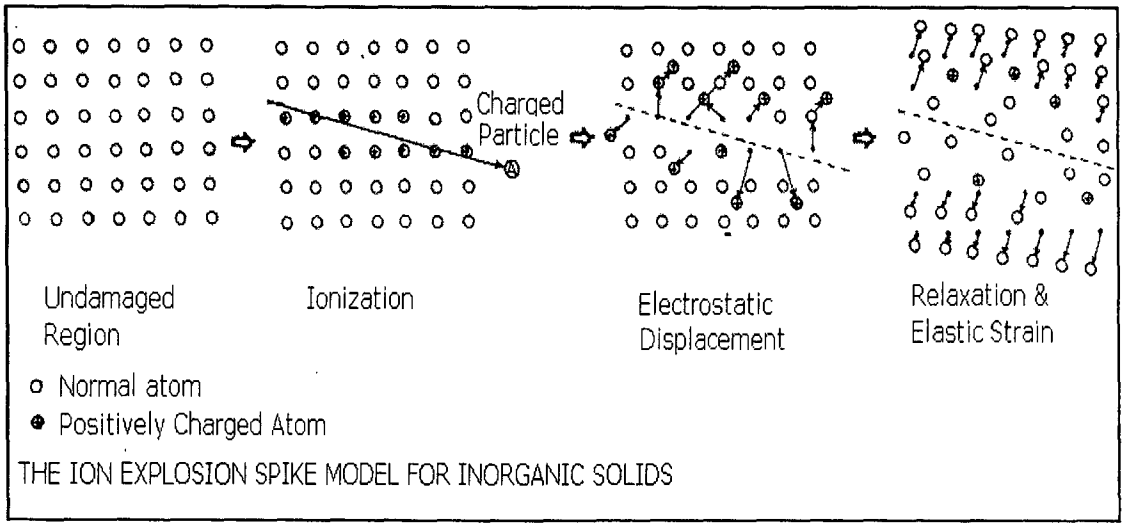

Figure 1.4: Ion explosive spike model.

Stage 4: Unetchable Particle track

There is a minimum velocity below which damage is insufficient to produce an etchable track and will be larger for detector materials with low sensitivities. The distance is called range deficit, where particle is moving but leaves no track.

Stage 5: Termination of the track

In this stage the particle comes to complete rest probably with complete electrons gained. Tracks which consist solely of stage five can occur for heavy particles of very low energy of ~1

keV/nucleon. They have been reported for heavy fragments from alpha decay of heavy nuclides[27] and for solar wind particles.[28,29]

iii) Radiochemical damage mechanism: Radiation damage in polymers involves scission or cross-linking of molecular chains. The rate of the polymer dissolution is enhanced by reduction of molecular weight caused by scission. This pattern of scission and dissolution is followed by the polymeric track detectors. But, tracks have been observed in polymers, such as polyethylene, which undergo cross linking. The cross-linking can render a polymer less soluble, but, the etchants attacks the polymer molecule more rapidly in the region of radiochemical damage. The composition of some etch products of polymers which degrade by chain scission indicates that the chemical reaction with the molecules plays a part in preferential dissolution.

The chain scission or crosslinking ability of a polymer on irradiation can be predicted by an empirical rule.[30] The rule says that chain scission on irradiation is possible in polymers having general formula:

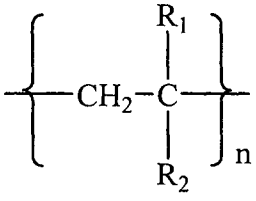

While those which cross link are of the type:

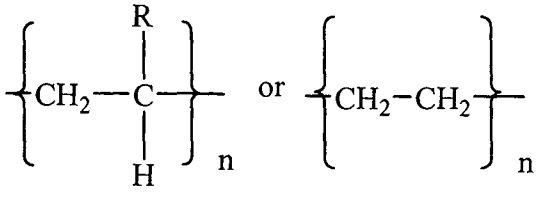

However, cellulose derivatives, polycarbonate or polyethylene terephthalate does not adhere to this rule. Radiation degradation of polymers can create free radicals by breaking C-C backbone bonds:

The C-H bond can also be broken,

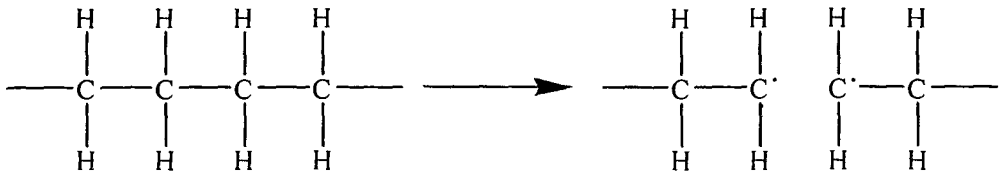

1.1

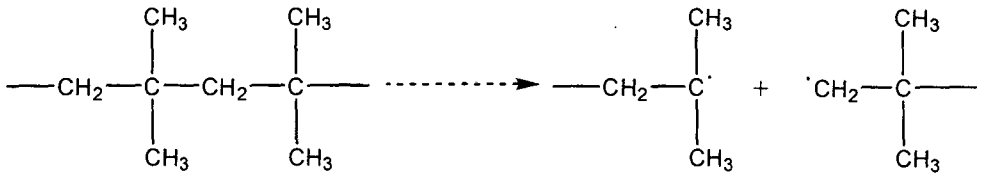

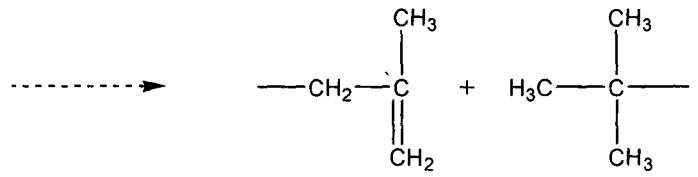

1.2

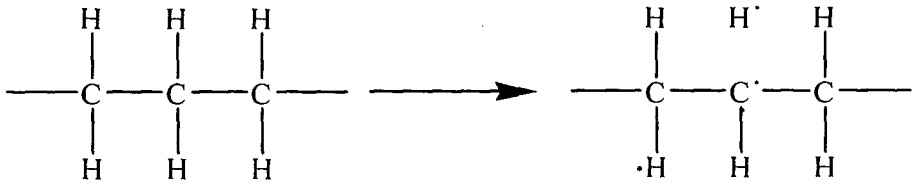

1.3

The free radicals in the first stage can readily recombine in case of polyethylene as the broken ends do not have to approach each other in a highly specific orientation before recombination. The slightly greater stability of the C-H bond compared to that of a C-C bond makes the second reaction difficult to occur. Furthermore, the high mobility of the hydrogen radical means that recombination is much less likely and rendering appreciable lifetime for carbon radical. The probability of recombination is reduced marginally in doubly substituted molecules due to formation of stable terminal groups. For e.g. the stabilization of the scission event is seen to occur in polyisobutylene as shown below.

Thus, in case of polymeric track detectors the damage process has several stages. In polymers it is likely that the mecha-

nisms exist which can propagate from the damage of the track and hence the primary ionization density required for etchability will be significantly low. In case of polycarbonates, damage mechanism is available in addition to the ion explosion spike. Polymers can be degraded at energies below that required for ionization. The lower energies necessary for polymer degradation mean that the δ-rays also contribute significantly to the damage leading to enhanced etching rates comparatively remote from the track core in which the ion explosion mechanism predominates.

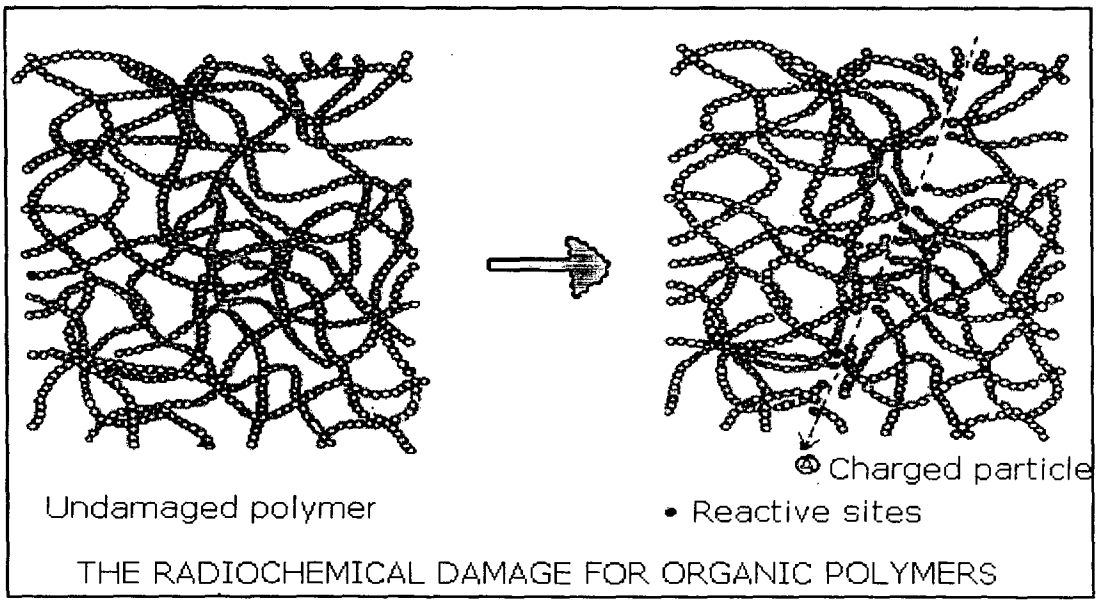

Figure 1.5 : Radiochemical damage mechanism.

Thus, the penetration of an energetic charged particle creates an array of radicals along its trajectory as shown in Figure 1.5. The formation of free radicals can lead to chain scission, degradation of side groups into low molecular weight species. The chain ends are also involved in the formation of intermident cross links, thereby forming a latent track. Chemical etchants like alkali hydroxides are able to degrade predominantly these regions of the latent track as compared to the bulk of the detector material used.

1.2.10 Track visualization techniques: As discussed earlier, a latent track is formed when a nuclear particle traverses a detector material at a sufficient energy called the threshold energy. These latent tracks have very fine dimensions and therefore can only be directly viewed under a transmission electron microscope. The various methods used to view these latent tracks are enlisted below.

i) Electron microscopy: The particle tracks in an unetched detector are not visible under an optical microscope. However, transmission electron microscopy has been successfully used to reveal these tracks in early stages.[6]

ii) Selective chemical etching:[14] The most widely used technique among the track detection workers for track visualization is the chemical etching process. The latent track of a charged particle is a region of enhanced activity towards chemically aggressive reagents. The material containing latent track is immersed into a solution called 'etchant' which degrades the latent track at much higher rate than the surrounding bulk region. The process increases the size of the latent track. When the dimensions of the tracks become comparable to that of the wavelength of visible light they act as strong scattering center appearing black in normal bright field illumination and white in a dark field under the optical microscope. This process of chemically enlarging the latent damages into visible tracks under the optical microscope is called chemical etching. Once the chemical etching process is over the detector is removed and washed with distilled water. The detector is dried under IR lamp and observed under optical microscope. Table 1.6 summarizes typical chemical etching methods used to etch some commonly used detectors.[14]

Category	Track detector material	Etching conditions
Crystal	Feldspars	1 g NaOH + 2 g H_2O under reflux.
	Olivine	KOH solution, 160 °C, 6 min.
	Mica	48 % HF at 20-25 °C, ~ 40 min.
	Quartz	KOH solution, 210 °C, 10 min.
Glass	Sodalime glass	48 % HF, at 20 - 25 °C, 3 sec.
	Phosphate glass	48 % HF, at 20 - 25 °C, 3 sec.
Plastics	CR-39™	1-12 N NaOH at 40-70 °C, 1-4 hrs.
	Polycarbonate	6 N NaOH at 50 °C, 60 min.
	Cellulose nitrate	3-6 N NaOH at 50 °C, 40 min.

Table 1.5: Different etching conditions used for etching nuclear tracks in different detector materials.

There are a large number of etchants which can be used for track revelation. The plastic track detectors are normally etched by using strong alkali hydroxides such as NaOH, KOH etc. To increase the effectiveness of attack aqueous etchants etch promoters such as ethanol, methanol, propanol is added to the solution. These organic solvents accelerate the rate of dissolution of the degraded polymer fragments formed during etching. Detergents are also added in some instances which can be used for generating cigar-like shapes of the tracks.[31] Oxidizing agents such as $KMnO_4$, $K_2Cr_2O_7$ have also been tried. However these etchants leads to highly resistant deposits of partially reduced metal oxides of low solubility. The chromium can attach to the polymers by covalent bonds and cannot be removed easily. For minerals and glass track detectors acids such as H_2SO_4, HF, HCl, H_3PO_4, glacial

acetic acid, HI etc are used as etchants.

iii) Electrochemical etching(ECE):[32] The chemical etching process is enhanced by using high voltage electric fields. The process increases the size of the tracks so that they can be counted by low magnification device. The method is advantageous for light particles such as protons, alphas at low intensities and makes track counting easier and faster. The process of ECE begins with the formation of conical tracks with a sharp tip similar to the tracks obtained by chemical etching. Under these conditions the influence of electric field at the conductive tip can be many times greater than that applied to the remaining surface of the detector material. The chemical action of the etchant combined with the electrical phenomena initiated by very high localized stress gradients can produce tree shaped track at the tip, the process being called treeing. The process can be visualized from the Figure 1.6.

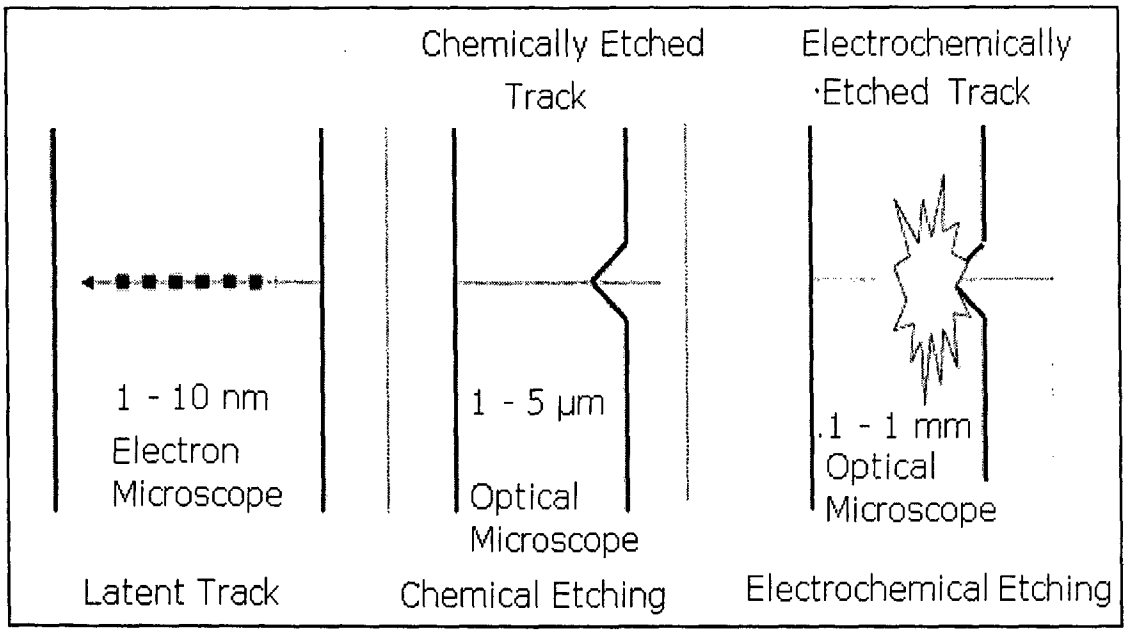

Figure 1.6: Electrochemical etching process.

The ECE consists of two volumes of electrolytes which are separated by the detector film. One of the electrolytes is the

etchant used for chemical etching of the detector. The two electrodes are dipped in the two electrolytes and alternating current of high voltage is applied across the foil. The ECE electrical field ranges from 20-40 $kVcm^{-1}$with the frequency values of the order of kHz. The detector film behaves as insulator between the two electrolytes. The AC voltage also leads to electrical phenomena that lead to electrical stress in the polymer. The high voltage produces the thermal phenomenon which increases the etch rate of the detector. The etching process is carried out at a temperature between 25 - 70 °C. In the ECE process the first step is the formation of a cone as is the case in chemical etching. Once a conical track is formed the tip of the needle shaped track attains a high electric field than that of the remaining detector. The high electrical field generates a local stress and can initiate electrical phenomenon which when combined with chemical action of the etchant produce a tree shaped track and the process is called treeing. A typical ECE assembly is showed in the Figure 1.7 below.

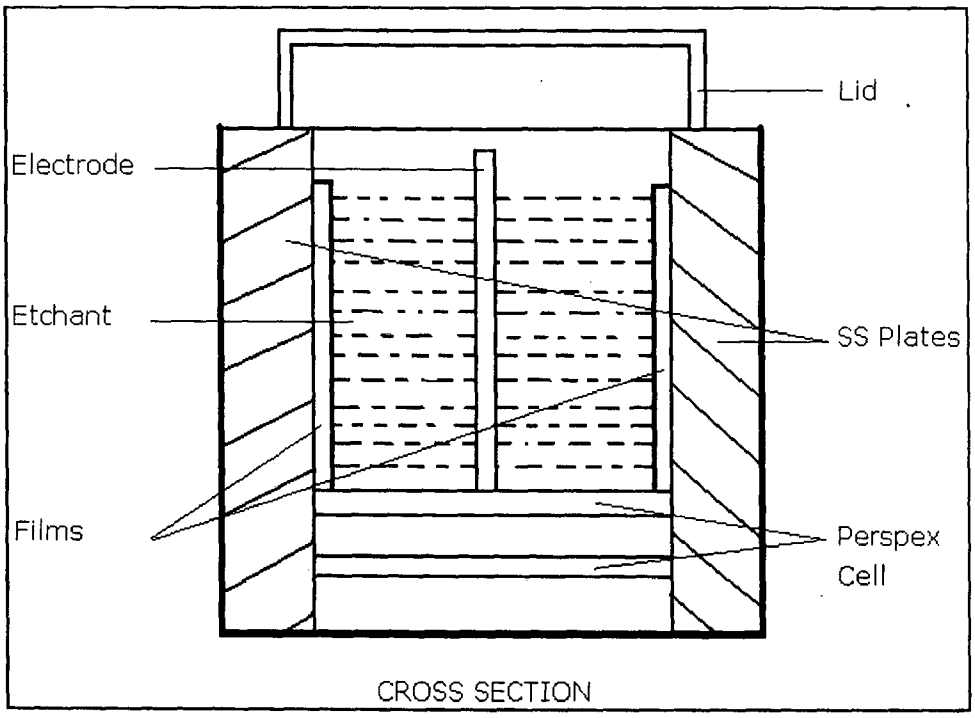

Figure 1.7: Electrochemical etching assembly.

The disadvantages of the technique are that the presence of high track density (above 103 cm^{-2}) makes the technique unsuitable due to intersecting track geometries. Secondly, the specific information of the track is lost upon EC etching. Moreover, tracks similar to radiation particle tracks are obtained if the detector contains imperfections or contaminants.

1.2.11 Factors influencing etch rate in a detector during chemical etching: The factors affecting the etch rate of polymer are

i) Etching conditions: The bulk etch rate is effected by different etching conditions used for track revelation. The increase in temperature has a marked effect on the bulk etch rate. The rate of etching increases exponentially with the increasing temperature for the plastic track detectors. The plastic track detectors are etched in aqueous alkali hydroxide solutions. The bulk etch rate of a polymeric detector increases with the increase in ionic radii of alkali metal ion used.[33]

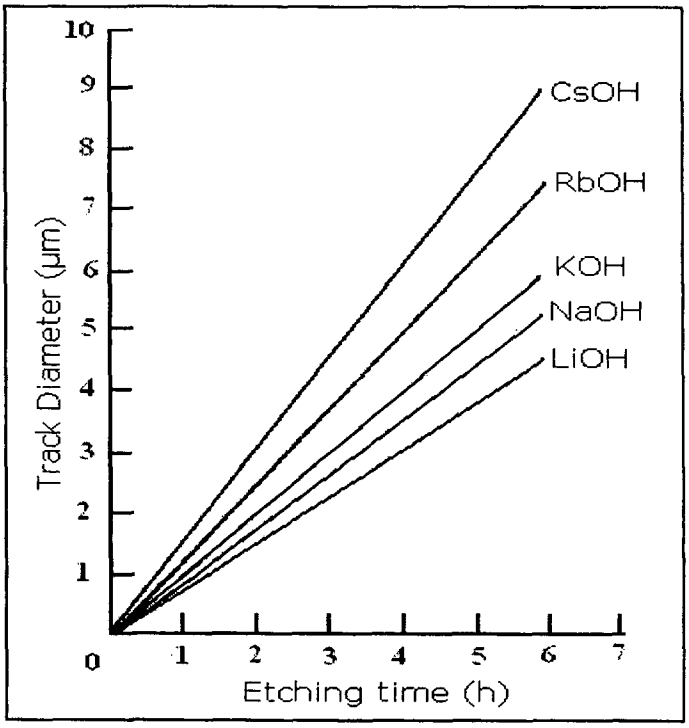

Figure 1.8: Effect of the alkali hydroxide on the track etching rate.

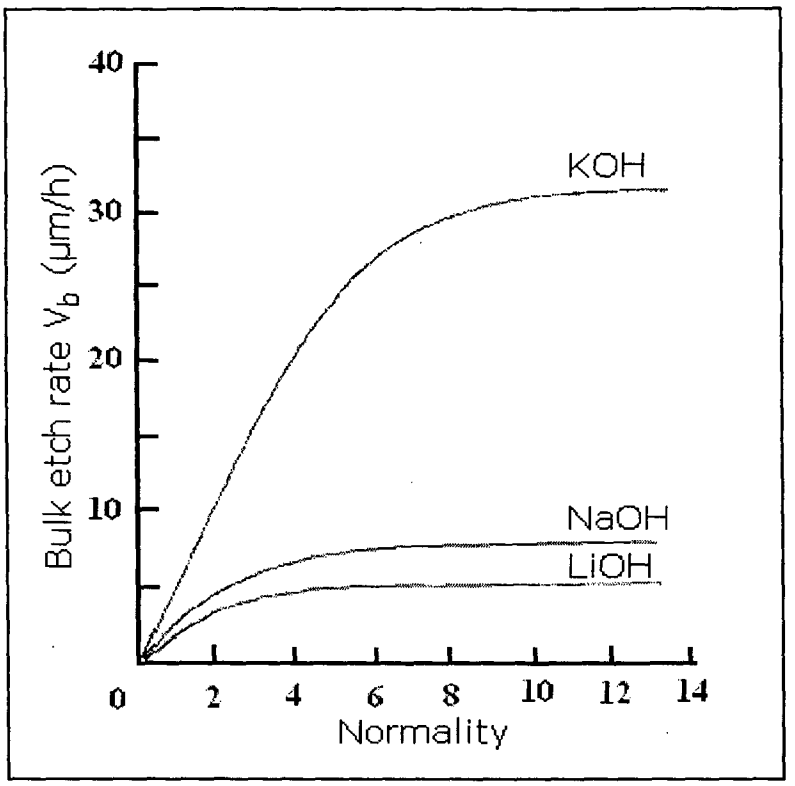

Figure 1.9: Effect of etchant concentration on the bulk etch rate of cellulose nitrate detector at 50 °C.

Figures 1.8 and 1.9 depict the variation in the bulk etch rate with the type of alkali and concentration respectively. The bulk etch rate was found to increase exponentially with the increase in the concentration of the etchant. In addition to concentration and temperature, the stirring of the etchant solution also plays vital role in etching process. The detectors etched in unstirred etchant tend to etch the material at a slow rate.[34]

ii) Ageing of the detector: The polymer film ageing can affect the etching properties of the material. The ageing of the detector depends on the storage conditions. The storage moisture content of some detectors can affect the bulk etch rate of water sensitive polymers like cellulose nitrate.[6] Environmental degradation of CR-39™ may take place by auto-oxidation. The tertiary hydrogen of the allylic part of the polymer can be attacked by oxygen to form peroxides.[35] The formation of peroxides on the substrate will pref-

erentially occur with tertiary hydrogen atoms in the structure.[36]

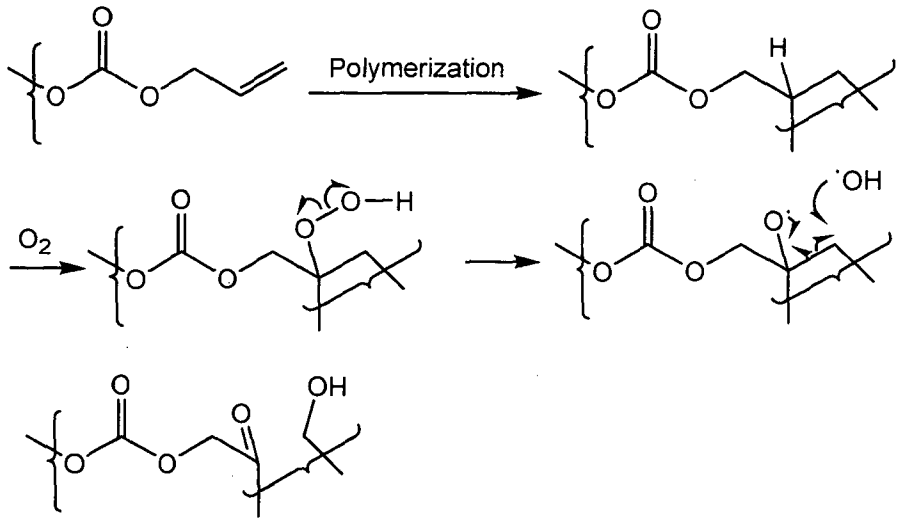

1.4

The process leads to scission of hydrocarbon chain in the polymer matrix. A neutral environment of vacuum or nitrogen atmosphere decreases the track etching rate. Detectors older than 5 years show odd behaviors of V_b which decreases with increasing age.

iii) Irradiation of detector before etching:[17] Irradiation of detector material before etching with radiations such as, gamma radiation, electrons, Proton beams, ultraviolet and infrared radiation increase the bulk etch rate. Polymer surface on exposure to radiation undergo various changes which causes either localized hardening/bulk surface hardening or softening. The hardening caused by ageing or heating is usually associated by decrease in V_b, while softening can lead to increase in etch rate.

The increase in the gamma dose on the detector increases the bulk etch rate as well as the sensitivity of the material.[37] The effect of gamma dose on PADC bulk etch rate was not profound till a dose of 10^4 Gy as V_b was unaffected. However, further increase

in dose enhanced the V_b.[38] The ultraviolet radiations, proton beams, the infrared radiation and electrons also increases the rate of etching. The increase in the V_b was due to the chain scission of the polymer matrix.

iv) Influence of homogeneity:[39] The latent ion tracks are formed due to rapid thermal quenching of the bombarding charged nucleus to an amorphous ion track core, according to the thermal spike model. The selective removal of this amorphous part leads to the formation of track and is the key step in ion track etching. Crystalline solids are therefore, ideally suited for ion track etching, but, large mono crystals rarely occur. Muskovite, Mica and Quartz are some of the mono crystals which can be used. These systems are very promising candidates for research, due to their high homogeneity down to the atomic scale, they enables well-defined nanostructures down to less than 10 nm. Dislocations and pronounced grain boundaries will compete with latent tracks during track etching in case of polycrystalline solids and hence are excluded.

Polymers are preferred to ionic crystals as the polymer chain scissions easily occur and are much more susceptible to radiation effects than ionic crystals. In polymers however, a mono crystal is not feasible and completely amorphous materials like polycarbonate (PC). Polyethylene terephthalate which is about 50 % crystalline is mechanically and chemically more resistant. However, the grain structure appears acceptable for tracks of 100 nm diameter since the size of its crystal grains (around 20 nm) is of the order of the track diameter. The partly crystalline polymers with large crystal grains in comparison with the track core diameter are not suited for ion track etching.

1.2.12 Mechanism of surface degradation in detectors during chemical etching:[39,40,41,42] In inorganic materials, once the material containing latent track is immersed in the etchant, the positive end of the water solvates the cation and the negative part solvates the anion thereby making the material soluble. Inorganic salts are mostly soluble in aqueous acids and therefore the material dissolution is simple process due to the polar nature of water. However, the solubility is enhanced at the sites of latent tracks as it renders the material highly active and the etchant can diffuse into the material at a faster rate. The mechanism of track development or polymer dissolution is completely different than that of inorganic materials. The etchant actually attacks the functional groups present in the polymer and degrades the material. The polymers containing different functional groups can be etched as follows.

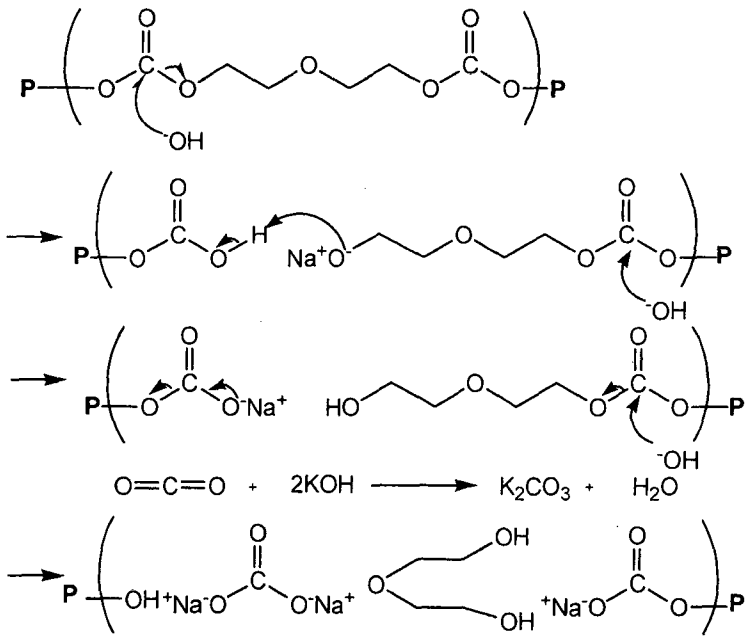

1.5

i) The carbonate containing polymers(CR-39™): The polymers containing carbonate groups are very commonly used as plastic

nuclear track detectors. The most common example of this type is PADC(CR-39™). The polymer degrades in alkali solution as follows

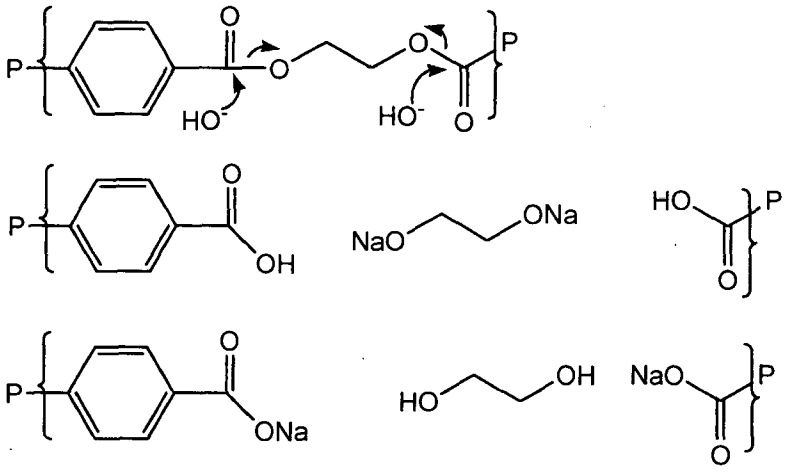

1.6

The base first attacks the carbonate moiety thereby rendering the bridging ethylene glycol free which goes in the solution. Decarboxylation of the carbonate moiety followed by absorption of the liberated carbon dioxide in alkali hydroxide solution completes the dissolution process. It can also happen that the ethylene glycol along with the carbonate moiety can be removed as a single fragment. An analogous mechanism exists in all the other polymers having carbonate group.

ii) The ester moiety in Polyethyleneterephtalate (PET): The end products of hydrolysis of the polymer are disodium terphthalate and ethylene glycol. The products can be accounted for, only if, the main points of etch attack are the partially charged ester groups, which are hydrolyzed by alkali.

iii) Polypropylene (PP): The monomer is not having any functional group but acetic acid is found to be one of the etch products under oxidizing etchants. The tertiary carbon is attacked by the strong oxidizers breaking the carbon hydrogen bond, creating peroxides or hydroperoxides and subsequently carbon-carbon bonds

adjacent to the tertiary carbon. The polymer is etched in acidic CrO_3 as an etchant.

For polycarbonates, track etch ratios above ten thousand have been observed. Addition of organic solvents, such as methanol, ethanol or propanol can dramatically decrease the track etch ratio, in case of PET, leading to wide cone angles. For example, these cones can be placed on both ends of a cylindrical track section. In general, heavier ions lead to more precisely defined ion tracks.

1.2.13 Techniques to improve track visibility: The chemical etching process and subsequent observation of nuclear tracks under an optical microscope can be facilitated by using following techniques

i) The track visibility can be enhanced by using polarized light and a crossed polarizer. The crossed polarizer enables easy detection of light scattered from track surfaces.[43]

ii) Polyester film is coated with a thin layer of 8 to 12 μm with red-dyed cellulose nitrate. After etching holes of particle tracks are observed against a red background. The tracks can be subsequently enlarged and recorded permanently on high contrast film or photographic paper.[13,44,45]

iii) Bright tracks on a dark background can be observed on a film if a fiber optic is used to introduce light at the edge of a detector through light tight jaws. The trapped illumination escapes from the surface when a hole is encountered. The tracks can then be easily counted against a dark background.[46]

iv) The surface of the track detector is coated with silver layer which reflects the light. The reflected light can be used to illuminate the tracks and assist counting purposes.[47]

v) The etching of the detector is carried in such a way that track perforation takes place and the chemical reacts with the markers underlying the material which produces localized absorption spots.[48]

vi) A fluorescent dye can be used to penetrate etched tracks which are then viewed using ultraviolet light.[13]

vii) Tracks can be visualized easily if the holes in a detector are exposed simultaneously to HCl gas on one side and NH_3 gas on the other. The reaction produces white NH_4Cl crystals at each hole.[49]

Visual counting of tracks is usually a tedious and lengthy procedure and necessitates automatic techniques when speed, high accuracy, evaluation of many detectors or of large areas is required.

1.2.14 Techniques to evaluate dose of recorded tracks: The latent nuclear tracks in a material as earlier stated can be visualized by TEM analysis. However to exactly determine the dose amount and the density of tracks, one can use several microscopic and macroscopic methods.

i) Microscopic Methods: The microscopic techniques are the most widely used for track counting and analysis. In all of these techniques the detector is initially etched in etchant.

1) Visual track counting: The method involves counting the number of tracks per view under an optical microscope to average out tracks/cm^2 for the detector. The method is time consuming and a low track density of < $10^5/cm^2$ is required for accurate analysis. Image projection techniques and image analyzing systems have now made the method more simple and effective.

2) Optical densometry: For high track density measurements optical densometric techniques are possible. The technique comprises of measuring the amount of scattered light proportionally

between etched and unetched surfaces.[50,51] A red dye is used to accentuate the material.[52]

3) Confocal microscopy:[53] The technique includes 3D construction of a nuclear track after etching. The method is very important as can be used to determine the charge, energy and mass of the particle.

4) Atomic force microscopic analysis: The technique has been rarely used to determine tracks in a detector material. However, one can use it accurately for bulk etch rate determination and to determine the post etch surface of detector.

ii) Non-microscopic methods of counting or estimation of dose: There are various methods for track detection or counting without the use of an optical microscope.

1) A detector material is etched and then treated with ammonia gas. The gas penetrates the track perforations which are subsequently recorded on Ozalid reproduction paper. The resulting image can be enlarged by projection through a microfilm reader, photographic enlarger or slide projector. The method can be used to scan surfaces of large areas.[54]

2) In this method the detector is coated on one side with an aluminium film and etched on the other side. The reagent first etches the track and then the aluminium. The process results in giving transparent apertures of 0.1 to 0.5 mm diameter.[55]

3) This technique uses the process polymer grafting[56] as a means of detecting charged particles. The passage of charged particle leaves an array of reactive species along its path. The high concentration of reactive chain ends and free radicals along the radiation tracks in a polymer, cellulose triacetate, are used to initiate polymerization of a monomer. The active centers in the polymer

are graft polymerized with propenoic acid, to give a cellulose triacetate-propenoic acid graft copolymer. The grafting of the propenoic acid at the latent tracks renders polymer acidic and hydrophilic at these sites. The co-polymer can then be dyed with rhodamine B and the tracks can be easily observed using fluorescence microscopy. ^{252}Cf fission fragments has been analyzed by this method with 100 % detection efficiency.

4) The tracks will appear bright against a dark background if they are illuminated with dark-field. A photomultiplier tube is placed in the eye piece to measure the total light scattered into a microscope objective.[57] In all techniques based on the measurement of macroscopic effects instead of individual track recognition, the optical density depends on both track density and etching time.

1.2.15 Applications of Solid State Nuclear Track Detectors:[6,17,13,13] The SSNTD technique has grown vary rapidly since its inception in the late 60's. The nuclear track detectors are used almost in all fields of nuclear chemistry/physics and also for biomedical and cosmos studies. Environmental studies and health effects are the topics of great interest to the current track detector workers. The nuclear track detectors are used in following diverse fields

i) Nuclear Physics and Technology: The track development field is extensively used in the field of nuclear physics and technology. The uses include

1) Fission track dating: The fission track dating method is used for archaeological dating. All minerals contain uranium which gives out fission fragments by spontaneous fission reaction. These fission fragments can be trapped on a track detector and counted after etching.

2) Uranium and Thorium exploration: The uranium decay product contains noble gas radon. This gas can diffuse or be transported to some distance in the soil and surrounding through the fissures in the rocks. The detector is exposed to alpha particles from radons, which gets registered, are counted on etching. The alpha track density gives the measure of radon concentration in the soil.[58]

3) Alpha estimation in waste water fields: The waste water from radioactive source contains alpha activity which has to be below 0.037 Bq/ml. Plastic track detectors can be used to assay the alpha activity in the solution.

4) Heavy ion reactions: The nuclear track detectors are used to study the reactions induced by heavy ions of low energy as well as of high energy. The product track analysis gives projectile charges, mean free path of ion fragments and other vital information.

5) Astrophysics and cosmic rays: SSNTD's have been extensively used to study the elemental and isotopic composition of primary galactic cosmic rays. The data obtained can be used to construct a modified model for the fluxes and spectra of cosmic ray protons and heavy nuclei.

6) Search for super heavy elements: The technique can be used to detect super heavy ions in artificial transformation reaction or of natural origin.

ii) Environmental and health physics: The use of nuclear track detectors has been extensive in the field of personnel protection dosimetry. The areas of interest includes

1) Radon dosimetry: Measurements of radon levels to monitor and control indoor radioactive pollution continues to be a significant activity pursued by the users of SSNTD's.

2) Neutron dosimetry: The use of track detectors to estimate neutrons exposure at nuclear reactors and other installations has been of great importance. To monitor the neutron flux at irradiation chambers of a nuclear reactor and to avoid risk of neutron exposure at the sites are the two important uses of SSNTD's.

3) Exposure at spacecrafts: During the visits at international space station, lunar landings and other flybys the cosmonauts are exposed to various radiation sources like ultra heavy, cosmic rays, interplanetary dust particles and the particles from solar flares. The nuclear track detectors are handy to measure dose levels of such particles.

iii) Biomedical science:

1) Boron neutron capture therapy: The therapy is used to scan and destroy malignant brain tumors. A boron containing compound is given to the patient which is absorbed by tumor and whose head is then irradiated with thermal neutrons. The spatial distribution of alpha particles produced by the reaction $^{10}B(n,\alpha)^{7}Li$ can be examined for research and treatment planning purposes.

2) Alpha content of blood: The workers at the uranium mines and reactors are exposed to uranium which gets inhaled into the body. The blood samples of these workers can be analyzed for radioactive substance by their alpha activity by immersing the detectors in frozen blood.

3) Lead content in the bones: The lead absorbed in the body gets accumulated in bones and teeth, which can be found by using nuclear track detectors.

iv) Technological Sciences:

1) Nucleopore filters: Filters are manufactured with cylindrical holes in detector material of predetermined size by irradiating a

thin polycarbonate sheet with roughly collimated fission fragments and etching to the desired pore size. The filters are used to study bacteria, algae and other microscopic organisms.[59,60]

2) Magnetic nanowires: Magnetic nanowires are of great interest and can be used as magnetoresistive sensors for miniaturized pickup sensors for magnetic hard-disk memories and as non-volatile magnetic bit memories.

In 2005, Dr. P. B. Price, one of the founding father of SSNTD technique, summarized the highlights of the research in the field of SSNTDs over a period of 45 years as given in Table 1.6.[60]

Year	Techniques and practical applications	Fundamental science applications
1958	Etch pits in LiF irradiated with fission	
1959	Observation of fission tracks in mica using TEM	
1962	Ancient tracks etched in mica	
1963	Use of minerals, glasses, polymers as track detectors. Neutron dosimeters.	Fission track dating
1964	Nuclepore filters	^{238}U Spontaneous fission Decay constant and fosil tracks of Fe-group cosmic rays of in meteorites
1965	Track formation by ion explosive spike model	Determination of age of ancient hominids
1966		400 MeV Ar ions ternary fission on $ThSiO^{n}_{4}$
1967	Etch rate criteria for charge resolution of energetic nuclei and alpha-recoil tracks in mica	Ultraheavy cosmic rays in meteorites (Z >30)

1969		Magnetic monopoles search
1970	Submicron particles counting	
1971	Lengths of fully confined tracks	Preferential emission of hi-Z nuclei in solar flares
1972	Detection of Radon and search for Uranium	$10^{11}/cm^3$ tracks of energetic solar particles in lunar soil
1978	CR-39 track detector	Charge spectrum of UH cosmic rays on Skylab
1980		Peking Man fission track dating
1981	Ion track micro technology	Mountain altitude Cosmic rays with Z = 3
1983		Fractionally charged projec tile fragments search
1984		Search for slow monopoles with ancient mica
1985		Cluster radioactivity
1988	BP-1 glass track detector	
1989		Strong evidence against cold fusion
1991	Treatment of burns using Particle track membranes	
1993		Singly ionized low-energy heavy cosmic rays
2000	Workable alpha-recoil track dating method	
2004	Particle tracks of interplanetary dust in aerogel collectors	

Table 1.6: Major discoveries in the field of SSNTD.

1.2.16 Major areas of SSNTD research in India:[61] The visit of P. B. Price to the Tata Institute of Fundamental Research, Mumbai marked the beginning of SSNTD research in India. At present there are at least 20 active research groups and specialized centers in India working in the field. A brief outline of the major areas of SSNTD research in India is given below.

i) Cosmic rays and space science: Indian scientists were actively involved in analyzing cosmic ray tracks recorded in a Lexan stack on the Skylab in 1973 - 74.[62] Other interesting results were the observation of anomalous cosmic ray components in near earth orbit and the first and direct/unambiguous results on the ionisation states of the anomalous cosmic ray components.[63]

ii) Fission track geochronology: Indian scientists also contributed substantially in the development of this concept and have provided ample data on fission track ages of co-existing minerals, estimation of cooling and uplift rates and determination of cooling uplift paths for various orogenic belts in India.

iii) Country-wide survey of radon and thoron levels in Indian dwellings: Preliminary survey regarding the concentration of radon and thoron were estimated in different parts all over India. BARC carried out a preliminary survey to monitor the air-borne alpha activity levels due to radon, thoron and their daughter products in the residential and industrial areas.

iv) Studies on fullerenes: Synthesis of one Buckminsterfullerene (C_{60}) and other onion-shell fullerene structures (C_{120+}) in graphite on irradiation with energetic heavy ions has been major contribution in India.[64] Studies pertaining to diffusion and the release of energy upon destruction of Fullerenes were also carried out.

v) Nuclear track registration from solution: "The wet method"

of nuclear track detection was developed in BARC. The method involves particle track detection on a detector immersed in solution. The method has opened up new areas of studies involving SSNTD's and has found many applications in nuclear science and technology.[65]

vi) Absolute fission yield measurements in the neutron-induced fission of actinides: The measurement of absolute fission yields in the thermal and fast neutron induced fission of a large number of actinide has been performed by simple indigenous method known as "track-etch-cum gamma spectrometry". The method finds applications in evolving a proper reactor design, fuel handling, waste management, etc. Furthermore it can be utilized for a proper understanding of the fission process.

1.3 Nuclear track detectors: A literature review: The era of solid state nuclear track detection began in 1960's when charged particle tracks were revealed by chemical etching at AERE, Harwell by D. A. Young. A variety of commonly available materials can serve as track detectors after proper calibration. Natural minerals, glasses and plastics are all used as track detectors. There are approximately 4300 research papers/conference articles etc. that have been published by track workers during the period 1964-2009 regarding preparation/use of polymeric materials.

1.3.1 Organic polymeric track detectors: Although the cellulosics and polycarbonates were used as plastic track detectors, the introduction of CR-39™ as nuclear track detector was a milestone in use of such materials as nuclear track detectors. CR-39™ polymer showed excellent behavior both in track recording sensitivity, homogeneity and optical properties. The polymer could detect charged particles of Z/β greater than or equal to 6.[11] The polymer

was extensively used in neutron dosimetry, measurement of Uranium contents in various materials and for search of heavy nuclei in cosmic radiations.

According to one of the reports, numbers of publications in the period 1964-1994 on polymeric track detectors are about 2000 articles.[66] However, out of the large number of publications only about 2-3 % dealt with design/preparation of polymeric detector films. Furthermore, the enhancement in the quality of PADC and CN detectors constituted the most part of these 2-3 % articles. During the later years i.e. from 1995-2009 the number of articles on preparation of polymeric track detectors was further reduced. Table 1.7 gives the structures of the most important monomers of different polymeric track detectors used till date.

Sr. No.	Chemical name [CAS registry number]	Monomer/ Polymer structure [Trade name]
1	Cellulose acetate butyrate [9004-36-8] R^1= H, R^2= $-COC_3H_7$ and R^3= $-COCH_3$	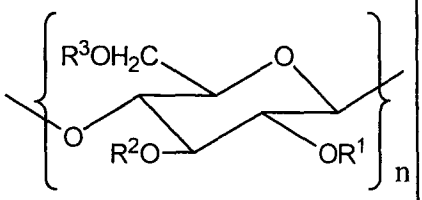
2	Cellulose acetate [9004-35-7] R^1= H, R^2= H and R^3= $-COCH_3$	T-Cellit
3	Cellulose diacetate [9035-69-2] R^1= H, R^2=R^3= $-COCH_3$	
4	Cellulose triacetate [9012-09-3] R^1= R^2= R^3= $-COCH_3$[Poroplastic]	Triafol-TN
5	Cellulose nitrate [9004-70-0] R^1= R^2= R^3= $-NO_2$	LR-115, CN-85, Daicel
6	Cellophane (Rayon) R^1= R^2= R^3= H	

7	Poly(ethylene) [9002-88-4]	$\{-CH_2-\}_n$
8	Bisphenol-A polycarbonate [78690-93-4]	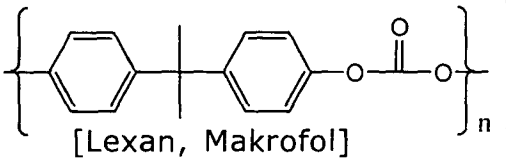 [Lexan, Makrofol]
9	Poly(imide)[13]	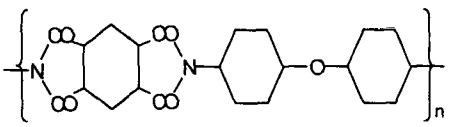
10	Poly(oxymethylene) [9002-81-7]	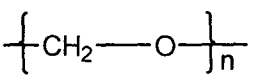 [Formaldehyde polymer]
11.	Poly(propelene)[13] [9003-07-O]	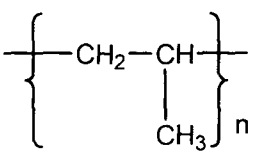
12.	Allyl diglycol carbonate[10] [142-22-3]	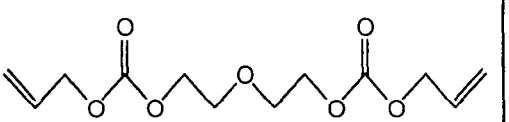 [CR-39™] [25656-90-0]
13	Poly(tetrafluro-ethylene)[9002-84-0][67]	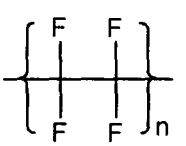 [Teflon]
14	Poly(vinyl acetate) [9003-20-7]	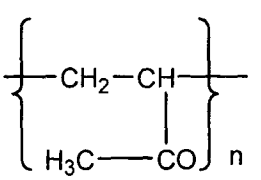
15	N-isopropyl acrylamide[68] [2210-25-5] copolymers with ADC	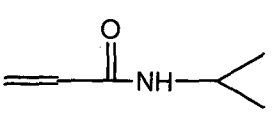 TNF-1

16.	Diallyl terphthalate[69] [959-26-2]	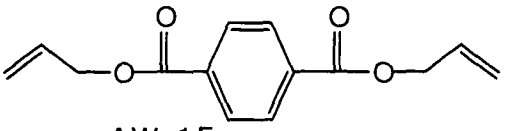 AW-15
17.	Diallyl isophthalate[70] [1087-21-4]	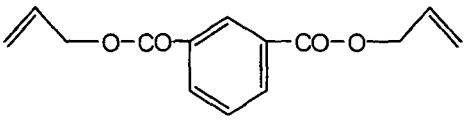 [Diallyl isophthalate homopolymer][25035-78-3]
18.	Bisphenol-A-bis(allyl carbonate)[70] [84000-75-9]	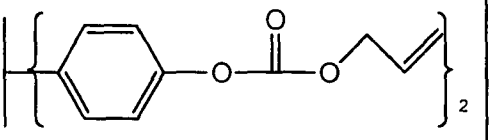 CR-73
19.	Triethylene glycol bis (methacrylate)[70] [109-16-0]	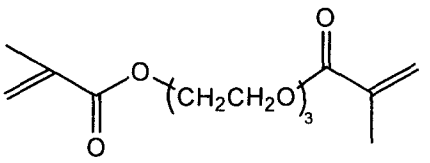
20.	Diallyl phthalate[71] [131-17-9]	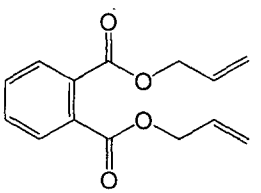 Poly(diallylphthalate) [25053-15-O]
21.	Poly(vinyl chloride)[6] [9002-86-2]	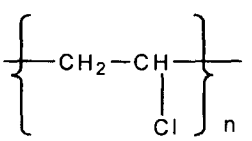 [Myraform]
22	Tetrafluoroethylene-ethylene copolymer[72]	$\{-CF_2CF_2-\}_n-\{CH_2CH_2-\}_m-$ PTFE-E
23.	Poly(methyl methacrylate)[73] [9011-14-7]	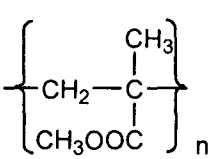

24.	Tris-(2,4-dioxa-3-oxohept-6-en-1-yl) nitromethane[73] [119845-30-6]	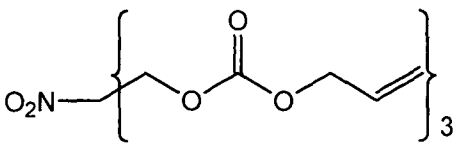 homopolymer and copolymers with ADC
25.	Allyl bis-(2-nitroxy-ethyl) carbamate[73] [1189124-70-6]	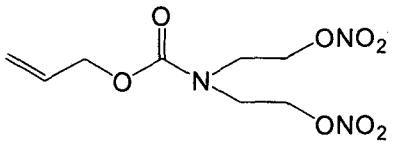 Copolymers with ADC
26.	Allyl diglycol sulfonate[74] [121752-04-3]	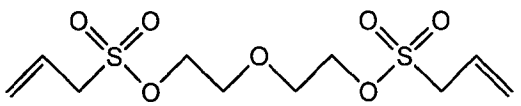 copolymers with ADC
27.	Alkanediol bis(allyl carbonate)[75]	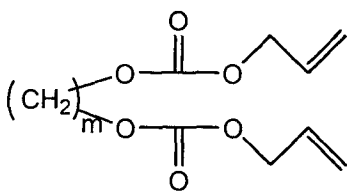
	a. Propanediol m=3	[70122-93-9]
	b. Butanediol m=4	[35236-67-0]
	c. Pentanediol m=5	[101069-79-8]
28.	Hexachlobutadiene[76] copolymer with ADC	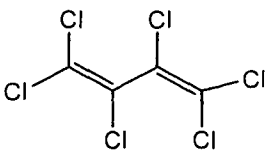
29.	Sulfur dioxide-ADC[77] copolymer	SO_2-*co*-ADC
30.	Poly(vinylidene fluoride)[79] [24937-79-9]	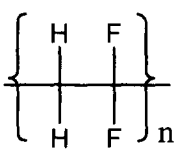

31	N-Allyloxycarbonyloxy-diethanolaminebis-(allyl carbonate)[78] [869885-52-9]	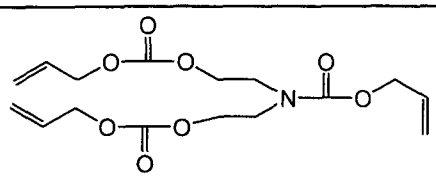 homopolymer and copolymer with ADC
32	2,2-bis(4-acryloyloxypoly-ethoxyphenyl)propane	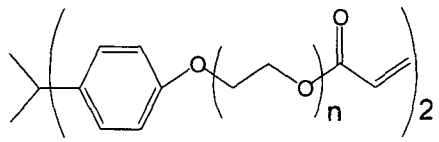
33	Methyl methacrylate-vinyl chloride copolymer	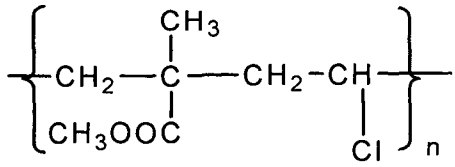 Viniproz
34	Poly(ethylene terephthalate) [25038-59-9]	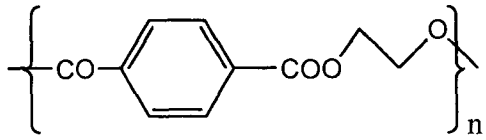 Lavasan, Mylar, Melinex-O

Table 1.7: Monomers and polymers of some previously examined plastic track detectors.

In most of the cases commercially available plastic sheets are tested as SSNTDs. Only CR-39™ out of this was investigated in detail. Baring few other materials, there have not been any attempts worldwide to design and prepare new polymers as track detectors. The main focus of research has always been in the improvement of the process for CR-39™ track detector. As a reason, therefore, no other polymeric materials than PADC, are commercially available. Some of these reports on investigation of CR-39™ suggests following important parameters which may be useful in designing track detectors.

1.3.2 Effect of radiation sensitive groups: The sensitivity of particular detector material is largely dependent on the nature of radiation sensitive group.

Type of bond	Energy KJ/mol
S=O	522
C=S	573
C=C	602
N=O	607
C=N	615
C=O	799
N-O	201
S-S	226
C-S	272
C-N	305
C-C	346
C-O	358
S-O	364
P-O	377

Table 1.8: Bond energies of different chemical bonds.

Table 1.8 enlists bond energies of different chemical bonds[80,81] and various common double bonds in the ascending order of bond energies i.e. bond strength. This clearly indicates that the ease of bond fission should be in the order,

P=O > S=O > N=O > C=O and N-O > C-P > C-C > C-O

Thus, monomers with S=O/N=O should result in polymers having higher radiation sensitivity than with C=O. Those having P=O could be even more sensitive. Even the etching process will occur rapidly. When this exposed detector is inserted in etchant, the etching process is predominantly higher at the latent track. The undamaged part of the polymer surface is etched at a very low bulk etch rate. Therefore, if weak functional groups which are

easily broken by passage of charged particle can be introduced into thermosetting resins the polymer will become more sensitive. The alpha sensitivity of SSNTD's can be represented by the ratio of track etch rate to the bulk etch rate. When a charged particle enters the detector, it brings about lot of chemical changes in the vicinity of its path inside the structure of the polymer. The track etch rate at this site will increase marginally compared to slight increase in the bulk etch rate of the track detector material used. This can be seen from following observations of different track detectors.

i) The effect of the radiation sensitive groups can be best exemplified by DEAS monomer.[74] The DEAS monomer contains a sulfonate linkage in place of carbonate linkage bridging the allyl group and diethylene glycol. However, the alpha sensitivity of the DEAS:ADC 20:80 w/w copolymer is much more than that of CR-39™. This is due to the weak linkages present in the sulfonate groups which can be easily affected by the charged particle.

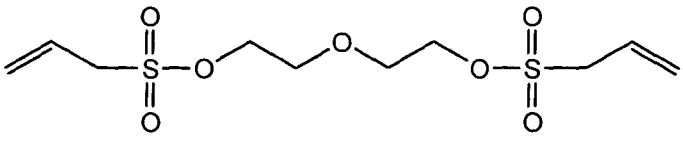

Diethylene glycol bis(allyl sulphonate)

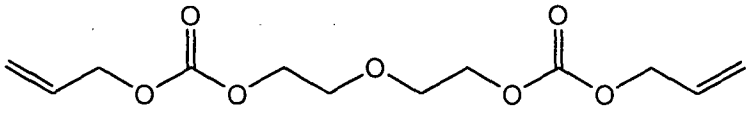

Diethyleneglycol bis(allyl carbonate)

ii) The Diallyl adepate contains four methylene's between two ester groups.[75] The Butanediol bis(allyl carbonate) also contains four methylene's between two carbonate linkages. However, the alpha sensitivity of the later is 10 times the alpha sensitivity of the former. Thus, the carbonate moiety provides higher sensitivity to the charged particles than the ester groups as the former is the

weaker linkage.

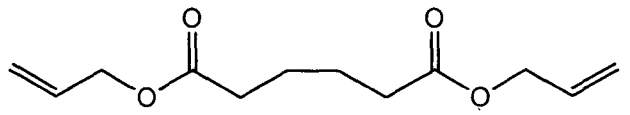

Diallyl adepate)

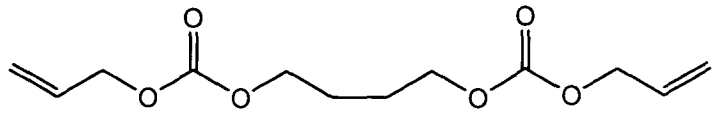

Butanediol bis(allyl carbonate)

iii) Cellulose esters and cellulose nitrate: The cellulose nitrate also is a classic example to show the effect of the radiation sensitive group on the sensitivity of the detector. The cellulose esters are sensitive to alpha particles of energy 3 - 4 MeV. However, the cellulose nitrate can detect protons with energy of the order of 0.55 MeV. This may be attributed to the more facile nature of nitrate ester group.

iv) Sulfur dioxide ADC copolymer:[77] The SO_2 ADC copolymer detects the alpha tracks in only one minute and the sensitivity of the material is also comparable to the CR-39™ films.

v) Chain bridging the radiation sensitive groups:[75] The CR-39™ polymer contains an important ethylene diglycol linkage between the allyl carbonate moieties which is responsible for its sensitivity to ionizing radiations. In order to understand the effect of ethylene diglycol linkage, pentanediol bis(allyl carbonate) (PeAC) monomer was prepared.

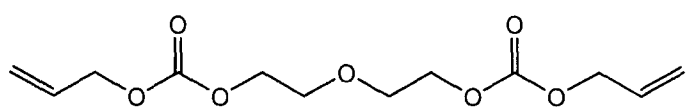

Diethylene glycol bis(allyl carbonate)

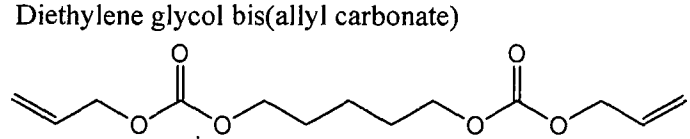

Pentanediol bis(allyl carbonate)

If, one observes the above two structures the only differ-

ence in the two molecules are the linkages joining the two carbonate moieties. However, the PADC polymer was four times more sensitive than the PPeAC. This means that the ether groups increases the sensitivity of the CR-39™ polymer significantly.

1.3.3 Additives in the polymeric detectors: It has been observed that the surface of a detector like CR-39™ becomes opaque after prolonged etching in alkali solution. This effect can be minimized by using a plasticizer which could stabilize the surface. A plasticizer normally increases the free volume of a polymer making the polymer chains more mobile.[82] The additives used must be soluble in the monomer. The molecular weight should be sufficiently low to increase the free volume without being low enough to diffuse out of the plastic.

Many commercially available additives have been tested which include diallyl phthalate, methyl methacrylate, diisobutyl phthalate, dioctyl sebasate, di(2-ethylhexyl) phthalate and dioctyl phthalate(DOP). However, good post etch surface properties of detector are obtained at the cost of the sensitivity of the polymer.[83] The edition of such additives changes the resolution and sensitivity of the material. With DOP in CR-39™ the resolution increases and the sensitivity decreases. This is because, the benzene rings in the DOP absorb the electrons/δ-rays without disturbing the polymeric structure.

1.3.4 Shrinkage during polymerization:[73] Shrinkage of the hardening polymer during polymerization is another important factor in preparing the films of high quality. In case of CR-39™ detector the shrinkage may reach upto 14 % and density increases from 1.15 g/cm^3 of monomer to 1.31 g/cm^3 of the homopolymer. To avoid thickness non uniformities and a possible cracking of the

detector film due to this effect, clamping of the mould glasses with uniform pressure is desirable.

1.4 Allyl monomers and their polymerization: The word allyl originated from the product of allium or onion family compound allyl sulfide. Ethylinic compounds with a general formula CH_2=CH-CH_2-X are called allyl compounds. The compounds show retarded rate of polymerization with low molecular weight oligomers being formed as compared to their vinylic counterparts.

1.4.1 Radical polymerization and the allylic monomers: In a free radical polymerization mechanism a free radical is the active species involved in the process. Free radical is an atomic or a molecular species with an unpaired electron. Under the appropriate conditions, a free radical is capable of reacting with an olefinic monomer to generate a chain carrier which propagates to generate a macromolecule. Thus, a rapid growth in the polymer unit takes place after chain initiation. Chain initiation, propagation and termination are the three steps involved in the polymerization process. The free radical polymerization is carried out in the presence of initiators which decompose on heating to afford free radicals.

i) Polymerization initiators:[84] The polymerization is initiated by various processes which generate free radicals. The free radicals can be generated by using heat, radiations or chemical reactions. The generated free radicals must be stable and should have sufficient life time to react with a monomer and create active sites. The free radicals can be produced by following methods

1) Thermal decomposition: The initiators are decomposed by applying heat. As the initiators are thermally unstable cleave the bond in homolytic fashion to give two free radicals *e.g.* organic

peroxides, peroxydicarbonates etc.

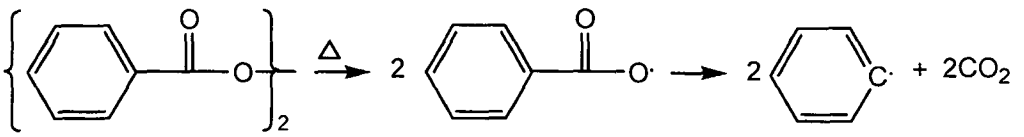

1.7

2) Photolysis: The method is applicable to metal iodides, metal alkyls and azo compounds e.g. decomposition of α,α′-azoisobis-butyronitrile.

3) Redox reactions: Involves use of redox reactions for generation of free radicals such as in the case of ferrous ion and the hydrogen peroxide.

ii) Initiator efficiency: The free radical initiator decomposes completely upon heating or the decomposition conditions normally employed for polymerization. However, the chain initiation may be less than 100 % efficient. The factors responsible for such things are

1) Primary recombination: Once the initiator is decomposed the diffusion of the radical fragment is restricted or completely retarded due to cage effects. In such cases the decomposed free radical may combine with the new free radicals.

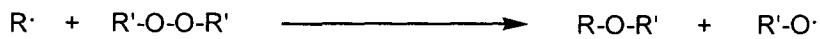

1.8

This produces only one free radical instead of potential three radicals.

2) Degradative chain transfer: Allylic monomers (mono allylic) can be considered as a class of vinyl type monomers (CH_2=CH-) which do not have any groups that withdraw or delocalize the p bond electrons. The double bond in such compounds, hence, is not active for polymerization by free radical methods. Thus, the allylic compounds have lower reactivity than vinylic compounds like styrene or acrylonitrile. The reluctant polymerization of mono allyl compounds is clearly due to lack of activating electron displacing

and/or resonance promoting groups attached to ethylene nucleus. Such groups when present prevent activity of hydrogen on third carbon (α – carbon) in degradative chain transfer. Thus, resonance and electron attraction by the group $-COOCH_3$ prevents methyl methacrylate from reacting like allylic compounds and it readily forms PMMA with free radical initiators.

In a monoallylic monomer ($CH_2=CH-CH_2-X$) removal of allylic hydrogen or halogen (X) results in resonance stabilized allyl radical which is inefficient in propagating polymer chain. The degradative chain transfer in mono allylic and mono allidine ($CH_2=CH-CH-X_2$) compounds is shown below.

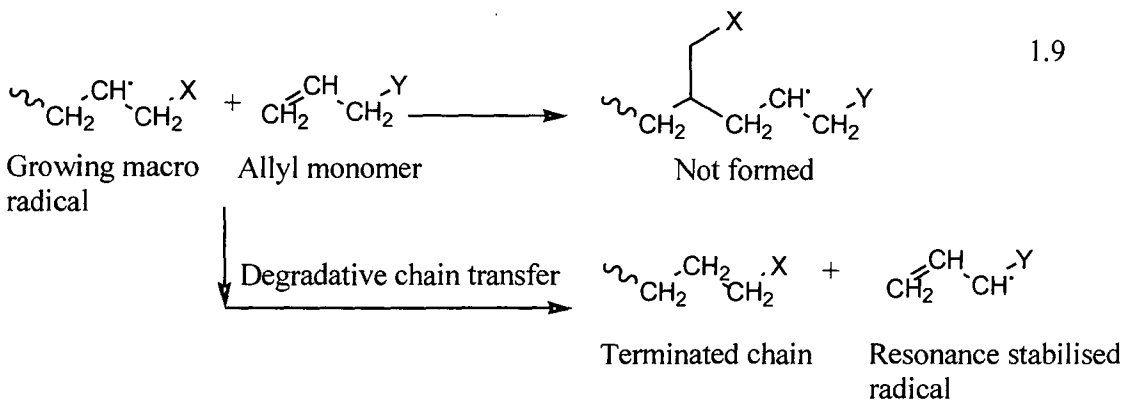

1.9

The free radical in the monomer is now resonance stabilized which combines only with the other stabilized allyl radical. The process is called autoinhibition of growing radical. Other process includes transfer to initiator or transfer to the polymer. This affects the effective molecular weight of the polymer and also the number of crosslinks. The auto inhibition process due to the abstraction of alpha hydrogen in allylic compounds was confirmed as the rate of polymerization and the molecular weight obtained increased by a large factor when deuterium substituted allyl acetate was used. However, allylic compounds having two or more allylic groups could be efficiently polymerized under free radical condi-

tions to give polymers, although degradative chain transfer occurs.

1.4.2 Kinetics of allyl polymerization: The thermoset polymers normally employed for track detection are prepared by cast polymerization process. The monomer can be cast polymerized by constant temperature polymerization wherein the monomer is heated along with the initiator at a constant temperature slightly above the decomposition temperature of the initiator. A constant temperature of 70 °C is used for BP and 45 °C for IPP. During constant temperature cast polymerization the rate of polymerization increases rapidly at the onset and then becomes slower and slower. A casting time of 60 - 72 hrs is required to develop essentially full cure. A further cure of 2 hrs at 115 °C is used to complete last stages of polymerization. This consumes any remaining traces of catalyst which might interfere with dimensional stability of the polymer. A very good quality casting can be obtained at the expense of time. Thus, a process of shorter time period would be desirable.[85] However, with such short time polymerization the depth dependency of etching may be observed.

The track recording properties of a plastic can be influenced remarkably by the type of conditions used for polymerization. At a fixed catalyst concentration, the rate of polymerization increases exponentially with temperature. Unless the temperature is kept low early in the heating profile, center of the mold will warm more due to the heat of polymerization, prompting more polymerization at the centre of the sheet.[86] Monomer is converted in gel form only at about twenty percent initiator conversion and 4 % of shrinkage has occurred. The gel is very fragile and if polymerization is carried more rapidly the remaining 10 % of shrinkage will occur differ-

entially from the center of the sheet to the two surfaces, producing sheered strata.[87] This strata have lower density of bonds and hence have a higher etch rate.

As polymerization reaction is exothermic and hence samples can lead to temperature excursions due to relatively low thermal conductivity of the sample.[88] This large thermal gradients, thermal excursions and even local or extended thermal runaways can lead to non uniform polymerization in the bulk of hardening polymer. Usually, the rapidly curing mass than fractures from the high forces developed and, because of excessive temperatures the polymerization catalyst is not effectively used.[89]

These temperature gradients during polymerization appear to contribute greatly to the lack of response in commercial CR-39™ films. In order to minimize costs, commercial manufacturers of CR-39™ sheet may complete the polymerization heating profile as quickly as possible. In order to minimize the depth dependency of the response of track detector and in an attempt to minimize differences between separate batches of plastics, interest focused on the kinetics of polymerization and calculations of expected internal temperature excursions from specific temperature time functions. In constant temperature polymerization treatments, only the beginning of curing process is highly exothermic. This suggests that the higher temperature and more rapid polymerization could be used in the later part of polymerization.[85] A constant rate of polymerization and peroxide decomposition would result in constant rate of exothermic heat evolution. Casting of the monomer must generally be carried out at relatively low temperatures and over extended periods of time.

In order to determine this heating profiles, Dial et. al. heated

a series of test tubes at a constant temperature and analyzed for its unsaturation and initiator concentration by iodometric analysis. The rate of the monomer conversion to that of the catalyst decomposition is of first order. Dial et. al. derived first order kinetic equations with the help of which, special heating profiles can be constructed. The polymerization process with this heating profiles leads to a constant rate of polymerization, giving rise to slow heat evolution and preventing the sudden rise in temperature due to exothermic nature of the process. The equations described by dial and coworkers are[85]

$$K_4 = Z_3 e^{-E_3/RT}(M_0 - K_4 t)\sqrt{C_0 - \frac{K_4 t}{Z_1 e^{-E_3/RT}}} \qquad 1.10$$

$$E_1 = \frac{T_1 T_2}{T_1 - T_2} Log_e \frac{K_1}{K'_1} \qquad 1.11$$

$$K_1 = Z_1 e^{-E_1/RT} \qquad 1.12$$

$$K_3 = -\frac{1}{t}\left[\frac{1}{\sqrt{C_0 - \frac{M_0}{K_1}}} \log_e \frac{\sqrt{C_0 - \frac{M_0}{K_1} + \frac{M}{K_1}} - \sqrt{C_0 - \frac{M_0}{K_1}}}{\sqrt{C_0 - \frac{M_0}{K_1} + \frac{M}{K_1}} + \sqrt{C_0 - \frac{M_0}{K_1}}} - \frac{1}{\sqrt{C_0 - \frac{M_0}{K_1}}} \log_e \frac{\sqrt{C_0} - \sqrt{C_0 - \frac{M_0}{K_1}}}{\sqrt{C_0} + \sqrt{C_0 - \frac{M_0}{K_1}}}\right] \qquad 1.13$$

$$E_3 = \frac{T_1 T_2}{T_1 - T_2} Log_e \frac{K_3}{K'_3} \qquad 1.14$$

$$K_3 = Z_3 e^{-E_3/RT} \qquad 1.15$$

Where Z_1, Z_3 are the Arrehenius constants; E_1 and E_3 are the corresponding activation energies; C_0 and M_0 are the initial con-

centrations of initiator and monomer, respectively; K_4 is the rate of polymerization. Dial *et.al.* has successfully calculated these constants for ADC polymerization using IPP catalyst and assuming that the constants would hold good, a number of authors have used these values for constructing the heating profiles. These equations have also been used to calculate heating profiles for hexafunctional monomer[90,91] and it may be interesting to study the rate of polymerization for other monomers and its effect on the sensitivity.

1.4.3 Effect of nature and concentration of initiator on allylic polymers:[92] The polymerization of allylic monomers can be performed by using different initiators. Decomposition temperature of different initiators varies and can affect the amount of crosslinks in the polymer matrix. The glass transition temperature of a polymer is dependent on the density of cross links. When the glass transition temperature and the curing temperature are same the rate of polymerization slows down due to restricted mobility of the participating groups. The peroxydicarbonate initiators are active in the region of 40-80 °C and hence increasing the curing temperature does not complete the polymerization of remaining ~5 % of unsaturation as high temperature completely destroys the initiator. This necessitates the use of initiators with higher decomposition temperature.

Table 1.9 gives the glass transition temperatures (T_g) of different polymers cured under different heating profiles having identical rate of initiator decomposition and concentration. Thus, the density of crossklinks can be increased by using the initiators having higher decomposition temperature. This is also evident from the complete polymerization of the samples cured with TBP.

Initiator	Curing range in °C	T_g in °C
Diisopropylperoxydicarbonate (IPP)	45-85	77
Benzoyl peroxide (BP)	70-115	90
Cyclohexylperoxydicarbonate (CHPC)	60-95	---
t-butyl peroxy benzoate (TBPB)	101-148	105
t-butyl peroxide (TBP)	123-171	109

Table 1.9: Glass transition for CR-39™ cured using different initiators.[92]

Thus, the density of crossklinks can be increased by using the initiators having higher decomposition temperature. This is also evident from the complete polymerization of the samples cured with TBP. The extent of crosslinks and thus the glass transition temperature also varies with the type and amount of initiator as can be seen from Table 1.10. The T_g increases with increase in initiator concentration up to a maximum level and decreases gradually as the initiator concentration is increased further. The bulk etch rate also decreases accordingly to a minimum and then increases as the concentration increases further.

Wt.% of Initiator		T_g in °C		% conversion	
IPP	TBP	IPP	TBP	IPP	TBP
1.5	0.23	22	104	76.3	95.8
3	0.45	77	109	92.8	97.9
4.5	0.9	91	112	96.2	100
6	1.8	90	109	97.1	100
8	2.7	83	106	98.2	100
10	3.6	75	101	98.3	100

Table 1.10: Variation of glass transition temperature with the amount of initiator.[92]

The increase in density of crosslink's also increases the sensitivity of the detector material. At higher initiator concentration the unsaturation left is zero, however the Tg decreases as the concentration increases and also the alpha sensitivity. This is because of the formation of lower molecular weight polymer chains. Thus the optimum initiator concentration is important as the detector under study attains maximum alpha sensitivity.

1.4.4 Glass transition temperature and the extent of polymer crosslinks:[93] The glass transition temperature (T_g) is the temperature above which the polymer is rubber like and soft. Below the glass transition temperature the polymer is glassy. This is due to the frozen nature of the polymer chains. Once the polymer has attained the T_g the chain segments move more cordially and the chains are relatively in the motion. The T_g occurrence largely depends on following factors.

i) Chain flexibility: The flexibility of the chain is the ability of a chain to rotate about the constituent chain atoms. Hence the long chain monomers have flexible chains and a less T_g. The chain flexibility is increased by the presence of groups -O-, -COO-, -O-CO-O- and the length of the bridging $-CH_2-$ groups.

ii) Polymer structure: The polymers containing more bulky groups and aromatic rings have higher T_g.

iii) Effect of crosslinks on T_g:[92] A highly crosslinked polymer is dense in its matrix which increases the T_g due to the decrease in the molecular motion of the densely packed molecular polymeric chains. Insertion of polar groups like $-SO_2-$, $-O-SO_2-$, -CON=, raises the T_g as they assist in stabilizing the extended forms in the crystallites. The increased crosslinks occupy the free volume in a sample which arises as a result of insufficient packing in the amorphous

region of the polymer.

1.4.5 Polymerization inhibition and acceleration:[94] Allyl polymerizations are inhibited in the presence of copper, lead, nitro compounds and atmospheric oxygen. Oxygen can act as both initiator and inhibitor. The polymerization inhibition in presence of oxygen takes place when peroxide formation is preferred to polymerization. However, these peroxides can sometimes decompose at higher temperatures and catalyze the polymerization process. Allyl alcohol has a little tendency to polymerize and slows the polymerization of other monomers. The presence of amines accelerates the decomposition of peroxides at an explosive rate. Aromatic sulfonic acids were found to increase the rate of polymerization of allylic compounds. Alkalis and amine hydroxides completely inhibits the polymerization of allyl ethers.

1.4.6 Allylic sulfur containing monomers: The sulfur compounds have been used in polymer industry from mid 19th century. The polymers containing sulfurous functionality find extensive use. The sulfonic group containing polymers are used as functional polymers as they can be modified into differential groups like sulfonic acids and their sodium salts, sulfonamides, sulfonyl chlorides, sulfonates, etc. Such polymers find extensive applications in industrial and water treatment applications. These polymers can also be used as polymer supports, ion exchangers etc. Some of the most common monomers are enlisted below.

i) Ethylene sulfonic acid: The monomer can be prepared by thermal elimination reaction.[95]

$$ClSO_2\text{-}CH_2\text{-}CH_2\text{-}SO_2Cl \longrightarrow CH_2{=}CH\text{-}SO_3H \qquad 1.16$$

The monomer can be prepared in higher yields by elimination of sodium hydroxyethyl sulfonate by phosphoric acid.[96] The sodium salt of the acid monomer is used as a comonomer in emulsion polymerization. It acts as emulsifying agent and stabilizes the polymeric emulsion.

ii) p-styrenesulfonic acid: The monomer can be polymerized to obtain polystyrene sulfonic acid. The other method to prepare polystyrene sulfonic acid is by sulfonation of polystyrene with conc. H_2SO_4.[97]

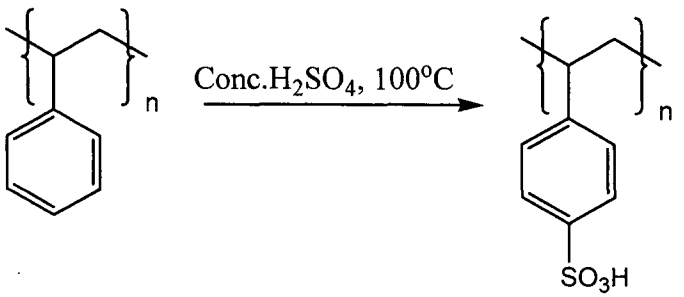

1.17

iii) N-allyl-vinyl sulfonamide: The monomer is used to prepare Poly(cyclic sulfonamide).[98]

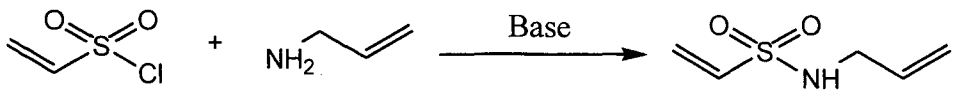

1.18

Polymerization in benzene with azoisobisbutyronitrile at 45 °C and 25 °C gave soluble polymers. The radical polymerization was considerably faster than various N-alkyl vinyl sulfonamides.

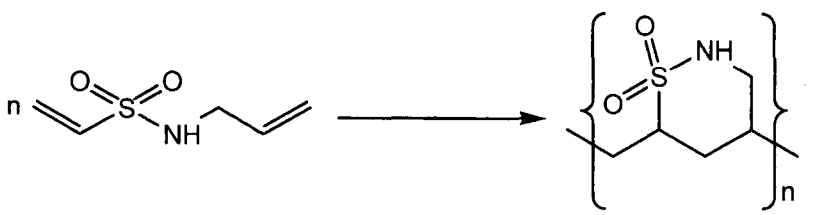

1.19

iv) Allyl isothiocyanates: Reactions of inorganic thiocyanates with allyl halides under mild conditions give allyl thiocyanates but it readily rearranges to give allyl isothiocyanates.[99,100]

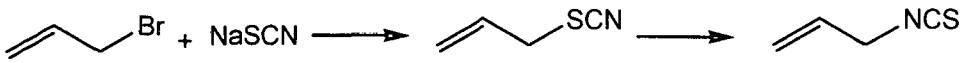

1.20

It is extremely pungent and in high concentrations it is used as a war gas. In high concentration it is acute and chronic irritant. It causes asthma, watery eyes and sneezing.

v) Allyl thiourea: can be prepared by reaction of allyl isothiocyanates with ammonia.

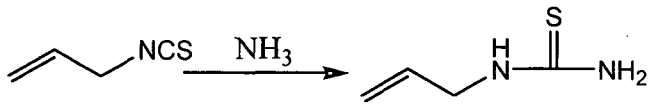

1.21

It is used in developing photographic film. N,N'-diallylthiourea was prepared by reaction of allyl isothiocyanates with allyl amine.[101,102]

vi) Diallyl sulfide: can be prepared by reaction of allyl halides with potassium or sodium sulfide.[103] Diallyl sulfide can be obtained from garlic oil by steam distillation.

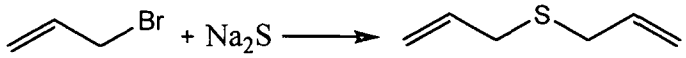

1.22

A small amount of diallyl sulfide is added during suspension polymerization of vinyl chloride. Mixtures diallyl sulfide reacts with SO_2 to give equimolar sulfone composition.[104]

vii) Allyl sulfoxides and sulfones: Diallyl sulfide is oxidized by benzoyl peroxide to give diallyl sulfoxide and diallyl sulfone.[105] The sulfoxide was also obtained by oxidation with hydrogen per-

oxide at low temperatures. Diallyl sulfoxide is hygroscopic liquid melting near room temperature. On heating with aqueous alkali ether sulfone is formed by way of normal addition of water.[106]

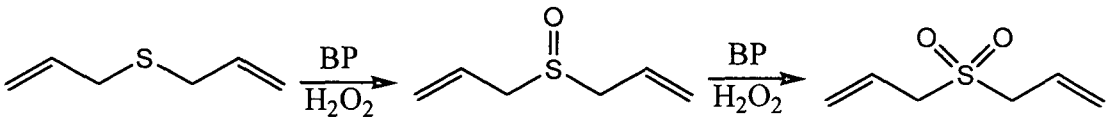

1.23

The hydrogen atoms in the cyclic compound trimethylene sulfone are quite acidic and can react with allyl chloride to form diallyl trisulfone. Solutions of the monomer in dimethyl formamide and diethylene glycol have given polymer on heating. Pentallyl trimethylene sulfone was copolymerized with unsaturated polyesters and styrene.

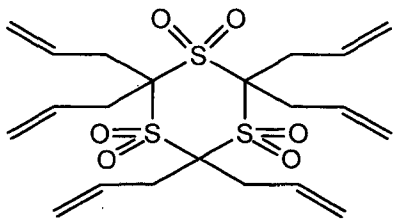

Pentallyl trimethylene sulfone was copolymerized with unsaturated polyesters and styrene. Hexallyl trimethylene sulfone has been suggested as crosslinking agent for acrylic acid in preparation of high viscosity mucilages.[107]

viii) Sodium allyl sulfonate: The monomer can be prepared by reacting aq. sodium sulfite with allyl halide. Copolymerization of sodium allyl sulfonate with methyl acrylate was used to prepare high polymers bearing sulfonate acid groups.[108]

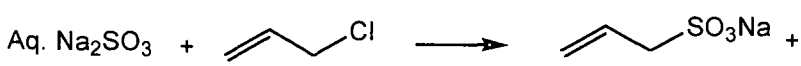

1.24

1.5 Statement of objectives: It can be observed that the SSNTD technique is in use for last more than 50 years. The technique is becoming increasingly popular in various branches of science and technology which require qualitative and quantitative measurements of radiations. Although there are three distinct classes of SSNTD materials i.e. crystals, glass and plastics, the plastics continue to dominate the scene. While thousands of polymeric materials are known, it is intriguing to note that about approximately 50 polymeric materials have been tested for SSNTD applications. Nitrocellulosics, PADC(CR-39™) is the most commonly used commercial SSNTD material.

It is also important to note that India still imports materials like PADC (CR-39™) or nitrocellulose (LR-115) from foreign agencies for various SSNTD applications. Almost all of the research groups working in the field of SSNTD in India, focus their attention on the use of such commercial detectors for various applications. In the present work, therefore, emphasis will be given on design and development of new indigenous materials keeping in mind the efforts taken earlier (1992 onwards) by our research group.[66,73] Since we have earlier studied detectors based on nitrocellulose and ADC in addition to use of ADC, efforts will be directed towards development of more efficient allyl carbonate monomers and allyl sulfur containing monomers. Thus, the aims and objectives of this research are briefly described as follows,

1] We have previously proposed a protocol for development and testing of track detectors from allylic monomers. While the protocol was based on experiments on allylic carbonate monomers, its effectiveness while dealing with allylic sulfur monomers will be verified.

2] From the introductory remarks it is clear that radiation sensitivity of polymer depends on vulnerability of various functional groups. Since S=O containing functional groups are known to be more labile compared to C=O containing functional groups, we wish to design various monomers containing sulfur and study them. The effects of combining S=O and C=O could also investigated.

3] The available literature emphasizes the importance of the nature of chain, bridging the functional groups like C=O or S=O in the monomer. It was noted that the diethylene glycol linkage -O-CH_2-CH_2-O-CH_2-CH_2-O- is most effective compared to other shorter or longer similar chains. In the present studies we want to investigate this fact further.

4] In some previous research work,[73] branched allylic monomers were studied and found to result in polymers with better radiation sensitivity. We wish to confirm this fact further by synthesizing monomers which have more branching and

a) Which do not have bridging chain like -O-CH_2-CH_2-O-CH_2-CH_2-O- as mentioned above.

b) Which have S=O containing group/groups instead of C=O. Since branched monomers with higher allylic functionality are expected to give polymers with higher density of crosslinks. Effect of the same on radiation sensitivity could also be understood.

5] It was previously established that the Dial's kinetic model for allylic polymerization could be extended for polymerization with higher functionality. In the present studies therefore we planned to continue applying the Dial's model and study kinetics of polymerization of all newly synthesized allylic monomers.

6] Literature also points out that copolymerization of ADC has favorable effects on radiation sensitivity. All newly synthesized monomers, therefore, will be copolymerized with ADC mono-

mers.

7] The polymeric detectors so designed will be evaluated in line with the testing protocol mentioned above and radiation sensitivity of PADC and newly synthesized polymers will be compared. This work will thus involve study of:

1. Bulk etch rate determination.
2. Sensitivity of the film to a particle.
3. Optimization of etching condition.
4. Variation in track density and etching time.
5. Comparison of track detection and imported film.
6. Alpha to fission fragment branching ratio.

Chapter II: Materials, Methods and Charecterizations

2.1 Materials: The materials used to carry out the current study were obtained as follows

2.1.1 Chemicals: The synthesis of the monomers and initiators were performed using the chemicals obtained from M/s e-Merck, India, M/s Sigma-Aldrich chemicals, USA, M/s Loba chemie, India, M/s Qualigens Fine Chemicals, India and M/s Molychem, India. The chemicals were purified whenever required and dried using the appropriate procedures given in the literature.[109]

2.1.2 Monomers: The monomers used in the study were synthesized in special laboratory, with controlled dust environment. The polymers were also prepared in similar environment. The monomers were purified using activated charcoal treatment followed by vacuum distillation wherever possible. Some of the thermally unstable monomers were purified by column chromatography, over 60-120 mesh silica gel, using the mixture of n-hexanes 60 - 80 °C and ethyl acetate.

2.1.3 Initiators: The initiators used for polymerization were IPP and BP. IPP was synthesized in our laboratory, and being highly unstable, was used without further purification. Commercially available moist BP (M/s Loba chemie) was crystallized from chloroform methanol mixture and used after drying.

2.1.4 Plasticizers: Commercially available dioctyl phthalate (M/s Loba chemie) of "GR" grade was used without further purification.

2.2 Mold design: Optical glass plates from (Schott, Germany) were used to assemble the mold. Commercial Teflon sheet of 500 μm thickness was cut in a square shaped gasket having a width of 1.2 - 1.3 cm as shown in figure below and a small opening to inject monomer was made. The gasket was sandwiched between the glass plates previously greased on the sides.

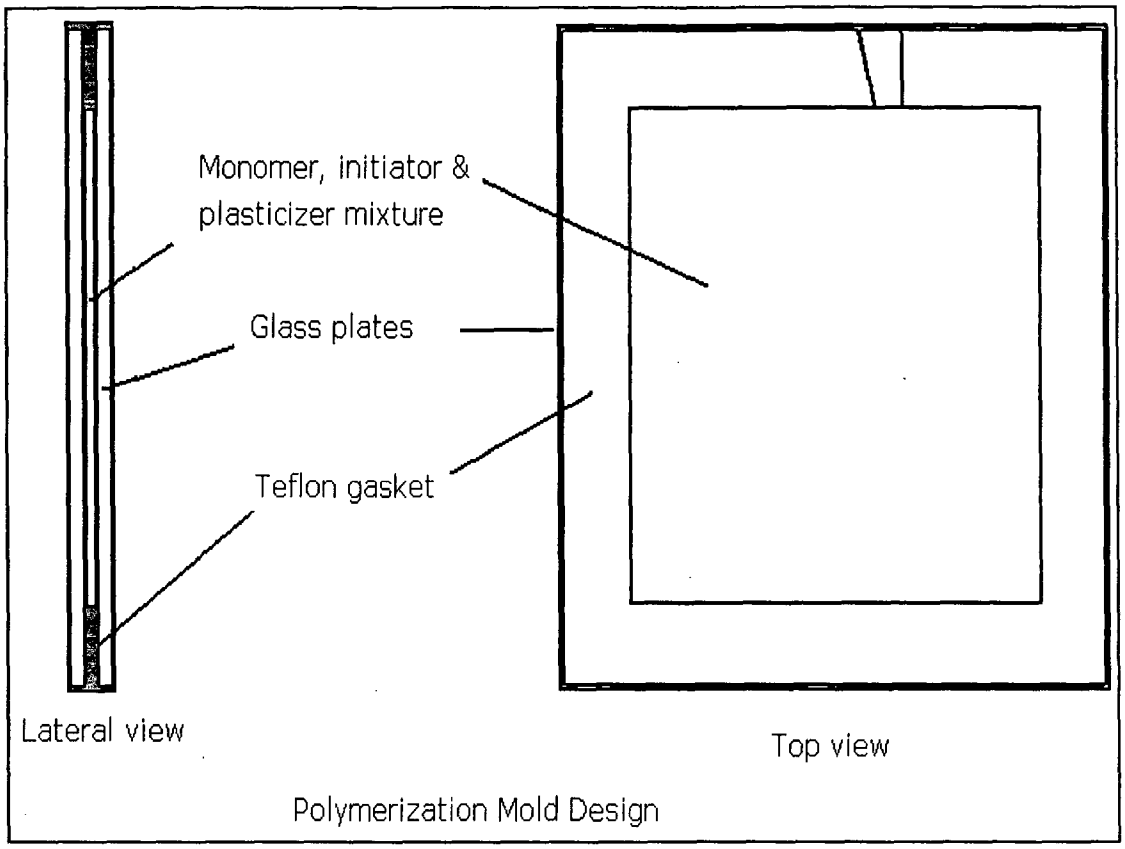

Figure 2.1: Polymerization mold design.

2.2.1 Preparation of films by cast polymerization:[73,91] Purified monomer is first filtered through a micro filter of pore 500 µm and then through 200 µm pore filter to remove any suspended particles. The monomer is held under a high vacuum of 0.2 mbar for 15 minutes and then dry nitrogen is flushed for 15 minutes to remove dissolved oxygen. The process is repeated twice to remove the dissolved oxygen from the monomer. Initiator and the plasticizer are added to the flask and the contents are homogenized by stirring. The polymerization mixture is taken into a syringe and carefully injected into the mold, through the opening in the teflon gasket. Care was taken to avoid the formation of air bubbles which hinders the process of polymerization. After completely filing the mold, the opening is sealed using a teflon plug and the molds were

sandwiched between flat aluminium plates as shown in the figure 2.2.

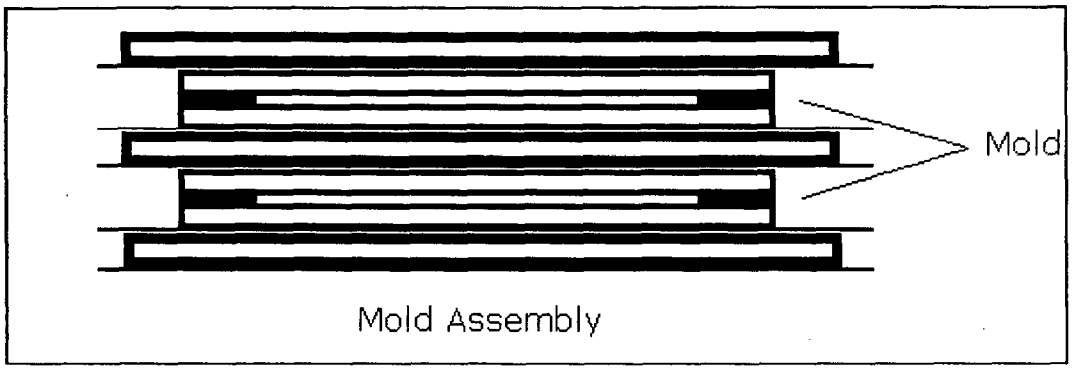

Figure 2.2: Mold assembly.

The above molds are placed in a mold pressurizing assembly. It consists of a stainless steel base and a screw-type piston which can be tightened to apply the pressure on the molds. The molds prepared are pressurized during polymerization from time to time using the mold polymerization assembly (Figure 2.3).

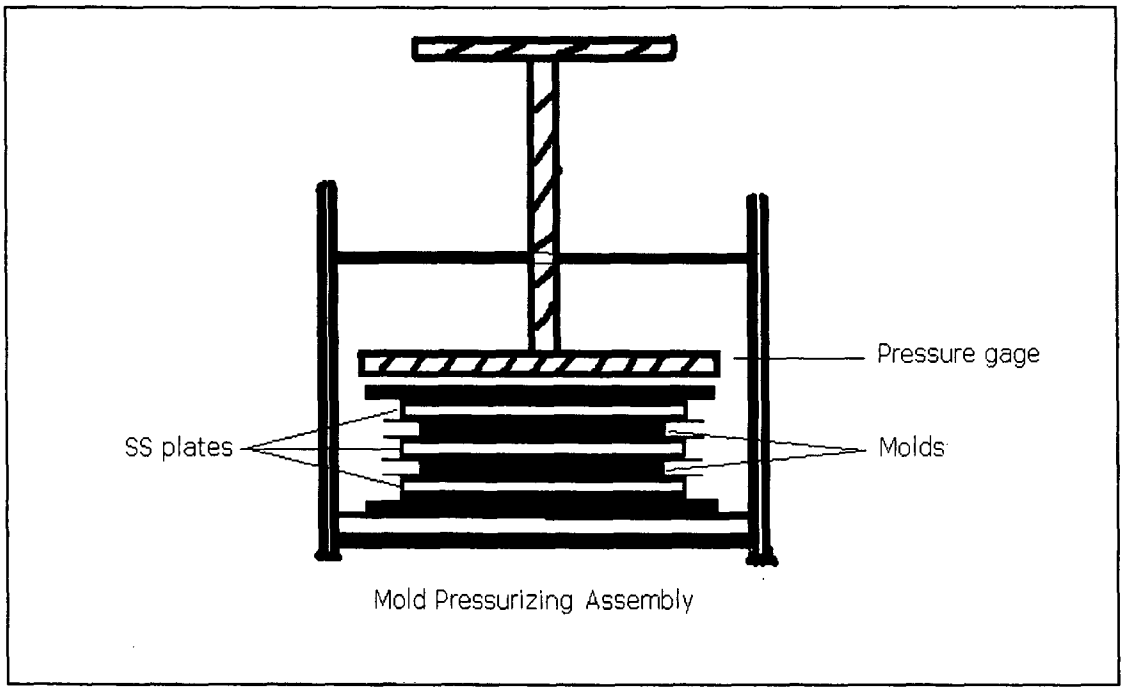

Figure 2.3: Mold pressurizing assembly.

The whole assembly is placed into the polymerization bath and heated according to the predetermined heating profile. The molds are tightened periodically to avoid the cracks from shrinkage dur-

ing polymerization. After completion of polymerization, the molds are allowed to cool for 12 hrs and opened.

2.2.2 Polymerization: The molds were sandwiched between aluminium plates in a pressurizing assembly. The polymerization is carried out using heating profiles having a temperature range of 40 - 95 °C and 70 - 95 °C depending on the type of initiator used. The different polymerization heating profiles used are depicted in figure 2.4.

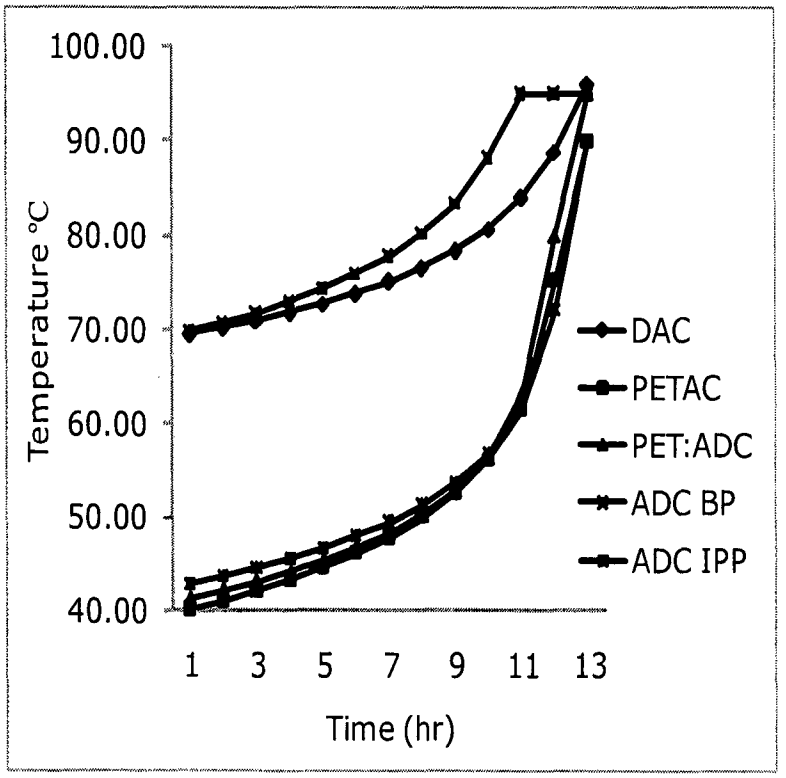

Figure 2.4: Heating profiles for polymerization of different polymers.

The whole assembly is placed between spiral heating coils (figure 2.5) in the polymerization bath. A constant temperature polymerization was employed for some thermally unstable mono-

mers. The bath temperature was controlled by external heating using programmable water bath (Julabo, F 25 HP, Germany) with a temperature accuracy of ± 0.01 °C.

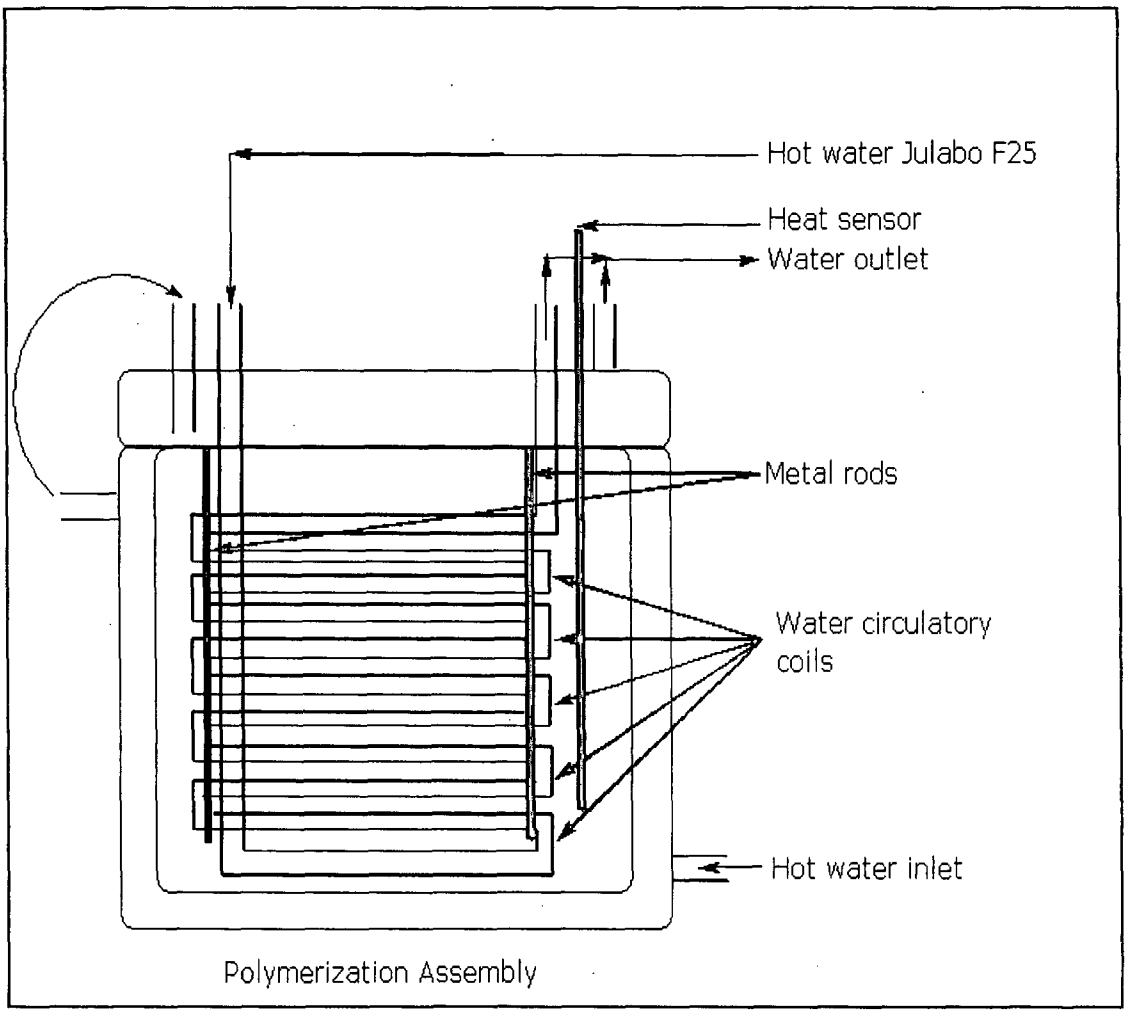

Figure 2.5: Polymerization bath.

2.3 Study of kinetics of polymerization: Kinetic of polymerization was studied by analyzing the amount of monomer and initiator concentration at different time intervals. 20 g of purified monomer is first taken in a round bottom flask and flushed with dry nitrogen for 30 minutes. The initiator is added as per the requirements and the contents are mixed thoroughly. 2 g of this mixture is transferred in 8 - 10 test tubes each and flushed again with dry

nitrogen and sealed with a rubber cork. The test tubes are then heated at a specified constant temperature and after particular time interval a test tube is removed and analyzed for its residual unsaturation and initiator concentration. Similarly, all the test tubes are analyzed at particular intervals.

2.3.1 Determination of residual unsaturation and initiator concentration: The amount of unsaturation left or the amount of monomer converted to the polymer can be estimated by Wij's iodometric estimations. The solutions of Wij's reagent (iodine monochloride in acetic acid), 0.1 N $Na_2S_2O_3$, 10 % KI solution, 0.1 N KIO_3 solution, starch indicator were prepared using the standard methods. The solutions were standardized wherever required.

i) Peroxide estimation:[110] A known quantity of initiator (30 - 50 mg) is dissolved in acetic anhydride and treated with solid KI. The mixture is swirled and kept in dark for 20 minutes. After 20 minutes the mixture is diluted with glacial acetic acid and water. The liberated iodine is titrated against standard 0.01 N $Na_2S_2O_3$ solution using starch indicator. The chemical processes involved in the reaction are

$$R\text{-}CO\text{-}O\text{-}O\text{-}CO\text{-}R + KI \longrightarrow I_2 + R\text{-}CO\text{-}O^-K^+ \qquad 2.1$$

$$Na_2S_2O_3 + I_2 \longrightarrow 2\,NaI + Na_2S_4O_6 \qquad 2.2$$

From the relation,

2000 mL of 1 N $Na_2S_2O_3$ is equivalent to molecular weight of initiator used. The relation can be conveniently used to determine the amount of initiator in the sample. The method can be used to estimate the amount of initiator left during the polymerization kinetic study. 1 g of monomer containing the initiator is dissolved in acetic anhydride and treated with solid KI. Further analysis remains same as given in the procedure above. The amount of initia-

tor can be determined by using the relation

$$X\ g = \frac{\text{Burette reading x Normality of } Na_2S_2O_3 \text{ x Molecular weight}}{2 \times 2000}$$

ii) Determination of unsaturation: The method involves a back titration of liberated iodine with standardized 0.1 N $Na_2S_2O_3$ solution. A known amount of monomer (30 - 50 mg) is dissolved in chloroform and a known amount of ICl in acetic acid is added. The mixture is kept in the dark for 60 minutes and 20 % KI solution is added. The liberated iodine is titrated against standard 0.1 N $Na_2S_2O_3$ solution using starch indicator. The chemical reactions involved in the process are

$$2\ P\text{-}CH_2\text{-}CH{=}CH_2 + ICl \longrightarrow P\text{-}CH_2\text{-}CHCl\text{-}CH_2I + P\text{-}CH_2\text{-}CHI\text{-}CH_2Cl$$

(P = Polymer chain) 2.3

$$ICl + KI \longrightarrow I_2 + KCl \quad 2.4$$

$$Na_2S_2O_3 + I_2 \longrightarrow 2\ NaI + Na_2S_4O_6 \quad 2.5$$

2000 mL of 1 N $Na_2S_2O_3$=1 I_2 = n x C = C, i.e. the molecular weight of the monomer, n is the number of double bonds. This method is used to determine the unsaturation amount during the kinetic studies. The 30 - 50 mg of mixture containing the monomer and initiator is dissolved in chloroform and analyzed as per the procedure. Reading corresponding to the initiator is subtracted from the main reading.

2.4 Instrumentation:

2.4.1 Optical microscope: The particle tracks were counted after chemical etching using a trinocular optical microscope. The microscope (Axiostar, Carl Zeiss, Germany) had optical magnifications of 5 x, 10 x, 40 x and 100 x.

2.4.2 Vacuum pump: A high vacuum pump (Hind Hivac, India) was used to generate vacuum of the order of 0.1 - 0.2 mbar re-

quired to distill monomers and to determine the alpha particle sensitivity of the polymer.

2.4.3 Thickness measurements: The thickness of the films prepared and analyzed is measured, over the entire surface of the films, randomly at 50 different points, for a film of size 8 cm x 8 cm, using a digital thickness gauge (Alpha meter, Para Electronics, India).

2.4.4 Exposure to radiation sources: Polymer samples of size 1 x 1 cm^2 are cut and exposed to ^{252}Cf source at a distance of 1 mm. In order to expose the detector to low energy alpha particles, the detector is exposed to alpha particles from the source at a distance of 1, 2 and 3 cm. The exposure assembly is as shown in the figure 2.6 below.

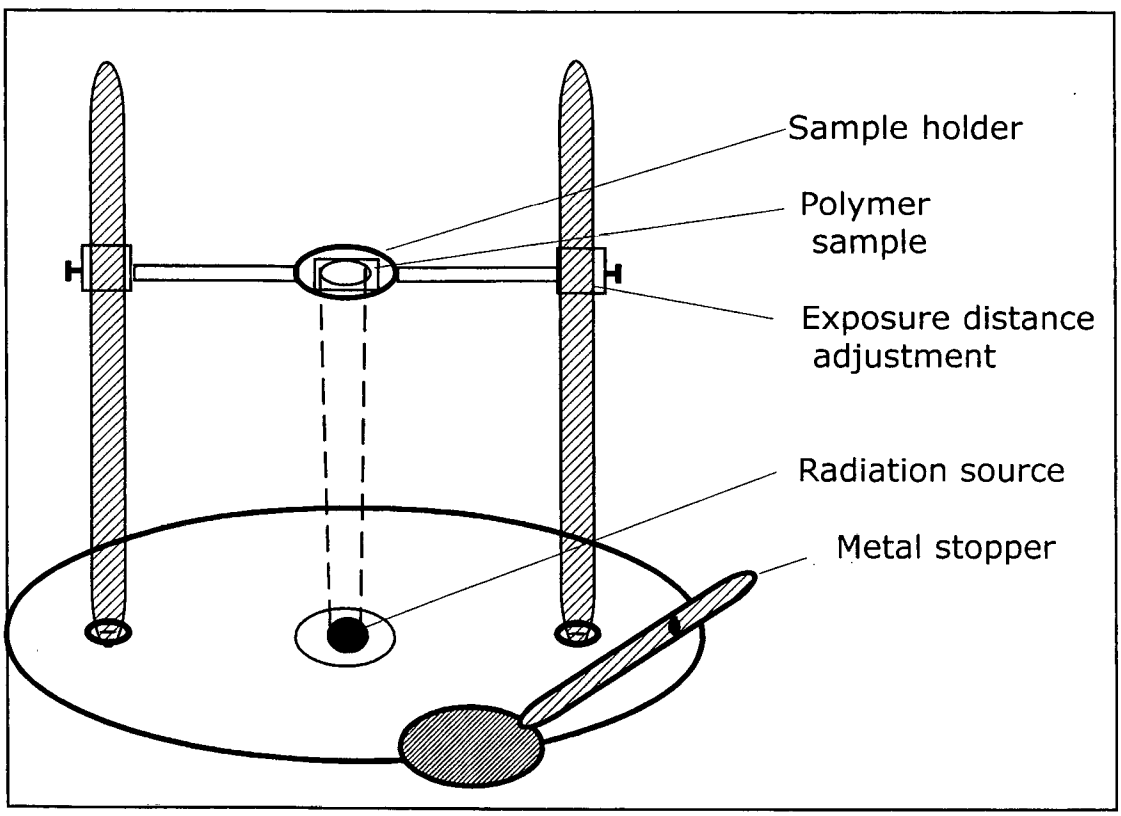

Figure 2.6: Exposure assembly.

The films are placed on the stage and the height can be adjusted by using the screw nuts.

2.4.5 Etching of the detector film: The films exposed to radiation source are etched in chemical etching bath made of glass as shown in Figure 2.7. The bath is provided with a thermometer, hot water jacket, stainless steel holder and a magnetic stirrer. The apparatus is filled with etchant and heated by external circulation of hot water through the jacket. The polymer samples are placed in stainless steel cage. Once the etching temperature is attained the cage is dipped into the etchant.

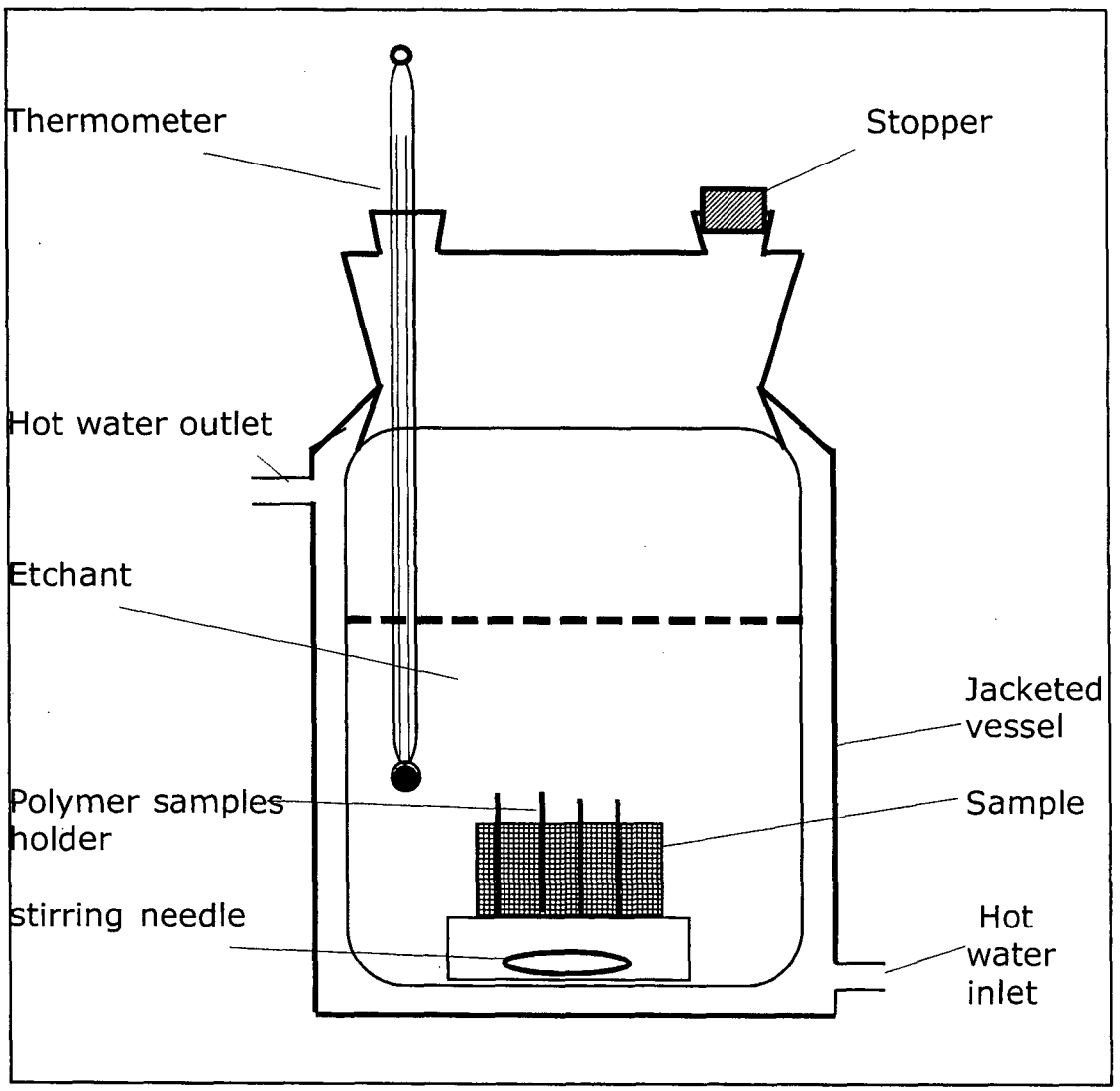

Figure 2.7: Glass assembly for chemical etching of polymer samples.

The bulk etch rate is the important parameter which is analyzed during the process of chemical etching. The bulk etch rate of

the polymer can be determined by following methods

i) Weight loss method: In this method the weight of the test film is determined before and after the etching of the polymer film. This method is sometimes referred to as gravimetric method and is limited by the accuracy of mass measurements. The bulk etch rate is determined by using formula.[66,73,111,112,113]

$$V_b = (M_1 - M_2)\, T_i / 2\, M_2\, t \qquad 2.1$$

Where, M_1 and M_2 are final and initial masses respectively, T_i is initial thickness and t is the time interval between the two measurements.

ii) Fission fragment track diameter method:[6,17,111,113] This is the most frequently used method for determination of bulk etch rate. The rate of change of diameter of fission fragments tracks in the detector material exposed to ^{252}Cf source after etching is determined at regular intervals. The diameters of fission fragments are determined by using an optical microscope. The bulk etch rate of the polymer was found by using the formula

$$V_b = D_f / 2\, t \qquad 2.2$$

Where, D_f is the diameter of fission fragment track and t is the time.

iii) The change in thickness method: The thickness of the material is determined using different methods of thickness measurements over its entire surface. The method can be used for detectors having uniform thickness. However the method renders error due to swelling of the polymer during chemical etching and hence is rarely used.

2.4.6 Counting of particle tracks under an optical microscope: The detector films after chemical etching are washed under running tap water and dried under an IR lamp. The dry films are

mounted on glass slide and placed on the microscope stage. The film is focused under the specific magnification and numbers of tracks per view are counted. In a 1 x 1 cm^2 film 100 views are counted using the X - Y stage. As per the given magnification, area under the observed view was determined using the stage micrometer. The track density was determined using the relationship.

$$\text{Track density (tracks / cm}^2\text{)} = \frac{\text{Total number of tracks counted}}{\text{Total number of views x area of the view}} \qquad 2.3$$

2.4.7 Sensitivity study: The polymer samples which detect alpha and fission fragment particles are anchored on alluminium support and are exposed to ^{252}Cf source in a vacuum dessicator.

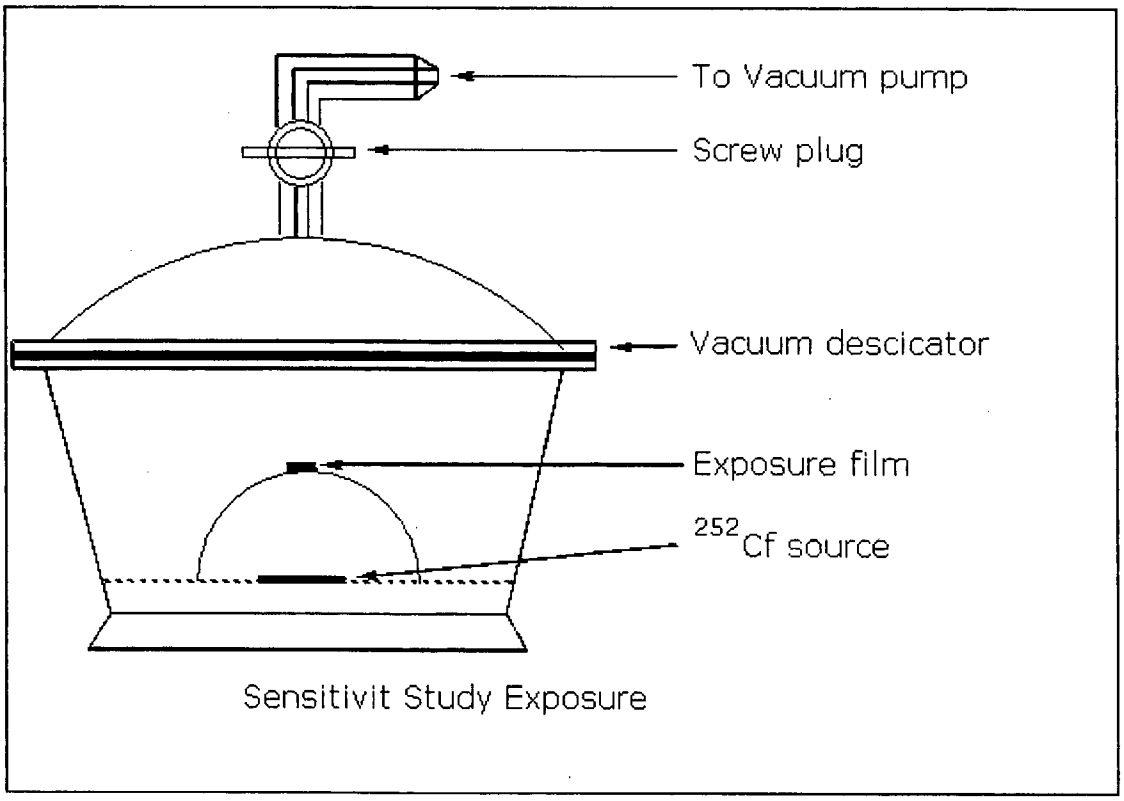

Figure 2.8: Exposure of SSNTD film to ^{252}Cf source for sensitivity measurements.

The distance of 5 cm is kept between the source and the

polymer. The films are exposed for 5 hrs at a vacuum of 0.2 mbar, applied using a high vacuum pump. After exposure, the films are etched and increase in the track diameter at every hour interval is noted. Once the diameters of the tracks are determined the alpha sensitivity of the detector film is determined by using the formula.[17,66,73,76,78,111,113]

$$S = \frac{1+ (d_\alpha / d_f)^2}{1 - (d_\alpha / d_f)^2} \qquad 2.4$$

Where

d_a is the diameter of the alpha particle track.

d_f is the diameter of fission fragment track.

2.5 Spectral characterization: The monomers after synthesis were characterized using various spectral techniques. IR spectra were recorded on Shimadzu FT-IR spectrophotometer with KBr discs for liquids and KBr/compound powdered mixture for solids. ^1H and ^{13}C spectra were recorded on Bruker 300 MHz spectrophotometer with $CDCl_3$ as solvent and TMS as an internal standard. Mass spectra were recorded on QStar XL MS-MS system.

2.6 Monomer synthesis:

2.6.1 Allyl chloroformate:[114,115] Triphosgene (9.3 g, 0.0316 mol) was dissolved in 70 mL dichloromethane in a two neck round bottom flask fitted with rubber septum. The mixture was cooled to 0 °C. Allyl alcohol (5.0 g, 0.086 mol) and pyridine (6.8 g 0.086 mol) were injected through the rubber septums in the reaction flask, simultaneously at such a rate that pyridine always remain in excess in the reaction mixture. After completion of addition, reaction mixture was stirred for 1 hr at 0 °C. The septum was removed and

reaction mixture was washed with 3 × 25 mL of ice cold water and the organic layer was dried over anhy. Na_2SO_4. Dichloromethane was removed by fractional distillation to afford (6.9 g, 67 %) allyl chloroformate. Figure 2.9 gives infrared spectrum of allyl chloroformate ν_{max}(KBr)/cm^{-1} 3091, 1770, 1267 and 1157 see next page 85).

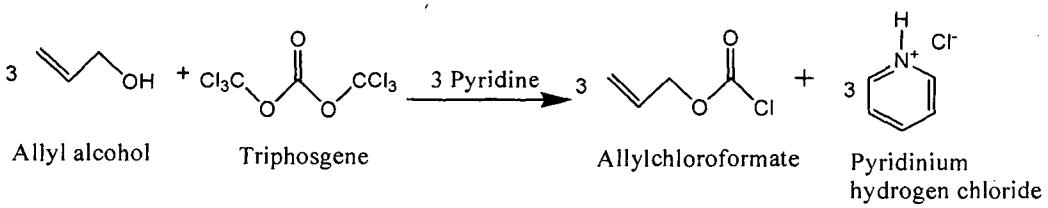

Scheme 2.1: Synthesis of allyl chloroformate.

2.6.2 Isopropyl chloroformate:[73,115] A procedure was same as that used for the preparation of allyl chloroformate (Section 2.6.1) except that, isopropyl alcohol was used instead of allyl alcohol.

2.6.3 Diallyl carbonate:[116] A process earlier standardized in our laboratory was used to prepare diallyl carbonate. Allyl alcohol (300 mL, 4.4 mol) was taken in a round bottom flask along with 60 mL of cyclohexane. The mixture was heated to 60 °C under vigorous stirring and KOH (1.5 g) was added. The reaction was heated to around 70 °C and drop by drop dimethyl carbonate (123.5 mL, 1.47 mol) was added through a dropping funnel. After completion of addition, the mixture of methanol and cyclohexane was removed by azeotropic distillation using a dufton column for 6 hrs. After removal of 60 mL of methanol the unreacted allyl alcohol and dimethyl carbonate were removed by downward normal distillation.

The unreacted allyl alcohol and dimethyl carbonate could be recycled in the next batch of monomer synthesis. The mixture was washed with 3 × 50 mL distilled water and dried over anhy. Na_2SO_4. The product was finally distilled under reduced pressure to give pure diallyl carbonate (118 g, 56.73 %) as a colorless liquid.

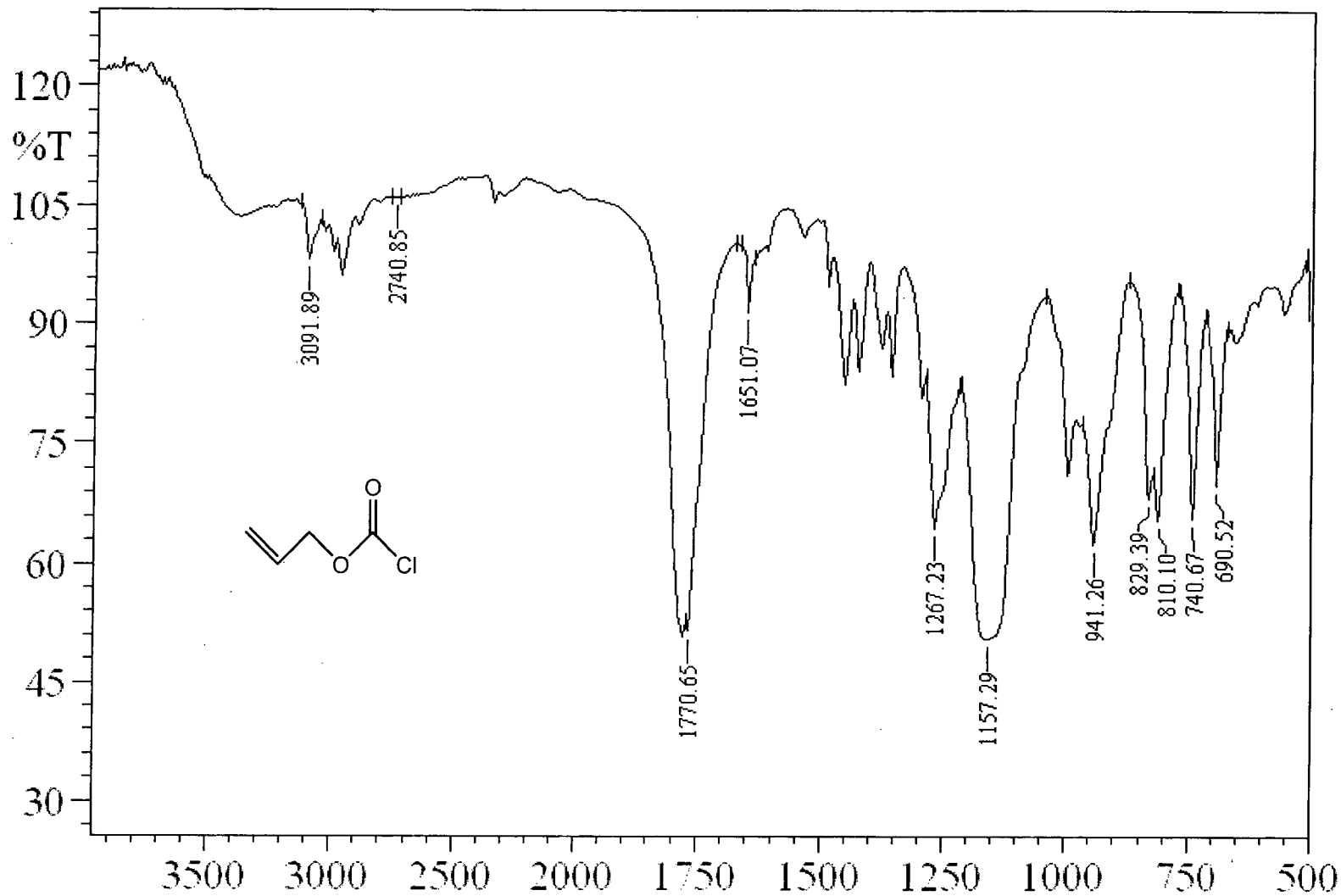

Figure 2.9: Infrared spectrum of allyl chloroformate.

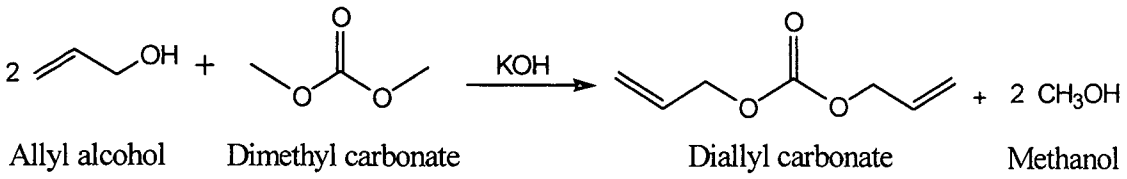

Scheme 2.2: Synthesis of Diallyl carbonate.

Infrared spectrum and the HRMS of DAC is given in Figures 2.10 and 2.11 respectively (pages 87-88). ν_{max}(KBr)/cm^{-1} 3088, 1747, 1253 and 968; m/z (TOF ES) 143.0708 (M^+ + Na. $C_7H_{10}O_3$ requires 143.0705)

2.6.4 Allyl diglycol carbonate: Diethylene glycol (12 g, 0.113 mol) was taken in a three neck flask equipped with thermometer, a dropping funnel and a magnetic stirrer. Diallyl carbonate (160 g, 1.13 mol) was charged in the flask and heated using oil bath under dry nitrogen atmosphere. At temperatures of around 60 °C, 500 mg of KOH was added. The temperature was raised to 114 °C and the allyl alcohol was continuously distilled out. After about 13 g of allyl alcohol was distilled, diallyl carbonate was distilled under reduced pressure. The crude ADC was suspended in 50 mL diethyl ether, washed with 3 x 30 mL of distilled water and dried over anhy. Na_2SO_4. Ether was carefully removed on water bath and finally, ADC monomer was distilled under reduced pressure of 0.2 mbar at 160 °C. Pure ADC (31.42 g, 80.63 %) was obtained as colorless liquid. The synthetic scheme for the process is as follows.

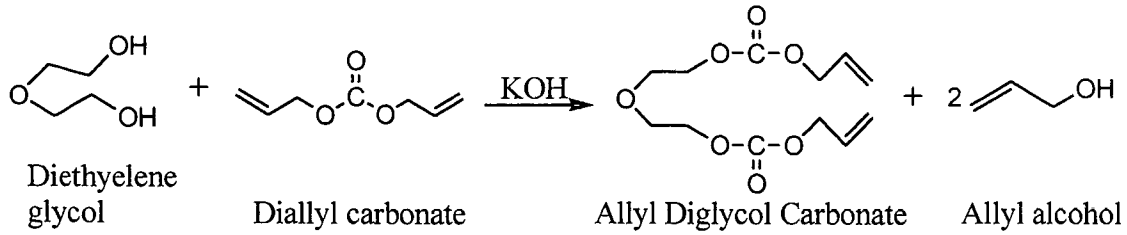

Scheme 2.3: Synthesis of ADC monomer.

The infrared spectrum of ADC monomer is dipicted in Figure 2.12 (Page 89) below. ν_{max}(KBr)/cm^{-1} 3088, 1749, 1295 and 1254.

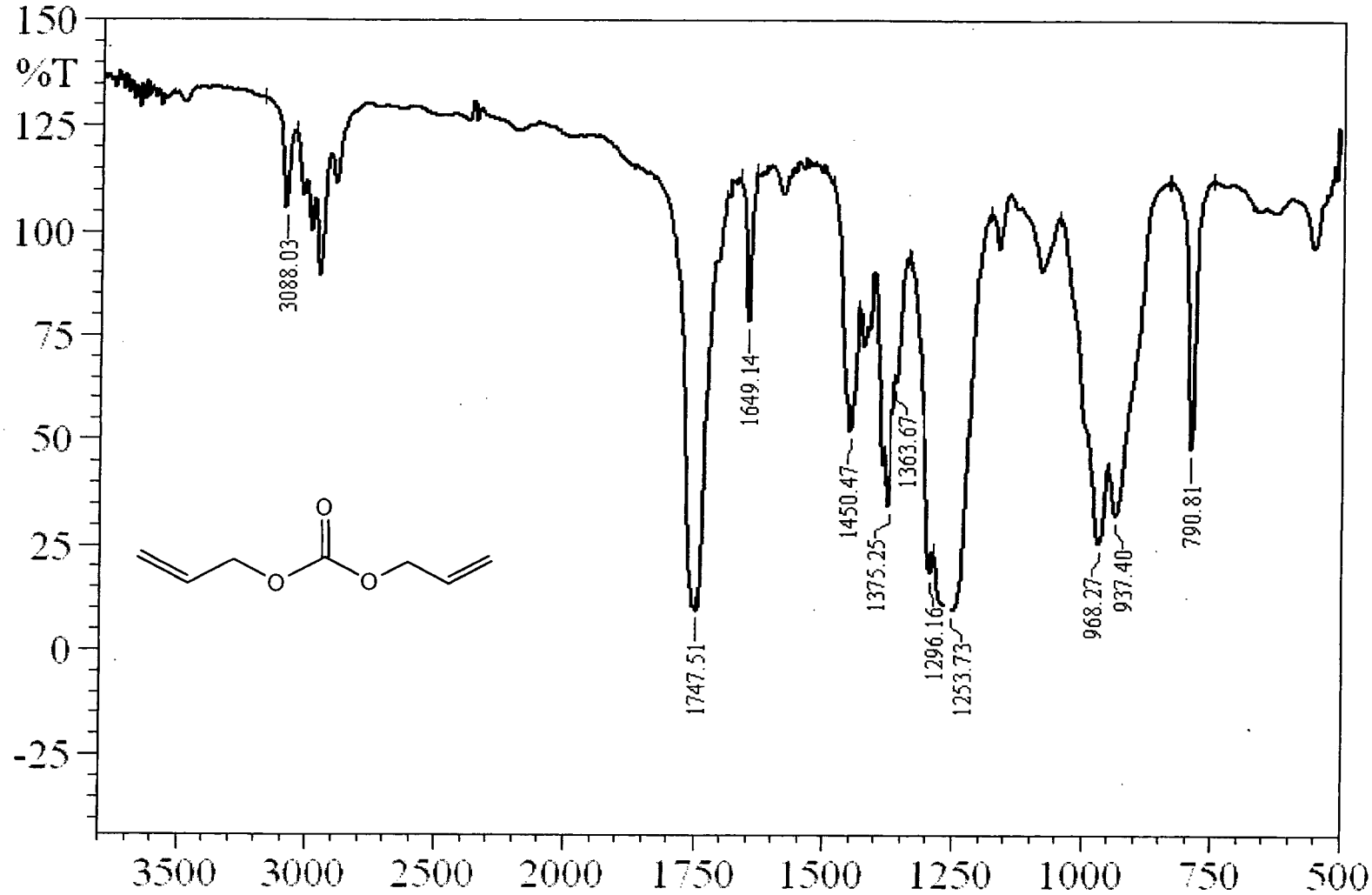

Figure 2.10: Infrared spectrum of diallyl carbonate.

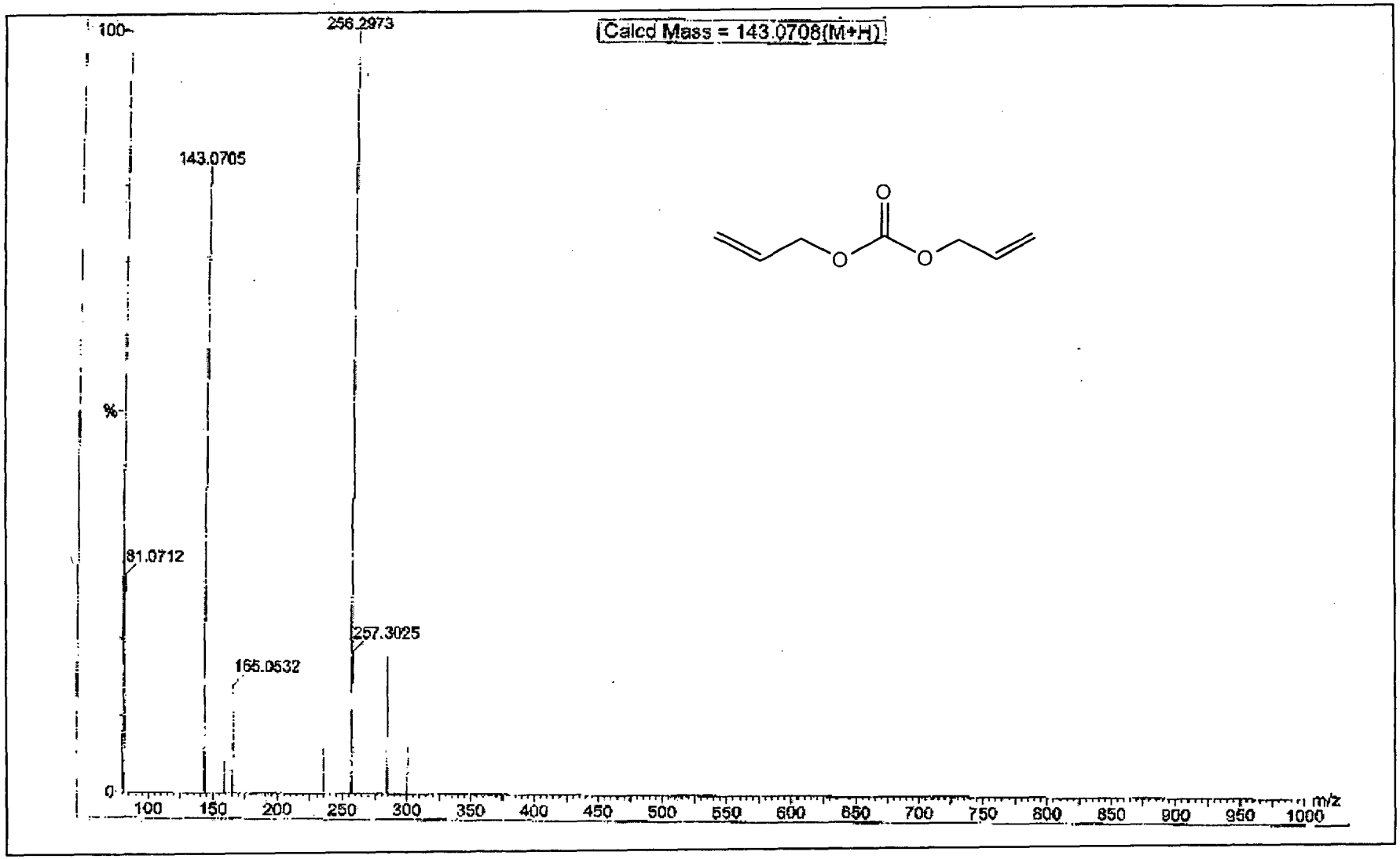

Figure 2.11: HRMS of diallyl carbonate.

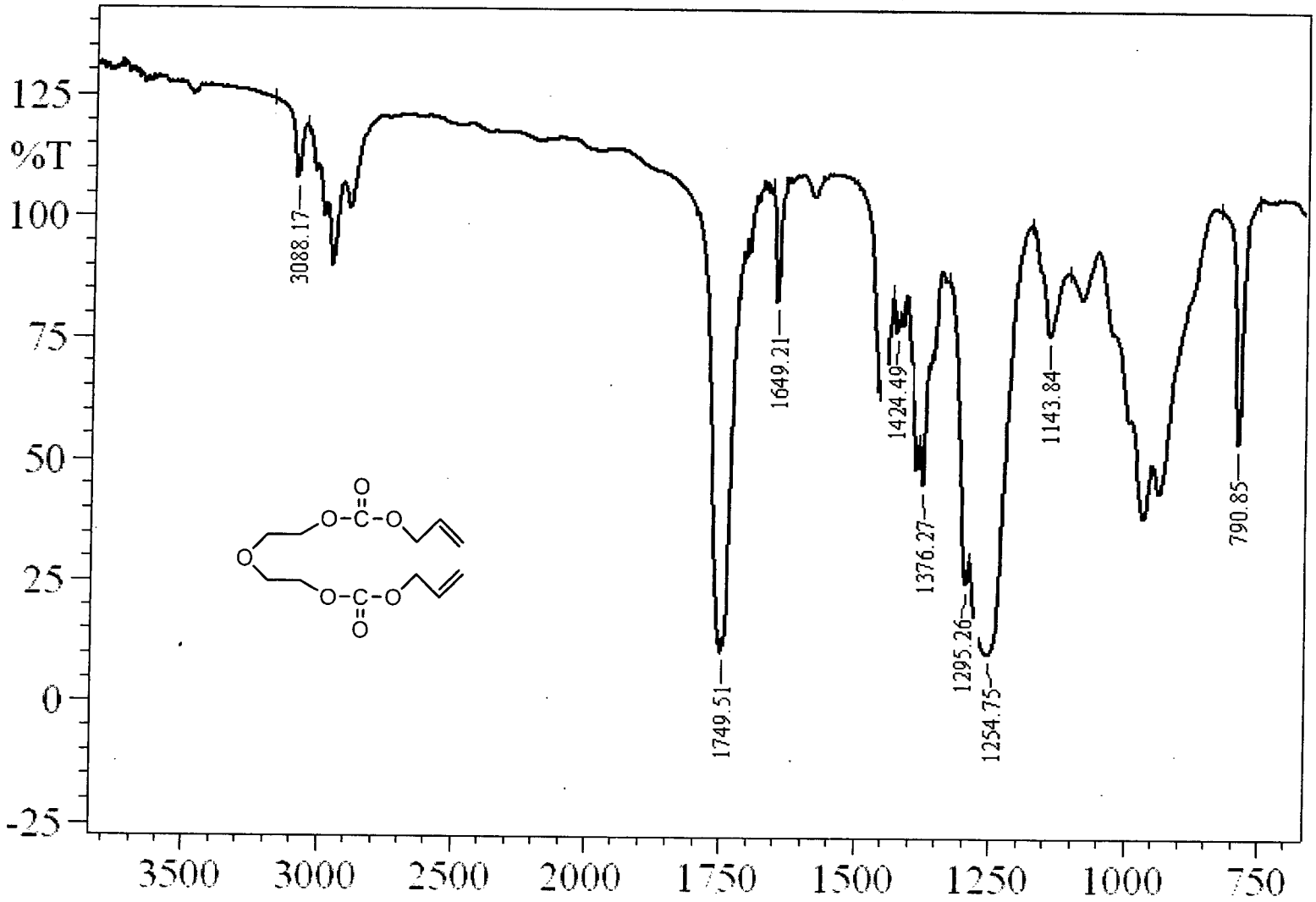

Figure 2.12: Infrared spectrum of allyl diglycol carbonate.

Diallyl sulphite (DAS):[118,119,120,121] Allyl alcohol (200 g, 3.44 mol) and 50 mL of dichloromethane was charged in a three neck flask fitted with a reflux condenser and a thermometer pocket. The reaction mixture was cooled to 10 °C and drop by drop thionyl chloride (205.81 g, 1.73 mol) was added to the reaction mixture. A vigorous reaction started and large amount of HCl gas was evolved. After complete addition of thionyl chloride the mixture was refluxed until no more gas was evolved. The solvent was removed and the product was vacuum distilled to get diallyl sulphite (180 g, 64 %) as a colorless liquid. The reaction scheme is as depicted below.

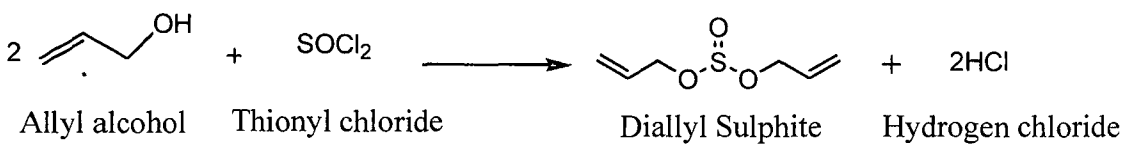

Scheme 2.4: Synthesis of Diallyl sulphite.

The structure of DAS was characterized by following spectral data. ν_{max}(KBr)/cm^{-1} 3088, 1647, 1207, and 972; δH(300 MHz; $CDCl_3$; Me_4Si) 4.45 (4H, m, 2 x SO-O-C$\underline{H}_2$), 5.23 (4H, dd, 2 x C$\underline{H}_2$=), 5.85 (2H, m, 2 x -C$\underline{H}$=); δC(300 MHz; $CDCl_3$; Me_4Si) 64.1ppm (2 x t), 120.3 (2 x t), 133.3 (2C x d). m/z (TOF ES) 185.0248 (M^+ + Na. $C_6H_{10}O_3S$ requires 185.0246)

The different spectra (IR, PMR, CMR & HRMS) recorded are given in Figures 2.13 to 2.16 respectively (pages 91-94).

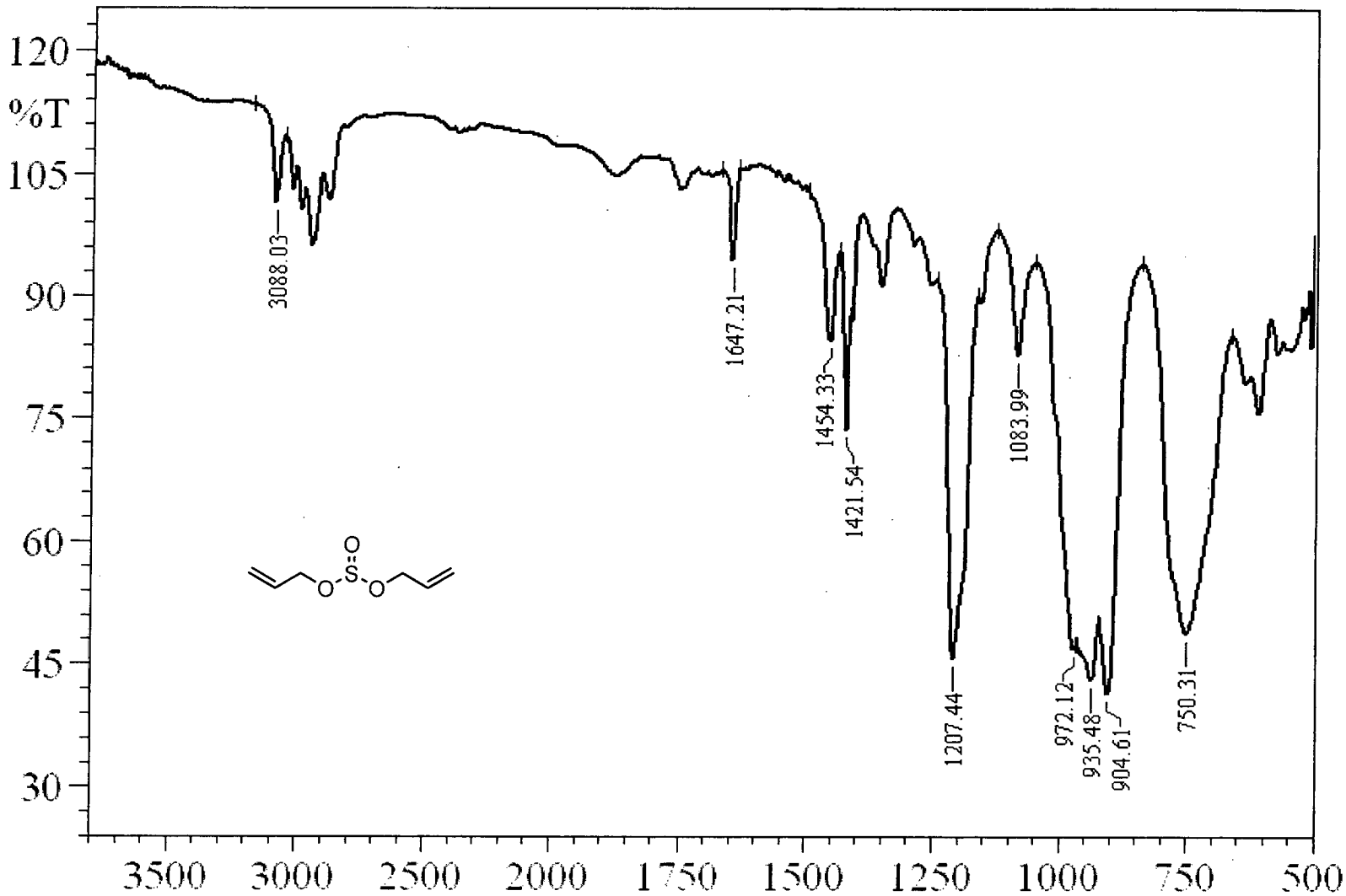

Figure 2.13: Infrared spectrum of diallyl sulphite.

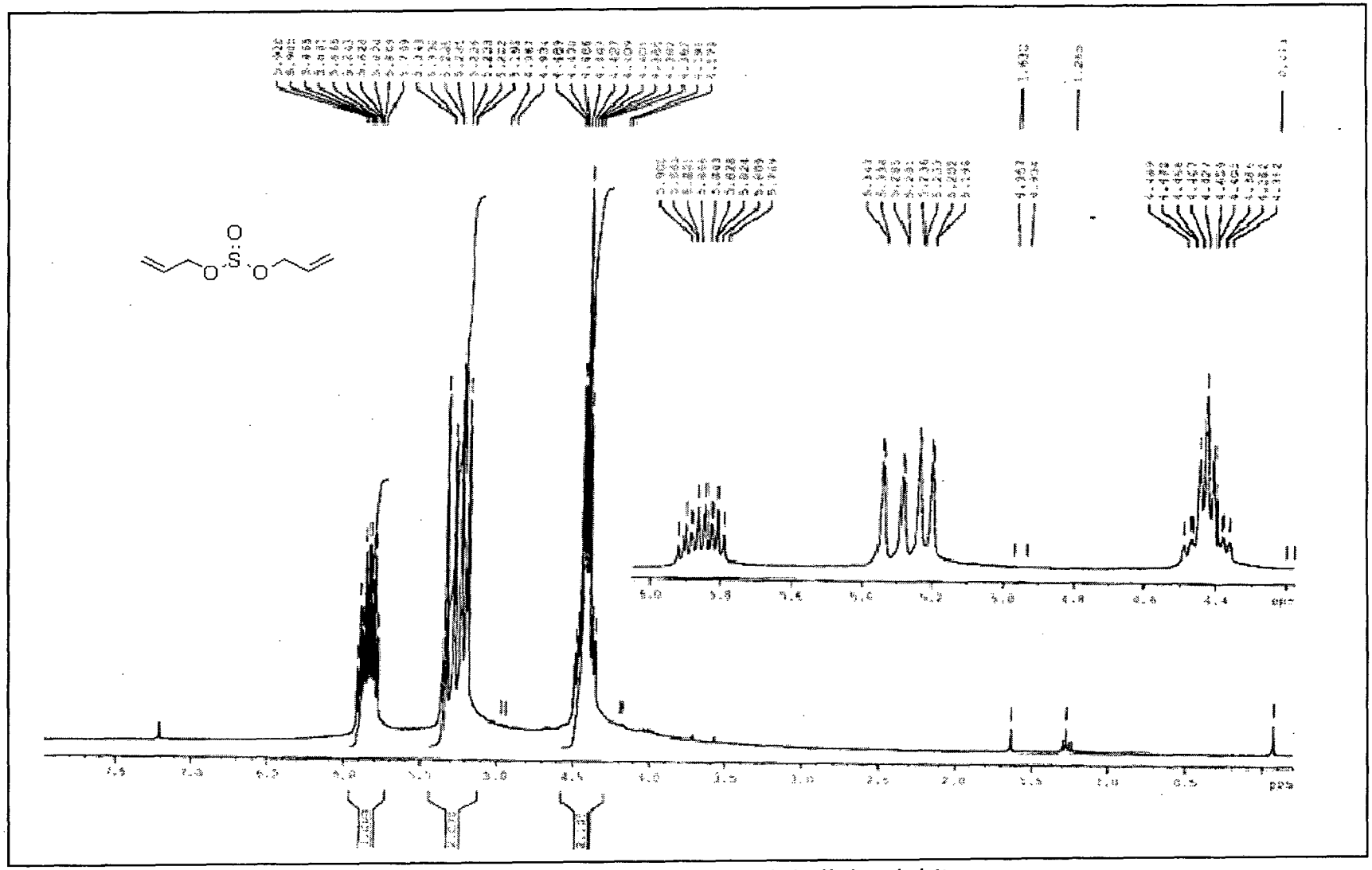

Figure 2.14: ^{1}H NMR spectrum of diallyl sulphite.

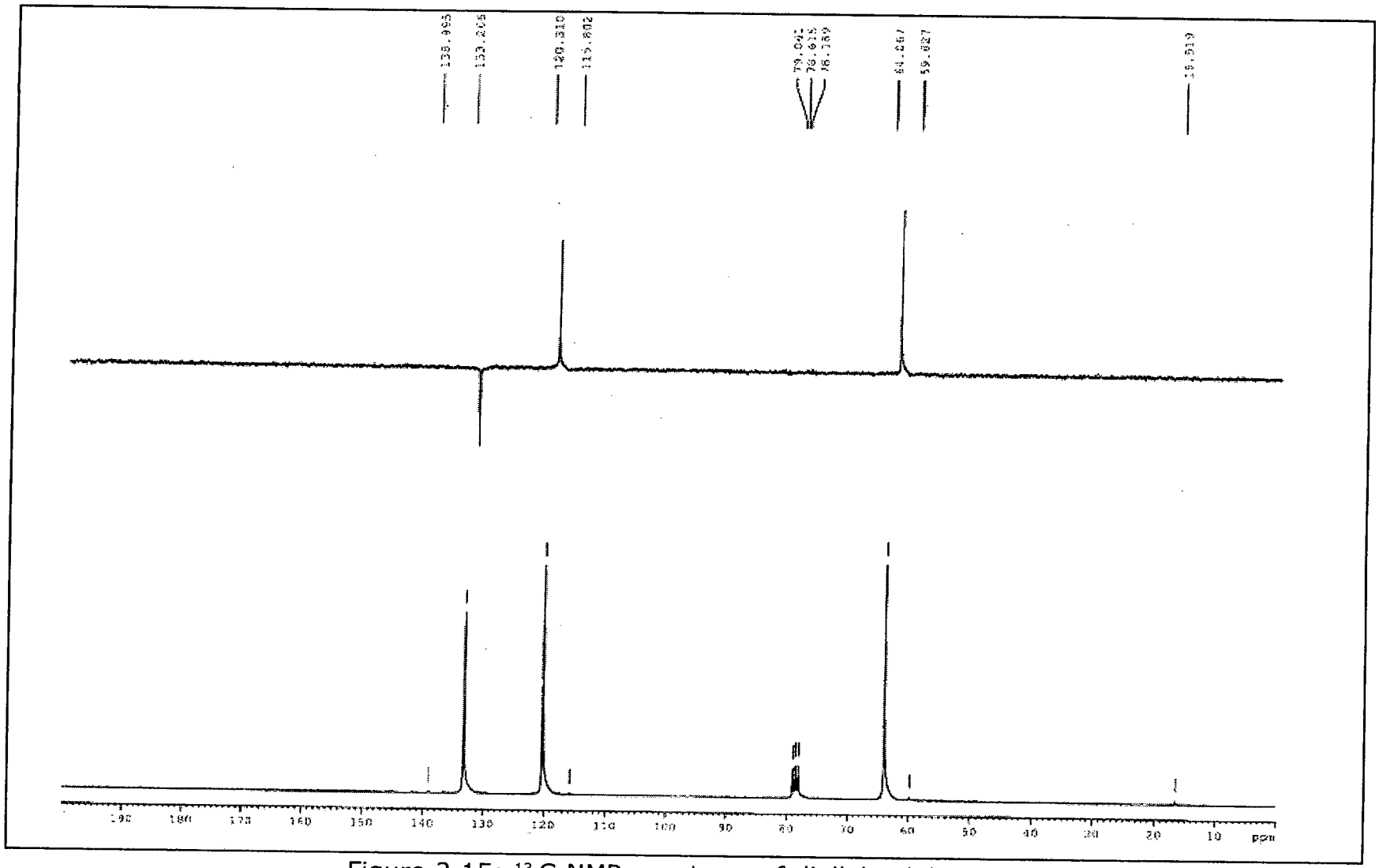

Figure 2.15: ^{13}C NMR spectrum of diallyl sulphite.

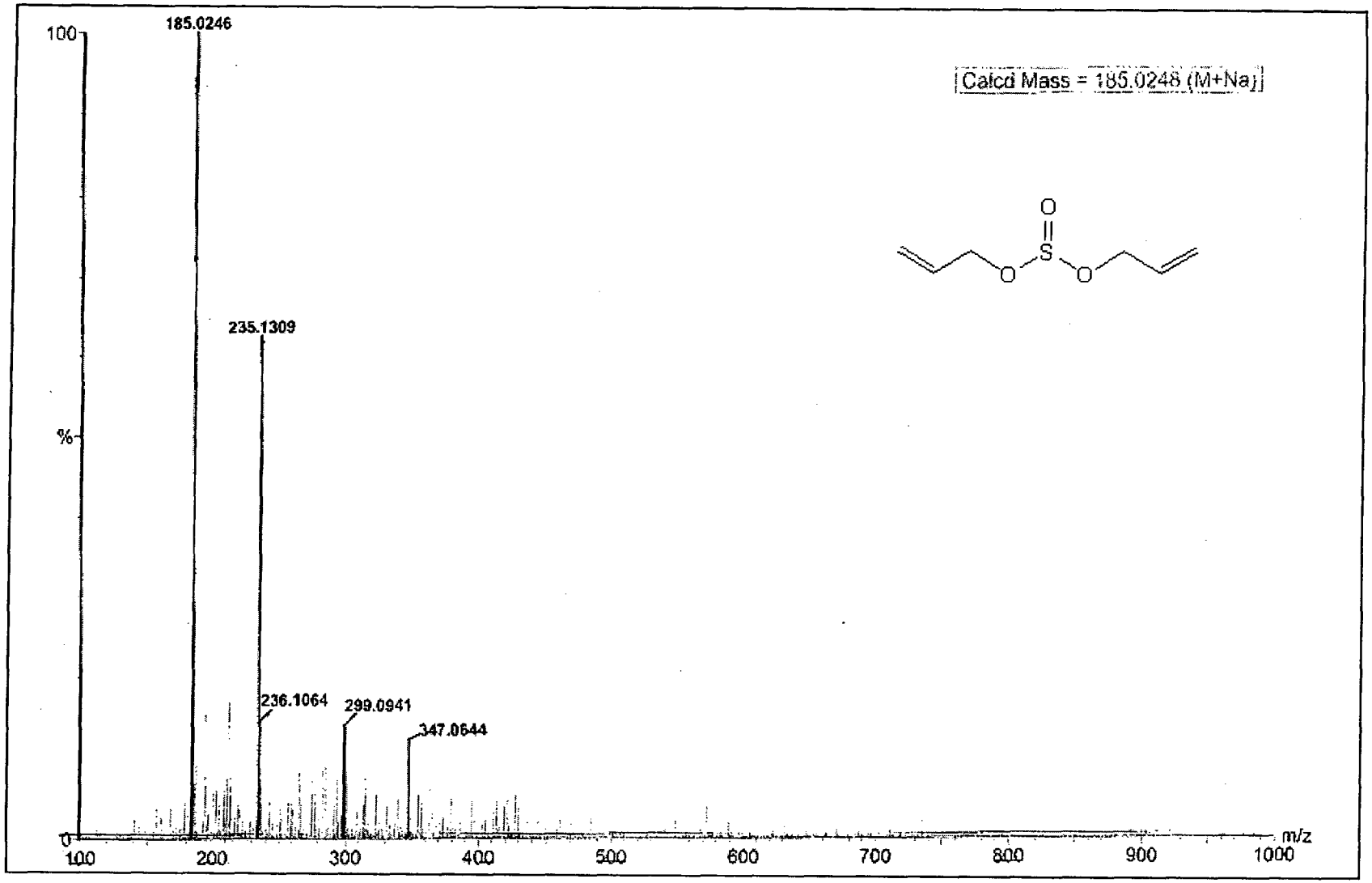

Figure 2.16: HRMS of diallyl sulphite.

2.6.6 Allyl diglycol sulphite (ADS):[122,123] In a three neck round bottom flask provided with a dry nitrogen gas inlet, a thermometer and a distillation assembly was charged (150 g, 0.93 mol) of DAS. Diethylene glycol (9.858 g, 0.093 mol) was added the mixture was flushed with a stream of dry nitrogen. The temperature of the reaction mixture was raised to 60 °C and 1 g of KOH was added. The mixture was heated under stirring to 110 °C and maintained until allyl alcohol (10.80 g, 0.17 mol) gets distilled. After completion of reaction the excess DAS was removed by vacuum distillation. The remaining mixture was taken in ether and washed with 3 x 50 mL of distilled water. The product was distilled under reduced pressure of 0.02 mbar at 160 °C to afford ADS (23.36 g, 80 %) as a light brown colored liquid. The reaction scheme is as depicted below.

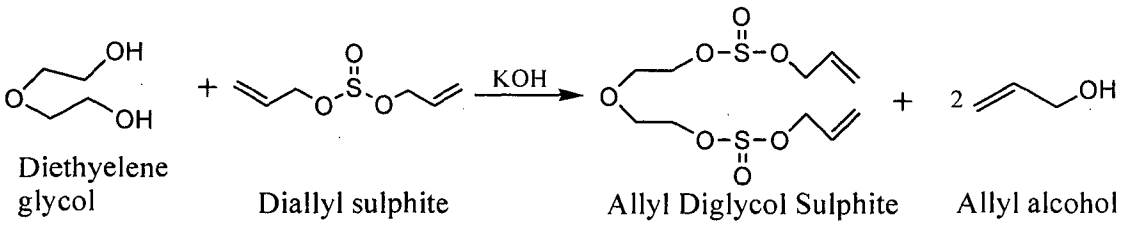

Scheme 2.5: ADS monomer synthesis.

The structure of ADS was characterized by recording its IR, ^{1}H NMR, ^{13}C NMR and mass spectral data and is given in Figures 2.17 to 2.20 (See next pages 96 - 100).

ν_{max}(KBr)/cm^{-1} 3089,1646, 1356, 1205; δH(300 MHz; $CDCl_3$; Me_4Si) 3.58 (4H, t, -O-C<u>H</u>$_2$-CH$_2$-), 3.88 (4H, t, 2 x SO-O-CH$_2$-C<u>H</u>$_2$-), 4.36 (4H, m, 2 x -SO-O-C<u>H</u>$_2$-,), 5.21 (4H, dd, 2 x C<u>H</u>$_2$=), 5.77 (2H, m, 2 x C<u>H</u>=); δC(300 MHz; $CDCl_3$; Me_4Si) 62.6 (2 x t), 64.2 (2 x t), 70.85 (2 x t), 120.5 (2 x t), 133.3 (2 x d), m/z (TOF ES) 337.0384 (M^+ + Na. $C_{10}H_{18}O_7S_2$ requires 337.0392)

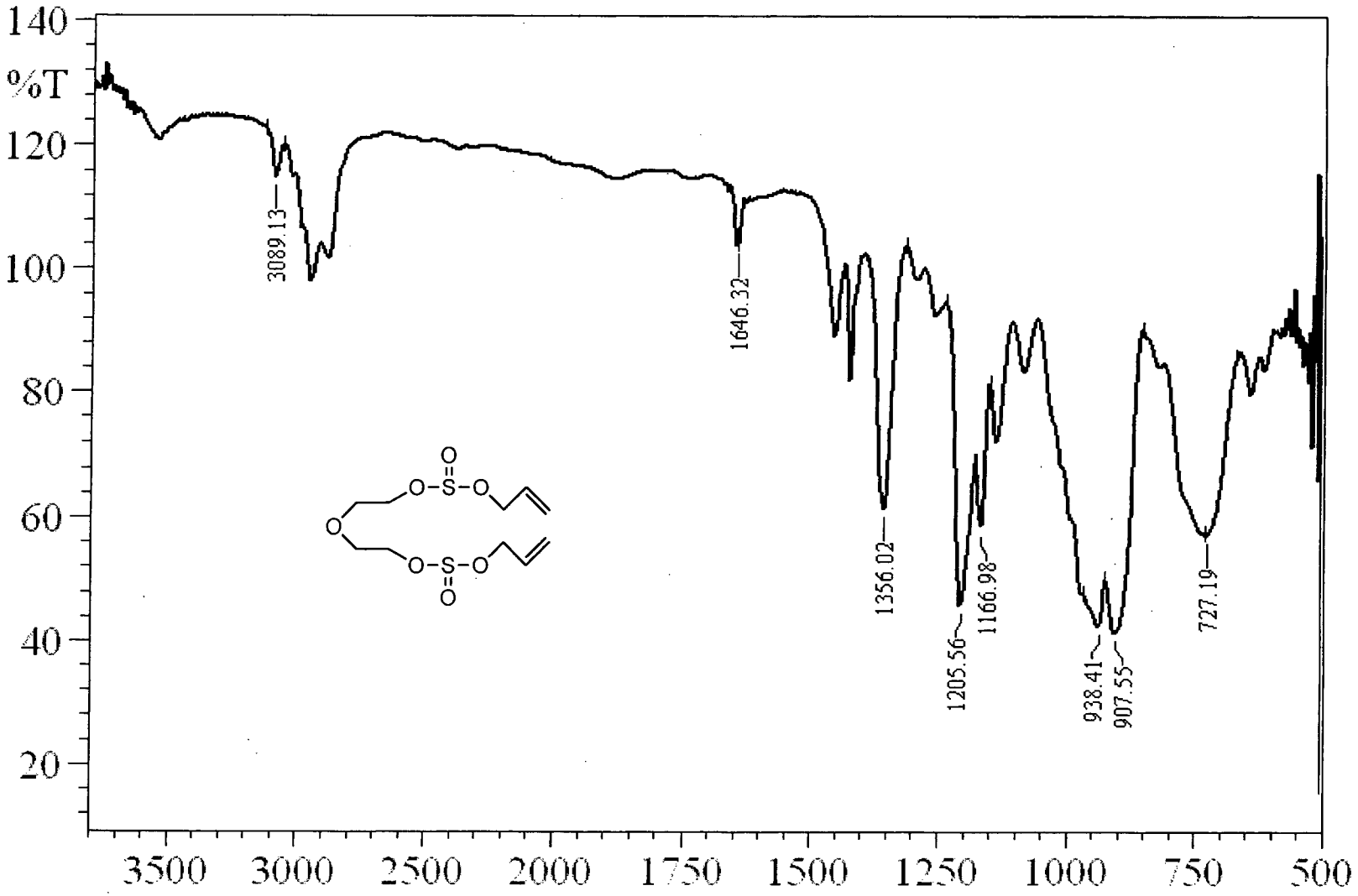

Figure 2.17: Infrared specturm allyl diglycol sulphite.

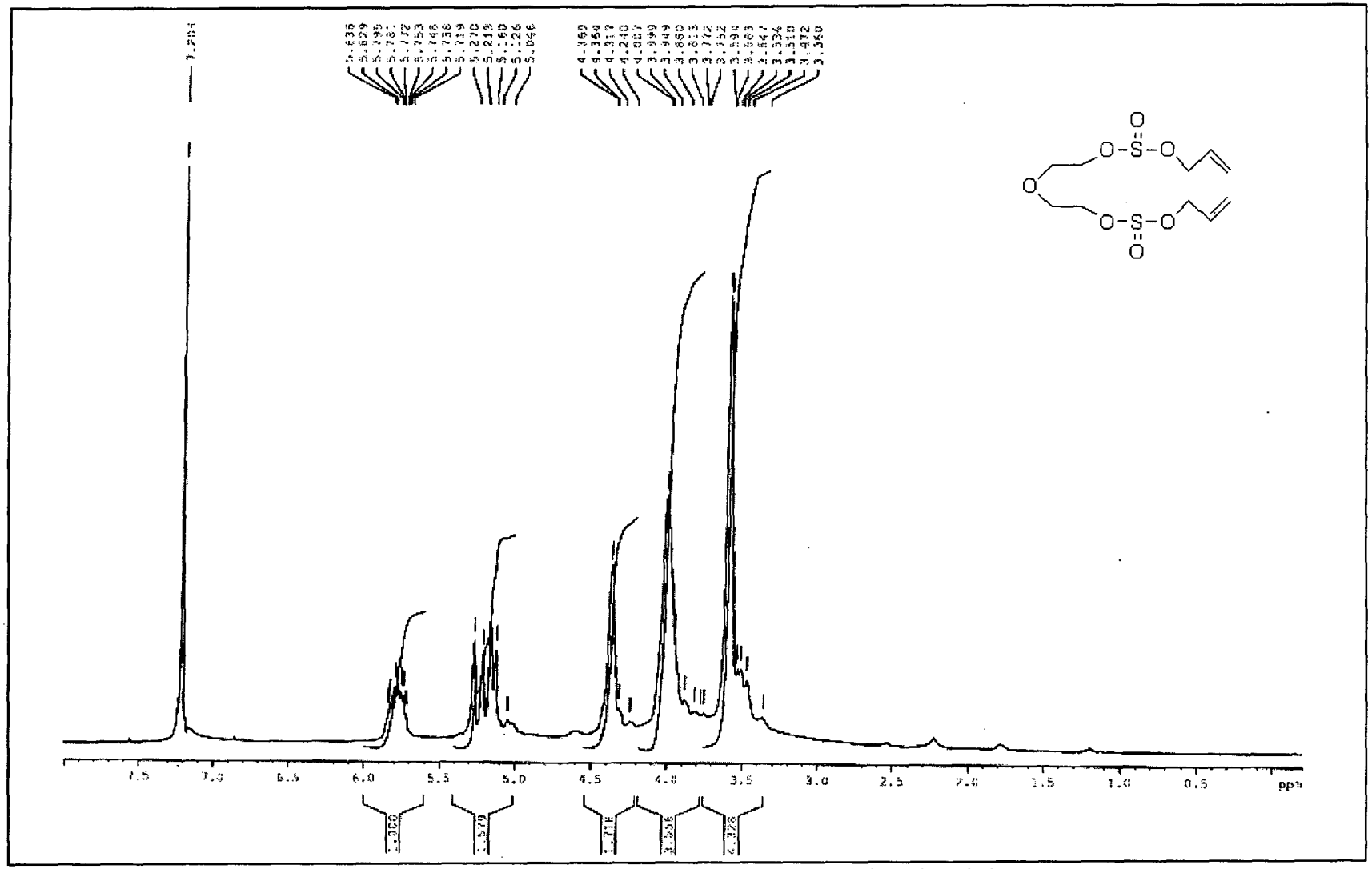

Figure 2.18: ^{1}H NMR spectrum of allyl diglycol sulphite.

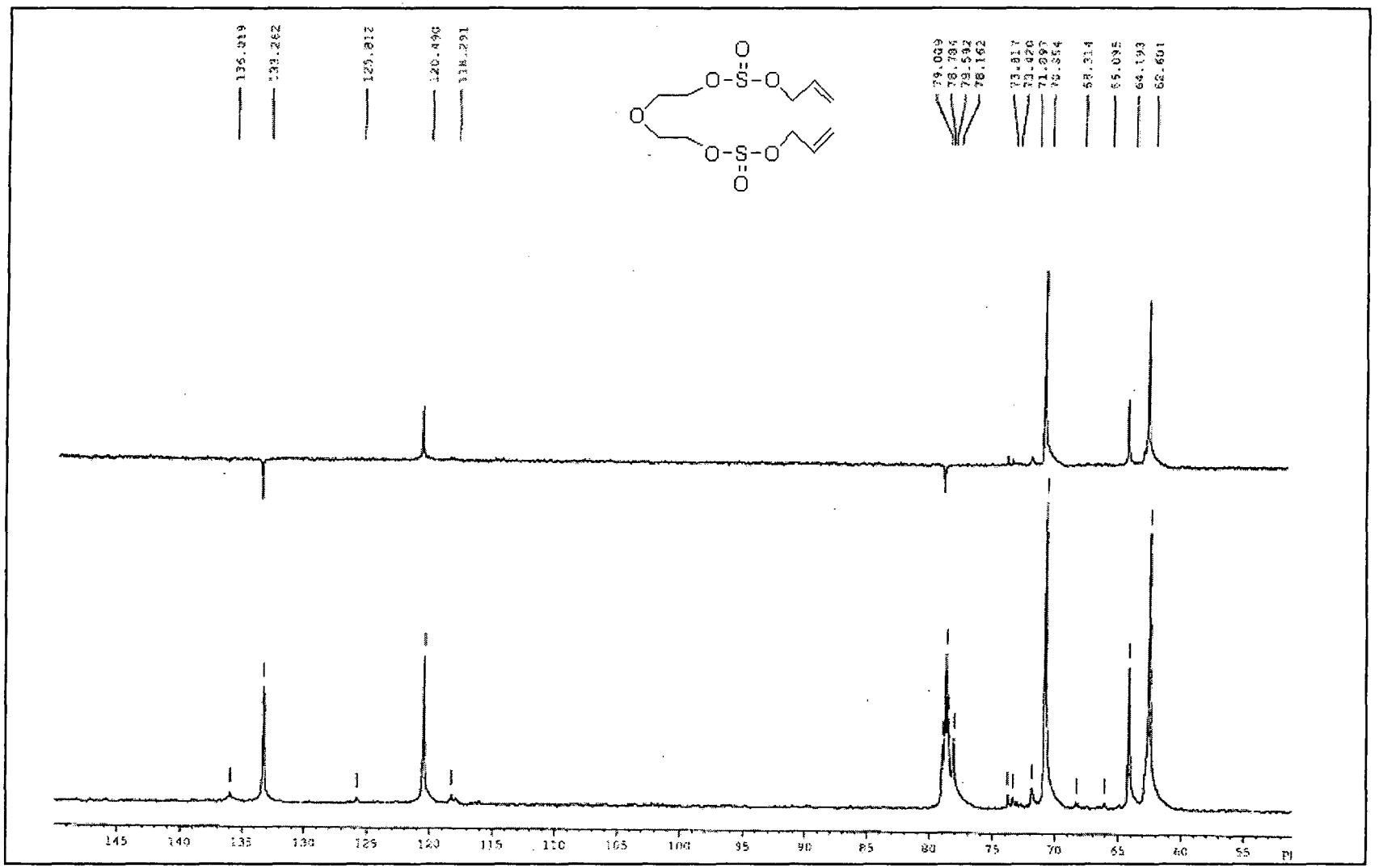

Figure 2.19: ^{13}C NMR spectrum of allyl diglycol sulphite.

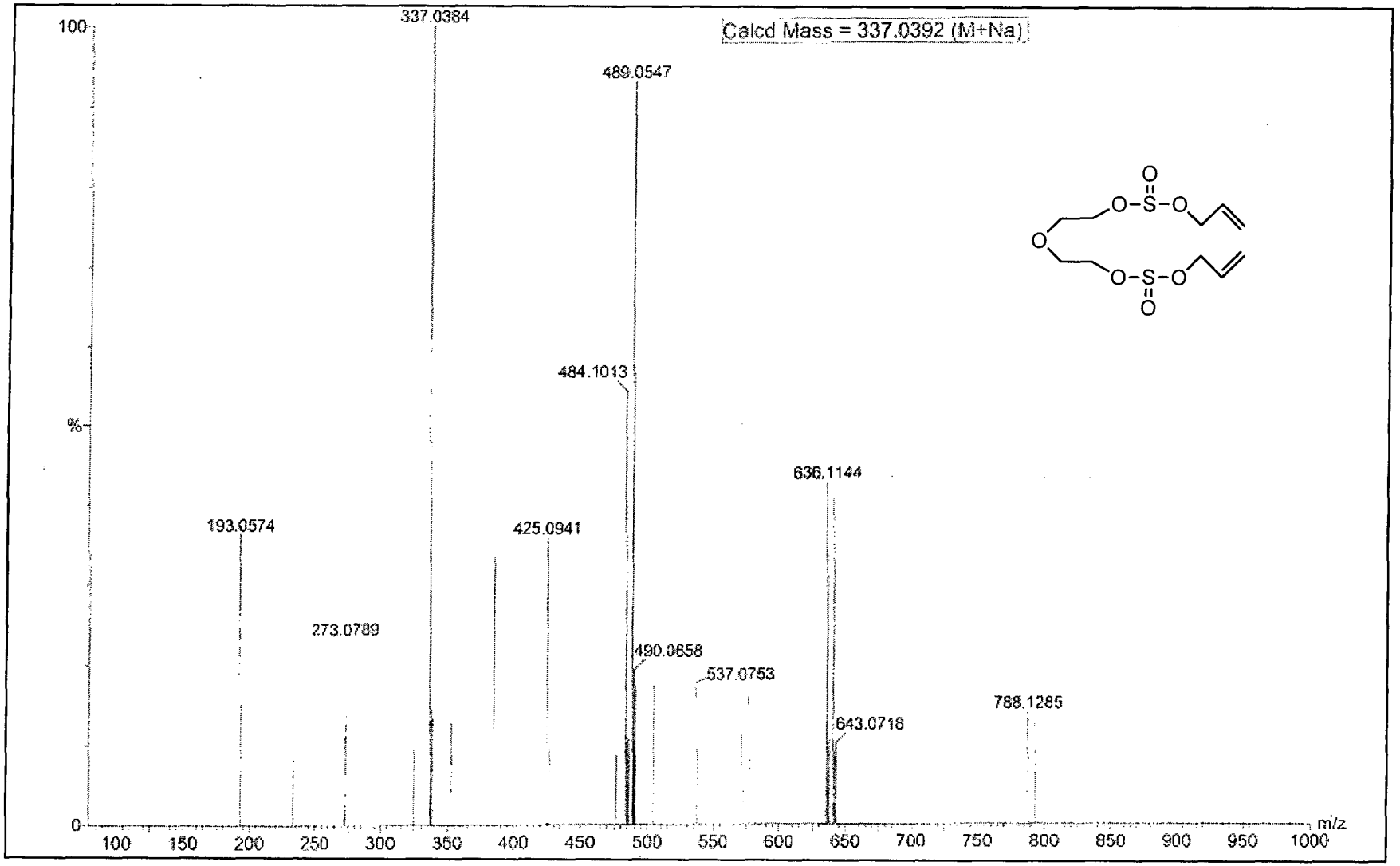

Figure 2.20: HRMS of allyl diglycol sulphite.

2.6.7 Diethyleneglycol bis(allyl sulfonate):[124,125,126]

i) Synthesis of sodium allyl sulfonate:- Allyl chloride (200 g, 2.61 mol) was added drop wise to a stirred solution of aqueous sodium sulphite (370.62 g, 2.62 mol) in a three neck flask provided with a reflux condenser and a thermometer. After completion of addition, the reaction mixture was stirred at 60 °C for 6 hr. Water was carefully removed by distillation and the solid obtained was recrystallized using 4:1 ethanol:water mixture. Sodium allyl sulfonate (263.52 g, 70 %) was obtained as a white solid. The IR spectrum is dipicted in Figure 2.21 (See page 101). ν_{max}(KBr)/cm^{-1} 3095, 1639, 1371, 1165. The synthetic scheme is given below.

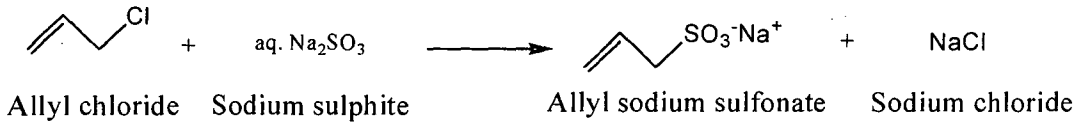

Scheme 2.6: Synthesis of allyl sodium sulfonate.

ii) Synthesis of Allyl chloro sulfonate:- Sodium allyl sulfonate (100 g, 0.69 mol) was reacted with phosphorous oxy chloride (107.45 g, 0.7 mol) and the mixture was heated at 120 °C for 8 hr. The brown colored mixture was poured in ice water under vigorous stirring and extracted in 4 x 50 mL diethyl ether. The ether was carefully evaporated and the mixture was vacuum distilled to get chloro allyl sulfonate (65 g, 67 %) as a colorless liquid. The synthetic scheme is given below. The IR spectrum of the compound is shown in Figure 2.22 (See page 102). ν_{max}(KBr)/cm^{-1} 3086, 1641, 1220, 1205.

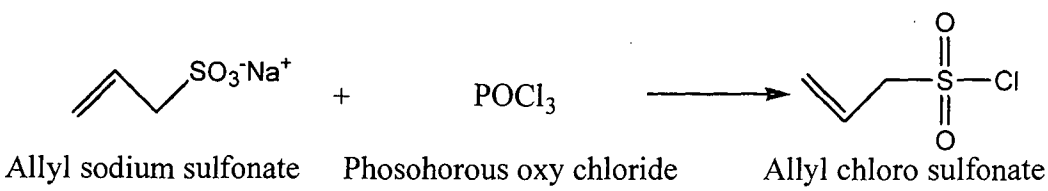

Scheme 2.7: Allyl chloro sulfonate synthesis.

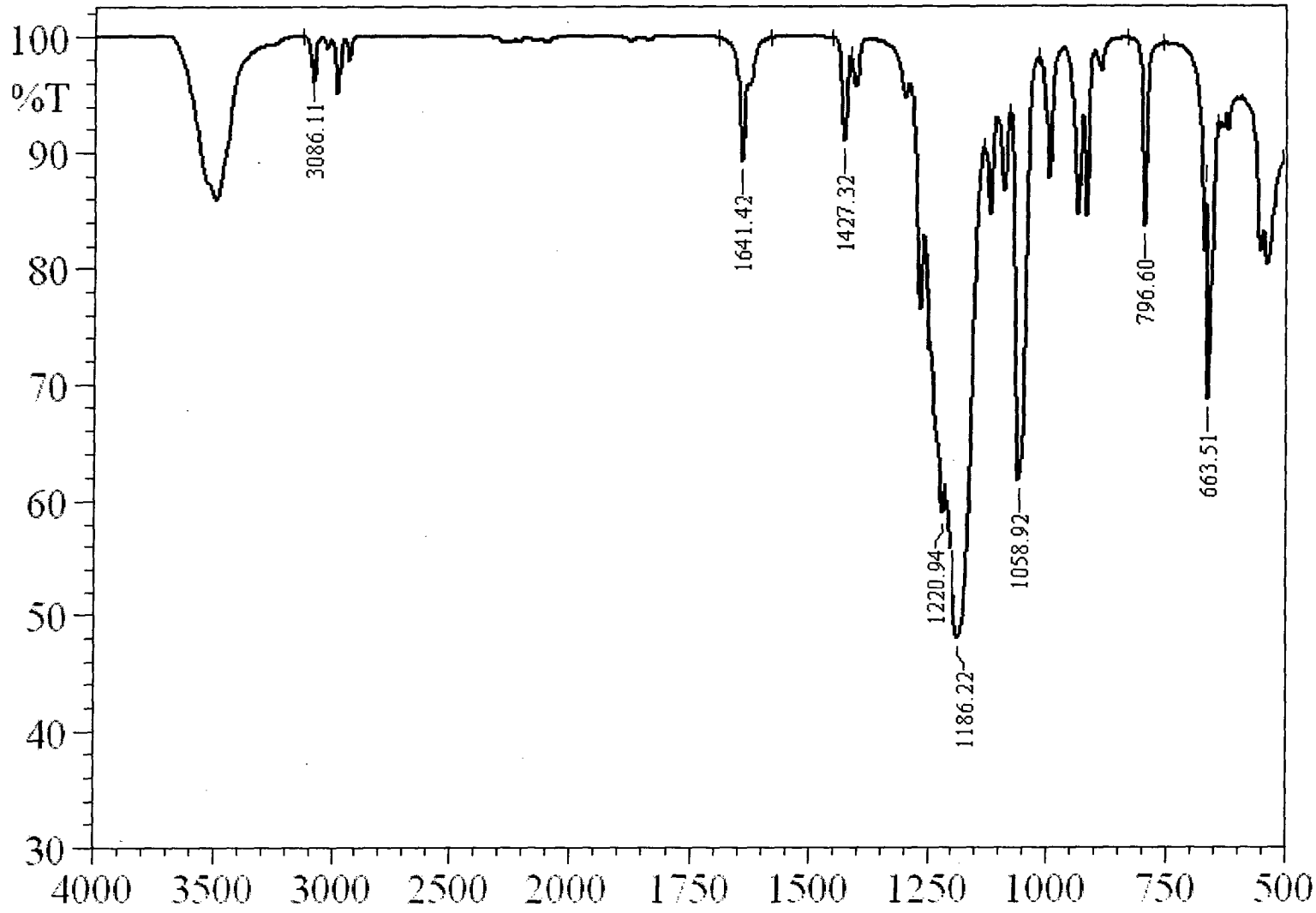

Figure 2.21: Infrared spectrum of sodium allyl sulfonate.

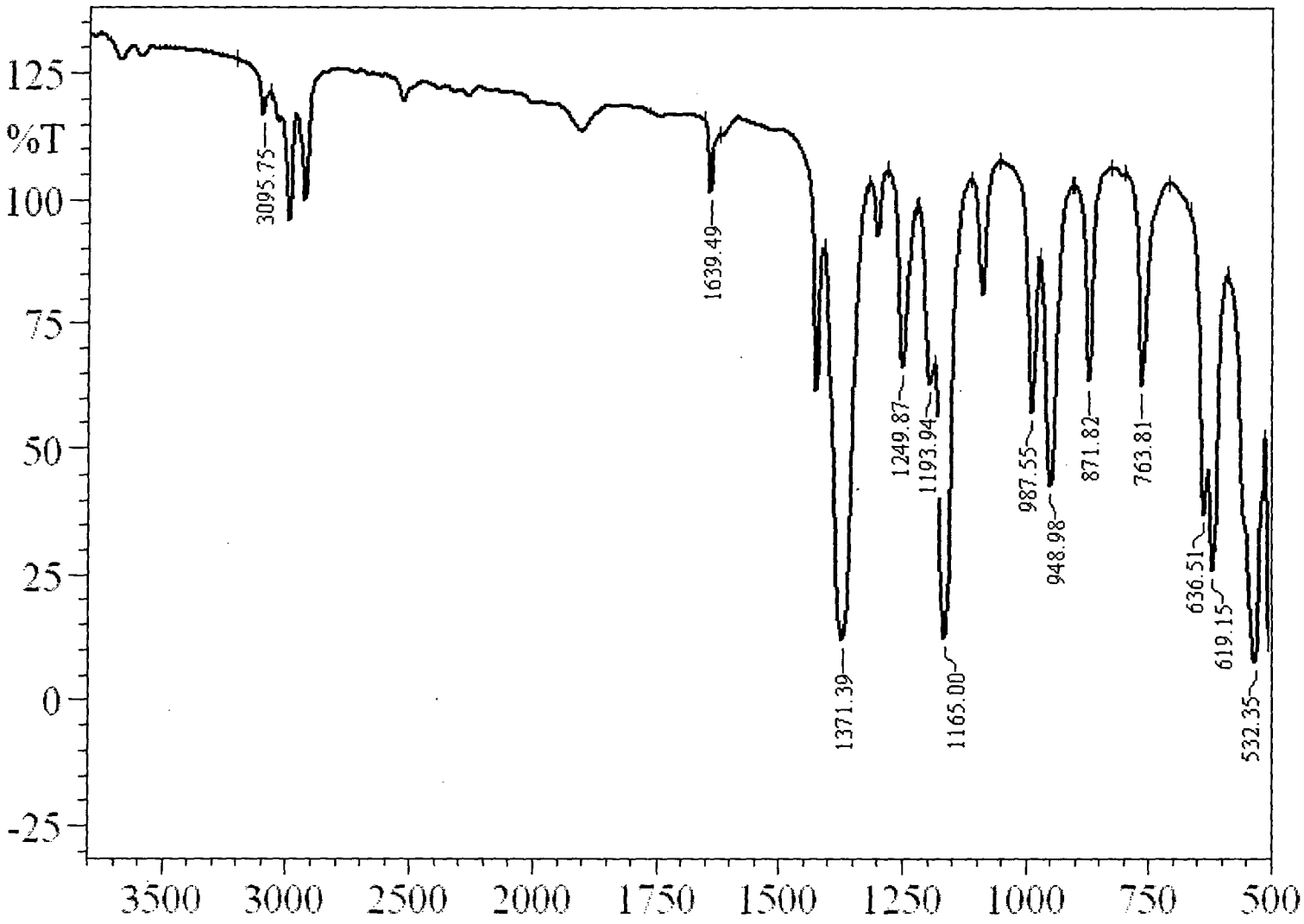

Figure 2.22: Infrared spectrum of allyl sulfonyl chloride.

iii) Diethyleneglycol bis(allyl sulfonate): Diethylene glycol (10 g, 0.094 mol) was cooled to 0 °C in a two neck flask having a thermometer pocket and dropping funnel. Chloro allyl sulfonate (26.7 g, 0.19 mol) was added to the flask and the mixture was stirred vigorously. Pyridine (15 g, 0.19 mol) was added drop by drop at such a rate that the temperature remained in the range of 0-5 °C. After this is complete, the mixture was stirred for further 1 hr. The product was suspended in 50 mL water and extracted with 3x50 mL of diethyl ether. The product obtained was purified by column chromatography using 3:7 v/v ethyl acetate/n-hexanes to afford DEAS (23.11 g, 78 %) as a white crystalline solid. The Scheme 2.8 depicts the reaction involved.

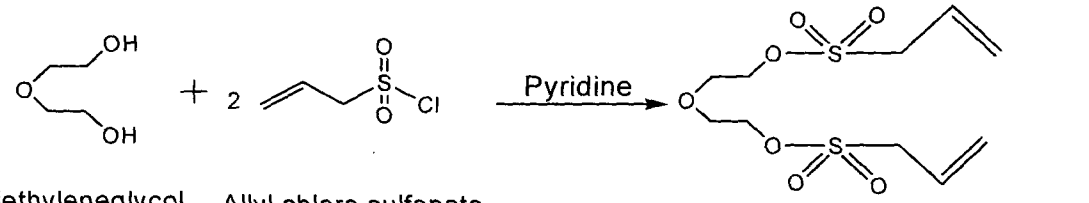

Diethyleneglycol Allyl chloro sulfonate Diethylene glycol bis(allylsulfonate)

Scheme 2.8: Synthesis of Diethyleneglycol bis(allyl sulfonate)

The structure of DEAS was characterized by recording its IR, ^{1}H NMR, ^{13}C NMR and HRMS data. Figures 2.23 to 2.26 (See page 104 - 107) give IR, PMR, CMR and HRMS spectra respectively, of DEAS monomer.

ν_{max}(KBr)/cm^{-1} 3089, 1641,1352, 1165; δH(300 MHz; $CDCl_3$; Me_4Si) 3.7 (4H, t, 2 x SO_2-C<u>H</u>$_2$-),3.8 (4H, t, 2 x O-C<u>H</u>$_2$-), 4.3 (4H, t, 2 x SO_2-O-C<u>H</u>$_2$-,), 5.4 (4H, dd, 2 x C<u>H</u>$_2$=), 5.9 (2H, m, 2 x C<u>H</u>=,); δC(300 MHz; $CDCl_3$; Me_4Si) 54.9 (2 x t), 69.1 (2 x t), 69.5 (2 x t), 124.4 (2 x d), 124.72 (2 x t), m/z (TOF ES) 337.0378 (M^+ + Na. $C_{10}H_{18}O_7S_2$ requires 337.0392)

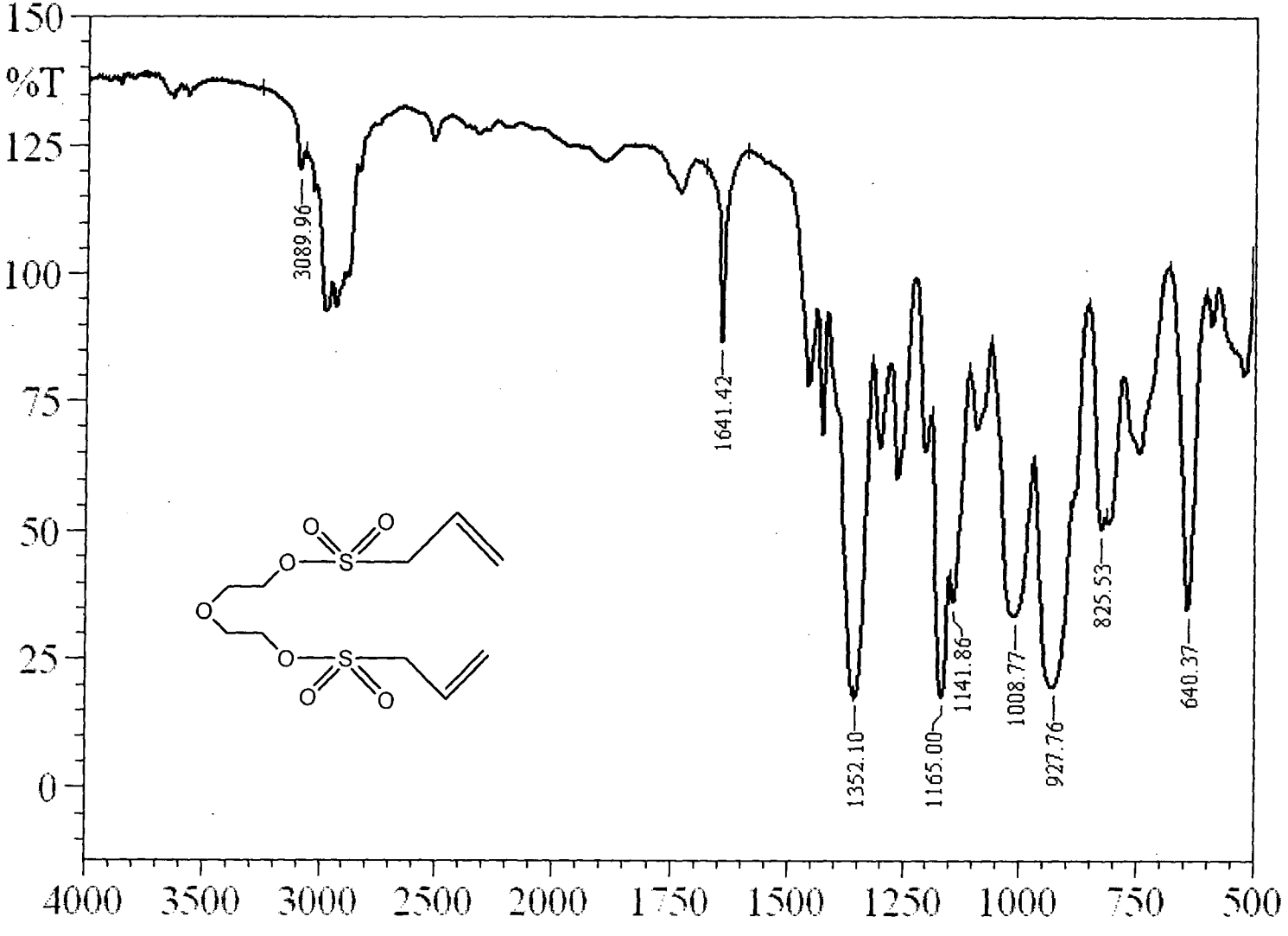

Figure 2.23: Infrared spectrum of diethylene glycol bis(allyl sulfonate).

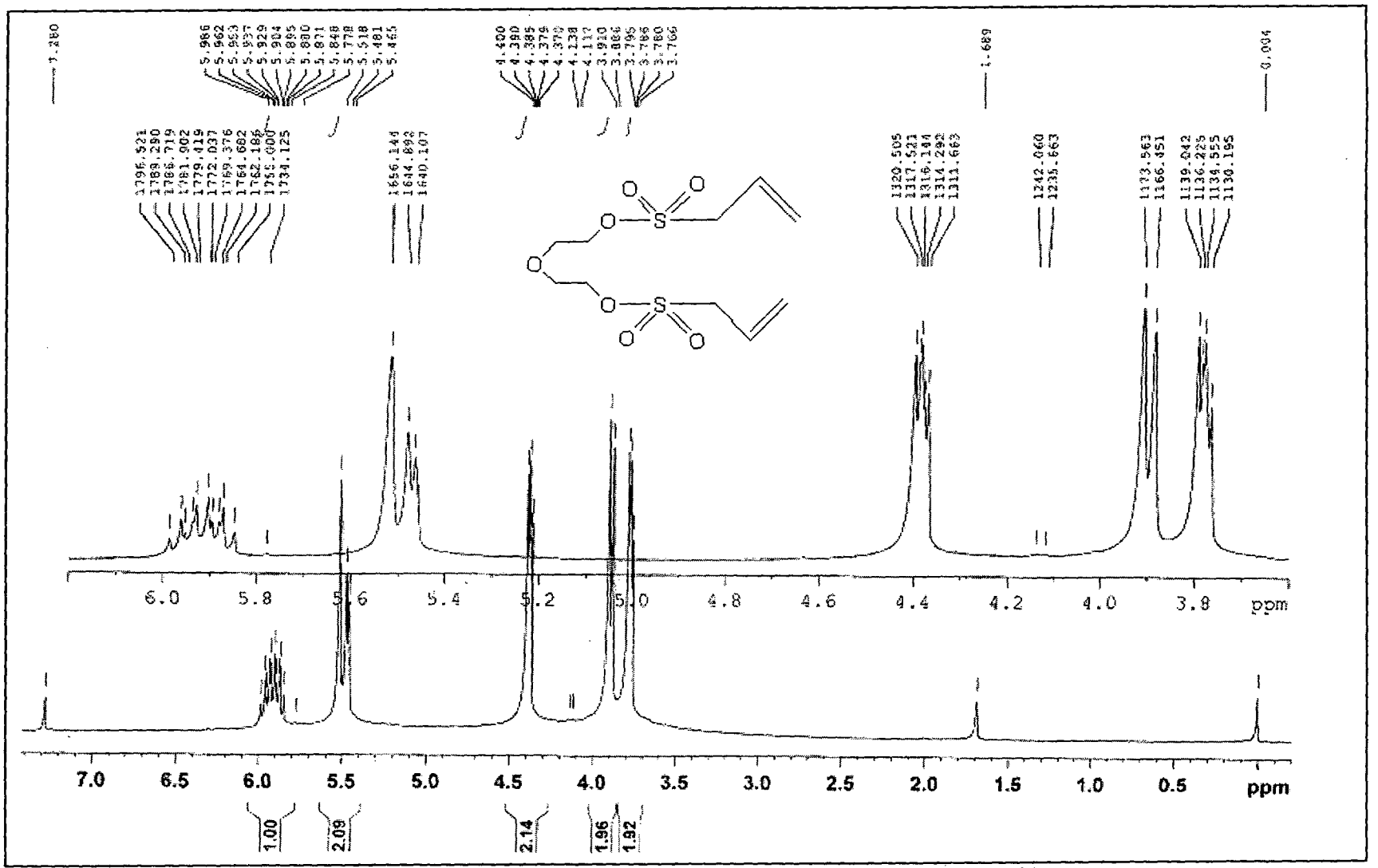

Figure 2.24: ^{1}H NMR spectrum of diethylene glycol bis(allyl sulfonate).

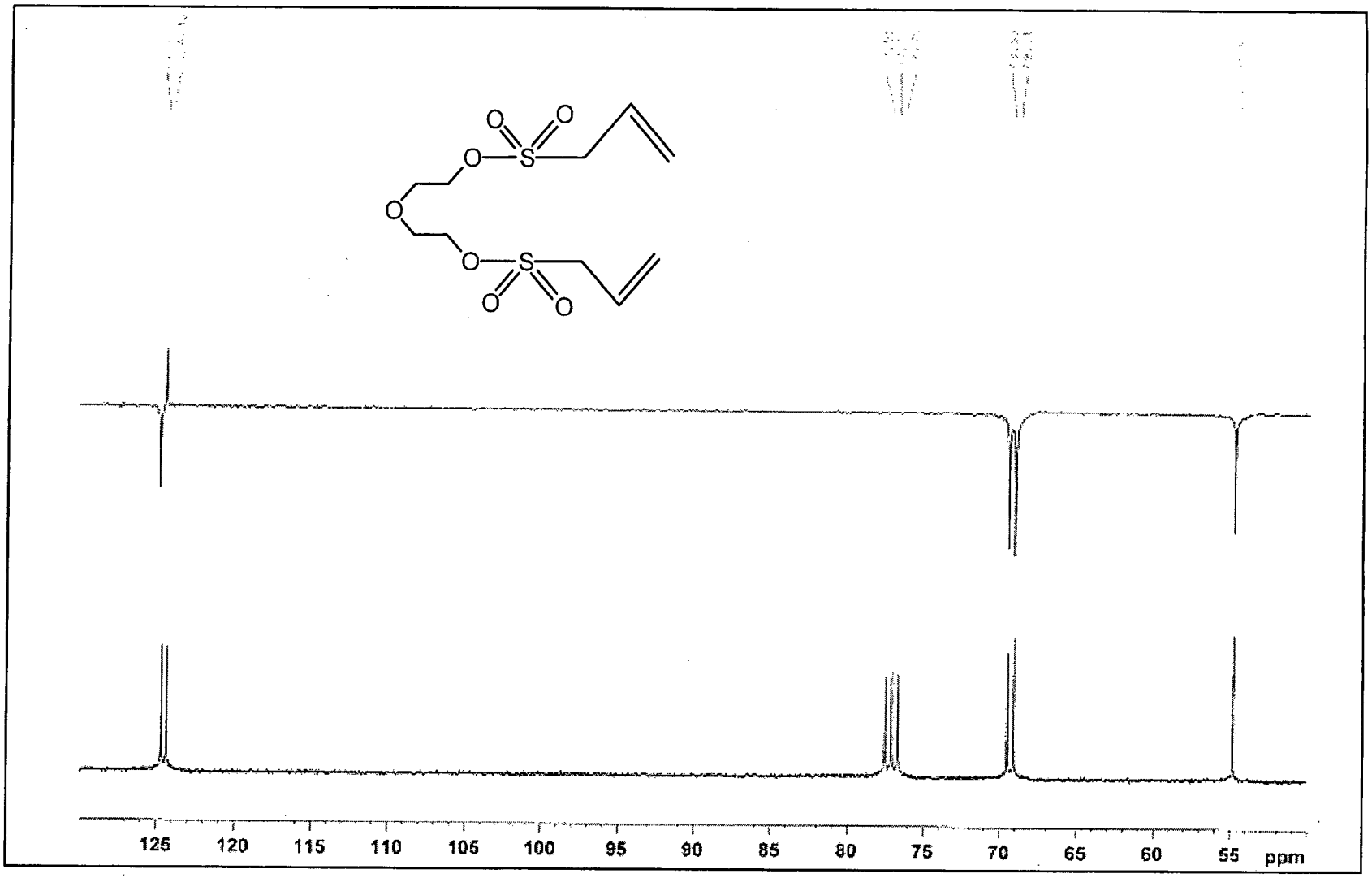

Figure 2.25: ^{13}C NMR spectrum of diethylene glycol bis(allyl sulfonate).

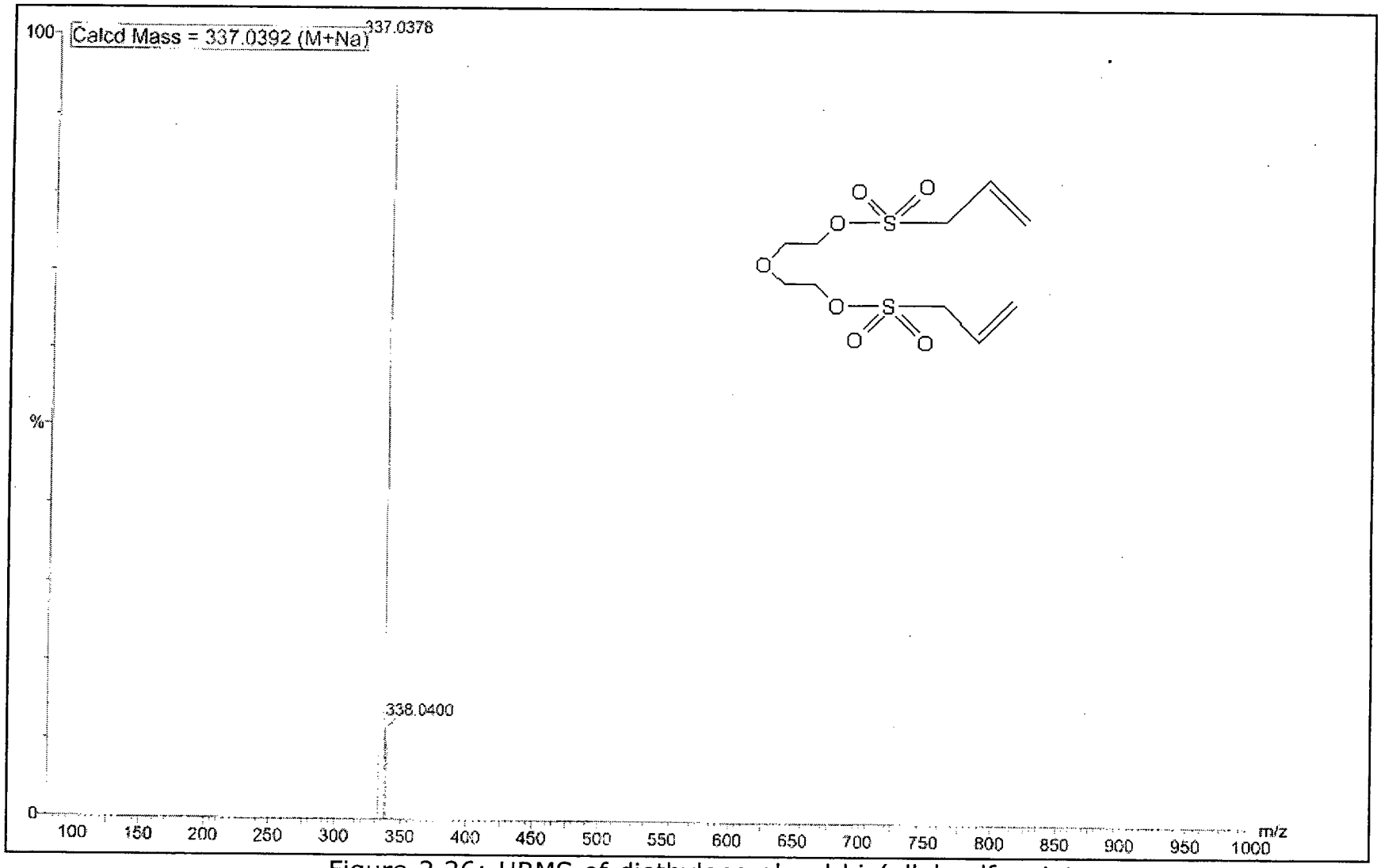

Figure 2.26: HRMS of diethylene glycol bis(allyl sulfonate).

2.6.8 Diethylene glycol bis(*n*-propyl sulfonate) (DEPS): DEAS (1 g, 3.2 mmol) monomer was dissolved in 20 mL ethyl acetate and 200 mg of 10 % Pd/C catalyst was added to the reaction mixture. The mixture was hydrogenated at 3 Kg/cm^2 of hydrogen pressure using the hydrogenation apparatus for 40 hrs. The reaction mixture was filtered and concentrated to get 0.888 g of crude product. The product was finally purified by column chromatography using silica gel and 1:1 v/v ethyl acetate/*n*-hexanes mixture as eluent to afford DEPS (0.754 g, 74 %) as a colorless liquid.

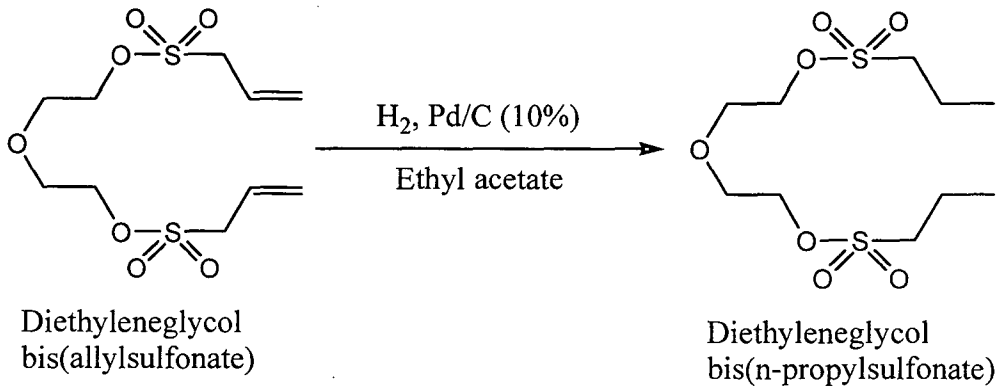

Scheme 2.9: DEPS monomer synthesis.

The structure of DEPS was characterized by using its IR, ^{1}H NMR & ^{13}C NMR spectral data (Figures 2.27 to 2.29, See page 109 - 111) ν_{max}(KBr)/cm^{-1} 1346, 1165, 935; δH(300 MHz; $CDCl_3$; Me_4Si) 1.1 (6H, p, 2 x -CH_2-$C\underline{H}_3$), 1.9 (4H, m, 2 x -$C\underline{H}_2$-CH_3), 3.1 (4H, p, 2 x -$C\underline{H}_2$-SO_2-), 3.8 (4H, p, 2 x -O-$C\underline{H}_2$-), 4.3 (4H, p, 2 x -SO_2-O-$C\underline{H}_2$-); δC(300 MHz; $CDCl_3$; Me_4Si) 12.8 (2 x q), 17.2 (2 x t), 52.2 (2 x t), 68.2 (2 x t), 69.1 (2 x t)

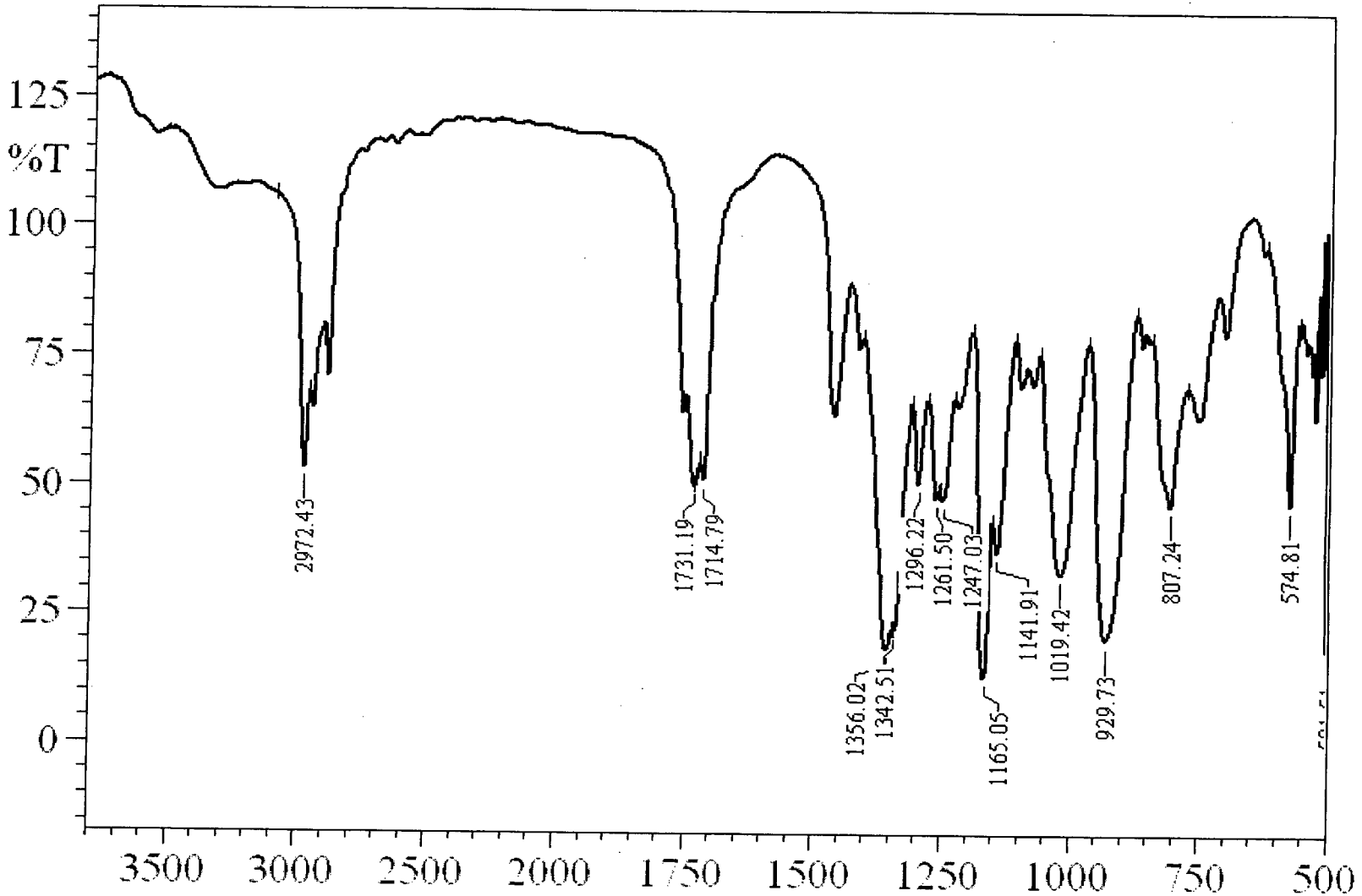

Figure 2.27: Infrared spectrum of diethylene glycol bis(n-propyl sulfonate) in ethyl aceate.

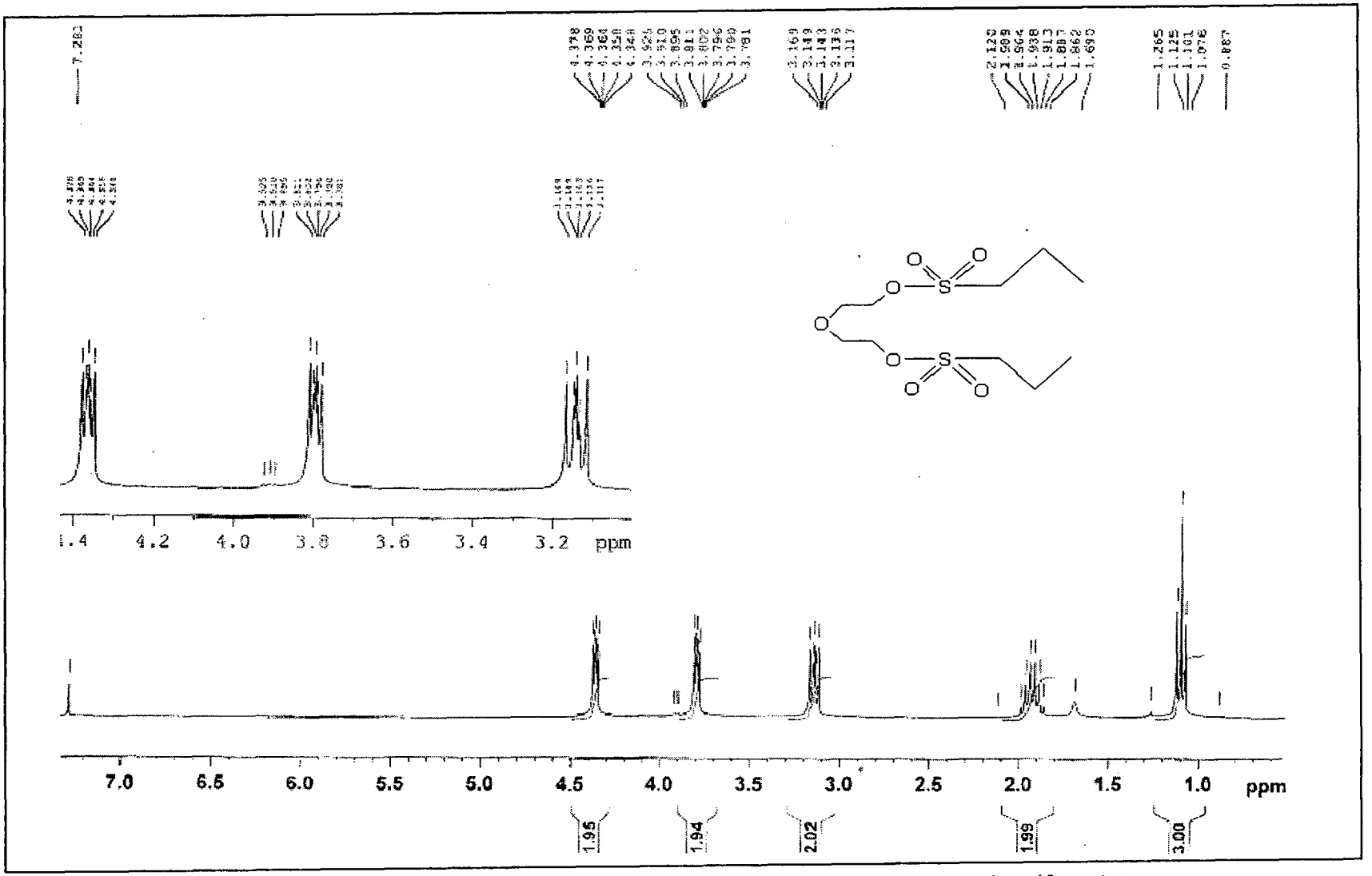

Figure 2.28: ^{1}H NMR spectrum of diethylene glycol bis(n-propyl sulfonate).

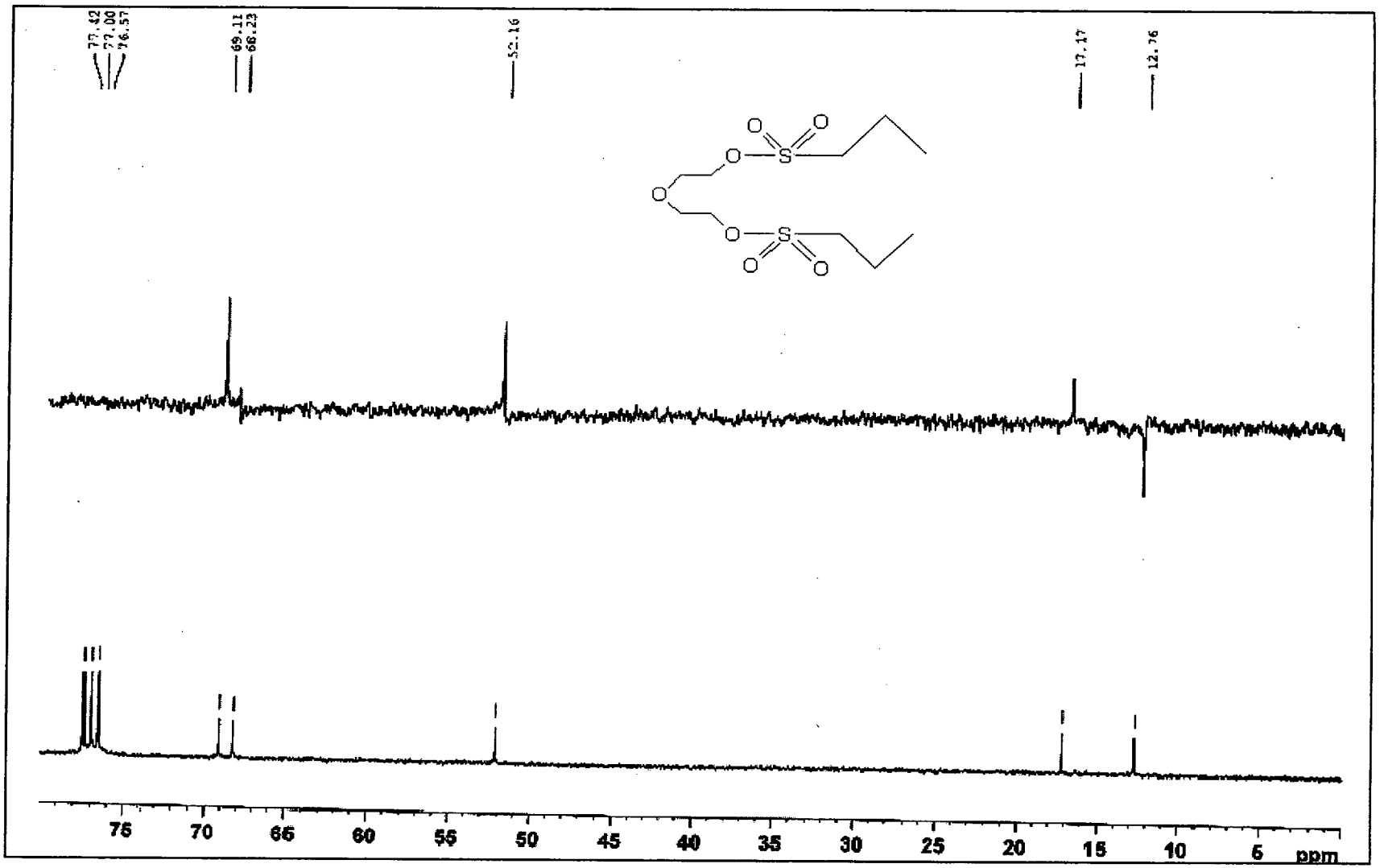

Figure 2.29: ^{13}C NMR spectrum of diethylene glycol bis(allyl sulfonate).

2.6.9 Pentaerythritol terakis(allyl carbonate):[115,127,128] In a three neck flask cooled to 0 °C, Pentaerythritol (10 g, 0.073 mol) was suspended in 50 mL benzene containing pyridine (23.82 g, 0.302 mol) The flask was provided with a mechanical stirrer, a dropping funnel and a thermometer. Allyl chloroformate (36.35 g, 0.302 mol) was added drop by drop with vigorous stirring. The temperature was not allowed to rise above 5 °C. After complete addition of allyl chloroformate the mixture was stirred for 1hr at room temperature. The mixture was washed with 1 × 50 mL 2 N HCL, 3 × 50 mL of water and organic layor dried over anhy. Na_2SO_4. The solvent was removed under vacuum to afford 27.21 g of crude product. The product was purified by activated carbon treatment followed by column chromatography using 3:7 v/v ethyl acetate/ n-hexanes mixture to get (26.13 g, 75 %) light yellow liquid.The structure of PETAC was characterized by its IR, PMR CMR and mass spectral data given in Figure 2.30 to 2.33 (page 113 - 116).

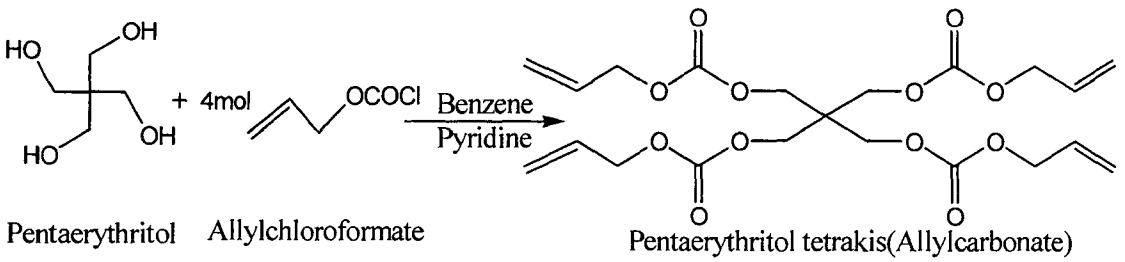

Scheme 2.10: Synthesis of PETAC monomer.

ν_{max}(KBr)/cm^{-1} 1751, 1371, 1244,986; δH(300 MHz; $CDCl_3$; Me_4Si) 4.18 (8H, s, 4 x -C-C$\underline{H}_2$), 4.54(8H, t, 4 x -O-C$\underline{H}_2$-CH=), 5.22 (4H, dd, 4 x -C$\underline{H}$=), 5.84(8H, m, 4 x C$\underline{H}_2$=);δC(300 MHz; $CDCl_3$; Me_4Si) 43.9 (1 x C), 66.6 (4 x t), 70.2 (4 x t), 120.6(4 x t), 132.6 (4 x d), 155.8 (4 x s); m/z (TOF ES) 495.1476 (M^+ + Na. $C_{21}H_{28}O_{12}$ requires 495.1478)

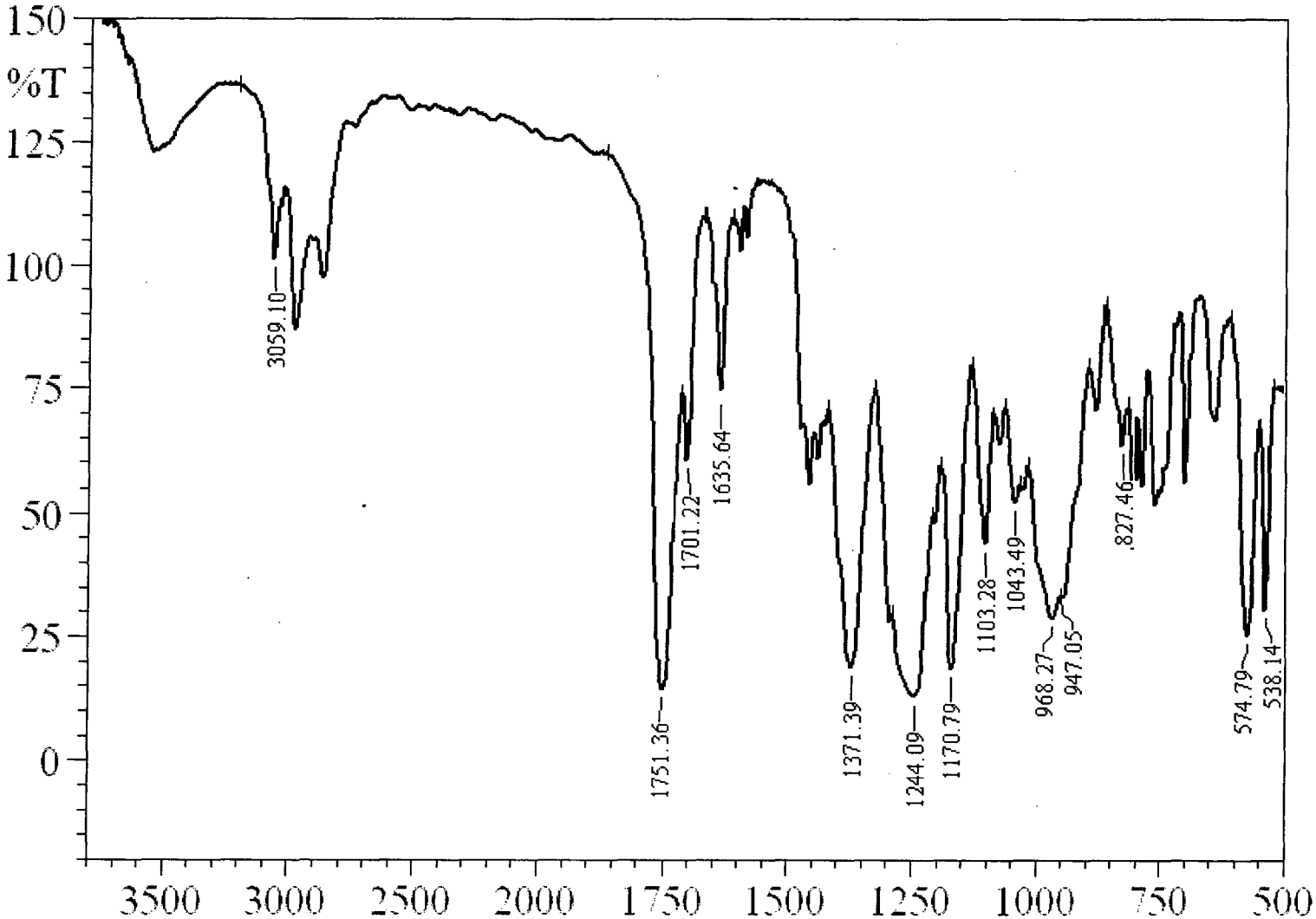

Figure 2.30: Infrared spectrum of Pentaerythritol tetrakis(allyl carbonate).

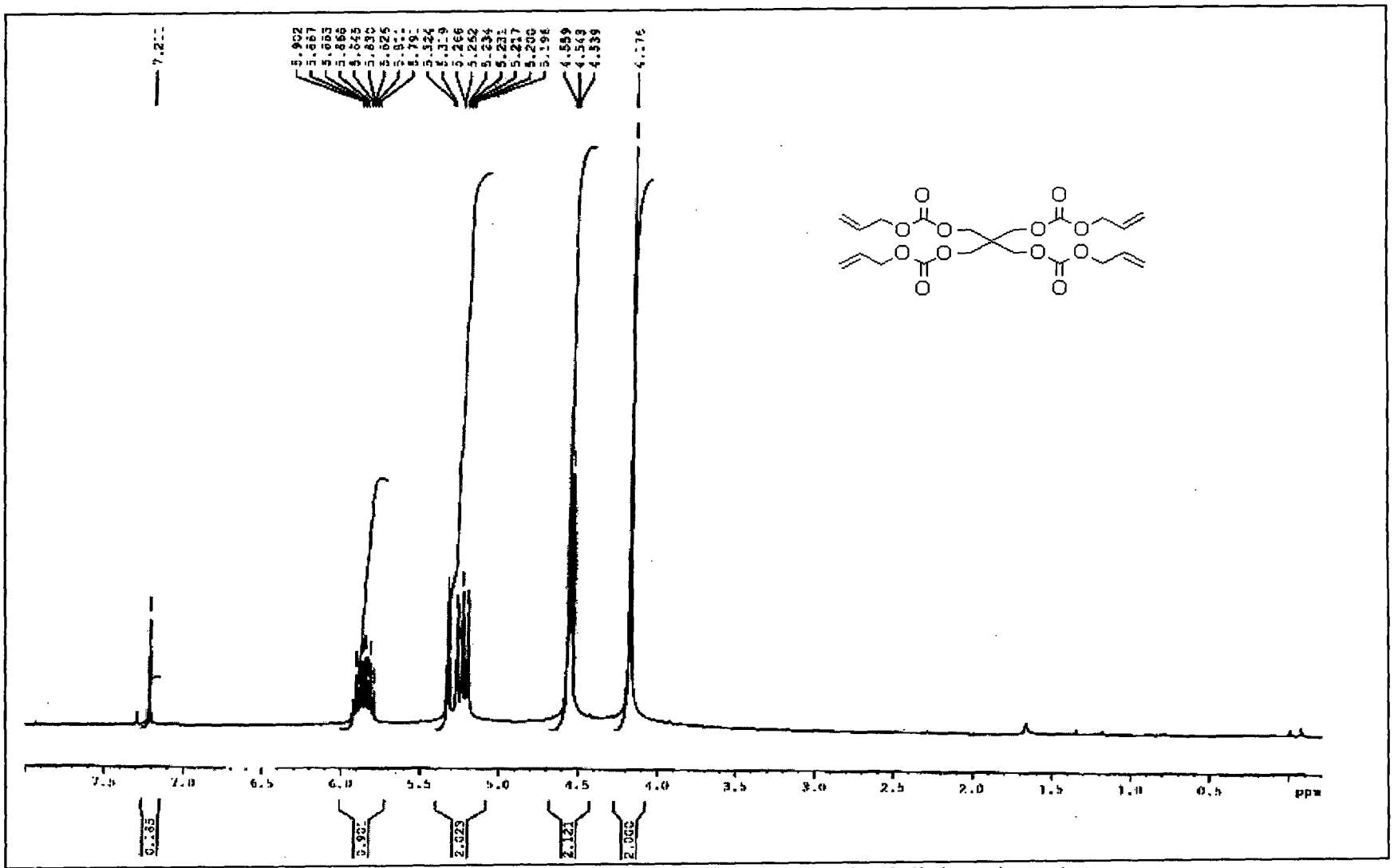

Figure 2.31:[1]H spectrum of pentaerythritol tetrakis(allyl carbonate).

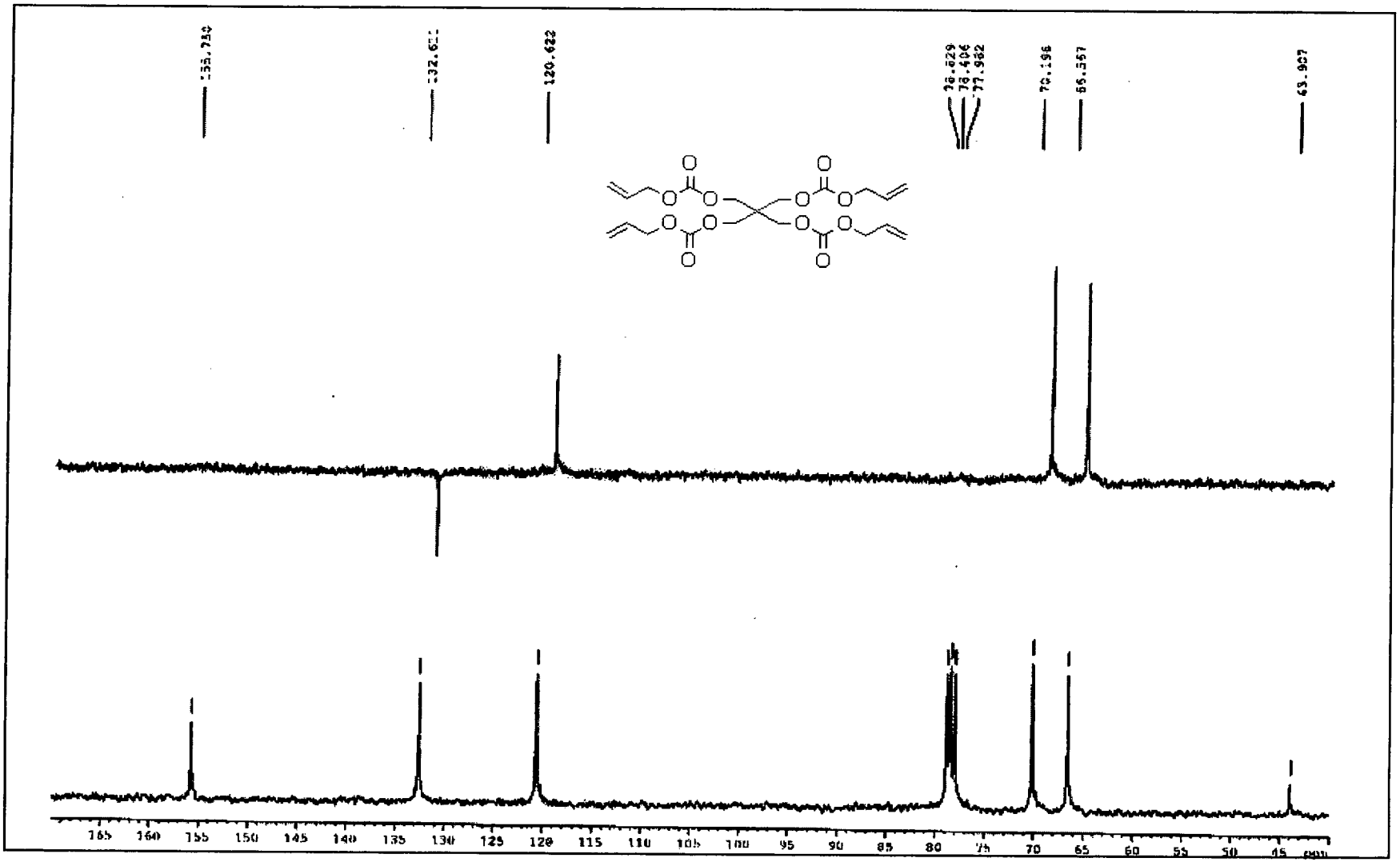

Figure 2.32: ^{13}C NMR spectrum of pentaerythritol tetrakis(allyl carbonate).

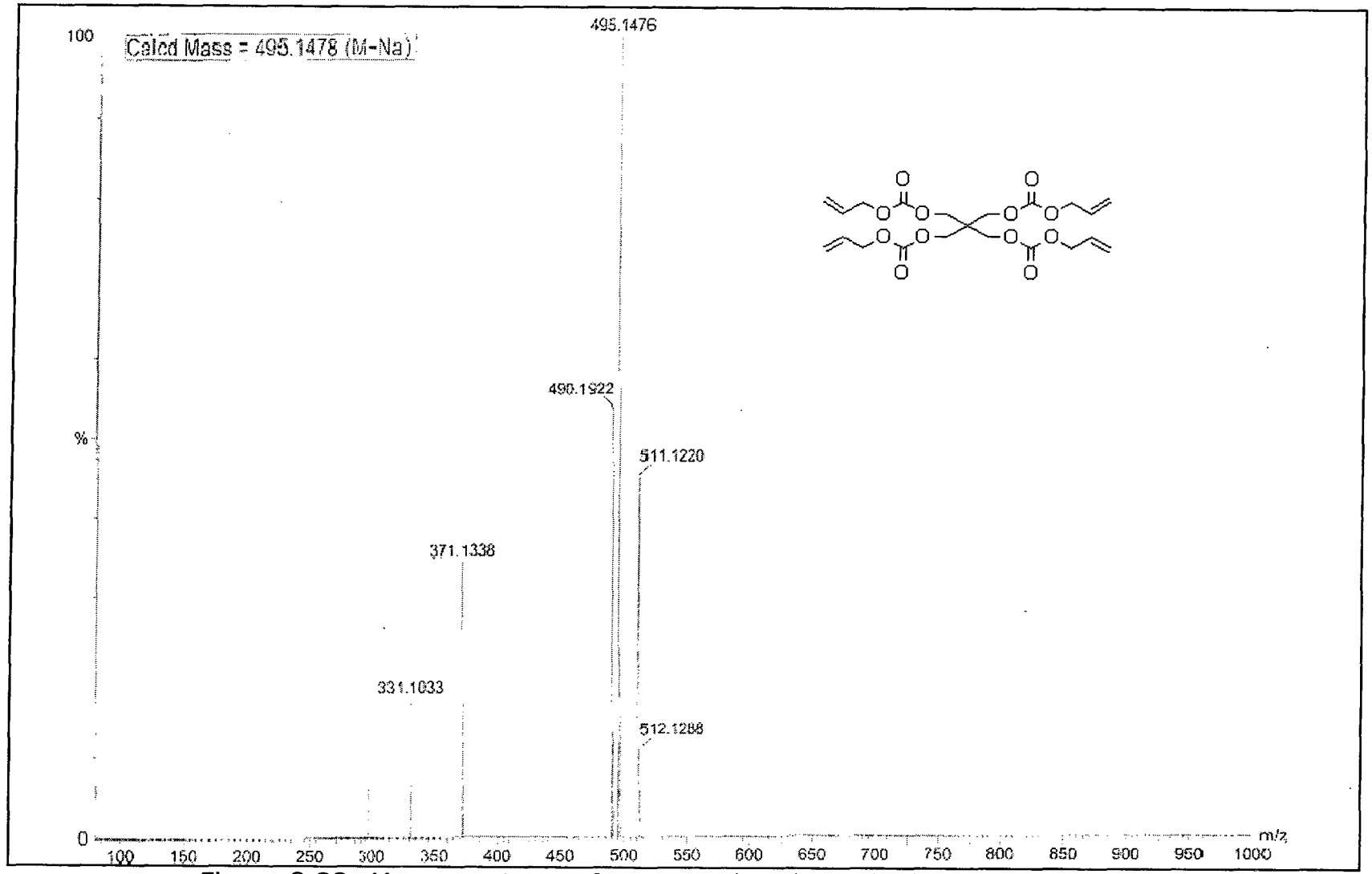

Figure 2.33: Mass spectrum of pentaerythritol tetrakis(allyl carbonate).

2.6.10 Isopropylperoxydicarbonate:[129] Isopropyl chloroformate (10 g, 0.082 mol) was taken in a two neck flask provided with a thermometer pocket and a magnetic stirrer. The flask was cooled using a cryostat and the temperature inside the flask was maintained at 2 °C. Na_2O_2 (3.28 g, 0.042 mol) prepared from aq. H_2O_2 and aq. NaOH was added drop by drop at such a rate that temperature inside the flask does not rise above 6 °C. After completion of addition, the mixture was stirred for further 1 hr at temperature between 5-10 °C. The product obtained was extracted in dichloromethane and washed with 2 × 20 mL ice cold water. The organic layer was dried over anhy. Na_2SO_4 and solvent evaporated under reduced pressure at a temperature below 20 °C. The product obtained was stored at temperature below 0 °C. The IPP initiator so obtained was analyzed by iodometry and used for polymerization without further purification. The IR spectrum of the compound is shown in Figure 2.34, page 118. ν_{max}(KBr)/cm^{-1} 2987, 1797, 1209,1095. The synthetic scheme is given below.

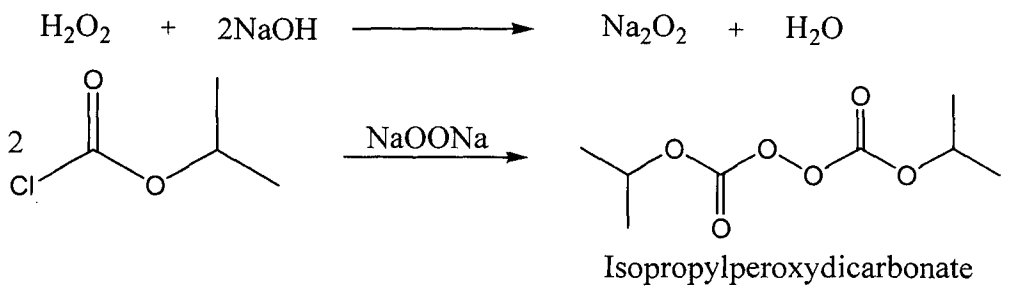

Scheme 2.11: IPP initiator synthesis.

PRECAUTIONS:

1) Initiator should not be prepared in large quantities as it de grades violently.
2) Initiator should be stored always below 0 °C.
3) Rapid drying should be performed on anhy. Na_2SO_4.
4) Initiator should be analyzed before use.

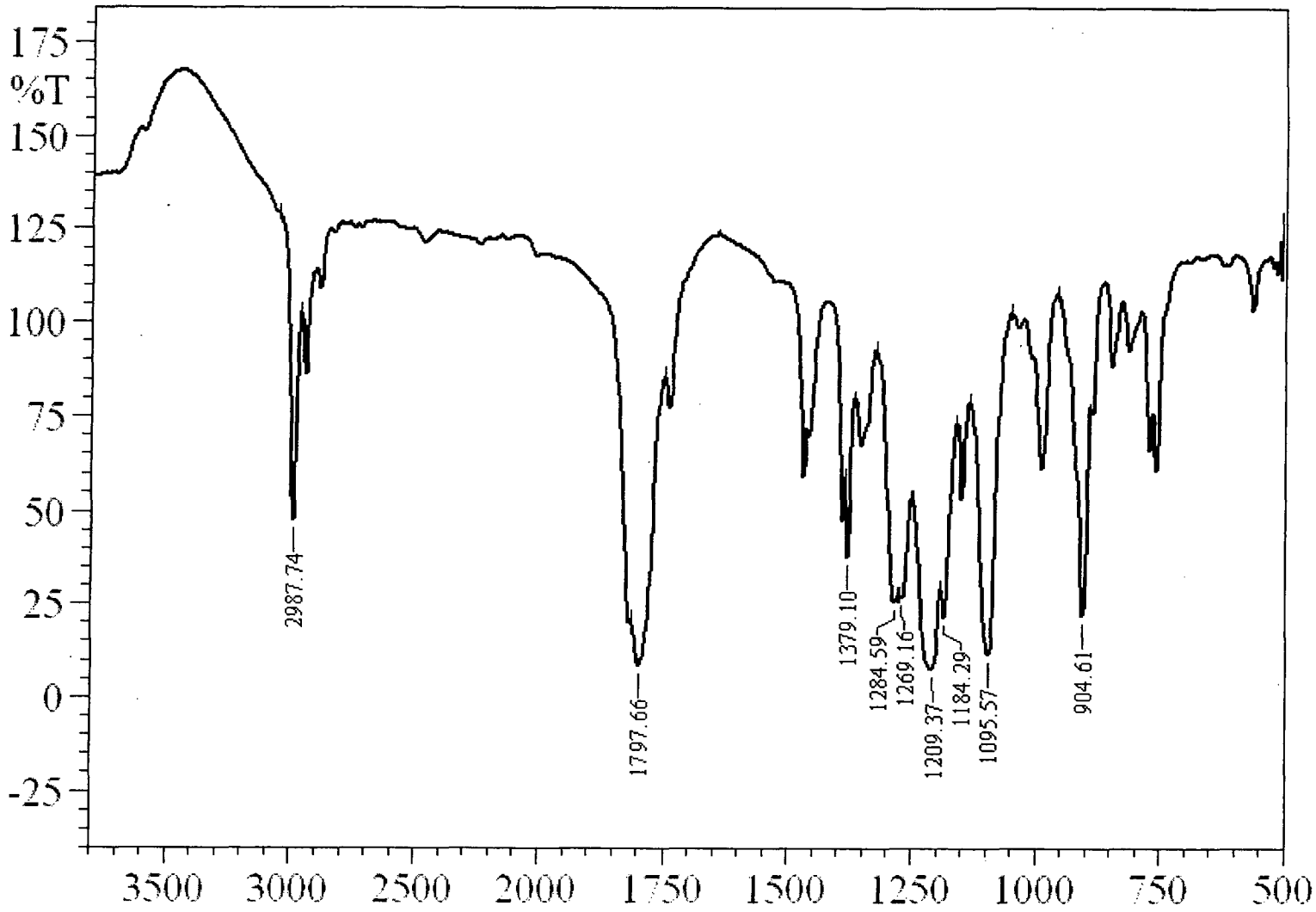

Figure 2.34: Infrared spectrum of IPP initiator.

2.6.11 Pentaerythritol bis(allyl carbonate) bis(allyl sulfonate): The monomer was synthesized as a white solid product using multi step stratergy . However the product is highly unstable and decomposes on storage. The synthetic is as discussed below.

Pentaerythritol mono(benzal):[130] Pentaerythritol (50 g, 0.37 mol) was dissolved in 360 mL water containing 2 mL of concentrated HCl in a three neck flask provided with magnetic stirrer, a dropping funnel and a thermometer. Under vigorous stirring, benzaldehyde (40.83 mL, 0.37 mol) was added to the flask drop by drop. After complete addition, the mixture was stirred for 1 hr. The white precipitate obtained was filtered on a Buckner funnel and washed with alkaline cold water. The solid product obtained was refluxed in 80 mL toluene and filtered. The filtrate obtained was cooled at 0 °C to crystallize the product which was filtered and dried to obtain the pentaerythritol mono(benzal) (56.37 g, 68.45 %) as a white solid.

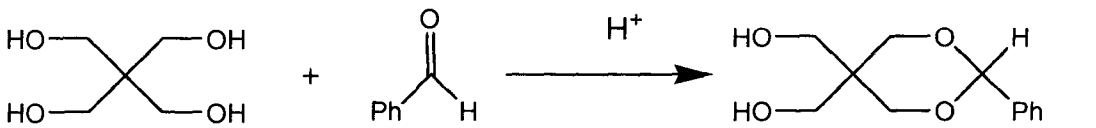

Pentaerythritol Benzaldehyde Pentaerythritol mono(benzal)

Scheme 2.12: Pentaerythritol mono(benzal).

Pentaerythritol mono(benzal) bis(allyl carbonate): Pentaerythritol mono(benzal) (25 g, 0.112mol) was suspended in diallyl carbonate (159 g, 1.12 mol) in a three necked flask fitted with a distillation head, dry nitrogen inlet and a thermometer pocket. Nitrogen was bubbled and the reaction was heated to 60 °C using an oil bath. 1 g of KOH was added and the temperature was raised to 110 °C, when allyl alcohol distills out from the mixture. After about (12 g, 0.224 mol) of allyl alcohol was distilled and reaction

was allowed to cool. The mixture was taken in ether and washed with 3 × 50 mL distilled water. The organic layer was dried over anhy. Na_2SO_4. Ether was evaporated and the mixture was vacuum distilled to remove diallyl carbonate. The product remained in distillation flask as a light brown liquid which was used without further purification in next step. The synthetic scheme is given below.

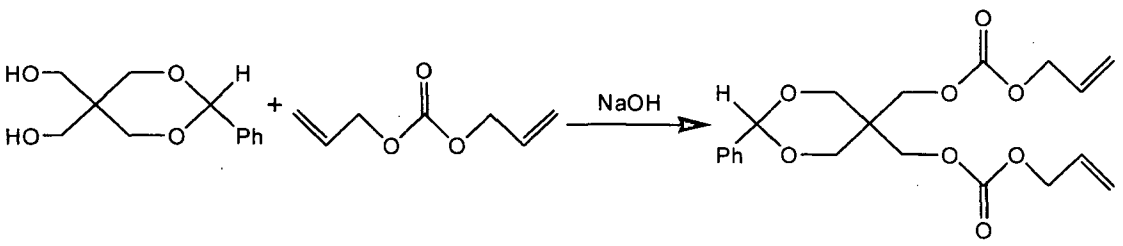

Pentaerythritol mono(benzal) | Diallyl carbonate | Pentaerythritol mono(benzal) bis(allylcarbonate)

Scheme 2.13: Synthesis of Pentaerythritol mono(benzal) bis(allyl carbonate).

Pentaerythritol bis(allyl carbonate): Pentaerythritol mono(benzal) bis(allyl carbonate) (20 g, 0.05 mol) was placed in a two neck flask provided with fractional distillation setup. 120 mL of 1:1 acetic acid:water mixture was added and the flask was heated to 120 °C. Benzaldehyde (5 g, 0.047 mol) was removed by azeotropic distillation. Finally, acetic acid and water was removed by vacuum distillation. Pentaerythritol bis(allyl carbonate) (11.32 g, 73 %) was obtained as a white solid.

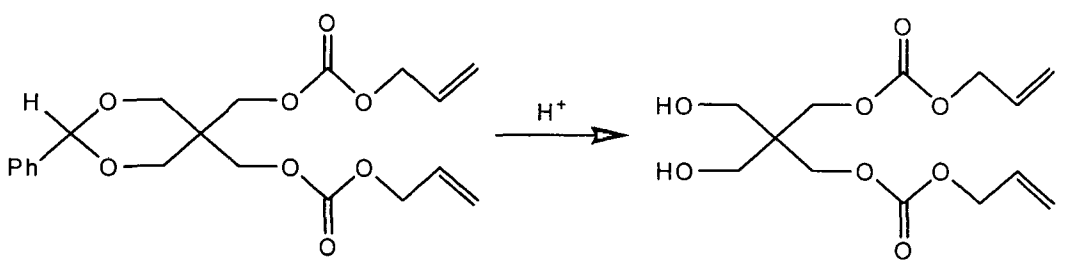

Pentaerythritol mono(benzal) bis(allylcarbonate) | Pentaerythritol bis(allylcarbonate)

Scheme 2.14: Synthesis of Pentaerythritol bis(allyl carbonate).

The IR specta of the compound is shown in Figure 2.35, Page 122.

ν_{max}(KBr)/cm^{-1} 3485, 3088, 1737, 1249.

Pentaerythritol bis(allyl carbonate) bis(allyl sulfonate): Recrystallised pentaerythritol bis(allyl carbonate) (5 g, 0.0164 mol) was cooled to 10 °C and pyridine (2.6 g, 0.0328 mol) was added along with 20 mL dichloromethane. Allyl sulfonyl chloride (4.6 g, 0.0328 mol) was added drop by drop and temperature maintained below 15 °C during the course of addition. The mixture was stirred for 1hr at room temperature. The organic layer was washed with 1 × 20 mL of 2 N HCl and 3 × 20 mL distilled water. The organic layer was dried over anhy. Na_2SO_4 and solvent was removed under vacuum. The product was purified by silica gel column chromatography using 3:7 v/v ethyl acetate/n-hexanes mixture as a white solid. The IR spectrum of the product (Figure 2.36, Page 123) showed complete conversion of the starting. ν_{max}(KBr)/cm^{-1} 3086, 1751, 1647, 1246, 968. However, the PMR shows more peaks in addition to the product peaks (Figure 2.36, Page 124). Decomposition can be seen in the HRMS (Figure 2.38, Page 125) of the product which suggest formation of the following product from the M+H peak observed at m/z 307 by nucleophilic substitution reaction.

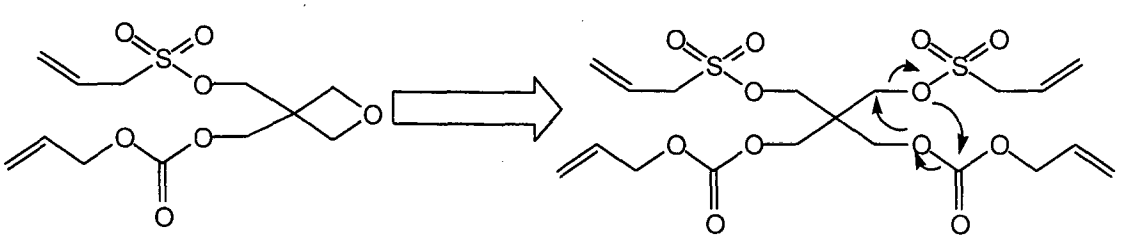

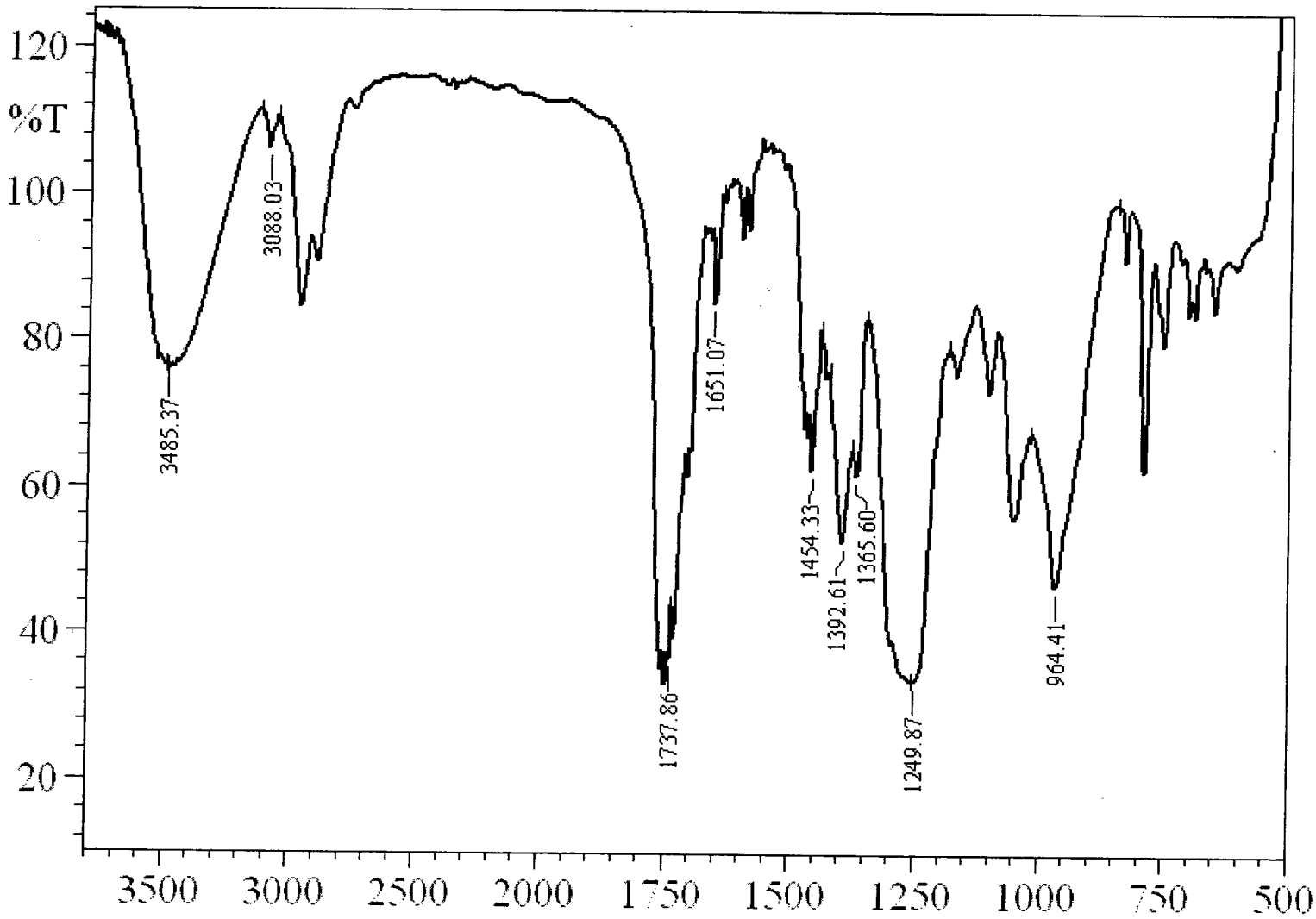

Figure 2.35: Infrared spectrum of Pentaerythritol bis(allyl carbonate).

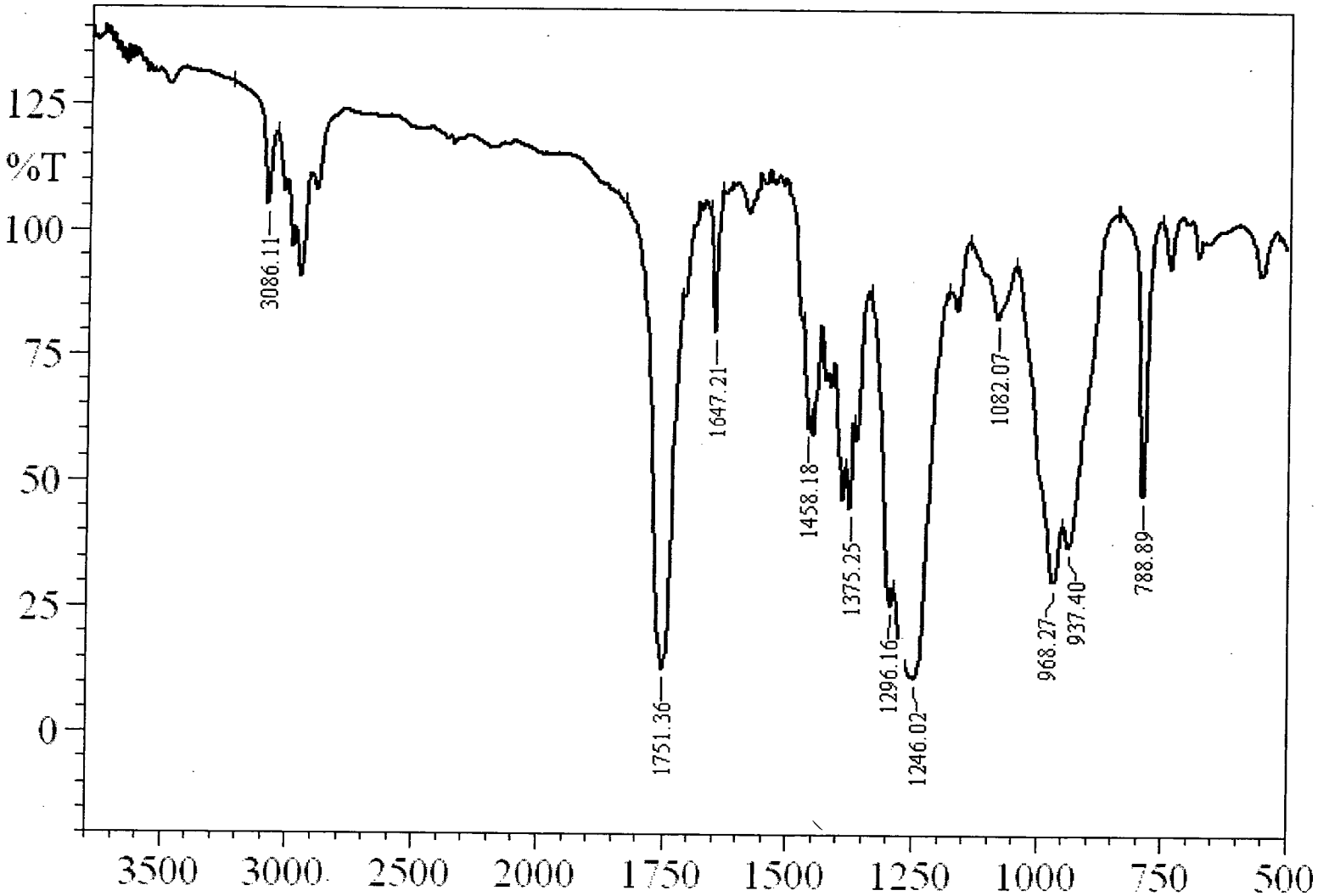

Figure 2.36: Infrared spectrum of Pentaerythritol bis(allyl carbonate) bis(allyl sulfonate) .

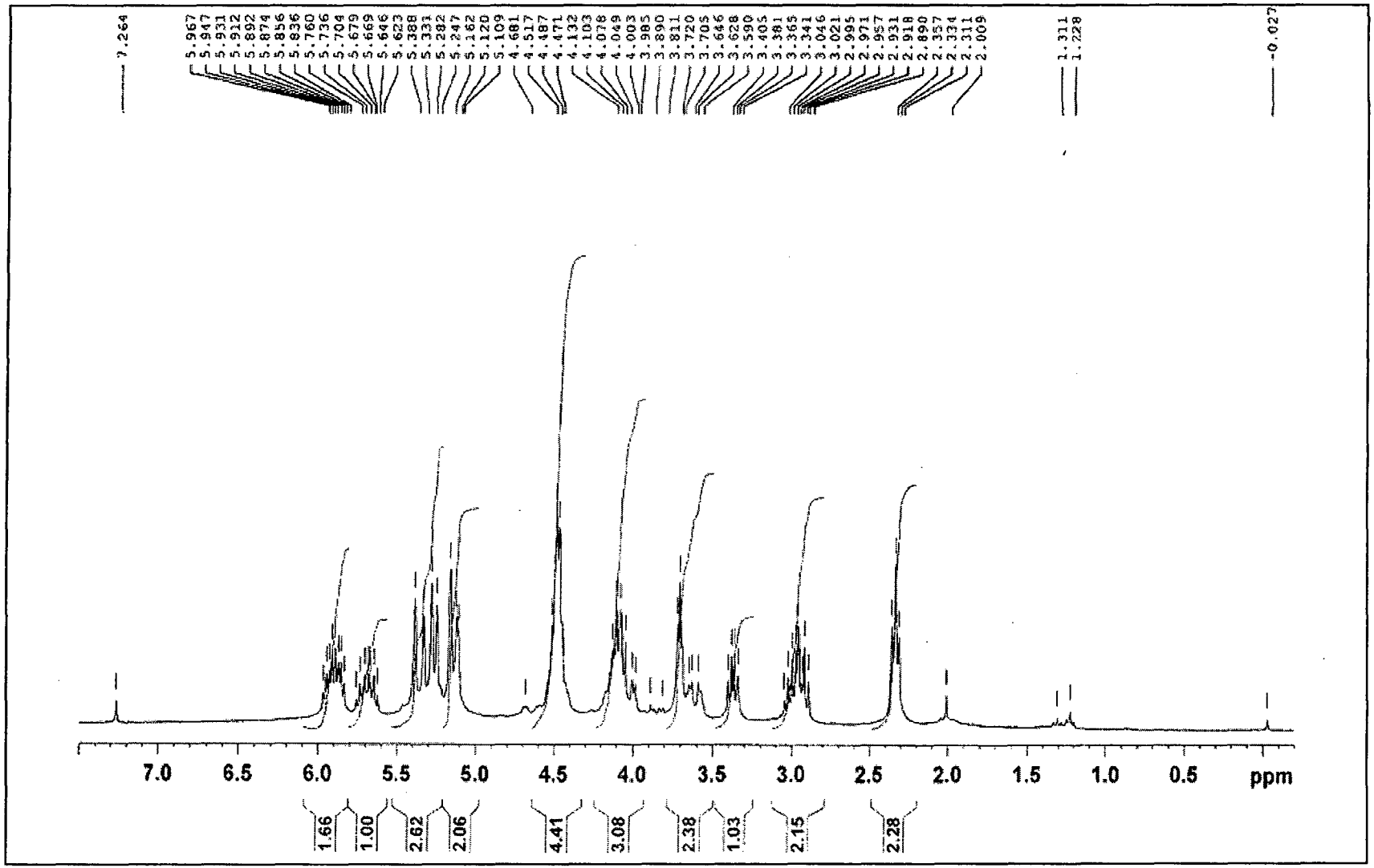

Figure 2.37: ^{1}H NMR of Pentaerythritol bis(allyl carbonate) bis(allyl sulfonate).

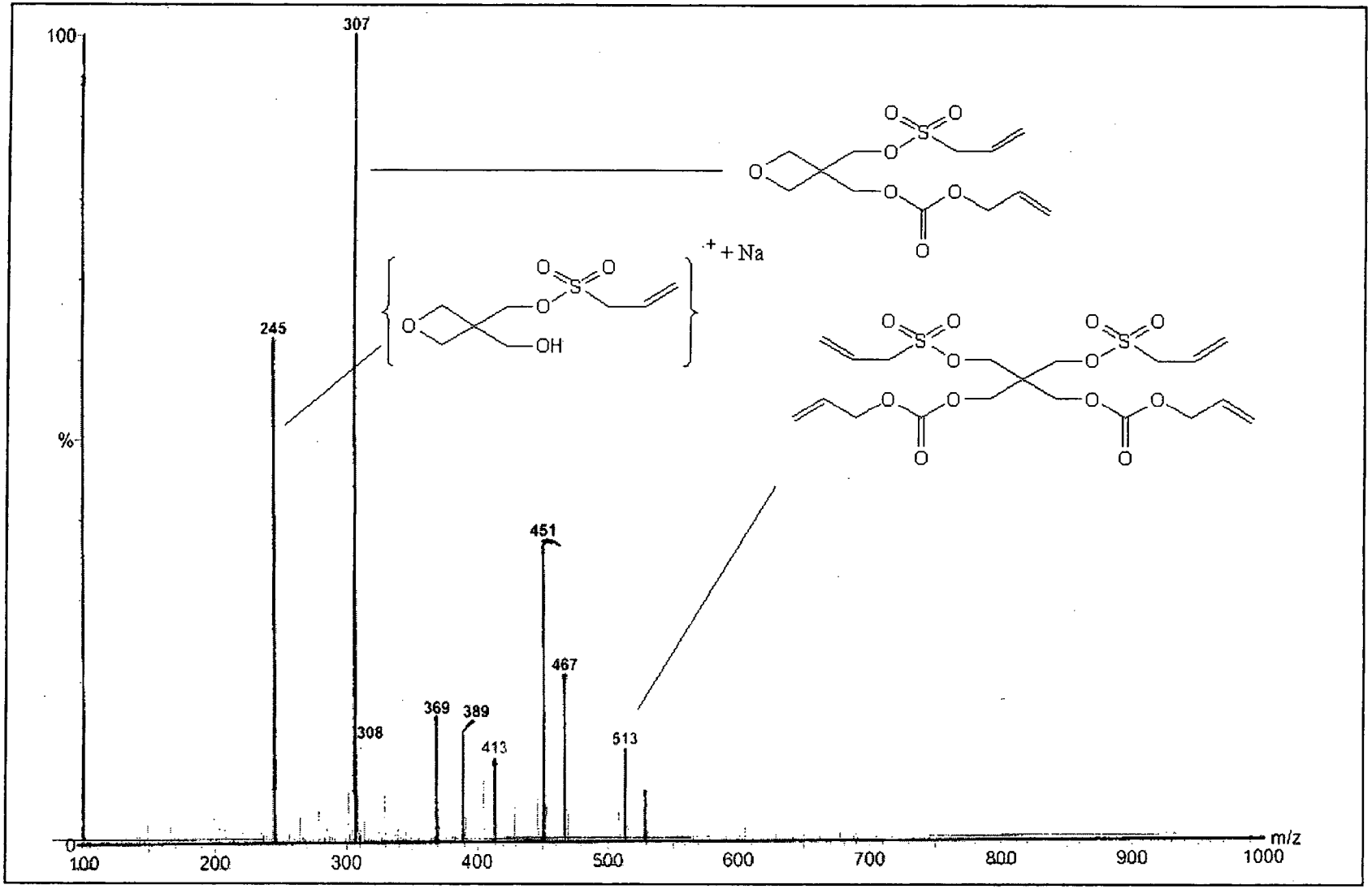

Figure 2.38: HRMS of Pentaerythritol bis(allyl carbonate) bis(allyl sulfonate) .

2.6.12 Pentaerythritol tetrakis(allylsulfonate)PETAS: The success of the PETAC monomer encouraged us to prepare the PETAS monomer as the polymer of the monomer would have had more vulnerable sulfonate group in addition to high crosslinks in the matrix. Pentaerythritol was reacted with allyl sulfonyl chloride in presence of base to get the desired monomer. The synthetic scheme proposed for the synthesis is as illustrated.

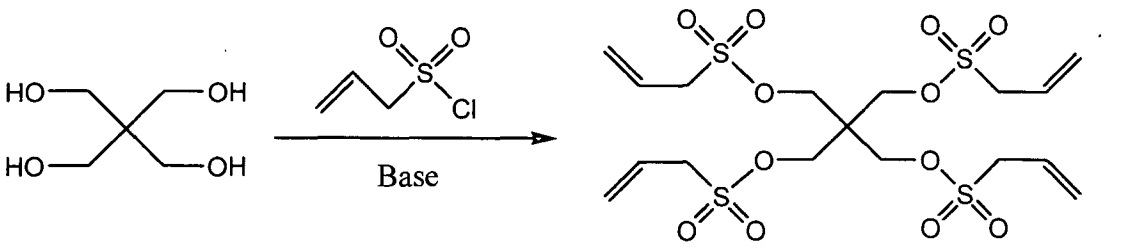

Pentaerythritol

Pentaerythritol tetrakis(allylsulphonate)

Scheme 2.15: Pentaerythritol tetrakis(allyl sulfonate)PETAS.

Table 2.1 gives different reaction conditions tried to prepare the PETAS monomer. However, all the attempts in this direction failed. In some cases, no product was formed, whereas, in other cases, a tarry product material was obtained. The IR spectra of the tarry product is shown in figure 2.39, Page 128. ν_{max}(KBr)/cm^{-1} 1635, 1372, 1166, 948.

Reaction condition	Base	Observations
Benzene reflux	Not added	No product
Neat	Not added	No product
RT, benzene	Pyridine	Black tarry product
0 °C, benzene	Pyridine	Black tarry product
0 °C, benzene	Triethyl amine	Black tarry product
0 °C, benzene	NaOH	No product
0 °C	aq. NaOH	No product
0 °C, Aliquat, DCM	NaOH	No product

0 °C, Aliquat, DCM	Pyridine	Black tarry product
0 °C	aq. Na2CO3	No product
0 °C, DCM	Pyridine	Black tarry product
0 °C, Dioxane	n-BuLi	No product
0 °C, Dioxane	NaH	No product

Table 2.1: Reaction conditions used for synthesis of PETAS.

2.7 X-Ray Characterizationof DEAS: It was observed that DEAS was solid and melted at 53 °C, whereas, it's functional isomer ADS with same molecular formula of $C_{10}H_{18}O_7S_2$ was liquid. The single crystal X-ray studies were performed on the monomer which showed that the molecules are involved in several weak C-H....O interactions.[131] The crystal structure of the title compound shows that the molecules are located with the ether oxygen atom (O_1) on a 2-fold axis with one half of the molecule constituting the asymmetric unit.

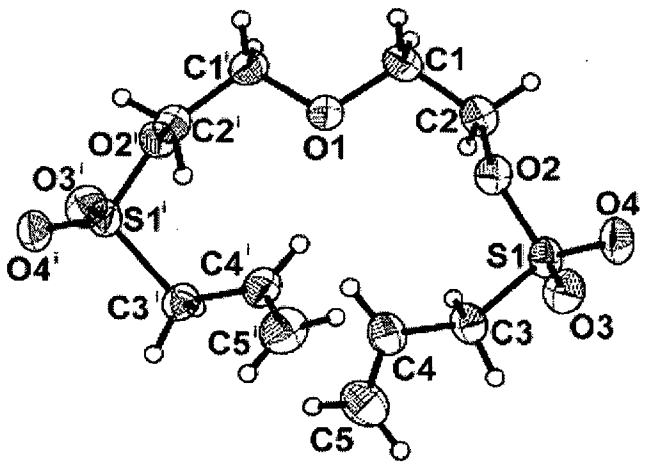

Figure 2.40: Crystal structure of DEAS showing the atom labeling scheme. Displacement ellipsoids are drawn at 30 % probability level. The O_1 atom is situated on a two-fold axis.

From the analysis of the structure of DEAS one finds that

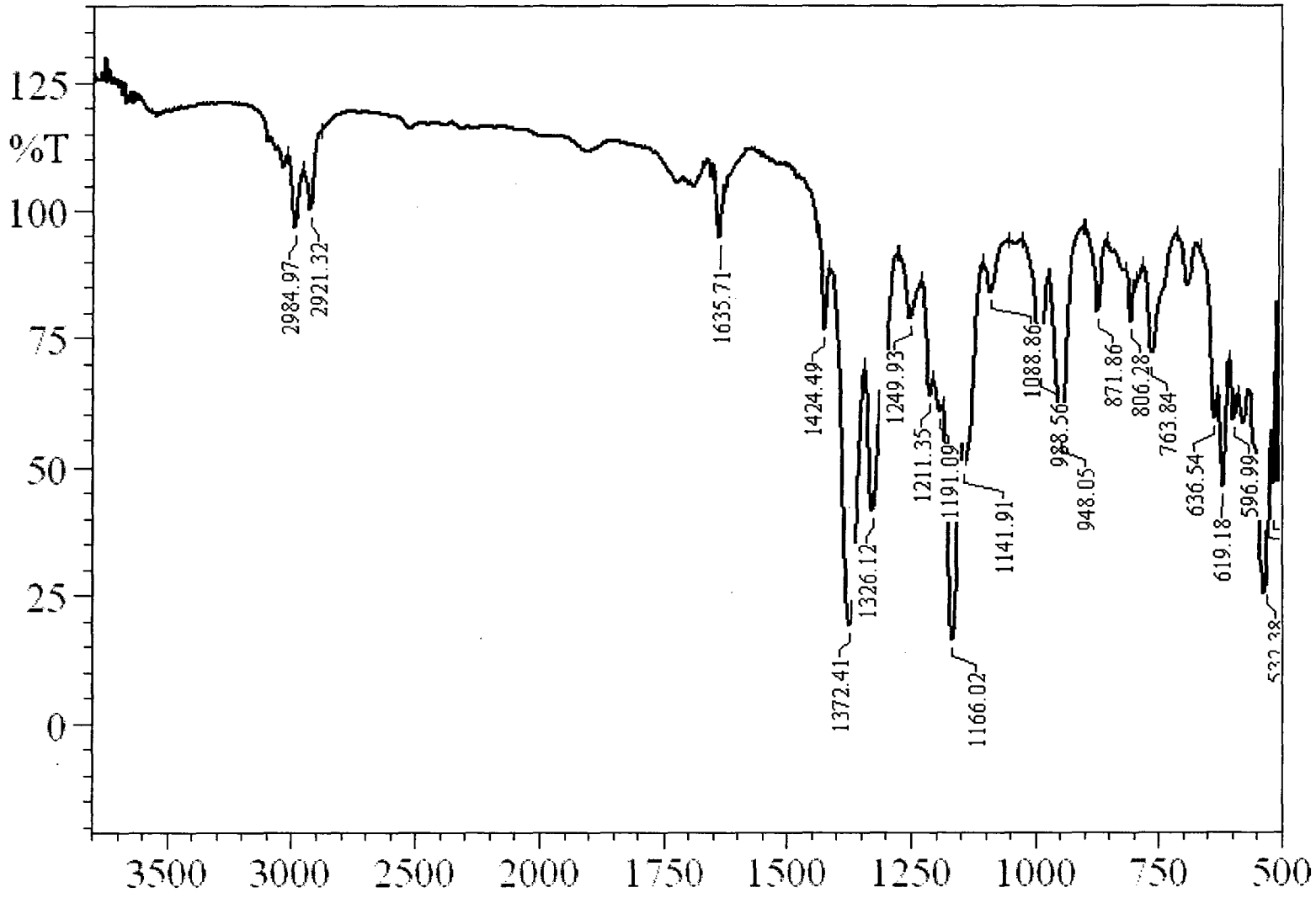

Figure 2.39: Infrared spectrum of Pentaerythritol tetrakis(allyl sulfonate). (tarry product)

each molecule is hydrogen bonded to four symmetry related molecules with the aid of C-H....O interactions. These O....H contacts are shorter than the sum of their Van der Waals radii.[132]

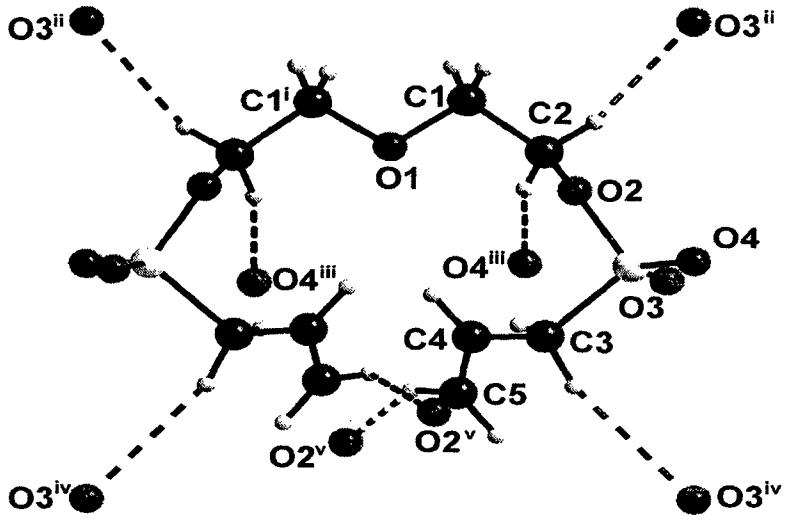

Figure 2.41: A view of the surrounding showing it's linking to four symmetry related molecules.

2.8 FTIR spectra of various polymers: The FTIR spectra of polymers were recorded and are given in Figures 2.42 to 2.49 (See next pages 130 - 137).

2.9 Photomicrographs of nuclear tracks in various polymeric track detectors.

Photomicrographs of nuclear tracks (alphas from ^{252}Cf or ^{239}Pu and fission fragments from ^{252}Cf) were recorded for various polymers prepared during this work. Some photomicrographs are given below. The expermental conditions are mentioned along with respective photomicrograph. (See next pages 138 - 142).

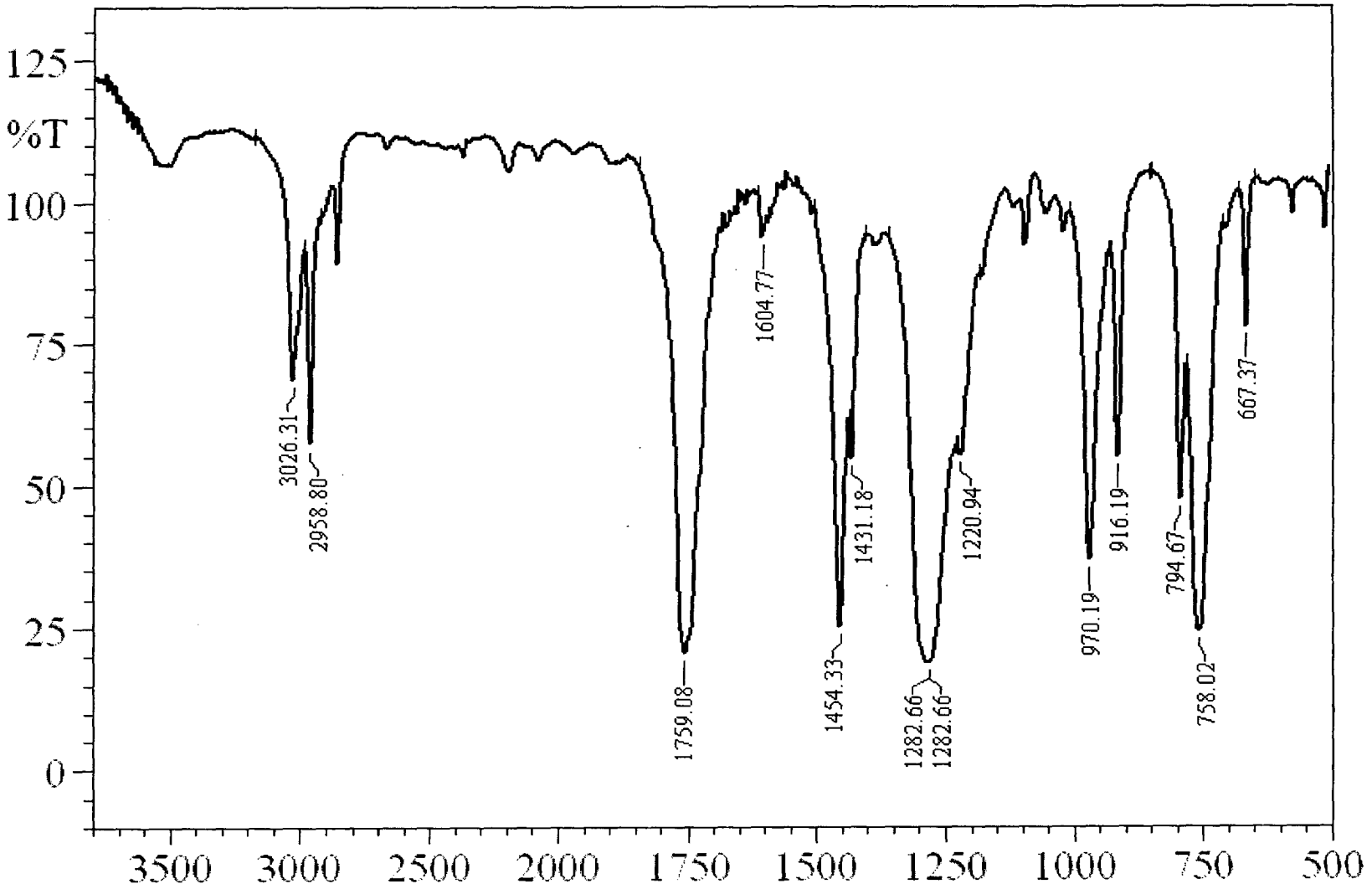

Figure 2.48: Infrared spectrum of PETAC homopolymer.

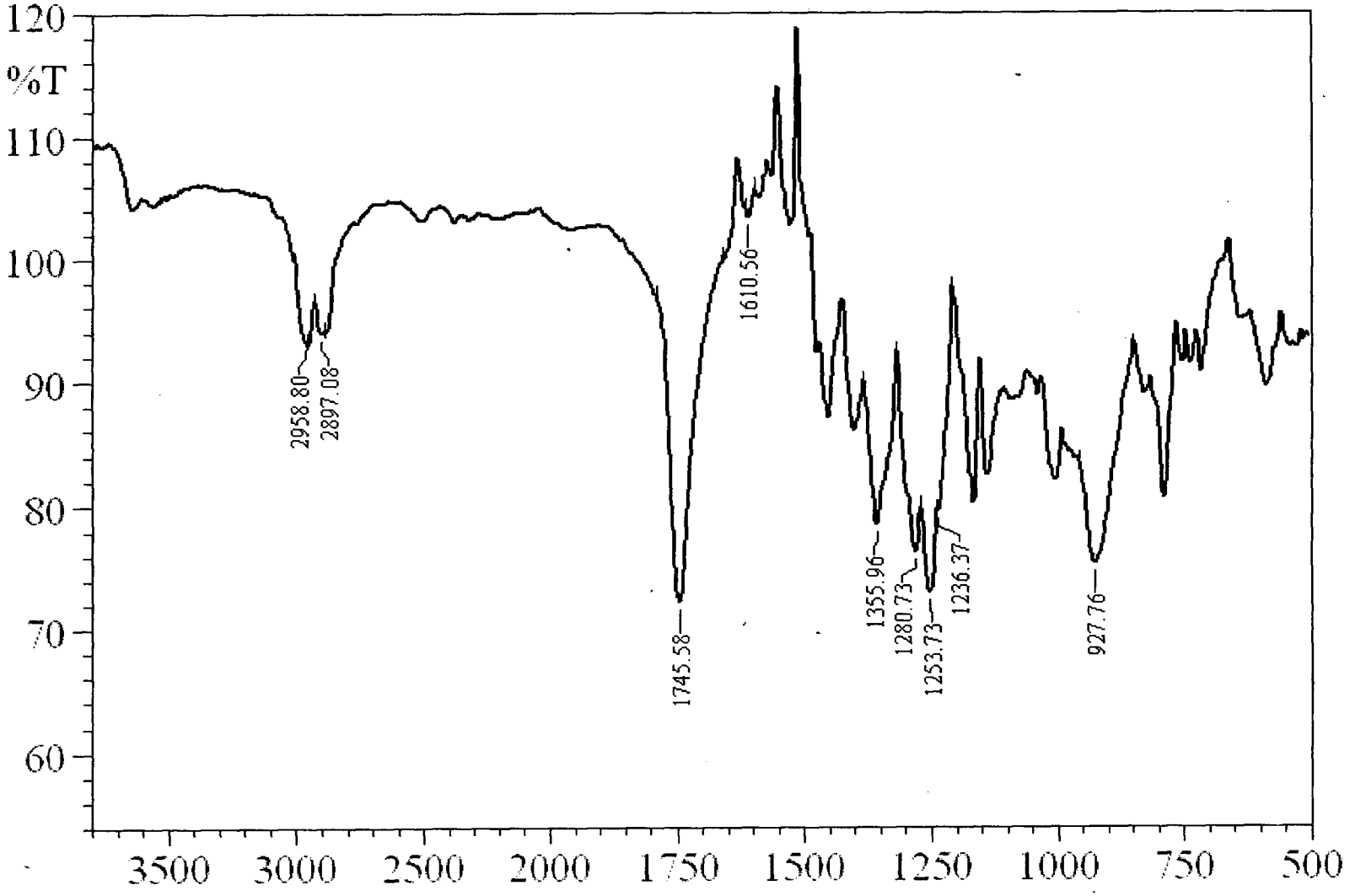

Figure 2.47: Infrared spectrum of DEAS:ADC 1:1 w/w copolymer.

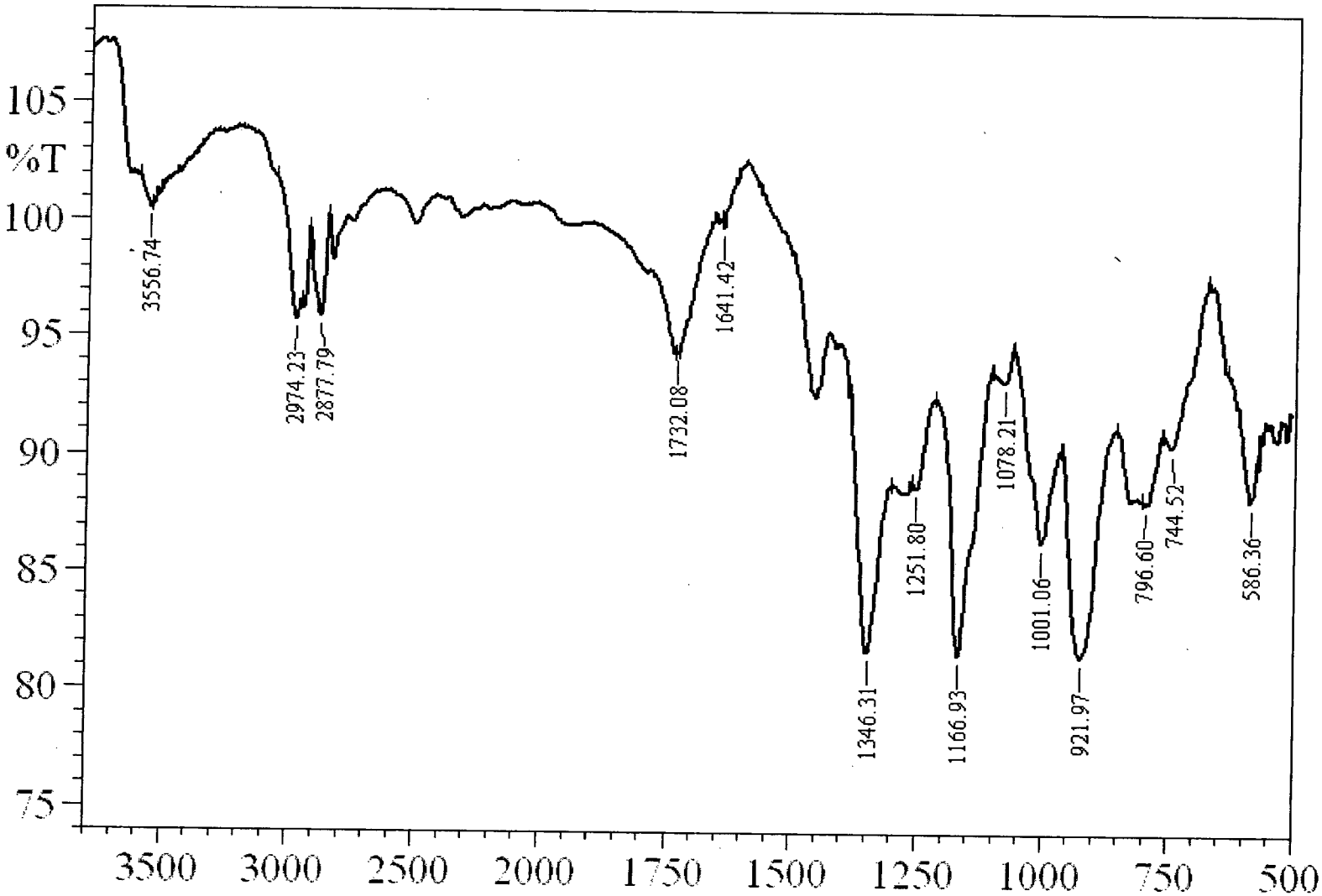

Figure 2.46: Infrared spectrum of DEAS homopolymer.

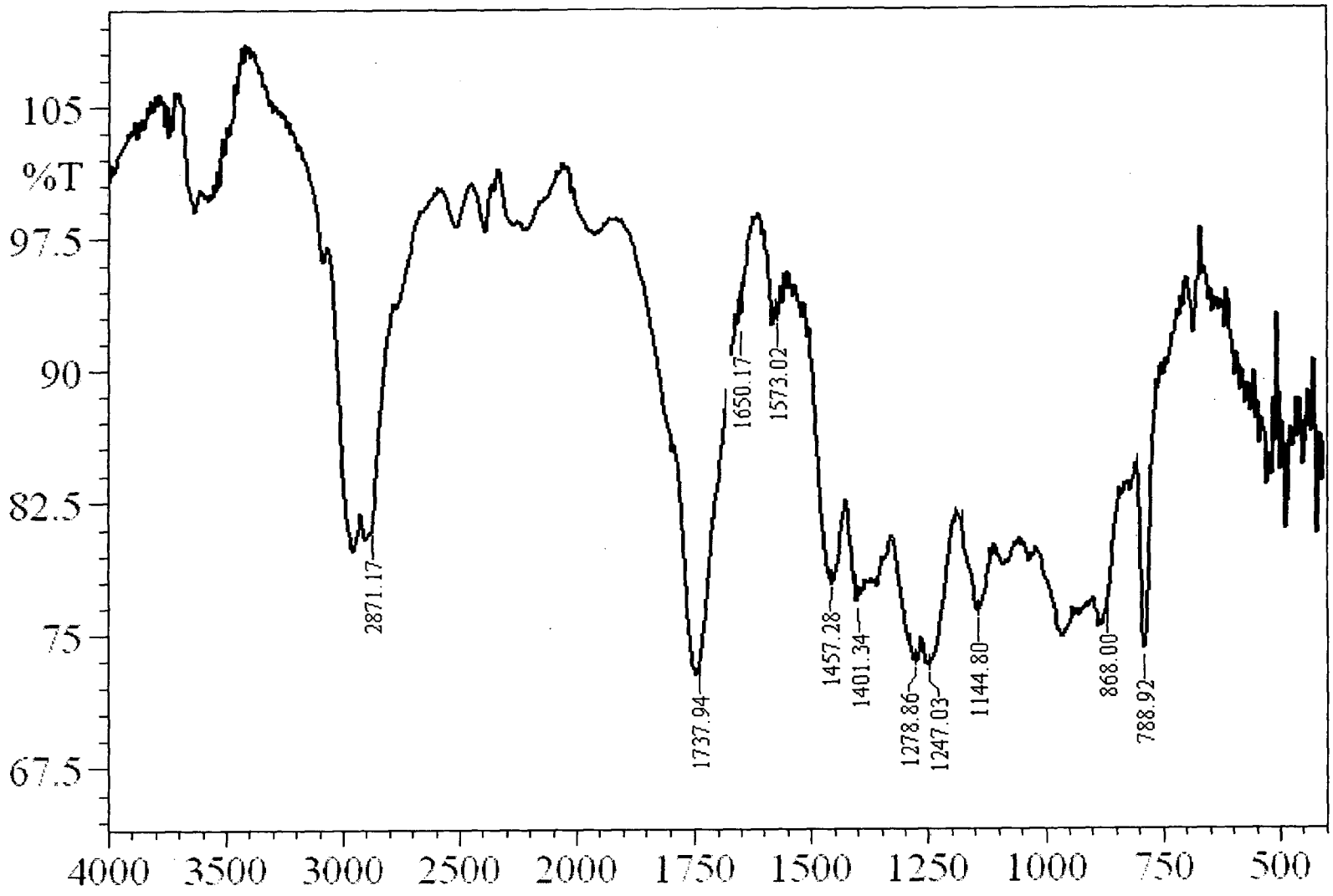

Figure 2.45: Infrared spectrum of ADS:ADC 1:9 w/w copolymer.

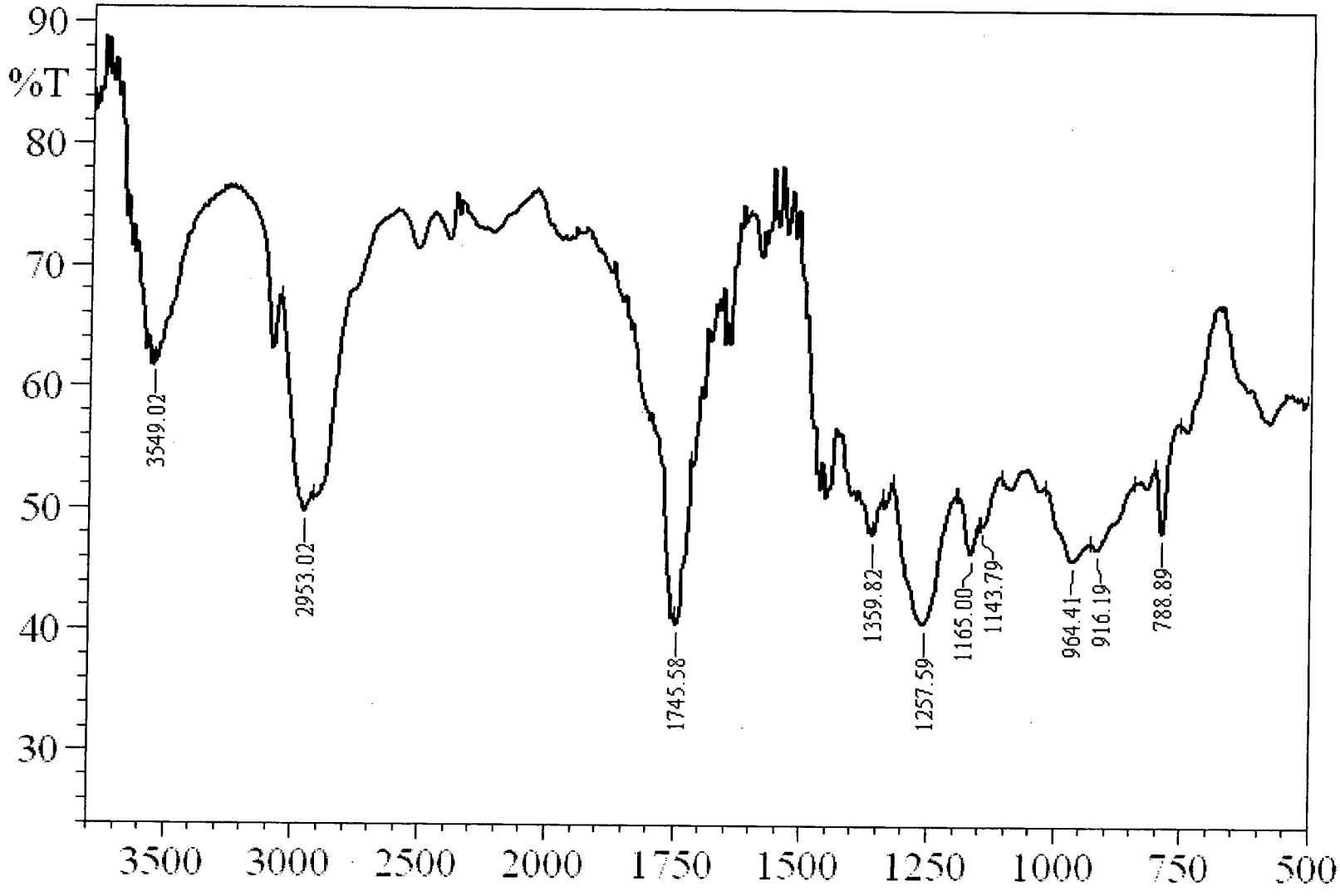

Figure 2.44: Infrared spectrum of DAS:ADC 2:8 w/w copolymer.

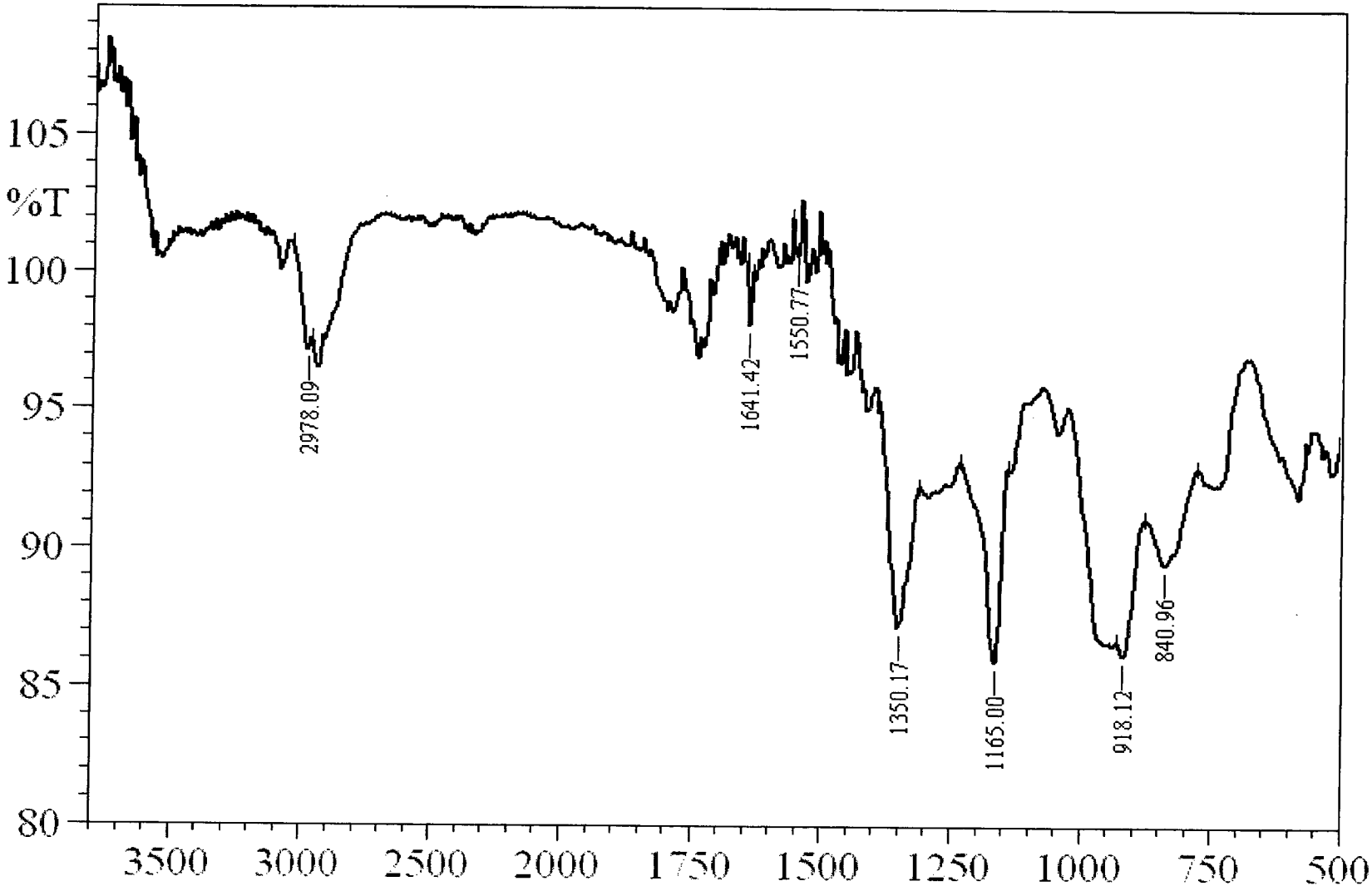

Figure 2.43: Infrared spectrum of DAS homopolymer.

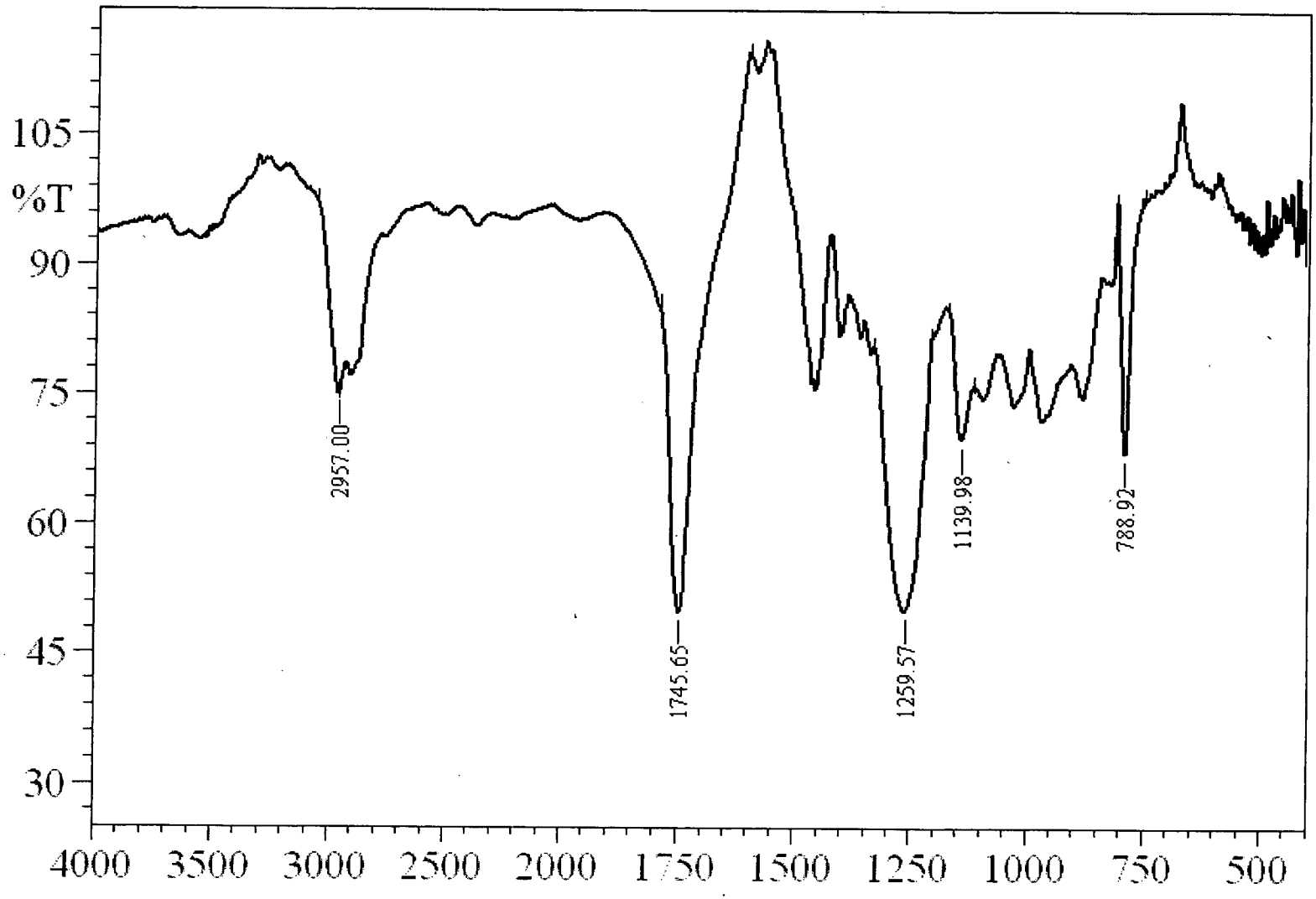

Figure 2.42: Infrared spectrum of CR-39™.

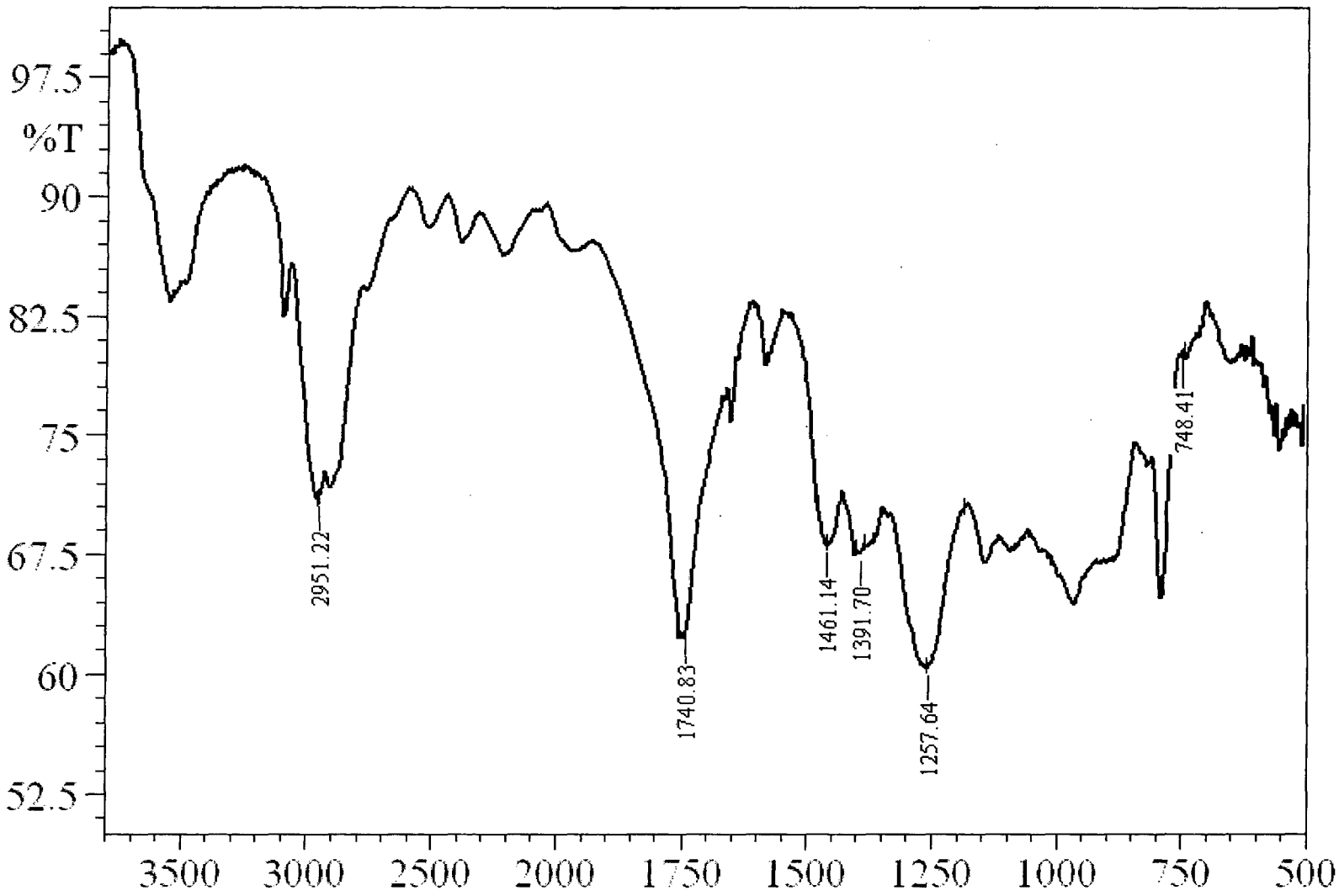

Figure 2.49: Infrared spectrum of PETAC:ADC 1:1 w/w copolymer.

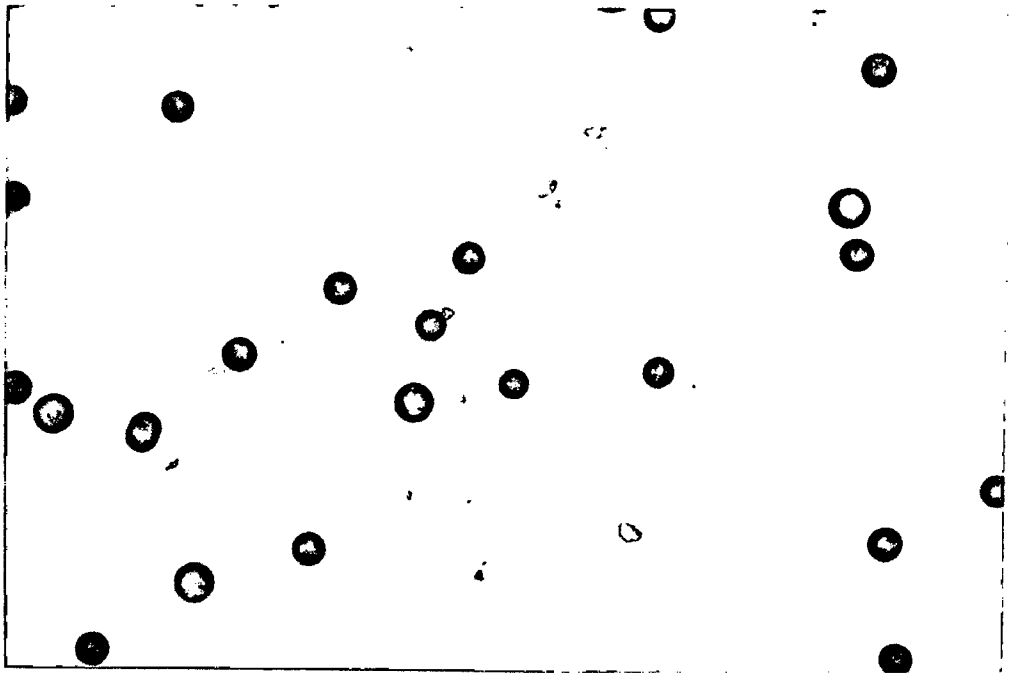

DEAS:ADC 3:7 w/w: Alpha and fission fragment tracks.
Exposed to ^{252}Cf, 5 cm at 0.02 mbar, Optical zoom: 100X

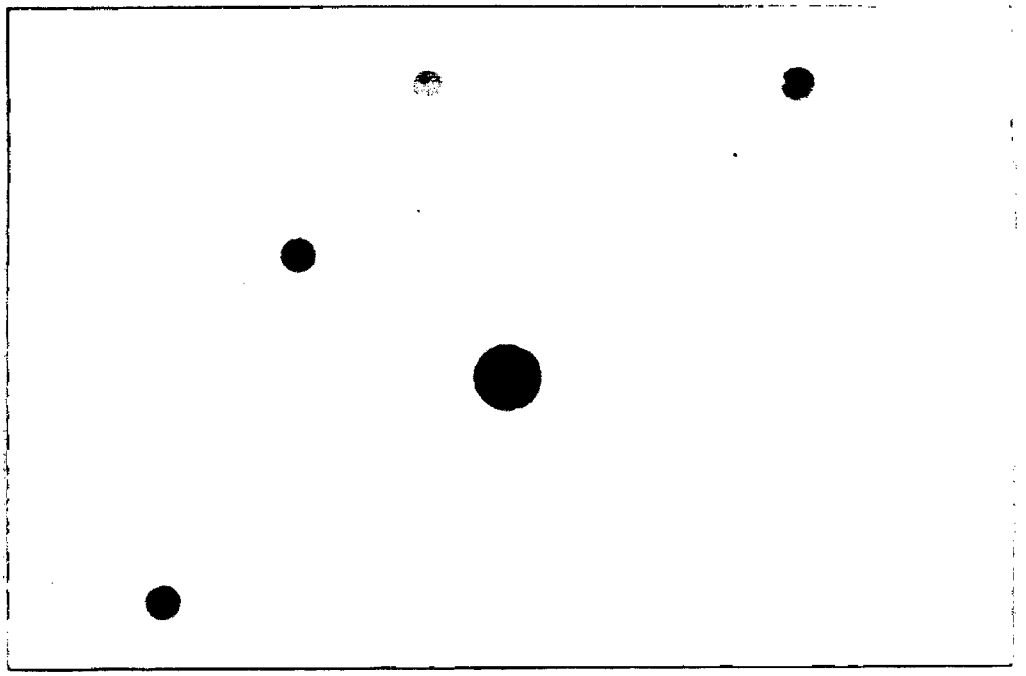

DEAS:PETAC 3:7 w/w: Alpha and fission fragment tracks.
Exposed to ^{252}Cf, 5 cm at 0.02 mbar, Optical zoom: 400X

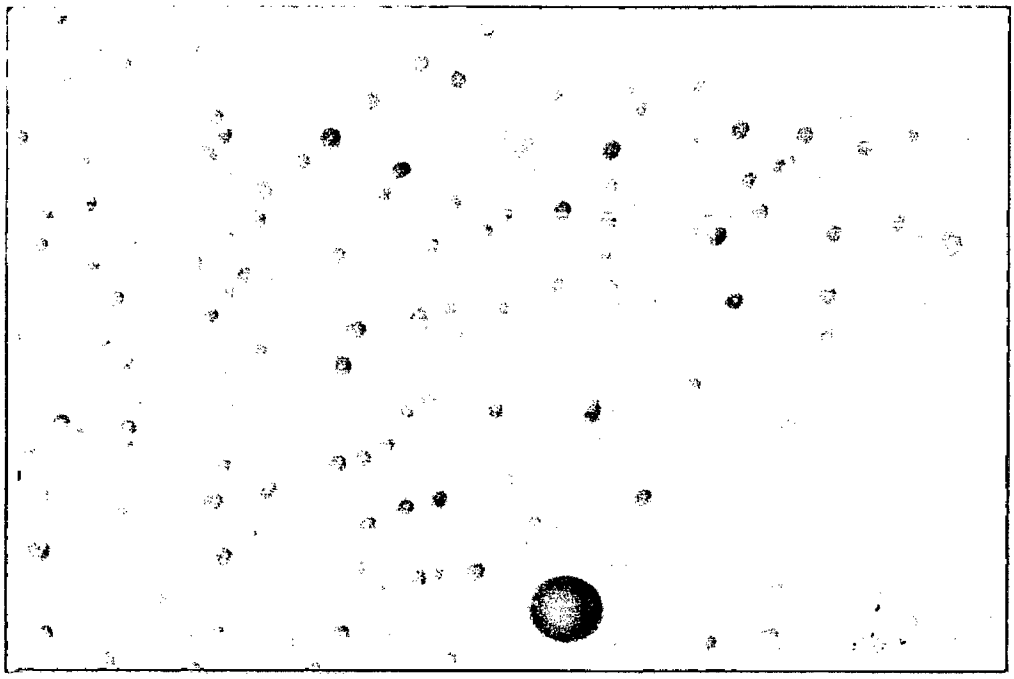

DEAS:ADC:PETAC 3:3:4 w/w/w: Alpha autoradiograph.
Exposed to ^{239}Pu, 1 mm, Optical zoom: 400X

DEAS:ADC 3:7 w/w: Alpha autoradiograph.
Exposed to ^{239}Pu, 1 mm, Optical zoom: 400X

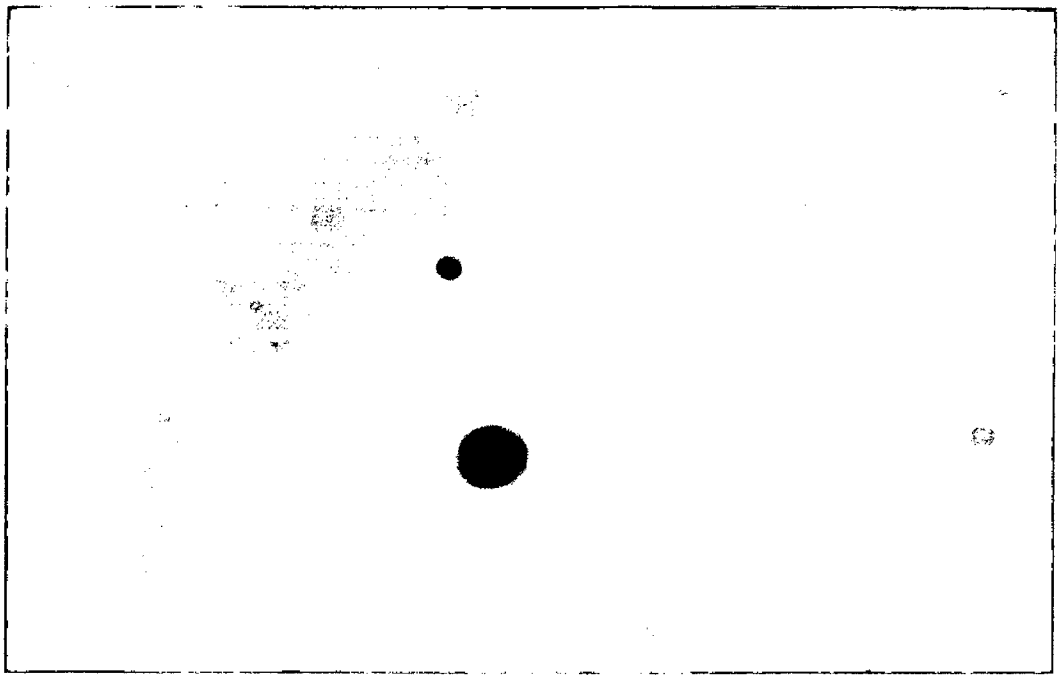

DAC:ADC 1:1 w/w: Alpha and fission fragment tracks.

Exposed to ^{252}Cf, 5 cm at 0.02 mbar, Optical zoom: 100X

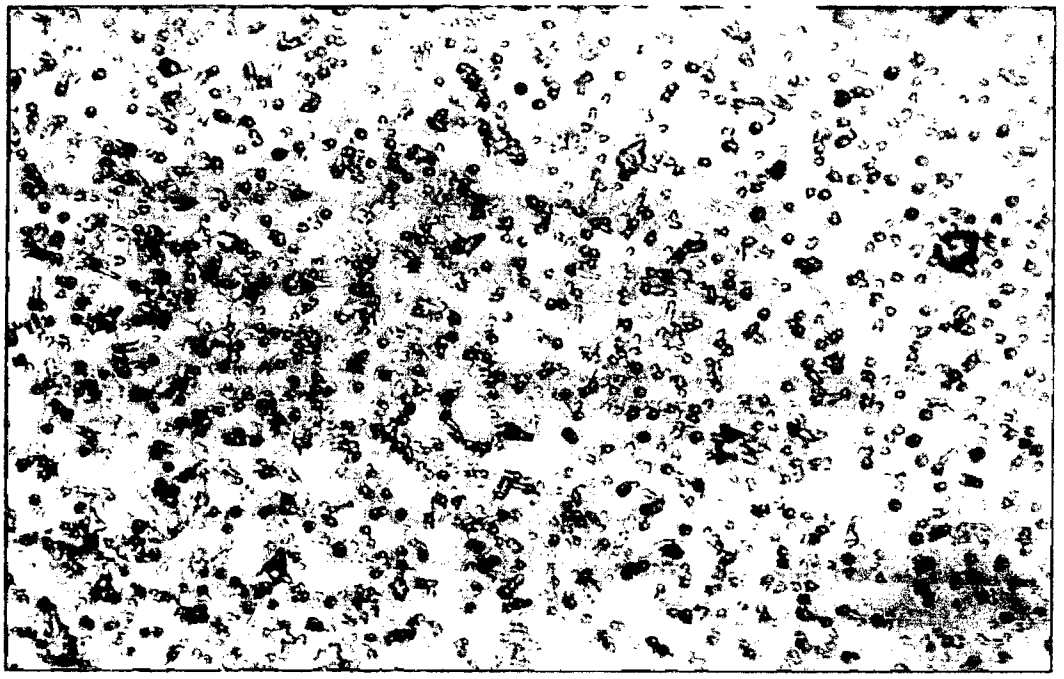

DEAS:ADC 2:8 w/w: Alpha autoradiograph.

Exposed to ^{239}Pu, 1 mm, Optical zoom: 400X

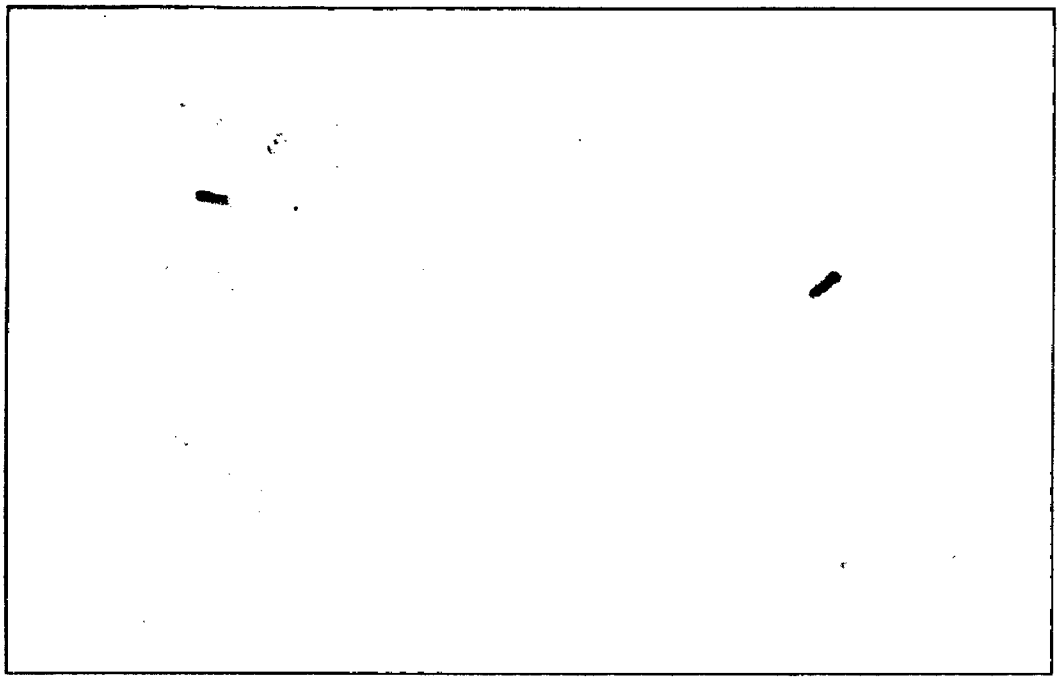

PETAC:ADC 4:6 w/w: Fission fragment tracks.

Exposed to ^{252}Cf at 1 mm, Optical zoom: 400X

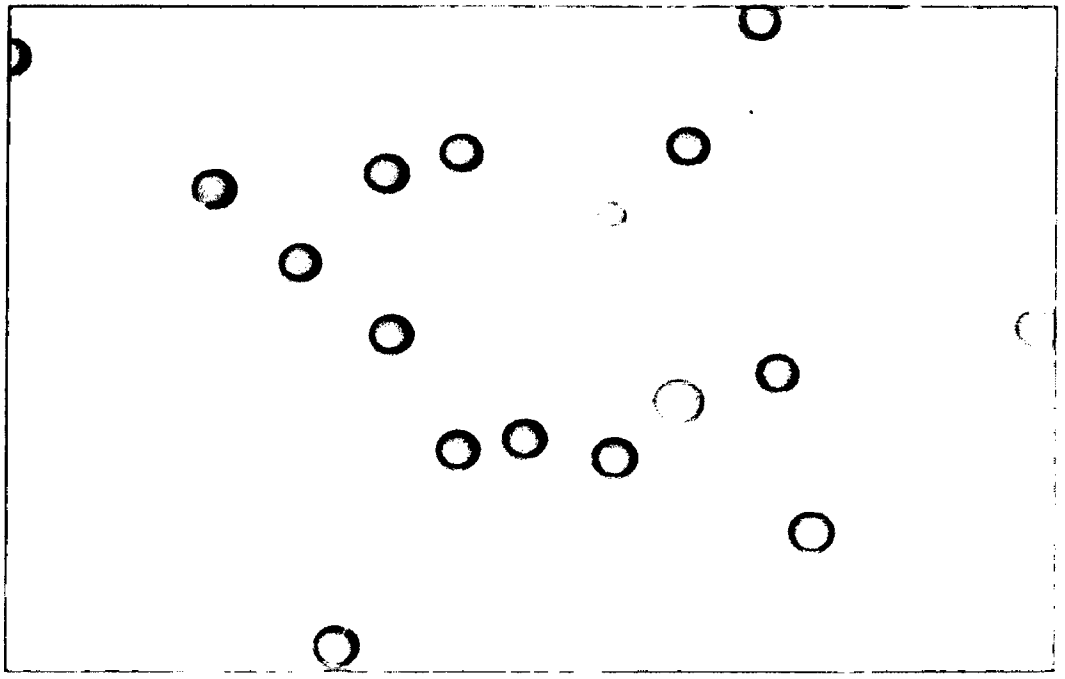

DEAS:PETAC 4:6 w/w: Alpha and fission fragment tracks.

Exposed to ^{252}Cf, 5 cm at 0.02 mbar, Optical zoom: 100X

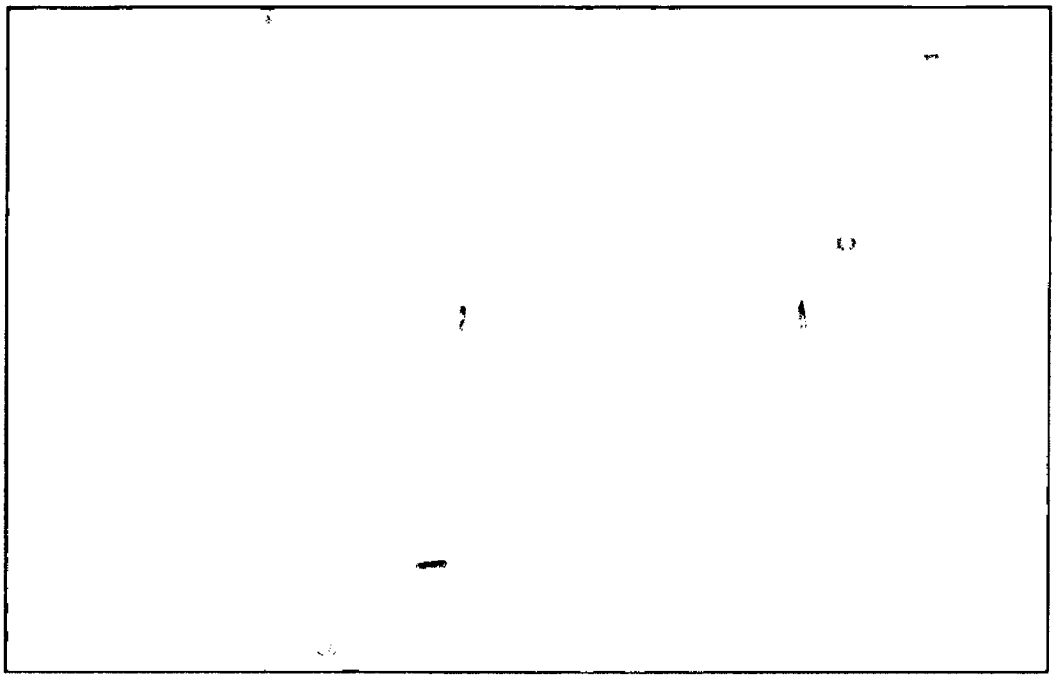

PETAC:ADC 1:1 w/w: Fission fragment tracks.

Exposed to ^{252}Cf, 1 mm, Optical zoom: 100X

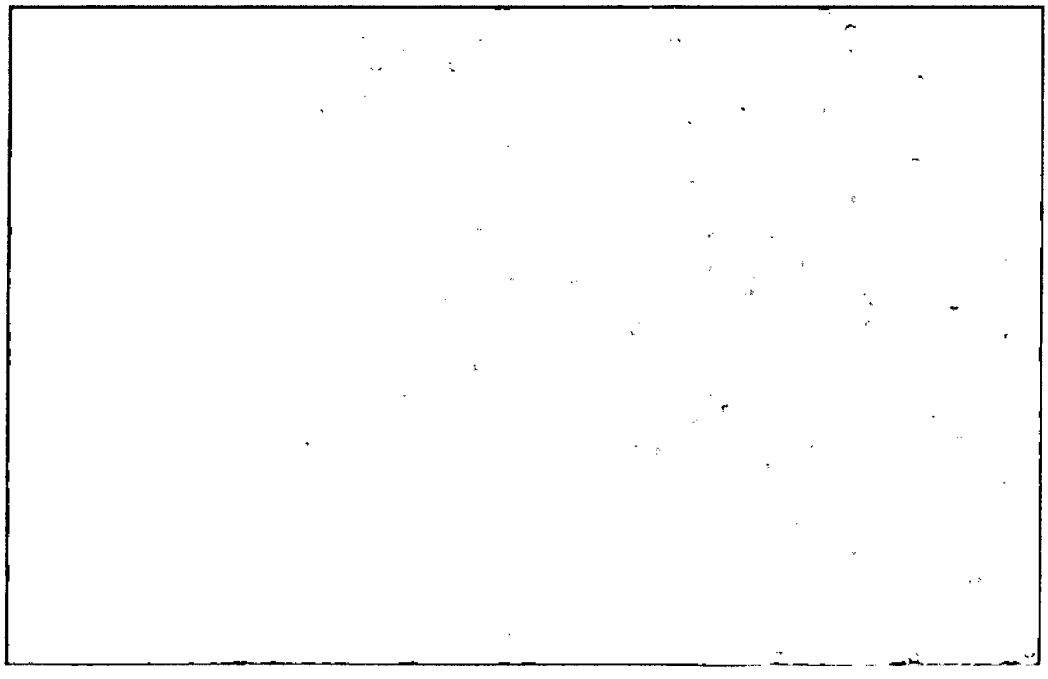

PETAC homopolymer: Alpha autoradiograph.

Exposed to ^{239}Pu, 1 mm, Optical zoom: 400X

Chapter III: Results and Discussion

In our endeavor towards development of novel materials for track detection, we decided to follow a uniform methodolgy based on our earlier experience and the same is outlined below.

3.1 Testing protocol for track detector films: It has been previously mentioned that, on the experience over last 15 years of work on preparation of polymeric SSNTDs, our laboratory has developed a protocol to synthesize and test polymeric detector films.[113] The process of polymerization requires monomers containing more than two allyl (CH_2=CH-CH_2-) groups. Allylic double bonds undergo polymerization and results in a 3 D polymer network as the functionality of the monomer is more than two. Furthermore, the introduction of allyl group also is easier job as compared to the introduction of vinyl group. If some functional groups containing hetero atoms (N, O, S, P) are introduced by suitable synthetic procedure between two allyl groups the polymer of the monomer can become more radiation sensitive. We have prepared monomers containing only one of the functional groups like -ONO_2, -O-CO-O-, -N-CO-O, O-SO-O-, -O-SO_2- or a monomer with more than one type of functional group. Further to improve density of crosslink's in a 3 D polymer chain network, we have used branched monomers which can efficiently crosslink.[73,78] We have also prepared some monomers which have pendant groups to see the effect on radiation sensitivity.[73]

Although the above mentioned protocol was proposed earlier its application and usefulness will be tested using the experimental work cited in this thesis. Therefore, following is the detailed description of the protocol and the same has been followed to the extent possible.

Step 1:Monomer synthesis and initial studies of monomer /

polymer:

a. Designing of the monomer, syntheses & its spectral characterization: The monomers are designed taking into account radiation sensitive group effect, chain bridging the two groups and the extent of crosslinks. The monomers are synthesized by using suitable chemicals. Finally, the monomer is characterized by infrared, ^{1}HNMR, ^{13}CNMR and the mass spectroscopy.

b. Thermal stability of the monomer-TG/DTA: A thermal study of the monomer gives a brief idea about the polymerization conditions that can be used to polymerize monomer under study. The TG/DTA analysis gives the maximum temperature above which monomer decomposes. This gives a brief idea of maximum temperature that can be used for polymerization. We observed that the monomers containing carbonate moiety are quite stable and can be easily heated up to 150 °C. The compounds containing nitrates ester group becomes unstable at around 70 °C and hence should be polymerized below 65 °C possibly using IPP initiator. The monomer containing sulphite groups are quite stable but, decompose on addition of IPP initiator at around 65 °C.

c. Casting of a test polymer sample & its characterization: To test the suitability of the designed monomer for track detection, a test polymer is first prepared. A homopolymer and a copolymer of the monomer with ADC are prepared by using appropriate heating profile. The polymers are than characterized with respect to the film properties such as color of the film, softness, % unsaturation left , average thickness and spectral properties.

d. Exposure to radiation source & etching in 6N NaOH at 70 °C: The polymer so obtained is cut into small pieces of size 1×1 cm^2 and exposed to alpha particles from ^{239}Pu source and to fission

fragments from ^{252}Cf source for track revelation properties of the polymer. The polymer is etched in 6 N NaOH at 70 °C to reveal tracks. If the polymer degrades or becomes opaque under above etching conditions than either the temperature of etchant is reduced or the concentration of etchant is changed.

e. Determination of bulk etch rate (V_b): The bulk etch rate of the film is a very important entity as it gives the rate at which the surface of the test polymer is degraded. The bulk etch rate of the polymer should be always less than the track etch rate V_t, in other words $V_t/V_b > 1$. During the etching, the surface of the test material is removed layer by layer thereby reducing the thickness of the material.

Step 2: Kinetics of polymerization: The monomer synthesized is heated with appropriate initiator at constant temperature to find its gel formation time. The Gel formation time gives a brief idea of the polymerization time required for the test polymer for its complete polymerization. The thermosetting polymers normally employed are prepared by cast polymerization process. The monomer can be cast polymerized by constant temperature polymerization wherein the monomer is heated along with the initiator at a constant temperature slightly above the decomposition temperature of the initiator. To minimize the depth dependency of the response and in an attempt to minimize differences between separate batches of plastics, the kinetics of polymerization and calculations of expected internal temperature excursions from specific temperature time functions are essential. A constant rate of polymerization and peroxide decomposition would result in constant rate of exothermic heat evolution. Thus a better polymer having uniform surface and bulk properties would be obtained.

Step 3: Optimization of initiator concentration: The amount of cross linking defines the sensitivity of particular detector. The cross linking in the polymer matrix is largely depends on the amount of initiator used. The density of crosslink's increases rapidly as the concentration of the initiator is increased up to a certain maximum value, followed by a gradual decrease. Thus, to find the optimum initiator concentration

a. Prepare films using different concentration of initiator/using different initiators.

b. Find the sensitivity by noting diameters of alpha/ fission tracks.

c. Repeat for all the films prepared with different initiator concentrations.

d. The initiator concentration where the sensitivity attains a maximum value is the optimum initiator concentration for the detector material.

Step 4: Optimization of etching conditions: The posts etch surface clarity of a film can be altered by using different conditions. To determine the optimum etching condition enough films at optimized initiator concentration are prepared and exposed to fission and alpha source. The films are etched at different temperatures keeping the normality constant. The films can also be etched varying the normality at constant temperature. V_b at every etching interval is noted along with the track appearance time. The optimum etching condition is one at which the surface of the film remains clear, has a moderate V_b and track development occurs within a reasonable time.

Step 5: Determination of alpha sensitivity at optimized etching conditions: At the selected optimum conditions, freshly exposed (to ^{252}Cf in vacuum) films and observe the variation of V_b

and sensitivity as a function of time to determine optimum etching time where S is maximum. Use the optimized etching conditions obtained above.

3.2 Monomer design and synthesis: As pointed previously, the literature survey indicates that the alpha sensitivity of a detector is largely dependent on the radiation sensitive groups, the three dimensional network in the polymer matrix and the chain bridging the two radiation sensitive groups. If one considers PADC (CR-39™) polymer, the sensitivity is mainly due to the presence of di-ethylene glycol linkage and the carbonate moiety. Fujii *et. al.* had synthesized some monomers analogues to ADC and confirmed that the ethylene diglycol linkage in the monomer is the most suitable bridging link between the two carbonate moieties.

The effect of radiation sensitive groups itself is not completely analyzed till date. To strengthen the observations by Fujii et. al. we thought of a monomer diallyl carbonate (DAC) having only one carbonate moiety flanked by two allyl groups. The monomer should form a hard polymer and one may expect that if $-CH_2-CH_2-O-CH_2-CH_2-$ and two carbonate groups impart some special properties, then in its absence the polymer from DAC should have poor radiation sensitivity than ADC. DAC was prepared by trans-esterification method using dimethyl carbonate and allyl alcohol.

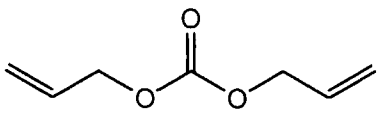

Diallyl carbonate (DAC)

Since, sulfur groups like $-O-SO_2-$ is known to give better radiation sensitivity, we thought of a monomer DAS. The DAS monomer was prepared by reacting thionyl chloride and allyl alcohol.

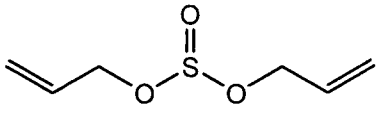

Diallyl sulphite (DAS)

One can further say that a monomer like ADS which has di-ethylene glycol linkage and SO_3 group should provide a polymer that has much better radiation sensitivity. The monomer was prepared by reacting Diethylene glycol and diallyl sulphite. It may be noted that ADS is a novel monomer and was not reported earlier.

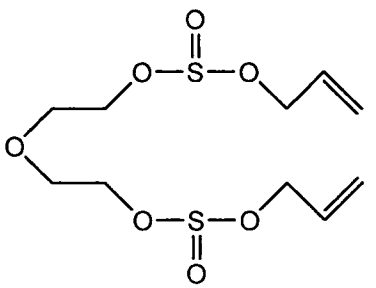

Allyl diglycol sulphite (ADS)

Fujji *et. al.* had first studied DEAS/ADC copolymers as track detectors. As DEAS homopolymer was not prepared their studies were incomplete. So we thought to study this monomer by preparing its homopolymer and copolymers with higher DEAS concentrations to observe one can prepare a polymer with much better track detection properties. The monomer was prepared by reacting di-ethylene glycol and allyl sulfonyl chloride in presence of base.

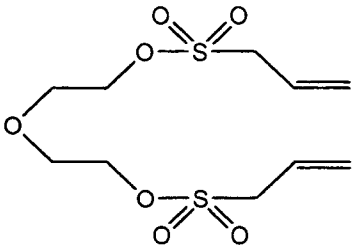

Diethyleneglycol bis(allyl sulfonate) (DEAS)

Having considered the effects of:

1) Removing diethylene glycol linkage from ADC.

2) Better sensitivity of S=O linkage than C=O linkages.

3) Higher alpha sensitivity polymers obtained by using branched monomers with higher functionality, like NADAC and TDONM, we thought of employing a more branched monomer with higher (octa) functionality. The resulting polymer should have a denser 3D-network of polymer chains with more cross linking from its eight linking points. PETAC monomer was prepared by reacting pentaerythritol and allyl carbonate in presence of base.

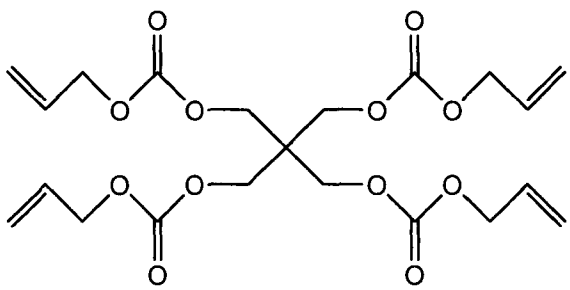

Pentaerythritol tetrakis(allyl carbonate)

If the above assumptions are true then, inserting few sulfonate groups in PETAC skeleton should give a polymer with much higher alpha sensitivity. This should provide more labile sulfonate groups in addition to higher crosslinking. So we sought to prepare PBCBS monomer.

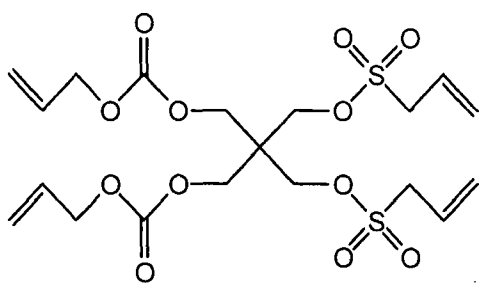

Pentaerythritol bis(allyl carbonate) bis(allyl sulfonate)

Further, by replacing all the four carbonate groups with -O-SO_2-

should result in a polymer that has still better radiation detection characteristics. Thus, synthesis of PETAS monomer was planned by reacting allyl sulfonyl chloride with pentaerythritol in presence of a base.

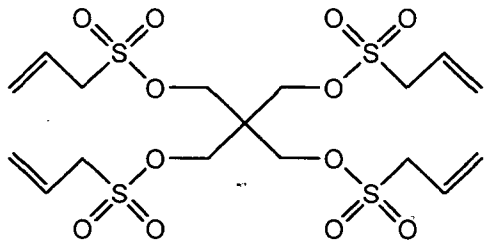

Pentaerythritol tetrakis(allyl sulfonate)

3.2.1 Thermal stability of the monomers: As discussed in the earlier chapter, the thermal stability of the monomer under study affects the polymer curing conditions and the type of initiator to be used for polymerization. The thermal stability of the monomers also determines the purification method to be used. Some of the monomers undergo polymerization or decompose under normal or vacuum distillation process. Such monomers are then purified by silica gel column chromatography. Table 3.1 gives the observed thermal stability of the monomers prepared.

Monomer	Thermal stability	Purification technique
DAC	Stable	Distillation at 166 °C
ADC	Unstable under normal distillation	Vacuum distillation at 0.1 - 0.2 mbar at 150 - 160 °C
DEAS	Unstable and forms black mass under vacuum distillation	Column chromatography with 7:3 v/v mixture of n-Hexanes-ethyl acetate
PETAC	Polymerizes under vacuum	Column chromatography

	distillation at 0.01 mbar at 160 °C	with 7:3 v/v mixture of n-Hexanes-ethyl acetate
DAS	Stable	Distillation 181 - 182 °C
ADS	Unstable	Vacuum distillation at 0.1 - 0.2 mbar at 140 °C
PBCBS	Unstable and forms black mass when vacuum distilled	Column chromatography with 8:2 v/v mixture of n-Hexanes-ethyl acetate

Table 3.1: Thermal stability of the monomers and their purification process.

3.2.2 Selection of initiator for polymerization: The polymerization of monomers is generally carried out using benzoyl peroxide (BP) or isopropyl peroxydiacarbonate (IPP) as initiator. Benzoyl peroxide is commercially available in moistened form and can be purified before use easily. The polymerization carried out using BP initiator ensures higher crosslinks in the polymer matrix due to the higher curing temperatures.[85] However, it has been observed that the use of BP initiator decreases the sensitivity of the plastic track detector.[73,92] The decrease in the sensitivity is due to the loss of particle energy to the ring vibrations of the benzene ring. With BP as initiator, polymerization is started in the temperature range of 70-95 °C which is much higher than IPP initiator. BP initiator cannot be used to polymerize monomers having sulphite moieties as the higher curing temperature makes the films completely dark. This is because the benzoyl peroxide attacks the sulphite moiety completely disrupting the structure and the nearest carbon is at-

tacked.[119]

The other initiator used and preferred for polymerization is IPP. The initiator has a lower decomposition temperature of 35 - 40 °C which allows the initiation of polymerization at lower temperature. The polymers obtained are generally more sensitive to alpha track detection than the polymers obtained from BP initiator. The main disadvantage of the initiator is that it cannot be purified before use due to instability and danger of explosion. The polymers cured with IPP initiator does not lead to maximum crosslink's as the polymerization slowly subsides due to the vitrification of the network.[92]

3.2.3 Monomer stability on heating with initiator: Some of the monomers prepared are stable in absence of initiator, but the stability of the monomers on heating in presence of initiator is also important to prepare a good polymer detector. The monomers having carbonate moieties are most stable and can be polymerized using IPP and BP initiators. DEAS is colorless monomer and their mixtures with ADC are stable in presence of initiators; however, the polymer films obtained after complete polymerization are light brown in color. The monomers having sulphite moiety are found to be unstable on heating with the initiator above 50 °C. The monomers form a black colored gel on heating with the initiator at higher temperature, probably due to formation of unstable higher oxides of sulfur. With higher initiator concentrations, similar results are obtained and the extent of colorization increases still more. Thus a constant temperature polymerization is best suited to polymerize these materials. Table 3.2 gives the stability study observations of DAS and ADS monomers.

w/w monomer mixture	IPP % w/w	Tempe-rature	Observations
DAS	4	50 °C	Dark gel brown in 12 hr
DAS	4	45 °C	Light yellow gel in 8 hr
DAS:ADC (1:1)	4	45 °C	Yellow gel in 4 hr
DAS:DAC (1:1)	4	45 °C	Yellow gel in 8 hr
ADS	4	50 °C	Light yellow Gel in 6.5 hr
ADS:ADC (1:1)	6	50 °C	Light yellow Gel in 4.5 hr
ADC:ADS:DAC (1:1:1)	6	50°C	Light yellow Gel in 2.5 hr
DEAS	6	50 °C	Light brown Gel in 3 hr
DEAS:ADC	5	50 °C	Colorless Gel in 3 hr
PBCBS:ADC (2.5:7.5)	4	50 °C	Brown gel in 4 hr

Table 3.2: Stability studies for the monomers in presence of initiators.

Table 3.2 shows that the samples having higher concentration of DAS and ADS are dark colored. It may be generally observed that unlike ADC which forms immobile gel with 3 % IPP at 50 °C within 2 hrs,[73] 4 - 6 % IPP is required to observe gel formation in case of the most of the sulfur containing monomers. This might be due to reactions of the initiator with the sulphite moiety of the monomer. The time required is also higher (4 - 8 hr) indicates that the initiator reacts with sulfur containing groups like -O-SO-O- or -O-SO_2 etc, rather than reacting with C=C. Thus, part of the radical initiator is distroyed by the sulfur containing moieties. Further, we observed that if these monomer-initiator mix-

tures are heated above 60 °C to reduce gelling time, the polymer becomes dark in color. As higher temperature and initiator concentration increases the dark color of the sulphite containing monomers the polymerizations were carried out at a constant temperatures below 50 °C and for extended time periods.

3.3 Cast polymerization of monomers to obtain test polymers: The test polymer of a designed monomer is prepared by cast polymerization. The test polymers enable us to know whether it is suitable to be used as track detector as such or some modifications are required. The monomer is also copolymerized with ADC monomer. Table 3.3 summarizes the curing conditions and the amount of initiator used for casting the test polymer. All the monomer mixtures were prepared in w/w ratio.

The monomers having sulfur containing moieties were polymerized using higher initiator concentration as part of the initiator might be destroyed by the reactivity of these monomers with sulfur groups. It was observed that the homopolymers having sulphite moieties are much soft in nature and could not be tested as track detectors.

Monomer mixture (w/w)	Initiator (% w/w)	Heating profile (Temperature range) used for polymerization
DAC	BP (3.3)	ADC polymerization[73] (71-95 °C)
DAC:ADC(1:1)	BP (3.3)	ADC polymerization[73] (71 - 95 °C)
DAS	IPP (8)	Constant at 45 °C for 24 hr
DAS:ADC(1:1)	IPP (3)	Constant at 45 °C for 24 hr
DAS:DAC(1:1)	IPP (8)	Constant at 45 °C for 24 hr
ADS	IPP (3)	Constant at 45 °C for 24 hr

ADS:ADC(1:1)	IPP (8)	Constant at 45 °C for 24 hr
ADS:ADC(2:8)	IPP (8)	Constant at 45 °C for 24 hr
ADC:ADS:DAC (1:1:1)	IPP (6)	Constant at 45 °C for 24 hr
DEAS	BP (6)	ADC polymerization[73] (71 - 95 °C)
DEAS:ADC (1:1)	BP (4)	ADC polymerization[73] (71 - 95 °C)
PETAC	BP (3)	ADC polymerization[73] (71 - 95 °C)
PETAC:ADC (1:1)	IPP (6)	ADC polymerization[73](71 - 95 °C)
PETAC:DEAS (4:6)	BP (4)	ADC polymerization[73] (71 - 95 °C)
PETAC:ADC:DEAS (4:3:3)	IPP (4)	ADC polymerization[73] (71 - 95 °C)
PBCBS:ADC* (2.5:7.5)	IPP (4)	PETAC:ADC 1:1 polymerization (42-90 °C)

* This work was done after studying PETAC polymerization kinetics.

Table 3.3: Curing conditions used for polymerization of different test polymers.

3.3.1 Track detection studies of newly designed test polymeric track detectors: The polymer films were cut into sizes of 1 x 1 cm^2 and exposed to fission fragments from ^{252}Cf source and alpha particles from ^{239}Pu source in close contact. The films were etched in 6 N NaOH at 70 °C. Some of the detectors had good alpha fission track response. Table 3.4 below (see next page) gives the physical properties and the track detection characteris

Sr. No.	Monomer mixture (w/w)	Thickness (μm)	Color and hardness
1	DAC	538 ± 10	Colorless, hard film
2	DAC:ADC(1:1)	625 ± 10	Colorless, hard film
3	DAS	----	Dark brown, soft film
4	DAS:ADC(1:1)	715 ± 10	Dark brown, soft film
5	DAS:DAC(1:1)	635 ± 10	Hard, light brown film
6	ADS	----	Soft gel like film
7	ADS:ADC(1:1)	----	Soft gel like film
8	ADS:ADC(2:8)	703 ± 10	Hard, light brown film
9	ADC:ADS:DAC(1:1:1)	626 ± 10	Hard, light brown film
10	DEAS	615 ± 10	Hard, light brown film
11	DEAS:ADC (1:1)	620 ± 10	Hard, light brown film
12	PETAC	636 ± 10	Colorless, hard film
13	PETAC:ADC(1:1)	594 ± 10	Colorless, hard film
14	PETAC:DEAS(4:6)	572 ± 10	Hard, light brown film
15	PETAC:ADC:DEAS (4:3:3)	634 ± 10	Hard, light brown film
16	PBCBS:ADC (2.5:7.5)	631 ± 10	Light brown film

Table 3.4: Physical and track detection properties of the polymer

tics of the polymers.

Most of the polymers can be easily used to reveal charged particle tracks. Some of the polymers can be used to reveal fission tracks in presence of alpha particles as they detect only fission tracks. The polysulphite homopolymers are not suitable as track detectors as all these polymers obtained were soft. The polymers were then studied with respect to their ^{252}Cf alpha particle sensitivity. The bulk etch rate of the polymers was also determined and is given in Table 3.5 (please see next page).

From the results obtained it is quite clear that the monomers having the sulphite moieties can reveal the tracks very quickly. The fission tracks are revealed first and could be seen easily, however, as the etching process is continued to reveal the alpha autoradiograph the film becomes opaque. Although the ^{239}Pu alpha tracks cannot be seen under the microscope an impression of alpha source can be observed easily. Thus, the polymers are best suited for quick analysis of fission fragment tracks. The copolymers of DEAS can reveal the tracks quickly as well, but, the homopolymer turns opaque after etching for 1 hr. PETAC homopolymers and copolymers can also reveal alpha and fission tracks quickly and the films remain clear under all etching conditions.

3.3.2 Sensitivity studies of the test polymer: Alpha sensitivity is a parameter which can be used to characterize a track detector. The method used for the purpose needs determination of diameters of both alpha and fission fragments at a given time and polymers with higher alpha sensitivity are preferred. Table 3.6 below gives the alpha sensitivity of the test polymers. The alpha sensitivity of the sulphite containing polymers and the DEAS homopolymer could not be determined as the films became opaque.

Sr. No.	Monomer mixture (w/w)	Time for track revelation in minutes in 6N NaOH , 70°C		Post et d
		Fission	Alphas	
1	DAC	50 - 60	-----	Clear f
2	DAC:ADC (1:1)	50 - 60	450 - 480	Clear f
3	DAS:ADC (2:8)	8 - 10	15 - 20	Opaque
4	DAS:DAC (1:1)	10 - 15	----	Opaque
5	ADS:ADC (2:8)	4 - 5	15-20	Opaque
6	ADC:ADS:DAC(1:1:1)	8 - 10	-----	Opaque
7	DEAS	50 - 60	160 - 180	Opaque
8	DEAS:ADC (1:1)	25 - 30	50 - 60	Clear f
9	PETAC	40 - 45	75 - 90	Clear f
10	PETAC:ADC (1:1)	25 - 30	50 - 60	Clear f
11	PETAC:DEAS (4:6)	20 - 25	40 - 45	Opaque
12	PETAC:ADC:DEAS (4:3:3)	12 - 15	25 - 30	Opaque
14	PBCBS:ADC(2.5:7.5)	25 - 30	55 - 60	Opaque
15	PADC	45 - 60	110 - 120	Clear f
16	CR-39™	45 - 60	110 - 120	Opaque

Table 3.5: Track recording time and post etch surface properties of diff

From the alpha sensitivity values one can observe that some of the test polymers have higher alpha sensitivity than CR-39™ polymer. The alpha sensitivity value can be increased further if the polymerization conditions and the etching conditions are optimized. The composition of the copolymer with respect to concentration of monomers is important as variation in the monomer concentration can affect the alpha sensitivity. The first step towards optimization of the polymerization conditions is to study kinetics of polymerization. The concentration of initiator can also affect the alpha sensitivity of the polymers. The bulk etch rates of the polymers are also comparable with that of the CR-39™ polymer.

Sr. No.	Monomer mixture w/w	Alpha sensitivity	Bulk etch rate (μm/hr)
1	DAC homopolymer	----	1.26
2	DAC:ADC(1:1)	1.18	1.17
3	DAS:ADC(2:8)	----	2.23
4	DAS:DAC(1:1)	----	2.25
5	ADS:ADC(2:8)	----	2.16
6	ADC:ADS:DAC (1:1:1)	----	1.86
7	DEAS homopolymer	----	2.08
8	DEAS:ADC (1:1)	1.36	1.65
9	PETAC homopolymer	1.38	2.07
10	PETAC:ADC(1:1)	1.67	1.64
11	PETAC:DEAS(4:6)	2.35	1.74
12	PETAC:ADC:DEAS (4:3:3)	2.36	1.38
14	PBCBS:ADC(2.5:7.5)	----	1.57
15	PADC	1.24	1.42
16	CR-39™	1.28	1.12

Table 3.6: Sensitivity values obtained for the test polymers.

3.4 Development of heating profile: It is well known that the curing conditions during polymerization vary the properties of the product. During polymerization, many processes like initiation, propagation etc takes place at a rapid rate in the initial stages. The processes are highly exothermic and hence favor further increase in the rate. However, due to higher polymerization rate many defects such as depth dependant bulk etch rate and strong angular dependence occur in the polymer matrix.[85] Thus, films prepared in different batches show different properties. Furthermore it is well known that the allylic polymerization leads to decrease in the bulk volume. In PADC the shrinkage in the volume is to the extent of 14 %. These factors lead to development of cracks in the polymer films.

Constant temperature polymerization reduces such defects considerably, but the time required for polymerization becomes long. Thus a need was felt for fast polymerization at a constant rate of heat evolution during polymerization. In order to overcome these problems, Dial et.al. studied the polymerization kinetics of ADC monomer using IPP initiator.[85] From the data obtained Dial *et.al.* derived a kinetic model with the help of which, special heating profiles can be constructed. Use of these heating profiles ensures constant rate of initiator decomposition and thus constant heat evolution due to allylic polymerization. The polymers cured using such heating profiles should have a better surface and bulk properties.

Mascarenhas et. al. have successfully used these constants for ADC monomer and a heating profile was obtained.[73] In addition to PADC, heating profiles for various hexafunctional monomers and monomers having nitrate ester functionality has been obtained by

performing kinetic study. We thought of extending this idea to newly prepared monomers to obtain a heating profile for individual monomers or number of allylic monomers.[90,91] Kinetic study involves analysis of the initiator and monomer concentration at constant temperature at different time intervals. The initiator concentration was determined using the iodimetric analysis and the unsaturation was analyzed by Wij's method. Determination of Dials Constants for most of the monomers cited above, kinetics of polymerization as per Dial's model has not been studied previously.

3.4.1 Kinetic studies of DAC monomer using BP initiator: Dial et. al., had performed the kinetic studies of ADC monomer with IPP initiator (3.3 %) at three different sets of temperatures viz. 40, 50 & 60 °C and heating profiles. Mascarenhas et. al. has also successfully used these equations for ADC polymerization kinetic study using BP initiator at 60, 70 and 80 °C.[73] This study was done for our indigenously prepared DAC monomer at 65, 70 and 75 °C based on the gel formation studies.

3.3 % BP initiator w/w was dissolved in DAC monomer and the mixture was flushed with dry nitrogen gas. The mixture was taken in test tubes and the time required for gel formation was noted at the specified temperatures. The results are given in the Table 3.7. The gel formation for a tetrafunctional monomers occur at approximately 75 % residual unsaturation. This was followed by further kinetics.

Sr. No.	Temperature(°C)	Time (hr)	Observation
1	65	7	Immobile gel
2	70	4	Immobile gel
3	75	2	Immobile gel

Table 3.7: Gelation time at different temperatures for DAC monomer with BP initiator.

The DAC monomer was mixed with initiator and transferred to a set of test tubes. Each test tube was filled with approximately about 2 g of the polymerization mixture. The mixture in the test tubes was flushed with nitrogen for 15 minutes each and test tubes were sealed with rubber stopper. The test tubes were then placed in thermostat bath and heated at a constant temperature of 65, 70 or 75 °C. A test tube was removed after particular time interval and chilled in ice bath to inhibit polymerization. The mixture was analyzed for its residual percentage unsaturation and residual initiator concentration with respect to time by using the standard analytical methods described in section 2.3. All the test tubes were analysed in similar fashion. The results are summarized in the Table 3.8 - Table 3.10.

Sr. No.	Time (hr)	Peroxide (%)	Unsaturation (%)
1	0	3.30	100.00
2	1	3.26	96.65
3	2	3.19	93.79
4	3	3.13	91.94
5	4	3.11	90.08
6	5	3.04	88.67
7	6	2.94	86.26
8	7	2.86	84.28
9	8	2.9	80.3

Table 3.8: Peroxide and rasidual unsaturation amount at 65 °C

Sr. No.	Time (h)	Peroxide (%)	Unsaturation (%)
1	0	3.30	100.00
2	1	3.24	97.26
3	2	3.14	94.25
4	3	3.10	90.77
5	4	3.01	88.06
6	4.5	2.92	85.11
7	5	2.87	83.07
8	5.5	2.79	81.68
9	6	2.73	78.70

Table 3.9: Peroxide and unsaturation amount at 70 °C

Sr. No.	Time (h)	Peroxide (%)	Unsaturation (%)
1	0	3.30	100.00
2	1	3.25	96.79
3	1.5	3.17	93.55
4	2	3.08	90.81
5	2.5	3.02	88.16
6	3	2.93	85.30
7	3.5	2.86	83.68
8	4	2.82	80.69
9	4.5	2.67	77.60

Table 3.10: Peroxide and unsaturation amount at different time intervals at 75 °C.

The results obtained are summarized in a graphical manner in Figure 3.1 below.

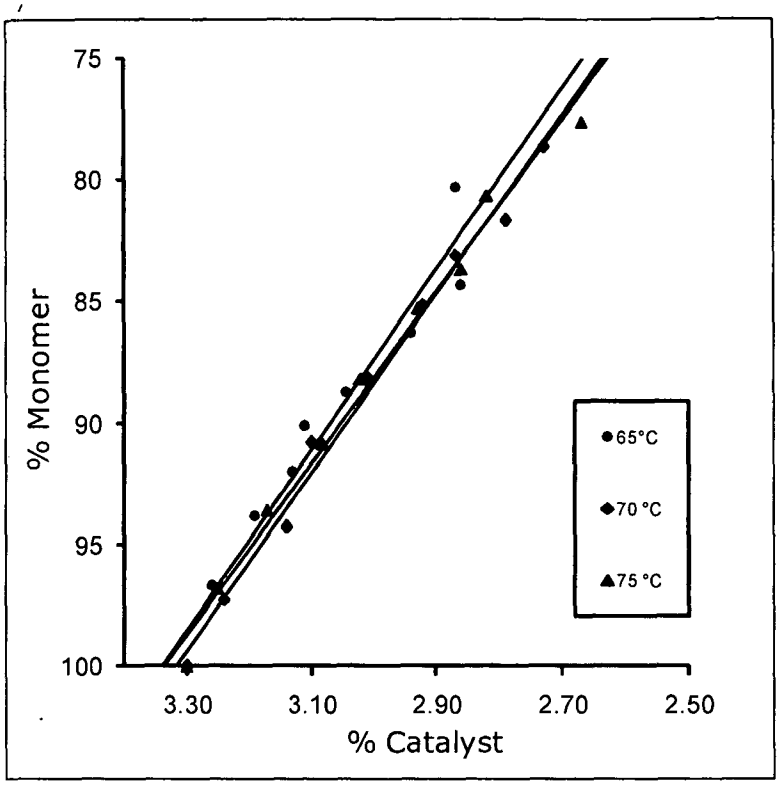

Figure 3.1: The amount of initiator and the unsaturation present at temperatures of 65, 70 and 75 °C.

From the Table 3.8 to 3.10 it is clear that the polymerization rate increases with the increase in the curing temperature. At the temperature of 75 °C, the test tubes were removed an analysed quickly due to early gelation of the polymerization mixture. Gelation of the polymerization mixture occured between 75-80 % of residual unsaturation.

The slopes obtained for the three lines were:

65 °C, K_1= 37.12

70 °C, K_1= 36.71

75 °C, K_1= 35.27

The values obtained are in decreasing order and are above the limiting values for the slope. Using these slope values, the constants E_1, Z_1, E_3, and Z_3 were obtained. The values are given below.

Sr. No.	Constant	Value
1	E_1	-1185.57
2	E_3	41752.87
3	Z_1	6.30E+00
4	Z_3	2.07E+25

Table 3.11: Values obtained for the constants given in the Dials equation.

Dial's equations were solved using a FORTRAN program[73] and a heating profile was calculated. However, the heating profile could be calculated for 10 hr as the roots of Dials equation become imaginary[85] after 10 hrs and the program fails to calculate the values. A graph was plotted for the 10 hr heating profile and was smoothly extrapolated further to obtain a 12 hr heating profile. The heating profile obtained for DAC polymerization is given in the Figure 3.2.

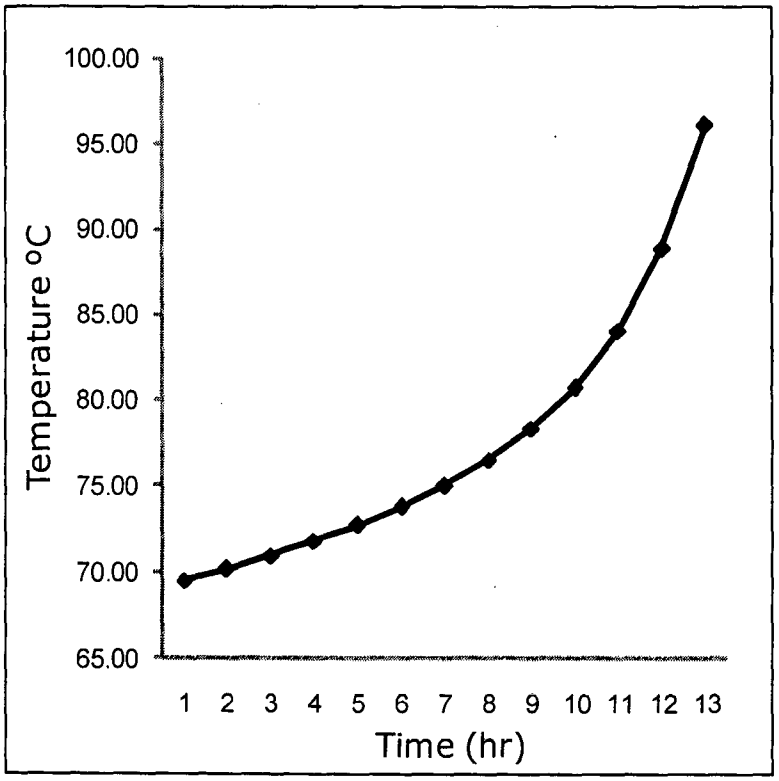

Figure 3.2: Heating profile obtained for DAC polymerization.

To see the effectiveness of heating profile, 12 test tubes were filled with polymerization mixture and heated in a water bath. The temperature of the water bath was raised as per the heating profile obtained. A test tube was removed after every hour and analyzed for the amount of residual unsaturation. The results obtained are shown graphically in the Figure 3.3 below. From the Figure it is clear that the polymerization occurs at a constant rate and a linear correlation is observed between yields of polymer as a function of time.

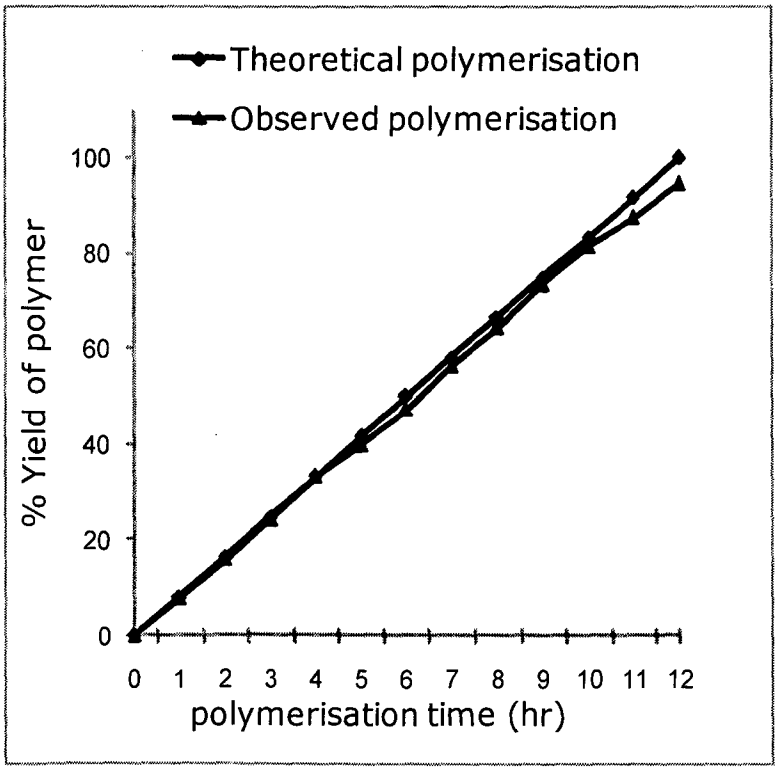

Figure 3.3: The monomer conversion at different time interval of heating profile.

This is supported well by the linear correlation coefficient (R^2) of 0.9996 obtained from calculated values at a given time interval. The deviation in the results might be due to the decreased

solubility of the polymer in the later stages as the polymer becomes very hard. Furthermore, experimental errors in estimating monomer/catalyst concentrations and efficiency of the electronic temperature controller bath used for heating of the monomer mixture can also contribute to the errors.

3.4.2 Polymerization kinetics of PETAC monomer using IPP initiator: Both the test polymers (PETAC homopolymer and copolymer with ADC) had a higher alpha sensitivity as compared to CR-39™. We thought of extending the Dial's model to study the polymerization of octafunctional, PETAC monomer and the PETAC:ADC 1:1 w/w copolymer. The kinetic studies for the polymers were performed using 6 % IPP initiator. The polymerization kinetics was studied using higher initiator concentration as the monomer is octa-functional and probably involves degradative chain transfer to higher extent. To overcome this, higher initiator concentration may be used. The polymerization kinetics was studied at 40, 45 and 50°C and the time required for gel formation is given in Table 3.12.

Sr. No.	Temperature (°C)	Time (hr)	Observation
1	40	3.5	Immobile gel
2	45	2	Immobile gel
3	50	0.75	Immobile gel

Table 3.12: Time required for gelation of PETAC monomer.

The residual unsaturation and the initiator concentration left at different temperatures are summarized in the Tables 3.13-3.15.

Sr. No.	Time (hr)	Peroxide (%)	Unsaturation (%)
1	0	6	100.00
2	0.5	5.90	96.53
3	1	5.81	93.51
4	1.5	5.61	91.08
5	2	5.50	89.11
6	2.5	5.40	86.00
7	3	5.29	85.72
8	3.5	5.20	84.28
9	4	5.07	82.84

Table 3.13: Residual peroxide and unsaturation amount at 40 °C

Sr. No.	Time (hr)	Peroxide (%)	Unsaturation (%)
1	0	6	100.00
2	0.25	5.88	96.05
3	0.50	5.68	94.68
4	0.75	5.53	92.74
5	1	5.36	90.31
6	1.25	5.27	87.19
7	1.50	5.09	85.17
8	1.75	5.05	83.60
9	2	4.88	77.80

Table 3.14: Residual peroxide and unsaturation amount at 45 °C.

Sr. No.	Time (hr)	Peroxide (%)	Unsaturation (%)
1	0	6	100.00
2	0.12	5.89	96.67
3	0.24	5.70	94.26
4	0.35	5.51	91.77
5	0.47	5.40	88.87
6	0.58	5.26	86.45
7	0.70	5.06	83.56
8	0.82	4.98	81.79
9	0.93	4.81	79.00

Table 3.15: Residual peroxide and unsaturation amount at 50 °C.

The unsaturation analysis indicates that the octafunctional monomer gelation occurs at around 88 % of residual unsaturation. This also indicates that the PETAC polymer would have a denser 3-D network. The PETAC monomer being an octafunctional monomer forms a gel very quickly due to incresed three dimentional cross linking. The monomer forms a gel at approximately 86-88 % residual unsaturation. Table 3.4 below dipicts graphical representation of the amount of residual initiator and rasidual unsaturation at 40, 45 and 50 °C.

The slopes obtained for three lines were:

At 40 °C, K_1= 17.82

45 °C, K_1= 17.67

50 °C, K_1= 17.16

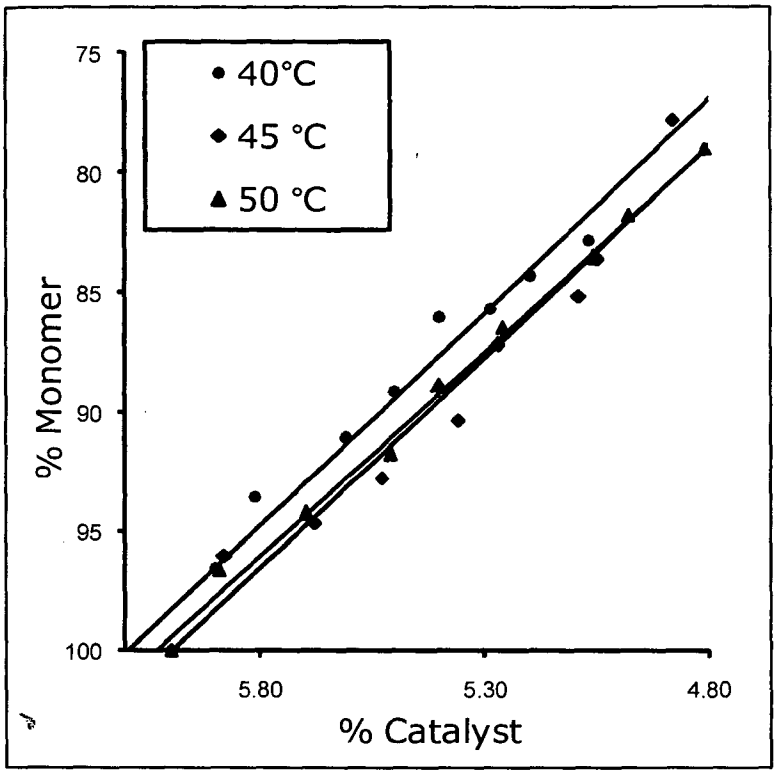

Figure 3.4: Graphical representation of the amount of residual initiator and unsaturation at 40, 45 and 50 °C.

The decreasing order of the values of the slopes of the line obtained was above the limiting value. The constants E_1, Z_1, E_3, and Z_3 were calculated by solving the kinetic equations using the values of the slopes of the lines. The values obtained for the constants E_1, Z_1, E_3, and Z_3 are dipicted in Table 3.16 below.

Sr. No.	Constant	Value
1	E_1	-746.29
2	E_3	26600.05
3	Z_1	5.33E+00
4	Z_3	1.29E+17

Table 3.16: Values obtained for the constants given in the Dial's equation.

Heating profile for 10.5 hr was obtained by using the Dial's equation as the roots of Dial's equation become imaginary and no further values were obtained. A graph was plotted for the 10 hr heating profile and was smoothly extrapolated further to obtain a 12 hr heating profile.The heating profile obtained for PETAC is shown in figure 3.5

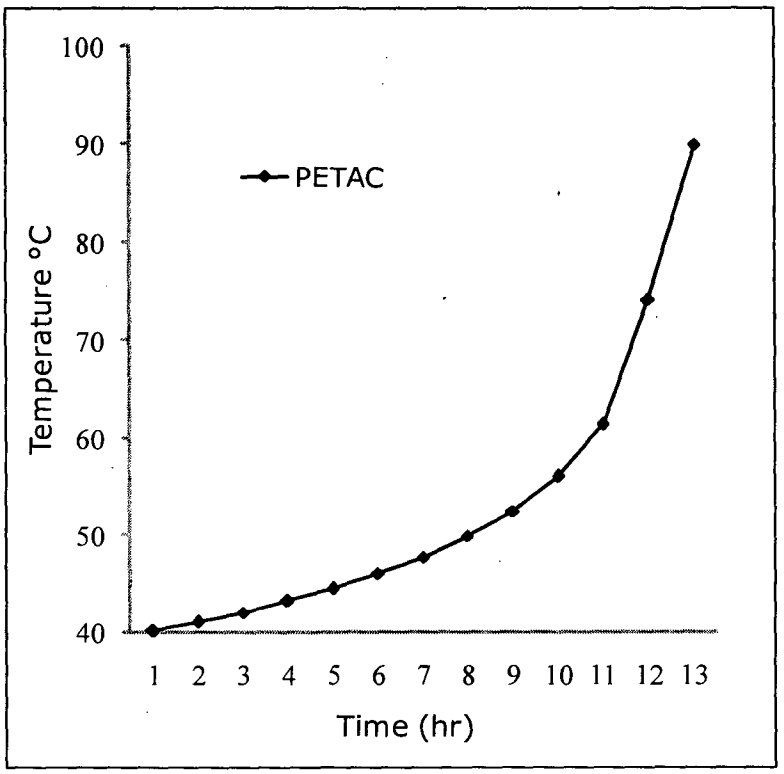

Figure 3.5: Heating profile obtained for PETAC monomer.

The heating profile obtained was also verified for its effectiveness. The polymerization mixture i.e. PETAC monomer with 6 % w/w IPP initiator was heated using the programmable water bath using the heating profile. From the data, Figure 3.6, it is clear that the heating profile obtained can be used for polymerization of PETAC monomer. This is supported well by the linear correlation coefficient (R_2) of 0.9993 obtained from calculated yields at a given time interval. As the polymer becomes more dense and hard at the

end the values obtained deviate towards the end of the profile.

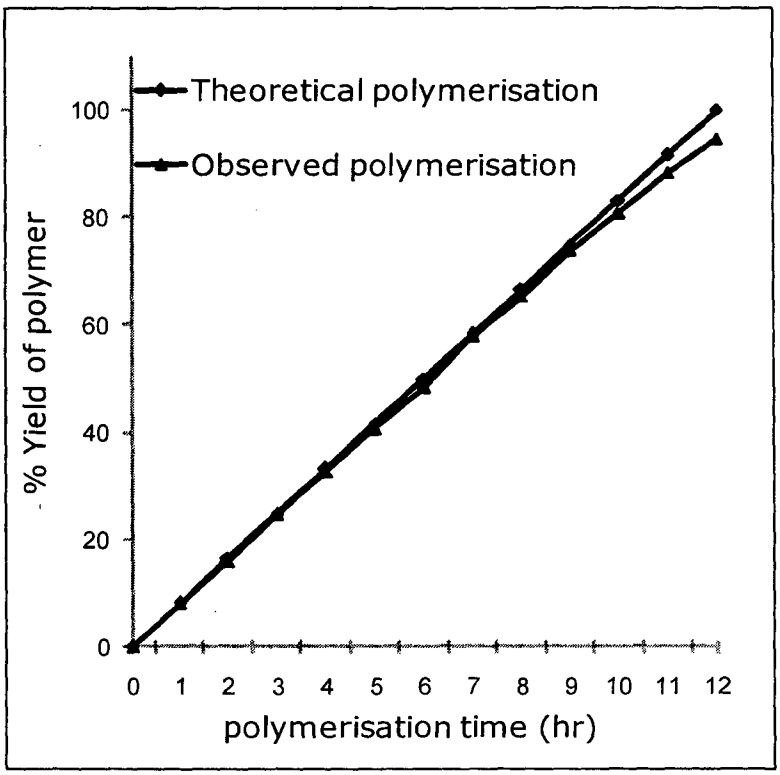

Figure 3.6: Verification of heating profile derived for constant temperature polymerization of PETAC monomer.

3.4.3 Polymerization kinetics of PETAC:ADC 1:1 w/w copolymer using IPP initiator: The copolymer of ADC have been always found to be more sensitive towards charged particle track detection. Polymerization of octafunctional PETAC monomer with ADC was also found to have higher alpha sensitivity than PADC (CR-39™. Hence the need for the kinetic studies of polymerization of ADC and PETACcopolymer with equal weight quantities and 6 % by weight IPP initiator was performed. The gel formation time for PETAC:ADC 1:1 w/w copolymer was recorded. The time required for gel formation is given in Table 3.17.

Sr. No.	Temperature(°C)	Time(hr)	Observation
1	40	4	Immobile gel
2	45	2	Immobile gel
3	50	1	Immobile gel

Table 3.17: Time for gelation of PETAC:ADC 1:1 w/w copolymer at different temperatures.

The above monomer mixture was heated in a set of test tubes at a temperature of 40, 45 and 50 °C. The testtubes were analysed for their residual unsaturation and initiator concentration.The results obtained at the three set of temperatures are summarized in the Tables 3.18-3.20.

Sr. No.	Time (h)	Peroxide(%)	Unsaturation (%)
1	0	6	100.00
2	0.5	5.89	97.89
3	1	5.77	95.15
4	1.5	5.62	93.16
5	2	5.47	89.35
6	2.5	5.33	86.65
7	3	5.28	86.30
8	3.5	5.17	84.36
9	4	5.06	83.00

Table 3.18: Peroxide and unsaturation amount at different time intervals at 40 °C

Sr. No.	Time (hr)	Peroxide(%)	Unsaturation (%)
1	0	6	100.00
2	0.25	5.87	97.70
3	0.50	5.73	95.18
4	0.75	5.61	94.38
5	1	5.49	91.51
6	1.25	5.43	89.71
7	1.50	5.29	87.50
8	1.75	5.17	85.42
9	2	5.10	83.83

Table 3.19: Peroxide and unsaturation amount at different time intervals at 45 °C.

Sr. No.	Time (h)	Peroxide(%)	Unsaturation (%)
1	0	6	100.00
2	0.17	5.86	97.89
3	0.33	5.74	95.34
4	0.50	5.61	93.02
5	0.67	5.41	90.01
6	0.75	5.25	87.05
7	0.83	5.18	84.51
8	0.92	5.09	84.42
9	1.00	4.96	83.37

Table 3.20: Peroxide and unsaturation amount at different time intervals at 50 °C.

The gelation of the monomer occurs at around 83 % residual unsaturation. The value indicates that the copolymer has a higher 3-D network than the ADC homopolymer and less denser than the PETAC homopolymer. The polymer also has enough ethylene diglycol linkages in the polymer matrix which also enhance the sensitivity of the polymer.

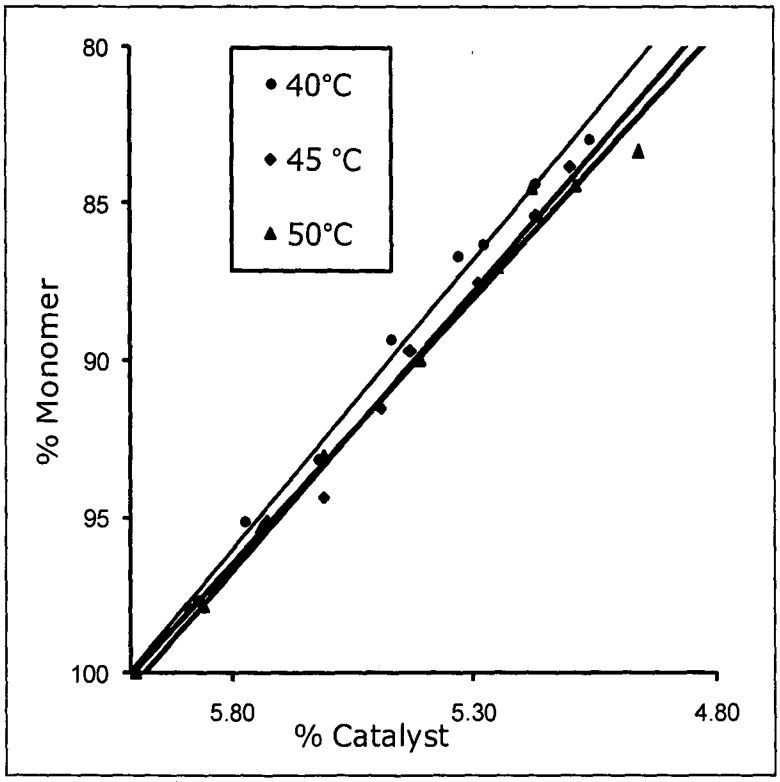

Figure 3.7: Graphical representation of the amount of initiator and unsaturation at 40, 45 and 50 °C.

The slopes obtained for three lines were:

At 40 °C, K_1= 18.53

45 °C, K_1= 17.90

50 °C, K_1= 16.97

The decreasing order of the values of the slopes of the line obtained was above the limiting values for the slope. The constants E_1, Z_1, E_3, and Z_3 were calculated by solving the kinetic

equations using the values of the slopes of the lines. E_1, Z_1, E_3, and Z_3 values obtained after solving the Dial's equations are given in the Table 3.21.

Sr. No.	Constant	Value
1	E_1	-1748.35
2	E_3	29728.76
3	Z_1	1.09E+00
4	Z_3	1.65E+19

Table 3.21: Values obtained for the constants given in the Dials equation.

The heating profile obtained is as shown in the Figure 3.8. The heating profile for 10 hr was obtained and thereafter it was smoothly extrapolated to obtain a 12 hr heating profile.

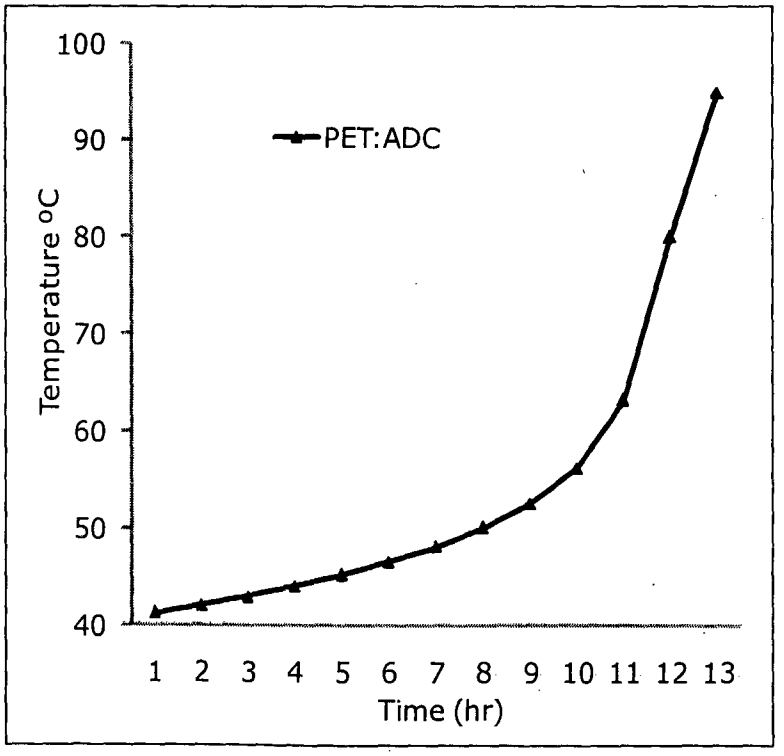

Figure 3.7: Time temperature heating profile for PETAC:ADC 1:1 w/w copolymer.

initiator are also close to one i.e. 0.9996, it can be said that they obey the same kinetic model as proposed by Dial *et. al.* The calculated and observed sets of data show a slight variation in the end of the analysis.

3.4.4 Kinetic studies of sulfur containing monomers using IPP initiator: Dial's kinetic model of allylic polymerization has already been successfully applied to monomers with functionality higher than 4 and to the monomers which have $-CO_3-$, $-ONO_2$, $-NCO_2-$, $-NO_2$ groups. This prompted us to develop the heating profiles for monomers containing sulfur based functional groups.

Attempts were made to apply Dial's kinetic model for monomers diallyl sulphite, allyl diglycol sulphite and diethylene glycol bis(allyl sulfonate). It was however observed that, during unsaturation estimation and initiator concentration analysis along with -C=C- bond, the S=O in the monomers also reacted with titrimetric reagents. This rendered error during the kinetic analysis. The monomers were however studied for gel formation. Table 3.22 gives the time required for gel formation for monomers and different copolymers.

Monomer	Initiator % w/w	Temperature	Time (hr)	Observations
DAS	4, IPP	45 °C	8	Light yellow, immobile gel
DAS	4, IPP	50°C	5	Light yellow, immobile gel
ADS	4, IPP	55°C	7	Brown mobile gel
ADS:ADC	4, IPP	50°C	6	Immobile gel
DAS:ADC	4, IPP	45°C	4	Light yellow, immobile gel
DAS:DAC	4, IPP	45°C	8	Immobile Gel formed
DEAS	5, BP	70°C	4	Light yellow, immobile gel
DEAS:ADC	5, BP	70°C	3	Colorless, immobile gel

Table 3.22: Gel point formation studies for sulfurous monomers.

The monomers also had a similarity with ADC and a heating profile derived for ADC polymerization would be feasible to polymerize these monomers.

3.4.5 Infrared spectroscopic method for kinetic estimation of monomers: The monomers containing sulfur moieties reacted with the analytical reagents used in the estimation of unsaturation. Thus, for polymerization of these monomers a heating profile could not be obtained as per Dials methodology. We, therefore, thought of studying the polymerization kinetics using on-line FTIR spectroscopy. For this purpose, we designed an assembly to hold the monomer mixture in form of a thin film (25 - 50 μm) between the two NaCl flats which are used to record IR spectrum. The assembly has a housing to hold the mold system made out of NaCl flats as shown in figure 3.9. A Teflon ring having an inner diameter of ~0.7 inch was placed on a NaCl window of 1 inch diameter. A special adhesive was used to make the mold leak proof. ADC monomer with 4 % w/w of IPP initiator was placed in the cavity and the mold was assembled with another NaCl window without allowing the formation of air bubble. The schematic of mold preparation is given in the Figure 3.9.

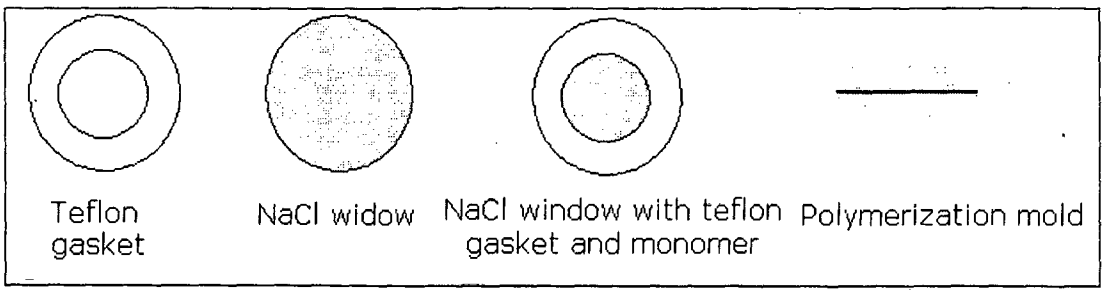

Figure 3.9: Schematic of mold preparation for kinetic study using IR spectroscopy.

The mold prepared was placed in a mold heating assembly specially devised for the purpose. It consists of an external hot water circulation to heat the polymerization mold with a temperature accuracy of ± 0.1 °C and a window of 0.7 inch diameter to scan the mold using the IR spectrometer. The temperature of the mold is recorded using the electronic temperature sensor attached to the instrument. The mold is placed in the polymerization assembly and heated to a constant temperature of 50 °C. An IR scan is recorded at the onset and thereafter continuously after interval of 15 minutes. Relative decrease in the peak heights at 1649 cm^{-1} and 3088 cm^{-1} due to -CH=CH_2 are recorded. The IR spectrum of the monomer at 0 hrs and after polymerizing for 11 hr are depicted in the Figure 3.10 (See next page). The Figure shows decrease in the peak height at 1649 cm^{-1} and 3088 cm^{-1} due to conversion of allylic double bonds to single bond and hence decrease in monomer concentration.

While testing the usefulness of this method, we observed that NaCl flats used in the study strongly adhered to polymer film that was developed. To overcome this, CaF_2 flats were used. Although, the adhesion was reduced, we observed (DEAS + IPP) mixture in CaF_2 flats that upon polymerization both the CaF_2 flats adhered very strongly to surface of DEAS homopolymer film formed. It took almost 90 days for softening of this film and detachment of the flats from the polymer surface. We therefore, stopped further studies in this regard.

The polymerization conditions used for polymerization of different polymers are given in the Table 3.23. Due to the structural similarity various sulfurous polymers were polymerized using the ADC heating profile. However, the copolymers derived from PETAC

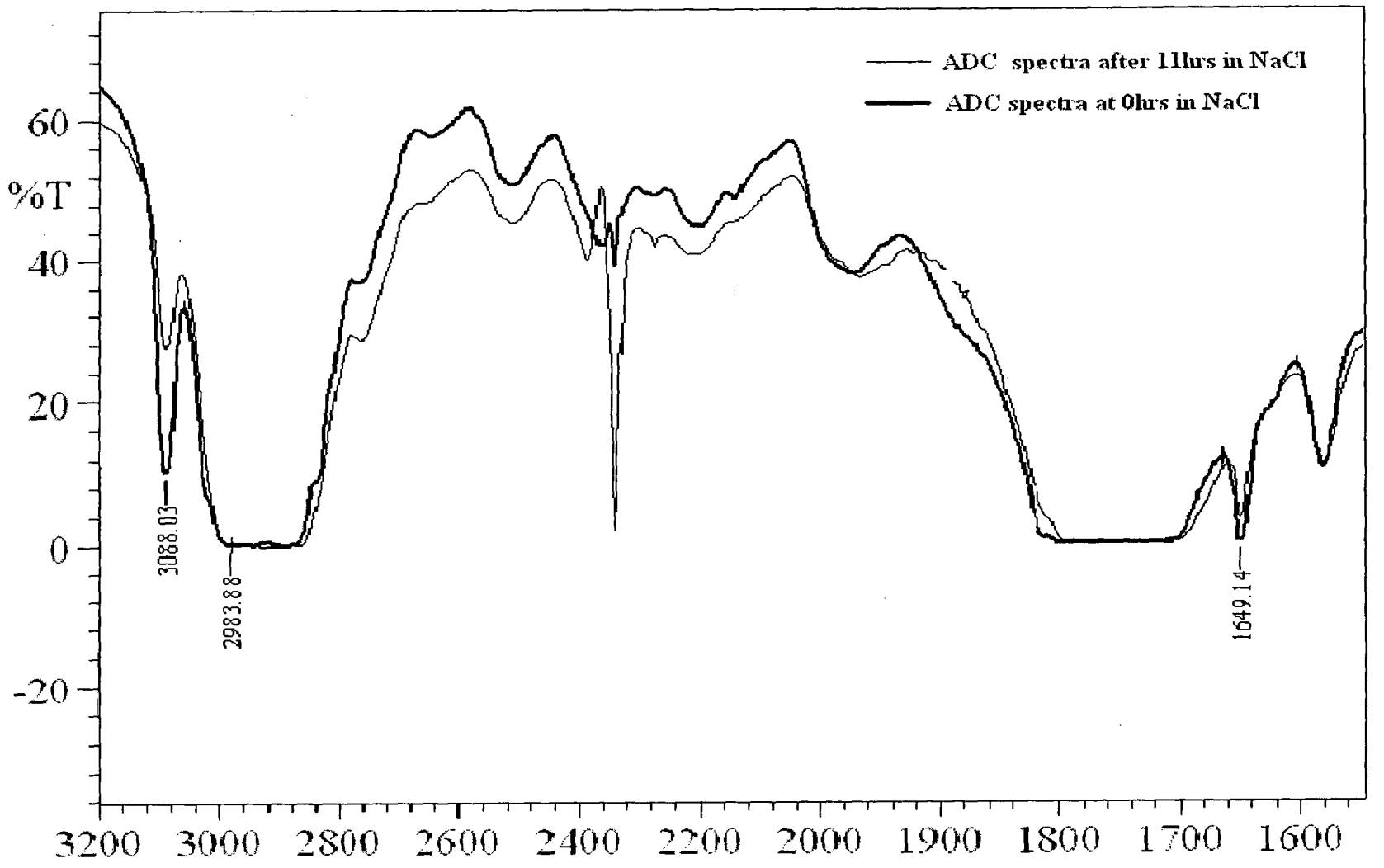

Figure 3.10. : IR spectrum of polymerization mixture at 0hrs and after 11hrs.

monomer and other sulfurous monomer were mostly polymerized using the PETAC and PETAC:ADC 1:1 w/w heating profiles.

Monomer	Heating profile used	Remarks
DEAS:ADC	ADC polymerization with IPP/BP	Structural similarity with ADC
DEAS	ADC polymerization with BP	Structural similarity with ADC
ADS	Constant temperature polymerization	Decomposed above 50 °C on heating with initiator
ADS:ADC copolymers	Constant temperature polymerization	Decomposed above 50 °C on heating with initiator
DEAS:PETAC copolymers	ADC polymerization with BP	Structural similarity of DEAS to ADC
PETAC:ADC: DEAS copolymers	PETAC:ADC 1:1 w/w polymerization	PETAC & ADC are major constituents
DAS:ADC copolymers	Constant temperature polymerization	Decompose at 50 °C on heating with initiator
PBCBS	PETAC polymerization with IPP	Structural similarity of PBCBS
PBCBS:ADC	PETAC:ADC1:1 w/w polymerization	Structural similarity with PETAC & ADC

Table 3.23: Polymerization heating profiles used for polymerization of different polymers of sulfurous monomers.

The sulfur containing monomers reacts with the titrimetric reagents during kinetic analysis and the study of their polymerization kinetics become difficult. The sulfurous monomers were therefore polymerised using the IPP or the BP heating profiles devised for different monomers. The heating profiles used for polymerization of different homopolymers and copolymers are given in Figure 3.11.

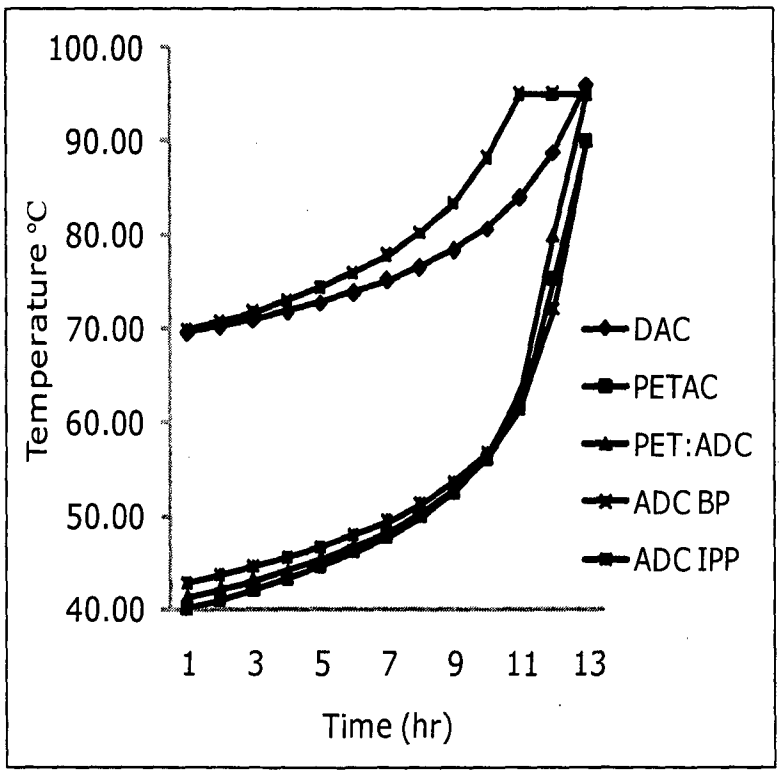

Figure 3.11: Polymerization heating profiles with IPP and BP initiators.

3.5 Optimization of monomer concentration: The monomer prepared is first homopolymerised and to find out its track detection characteristics. If a homopolymer of a monomer is found to detect charged particle it is often copolymerized with ADC monomer. The copolymers of ADC are prepared as the sensitivity of copolymer is higher than that of the copolymer.[73,74,77] This may be due to the fact

that the copolymerization leads to introduction of ethylene diglycol linkages in the polymer matrix. A series of copolymers of new monomers and ADC were prepared to find out the optimum composition where alpha sensitivity is maximum.

3.5.1 Optimization of DAC:ADC copolymer concentration: The test polymer of DAC monomer was able to detect only fission fragments particles from ^{252}Cf source. The various copolymers of ADC with DAC were prepared and their track detection properties were examined. The polymerization of the monomers was performed using the derived DAC heating profile. The mixtures having higher ADC concentration were polymerized using the ADC heating profile. The polymers were tested for the amount of residual unsaturation after complete polymerization. The thickness of the film was also noted. All the polymers prepared were colorless and could be easily used as track detectors. Table 3.24 gives the physical properties of DAC homopolymer and the various copolymers prepared from DAC and ADC.

Sr. No.	DAC:ADC polymer(w/w)	Film thickness (micron)	% residual unsaturation
1	DAC	589 ± 5	3.73
2	8:2	650 ± 5	3.78
3	7:3	573 ± 5	6.01
4	6:4	565 ± 5	4.68
5	1:1	604 ± 5	3.86
6	4:6	604 ± 5	5.73
7	3:7	562 ± 5	4.26
8	2:8	653 ± 5	4.55
9	1:9	680 ± 5	4.13

Table 3.24: Physical properties of DAC homopolymer and copolymers with ADC.

The polymers obtained were cut into the small pieces of size 1 x 1 cm^2 and were exposed to fission fragments from ^{252}Cf source and alpha particles from ^{239}Pu source in close (0.1 cm) contact. The polymer films were etched in 6 N NaOH at 70 °C and the time required to reveal the alpha autoradiograph and fission fragment tracks was noted. The Table 3.25 gives the time required for track revelation.

Sr. No.	Composition of ADC:DAC w/w	Time to observe ^{252}Cf fission tracks (hr)	Time to observe ^{239}Pu alpha tracks (hr)
1	DAC	1	Not observed
2	8:2	1	Not observed
3	7:3	1	Not observed
4	6:4	1	7
5	1:1	1	4
6	4:6	1	4
7	3:7	1	3
8	2:8	1	3
9	1:9	1	2
10	CR-39™	1	2

Table 3.25: Time required revealing alpha and fission fragment tracks.

The DAC homopolymer was found to detect only fission fragment tracks even after etching for more than 15 hr. When the concentration of DAC is increased to 60 %, the copolymer with ADC can be used to detect alpha autoradiograph. Thus, the copolymers containing ADC proportion more than or equal to 40 % were able to detect both alpha and fission tracks. The time re-

quired to reveal the particle tracks decreases with the increase in the ADC concentration. From the track revelation times recorded it can be seen that the time required to reveal alpha autoradiograph increases as the concentration of DAC monomer in the copolymer increases.

The alpha sensitivity studies were performed on the copolymers which were able to detect both the alpha and fission fragment tracks under the etching conditions used. The track growth of fission fragments were measured at every hour interval and is depicted in Figure 3.12.

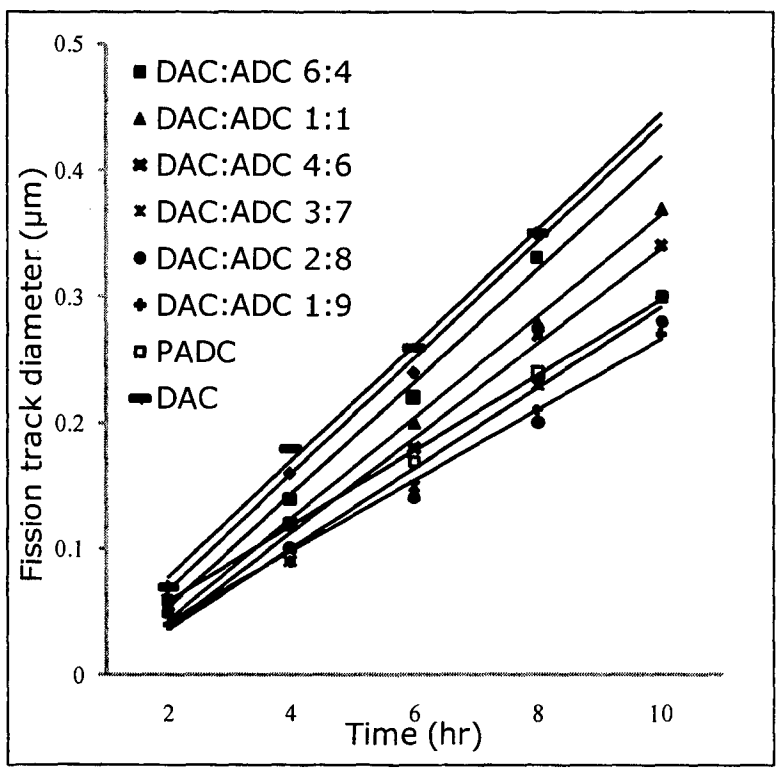

Figure 3.12: Variation of fission track diameter in different copolymers of DAC:ADC.

Thus, it may be observed that PDAC homopolymer has higher bulk etch rate than that of PADC which in our opinion, is due to lesser amount of polymer chain entanglement and lesser

crosslinking. The alpha sensitivity of the films was measured using variation of track diameters and is given in Table 3.26. From the data obtained it is clear that the ADC copolymers of DAC are not more sensitive than CR-39™. The sensitivity increases with the increase in the concentration of ADC which implies that the DAC monomer itself is not sensitive for track detection. The DAC homopolymer, however, can be used to reveal fission tracks in presence of large amounts of alpha particles. This also helps in concluding that the presence of diethylene glycol link is important for higher radiation sensitivity of CR-39™ and this observation is in line with what was observed by Fujii *et al.*

DAC:ADC Polymer(w/w)	Alpha Sensitivity	Bulk etch rate (Polymer μm/hr)
1:0	Not determined	----
8:2	Not determined	----
7:3	Not determined	0.018
6:4	1.08	0.015
1:1	1.13	0.013
4:6	1.16	0.013
3:7	1.20	0.013
2:8	1.19	0.013
1:9	1.25	0.010
CR-39™	1.28	0.010

Table 3.26: Sensitivity values and the bulk etch rate of different copolymers.

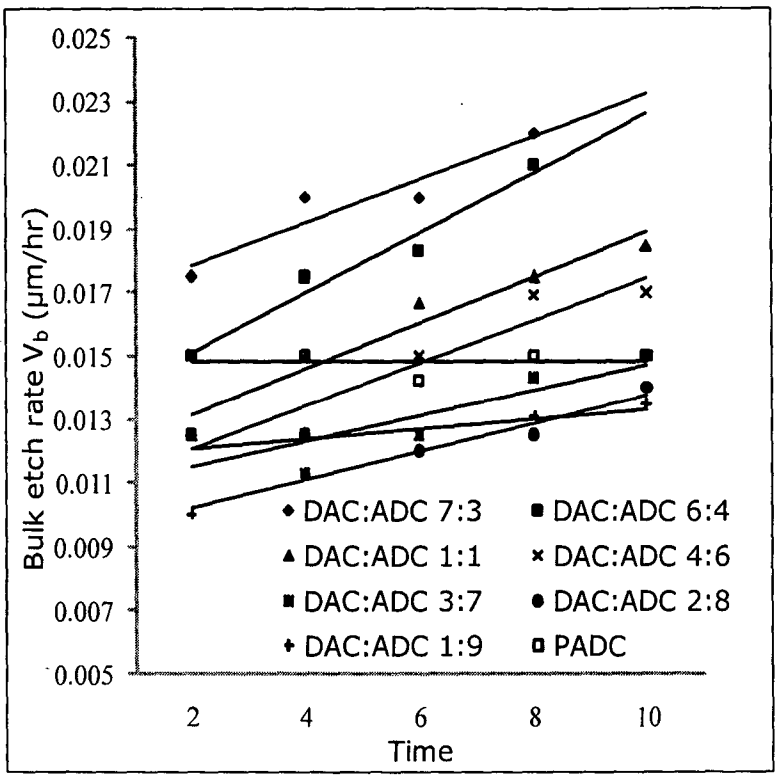

Figure 3.13: Variation of bulk etch rate in different copolymers.

The bulk etch rate of the copolymers was determined using the fission track diameter method. The bulk etch of the copolymers increased with increase in the concentration of DAC monomers. The variation of bulks etch rate for different copolymers is depicted in Figure 3.13.

3.5.2 Optimization of DEAS:ADC copolymer composition: Addition of DEAS monomer to the ADC monomer introduces relatively weak sulfonate linkage in the polymer matrix. Fujii et al. had first prepared copolymers of DEAS with ADC in 1:9 (SR-86(10)) and 2:8 (SR-86(20)) w/w ratio using IPP initiator. Copolymers of ADC with higher DEAS concentration was not prepared by them as the monomer was solid and had a limited solubility (20 % w/w) in ADC.[74] Both the copolymers were more sensitive than PADC i.e.

CR-39™ track detector. Fujii et al never tried to optimize the composition of copolymer to get better sensitivity. Based on our experiments, we expected that higher DEAS concentration ADC copolymers may show better track detection properties than CR-39™. Furthermore, no spectral characterization of DEAS monomer was reported by the authors. The DEAS monomer was synthesized by condensation method and purified by column chromatography. The monomer was characterized using the various spectroscopic techniques and also the melting point of the monomer was recorded.

The DEAS monomer was found to melt at a comparatively lower temperature of 53 °C. Thus a homopolymer of DEAS and other copolymers with ADC could be easily prepared by using BP initiator. BP has a decomposition temperature of 70 °C. Thus, ADC and DEAS monomers were mixed in specified concentration and heated on water bath at around 60 °C to get a homogenous molten mixture. BP 4 % w/w and the DOP 1 % w/w was added. The contents were mixed thoroughly until the initiator completely dissolves in the polymerization mixture. However, the co-monomers with higher DEAS concentration solidified during injection of the mixture. The mixture was injected in the mold preheated at around 60 °C as rapidly as possible through a 200 µm filter using a syringe.

The ADC heating profile was used due to the structural similarity of the DEAS and ADC. The DEAS was also homopolymerized using the same heating profile. The films obtained were hard and had a brown color. The brown coloring increased with the increase in DEAS concentration in the copolymer. The unsaturation analysis of the polymers was not performed due to analytical problems. The track detection properties and thickness of the films are given in Table 3.27 below (Please see next page).

Polymer of DEAS:ADC w/w	Thickness (μm)	Time to observe (min)	
		^{252}Cf fission	^{239}Pu alpha
DEAS	615±5	50 - 60	180
1:9	625±5	35 - 45	60
2:8	662±5	20 - 30	60
3:7	646±5	20 - 30	60
4:6	586±5	20 - 30	60
1:1	683±5	20 - 30	60
6:4	701±5	20 - 30	60
7:3	625±5	20 - 30	60
8:2	662±5	45 - 60	90
CR-39™	500±5	45 - 60	120

Table 3.27: Track detection properties of different copolymers of DEAS and ADC.

From the track revelation studies it can be seen that the copolymers can reveal the alpha and fission tracks rapidly. The time required to reveal tracks is reduced to almost half than that required for commercially available CR-39™. The post etch surface of the films was also very clear. Surprisingly, DEAS homopolymer did not show higher sensitivity than PADC. It is known that R-$SO_2^{\cdot}$ radical, if formed, undergo addition even with R-CH=CH_2 double bonds. The radical may also lose SO_2 to give a R· free radical.[133] Later we also noted from the literature that sulfonyl compounds under the influence of radical initiators, UV light or heat undergo cleavage releasing SO_2.[134]

It may therefore be expected that such reactions adversely affect formation of a rigid 3 D network, so that the bulk etch rate of the polymer increases and consequently radiation sensitivity decreases. The polymer also turned opaque when it was etched for more than 2 hrs. The physical appearance/impression of the alpha autoradiograph was seen but under the microscope the tracks could not be seen clearly due to large background and opaqueness of the film.

The copolymers of ADC with DEAS were able to reveal the tracks in quick time. The alpha sensitivity of the polymers was determined using the track diameter method. Table 3.28 (see next page) gives the alpha sensitivity and the bulk etch rate of different copolymers. One can see that the alpha sensitivity of the polymer DEAS:ADC 3:7 w/w copolymer is maximum. The sensitivity of the indigenous SR-86 (10) [DEAS:ADC 1:9 w/w] and SR-86(20) [DEAS:ADC 2:8 w/w] was less than the 3:7 copolymer. As the concentration of DEAS monomer is increased further the sensitivity of the copolymers decreases.

The sensitivity of the DEAS homopolymer was not determined as the polymer turns opaque after 2 hrs of chemical etching and the tracks of the alpha particles are not seen very clearly. The DEAS homopolymer was etched with 1 N - 7 N NaOH at a temperature range of 50 - 70 ^{o}C but the polymer turned opaque. Under milder etching conditions the polymer turned opaque after 3 - 4 hr but no autoradiograph was seen when the film was clean. Weight loss method was used to determine the bulk etch rate of the material DEAS homopolymer as the tracks cannot be observed clearly after 1 hr of chemical etching.

Composition of DEAS:ADC (w/w)	Maximum alpha Sensitivity	Bulk etch rate (V_b) µm/hr
CR-39™	1.22	0.015
PADC (indigenous)	1.20	0.011
1:9 *i.e.* SR-86(10))	1.41	0.020
2:8 *i.e.* SR-86(20)	1.74	0.022
3:7	2.38	0.022
4:6	1.60	0.035
1:1	1.36	0.030
6:4	1.23	0.036
7:3	1.21	0.051
8:2	1.20	0.052
PDEAS	Not determined	2.08*

* Weight loss method was used to determine the bulk etch rate of the material.

Table 3.28: Alpha sensitivity and the bulk etch rate of copolymers.

Composition of DEAS:ADC w/w	Alpha track diameter (µm) after etching		
	2 hr	3 hr	4 hr
CR-39	--	0.020	0.040
PADC	--	0.020	0.035
1:9 (SR-86(10))	--	0.010	0.030
2:8 (SR-86(20))	--	0.030	0.060
3:7	0.020	0.060	0.011
4:6	0.040	0.084	0.128
1:1	0.050	0.073	0.110
6:4	0.050	0.085	0.110
7:3	0.065	0.120	0.190
8:2	0.063	0.130	0.190

Table 3.29: Variation of alpha track diameters in DEAS:ADC co-polymers.

Composition of DEAS:ADC w/w	Fission track diameter (μm) after etching			
	1hr	2hrs	3hrs	4hrs
CR-39	0.030	0.060	0.095	0.130
PADC	0.021	0.050	0.080	0.115
1:9 (SR-86(10))	0.020	0.060	0.090	0.120
2:8 (SR-86(20))	0.040	0.080	0.120	0.160
3:7	0.042	0.090	0.170	0.265
4:6	0.047	0.095	0.203	0.269
1:1	0.060	0.127	0.206	0.228
6:4	0.050	0.160	0.264	----
7:3	0.101	0.210	0.310	----
8:2	0.103	0.210	0.320	----

Table 3.30: Variation of fission fragment track diameter in DEAS:ADC copolymers.

The track growth rate increases with increase in the concentration of DEAS monomer. The alpha track being in the early development stage poses difficulty in diameter measurements in first hour. Table 3.29 gives the diameter of the alpha tracks during the first four hours of chemical etching. It may seen that there is a considerable difference in the diameter of the alpha tracks observed in different polymers. From the results it is quite clear that the increase in the DEAS concentration increases the bulk etch rate of the polymer as well as the track etch rate. The increase in the fission track diameter (Table 3.30) also follows the same trend i.e. the track diameter increases with increase in DEAS concentration. This is due to more number of labile sulfonate groups in the polymer matrix. The higher DEAS concentration incerts more num-

ber of labile sulfonate moieties which are hydrolyzed more easily. The Figure 3.14 below shows the variation of bulk etch rate in different copolymers of DEAS:ADC when etched in 6 N NaOH at 70 °C. The bulk etch rate was determined using the fission fragment diameter method and increases with the rise of DEAS concentration .

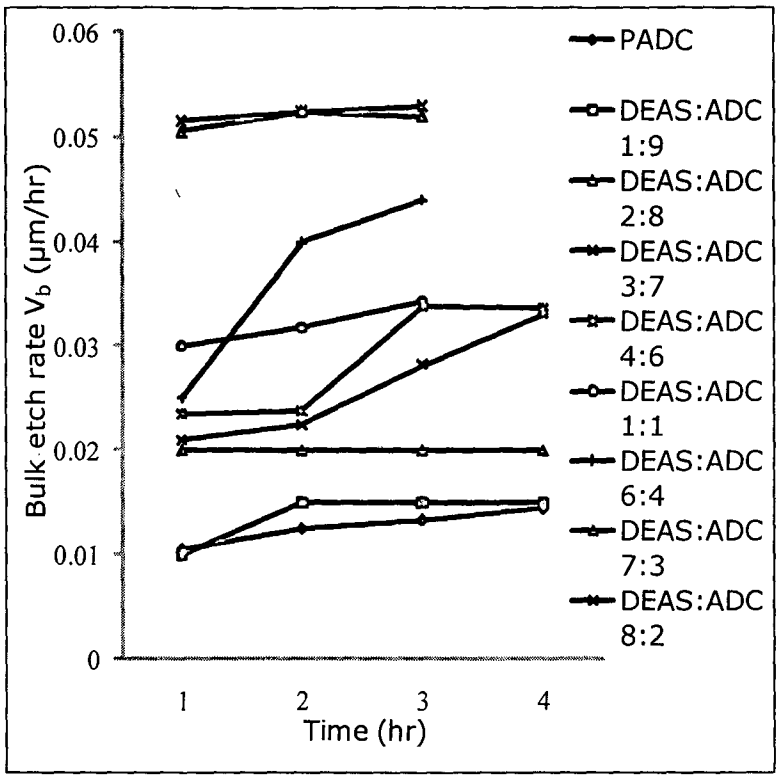

Figure 3.14: Variation of bulk etch rate in different copolymers of DEAS:ADC.

It was found that in addition to sulphite containing polymers, the DEAS based polymers (homopolymers and copolymers) become very soft within 2-3 months and further get converted into a viscous gelly liquid in nearly an year. The decomposition was observed even if they are stored in sealed plastic bags(0 °C). The IR spectrum of the decomposed brownish liquid of DEAS:ADC 1:1 w/w copolymeris is shown in figure 3.15 below (See next page) in

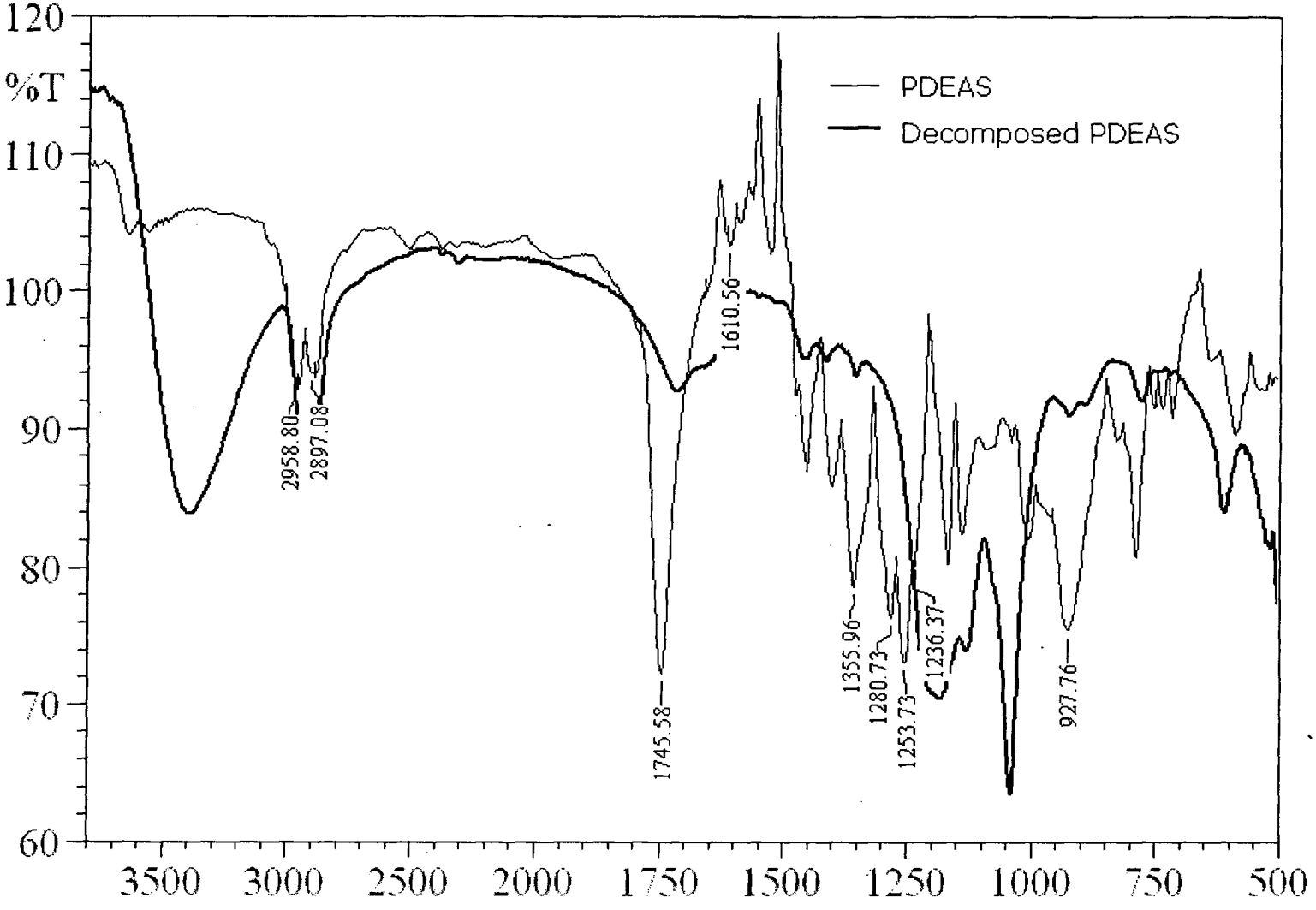

Figure 3.15: Infrared specturm of DEAS:ADC and decomposed DEAS:ADC polymers.

comparison with the IR spectra of newly prepared DEAS:ADC 1:1 w/w copolymer.

The spectra comparison clearly indicates decomposition of the copolymer. From the IR spectra of the copolymers it appeared that the liquid had a significant hydroxyl content but the charecteristics peaks of S=O at 1352 cm^{-1} and 1165 cm^{-1} were not much clear indicating that probably degradation of the polymer with loss of certain sulfur compounds takes place. The degraded gelly liquid was also found to give disagreeable odour. In a separate experiment to increase the shelf life of the DEAS copolymers it was observed that the samples irradiated with gamma radiation results in longer shelf life of the polymer so that degradation occurs after considerably long time.The variation in the sensitivity of DEAS:ADC 3:7 w/w, DEAS:ADC 2:8 w/w, DEAS:ADC 4:6 w/w and PADC are given in the Figure 3.16.

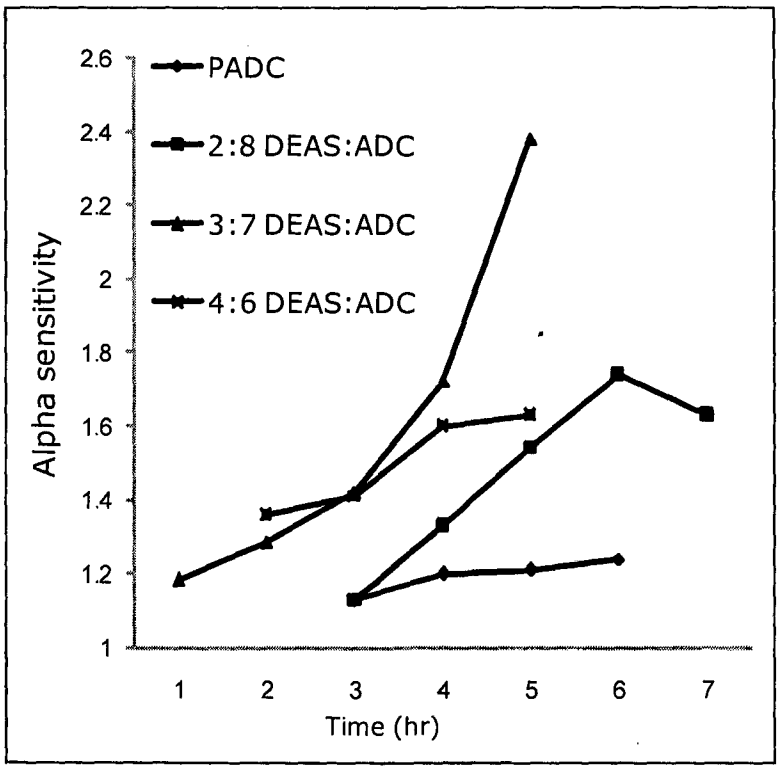

Figure 3.16: Sensitivity variation in most sensitive copolymers of DEAS and ADC.

Interestingly, the monomer mixture of DEAS:ADC 3:7 w/w remained liquid even after cooling at 25 °C. DEAS:ADC 3:7 w/w copolymer thus, can be prepared using IPP initiator as polymerization catalyst. The DEAS and ADC monomers were mixed in 3:7 w/w and heated on water bath to melt the DEAS monomer. The mixture was cooled to ~ 30 °C and IPP initiator 4 % w/w and DOP 1 % w/w were added. The mixture was homogenized and injected into the polymerization mold and polymerized using 12 hr constant rate heating profile of ADC IPP monomer.

The polymer obtained was hard, clear and had less brown color than the polymer prepared using the BP initiator. The thickness of the polymer film was 671 ± 10 μm. The polymer had almost identical track detection properties and the time required to reveal tracks was same. The difference in the two polymers was clear when the sensitivity studies was performed on the two polymer prepared using the IPP and BP initiator. Figure 3.17 (see next page) gives the variation in the track sizes of alpha and fission fragments in polymers prepared using different initiators after etching in 6 N NaOH at 70 °C. At the onset of etching process the track diameters were almost same after 1hr But, one can observe that in the polymer derived from the IPP initiator the rate of increase of track sizes of both alpha and fission was more than the polymer derived using BP initiator.

From Figure 3.18 (see next page) one can observe that the polymer prepared by using IPP initiator is more sensitive. The maximum alpha sensitivity for IPP initiated polymer is 2.54 whereas the polymer prepared using BP initiator has a maximum alpha sensitivity of 2.38. The time required to attain maximum alpha sensitivity was also reduced in the polymer prepared with IPP as compared to that of the polymer prepared using BP initiator.

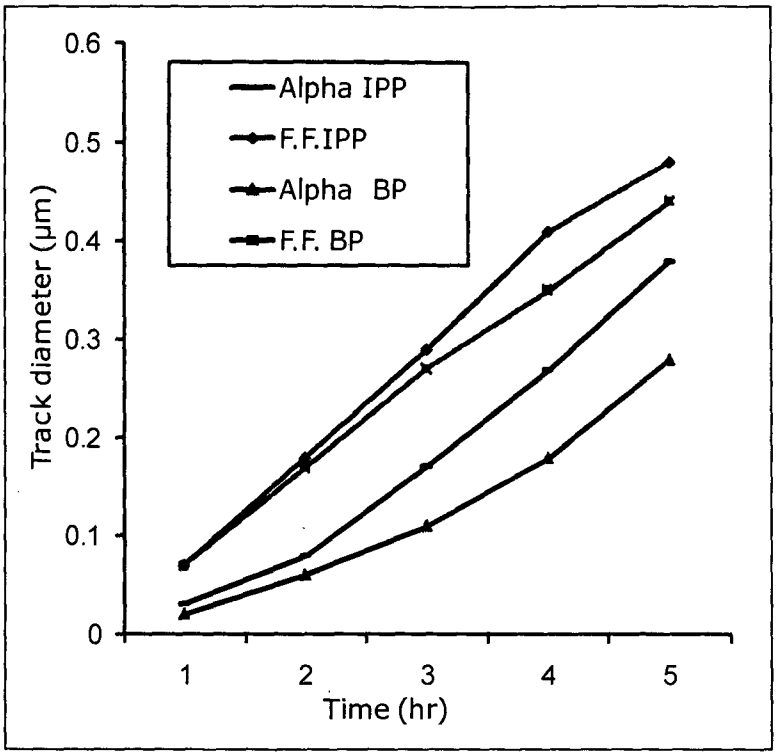

Figure 3.17: Track size of alpha and fission in copolymers prepared using BP and IPP.

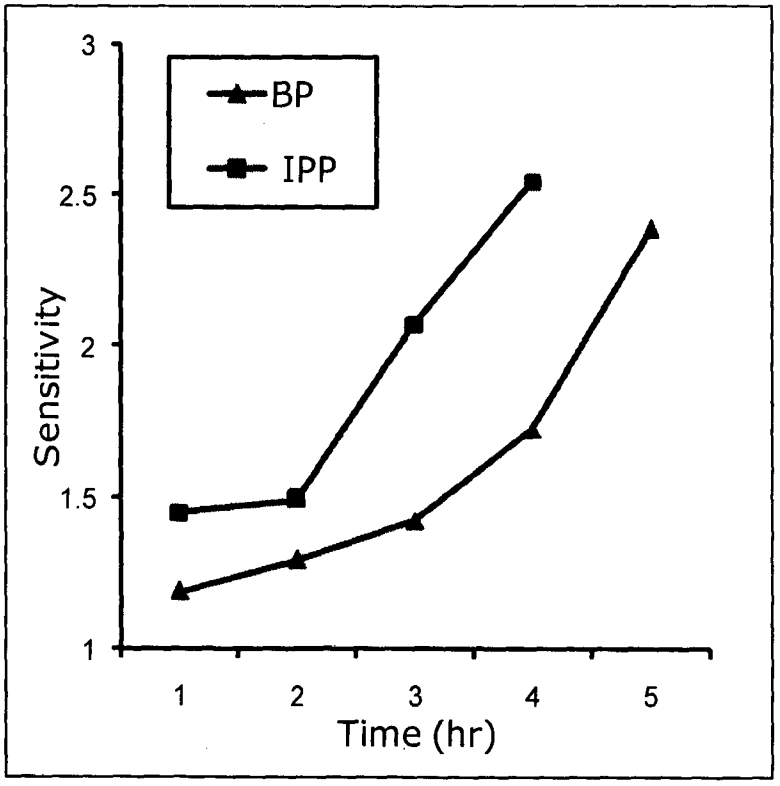

Figure 3.18: Sensitivity values for the copolymers prepared using BP and IPP.

3.5.3 Optimization of PETAC:ADC copolymer composition: The PETAC monomer is a octafunctional monomer and should form a denser 3-D network in the polymer matrix. This monomer is a colorless liquid and can be easily polymerized using IPP initiator. As monomer is thermally unstable at high temperatures (above 150 °C) it is purified using silica gel column chromatography with n-hexanes/ethyl acetate as eluent. The PETAC monomer is also copolymerized with ADC monomer in different w/w proportions. As the concentration of ADC monomer is increased in the copolymer mixture, more number of ethylene diglycol linkages would be introduced in the polymer which increases the sensitivity of the polymer. However, the 3-D network density would decrease in the polymer matrix. Thus, the new copolymers would have some interesting track detection and sensitivity relationship properties than either of the homopolymers.

The monomers were mixed in weight by weight ratio and stirred under nitrogen for 30 minutes. 6 % w/w IPP initiator and 1 % w/w DOP plasticizer was added to the monomer The mixture was injected in polymerization mold and polymerized according to the 12 hour heating profiles derived for PETAC, PETAC:ADC and ADC(IPP) monomer polymerization. The heating profiles used for the polymerization of different monomers are given in Table 3.31. The polymerization heating profile was chosen depending on the concentration of particular monomer. The molds were allowed to cool for 12 hours before opening them.

Sr. No	Heating profile used	Composition of PETAC:ADCw/w
1	PETAC polymerization	10:0, 8:2, 7:3
2	PETAC:ADC polymerization	4:6, 1:1, 6:4
3	ADC (IPP) polymerization	3:7, 2:8, 1:9, 0:10

Table 3.31: Polymerization heating profiles used for polymerization of different monomers.

The polymers obtained were colorless, hard and brittle. The thickness data of the polymers and the rasidual unsaturation obtained is given in Table 3.32.

Composition of ADC:PETAC w/w	Thickness (μm)	% residual unsaturation
CR-39™	250 ± 5	5.42
1:9	597 ± 5	5.33
2:8	610 ± 5	8.11
3:7	590 ± 5	6.22
4:6	635 ± 5	5.34
1:1	562 ± 5	4.75
6:4	615 ± 5	5.50
7:3	573 ± 5	4.98
8:2	608 ± 5	5.00
10:0	593 ± 5	6.23

Table 3.32: Physical properties of different polymers prepared.

Composition of ADC:PETAC (w/w)	Time to observe (min)	
	fission tracks	alpha autoradiograph
CR-39™	45-60	120
1:9	35-45	60
2:8	35-45	60
3:7	25-30	60
4:6	25-30	60
1:1	25-30	60
6:4	25-30	60
7:3	25-30	60
8:2	25-30	60
10:0	45-60	90

Table 3.33: Alpha and fission track revelation time for different polymers.

The polymers were subjected to track revelation studies and the results obtained are given in Table 3.33 abow (Please see previous page). The films were etched in 6N NaOH at 70 °C. The fission and alpha tracks in PETAC homopolymer were observed in 35 and 90 minutes respectively as compared to PADC/CR-39™ which require about 45 minutes for (fission tracks) and 120 minutes for (alpha) tracks. The track diameters increased with the increase in the concentration of ADC monomer in the copolymer mixture *e.g.* the diameter of alpha track in PPETAC after 4 hr was less than the alpha track diameter in PADC after 4 hr when etched unde identical etching conditions. The variation in track size of the alpha particles is given in Figure 3.19.

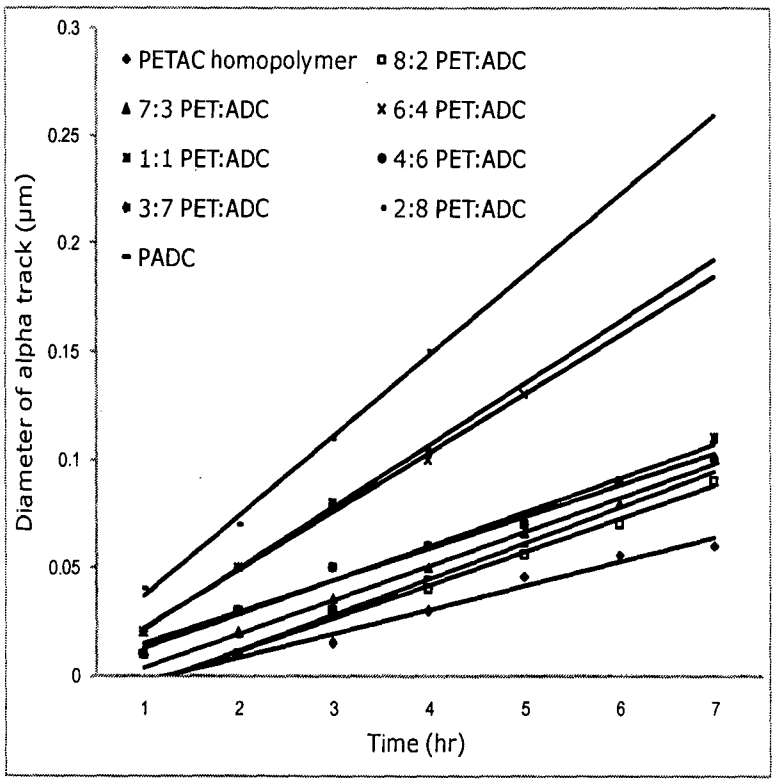

Figure 3.19: Variation of alpha track diameter in different copolymers of PETAC and ADC.

The fission track diameter also increased with higher ADC concentration in the copolymer. The increase in the ADC concentration decreases the 3 D network *i.e.* the crosslinks in the copolymer as compared to the PETAC homopolymer due to reduced functionality of the ADC monomer. The variation of fission track diameter in PETAC homopolymer and different copolymers of PETAC:ADC w/w is given in Figure 3.20.

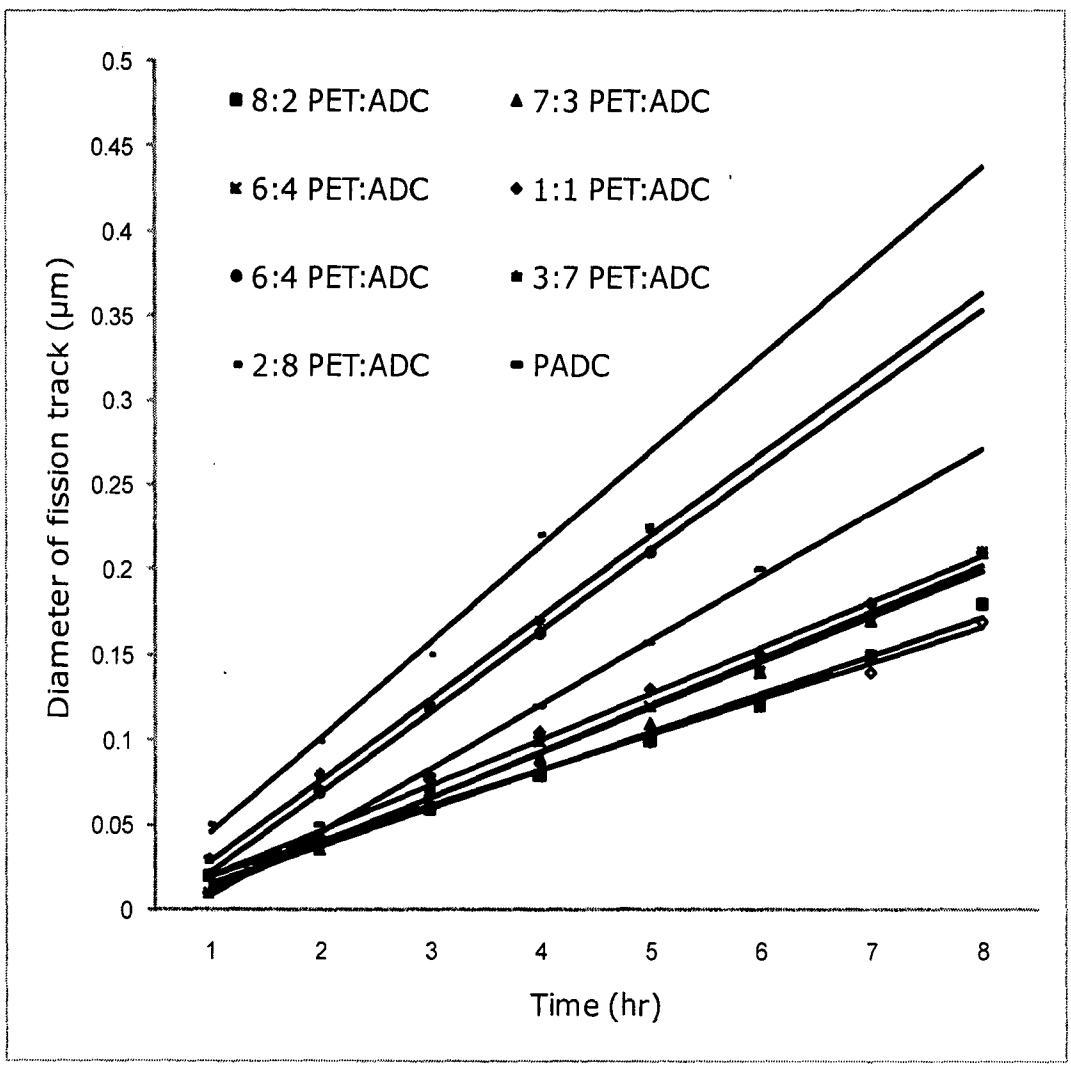

Figure 3.20: Variation of fission track diameter in different copolymers of PETAC and ADC.

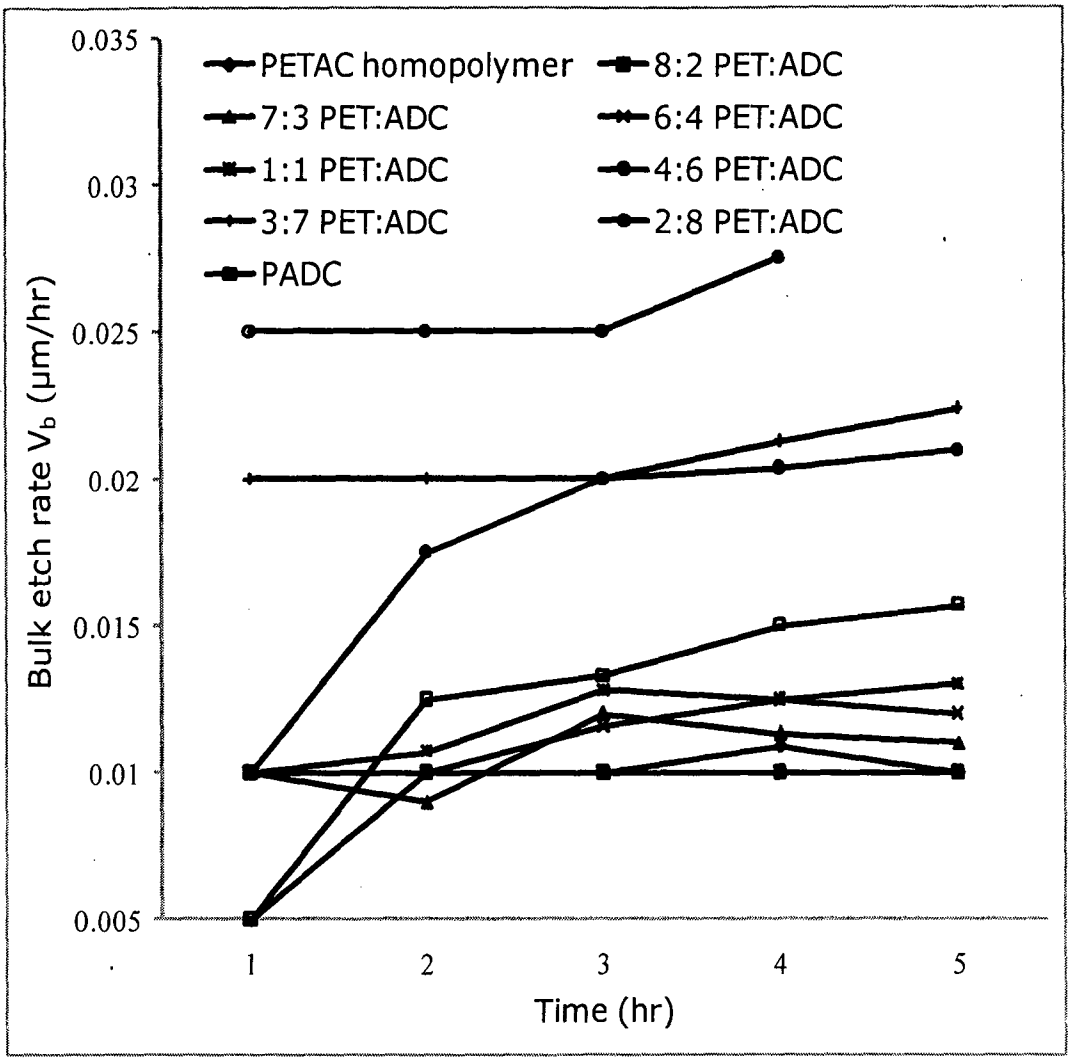

Figure 3.21: Variation of bulk etch rate of different polymers.

Figure 3.21 gives variation in the bulk etch rate of different polymers. From the Table 3.34 below (see next page) one can see that the alpha sensitivity of the PETAC homopolymer is more than that of PADC or CR-39™. Thus, the PETAC homopolymer has a very dense 3-D network which must effectively stops the charged particle. The large number of covalent bonds in the polymer interacts with the particle more efficiently. However, it was observed that the copolymer PETAC:ADC 4:6 w/w had a maximum alpha sensitivity. It may be argued that due to the induction of diethylene glycol linkage, in addition to the denser 3-D network, makes the polymer even more sensitive towards alpha particles.

Composition of ADC:PETAC (w/w)	Maximum alpha sensitivity	Bulk etch rate (V_b) (μm / hr)
CR-39	1.22	0.013
10:0	1.23	0.013
8:2	1.55	0.010
7:3	1.57	0.010
6:4	1.78	0.018
1:1	1.67	0.011
4:6	1.60	0.015
3:7	1.56	0.020
2:8	1.56	0.025
PPETAC	1.38	0.125

Table 3.34: Alpha sensitivity values for various copolymers of PETAC:ADC w/w.

The PPETAC polymer has higher alpha sensitivity than ADC. All the further studies of the polymers would be performed with respect to these polymers.

3.5.4 Optimization of DEAS:PETAC copolymer composition:

The PETAC:ADC 4:6 w/w copolymer was found to be the polymer with the highest alpha sensitivity. It was worth studying the sensitivity relationship of PETAC monomer copolymerized with DEAS monomer. The copolymerization of PETAC with DEAS would introduce a more labile sulfonate group in dense 3-D network and thus the copolymer must be more sensitive than PETAC:ADC 4:6 w/w copolymer. As the concentration of ADC:PETAC was optimized to 6:4 w/w respectively the DEAS:PETAC copolymers with 7:3, 6:4 and 1:1 w/w composition was prepared.

The monomers were mixed in specified w/w ratio and heated on water bath to melt DEAS monomer. The polymerization was carried using 4 % w/w BP initiator and 1 % w/w of DOP as a plasticizer. IPP could not be used as initiator in this case as, DEAS was found to have very limited solubility in PETAC at room temperature and therefore the PETAC:DEAS mixture. The mixture was held at 60 °C to ensure the dissolution. At this temperature IPP would undergo decomposition and hence BP was selected as polymerization initiator. ADC (BP) heating profile was used to polymerize the copolymers. The films obtained were cut into pieces of size 1x1 cm^2 and were used for track revelation studies. The time required to reveal alpha and fission tracks after etching in 6 N NaOH at 70 °C is given in Table 3.35.

Composition of DEAS:PETAC w/w	Thickness (μm)	Time to observe (min)	
		fission tracks	alpha tracks
7:3	545 ± 5	15-20	45
6:4	546 ± 5	15-20	45
1:1	698 ± 5	20-25	45
ADC:PETAC 6:4	635±5	25-30	60
DEAS:ADC 3:7	646±5	25-30	60
CR-39™	250±5	45-60	120

Table 3.35: Track revelation studies for different polymers prepared from PETAC and DEAS.

As expected, the time required to reveal the alpha and fission tracks was reduced in the copolymers of PETAC:DEAS as compared to PETAC:ADC of same w/w monomer ratio. The time re-

quired to reveal alpha tracks was reduced to 45 minutes in DEAS:PETAC 6:4 w/w as compared to 60 minutes required for ADC:PETAC 6:4 w/w and DEAS:ADC 3:7 w/w and 120 minutes required for CR-39™. The fission tracks were revealed in 15-20 minutes by DEAS:PETAC 6:4 w/w copolymer as compared to 25-30 minutes required for ADC:PETAC 6:4 w/w and DEAS:ADC 3:7 w/w and 60 minutes CR-39™ respectively.

The alpha sensitivity of these polymers was determined using the track diameter of the alpha and fission tracks. The variation in the alpha sensitivity of the polymers can be seen from Figures 3.22 to Figure 3.24.

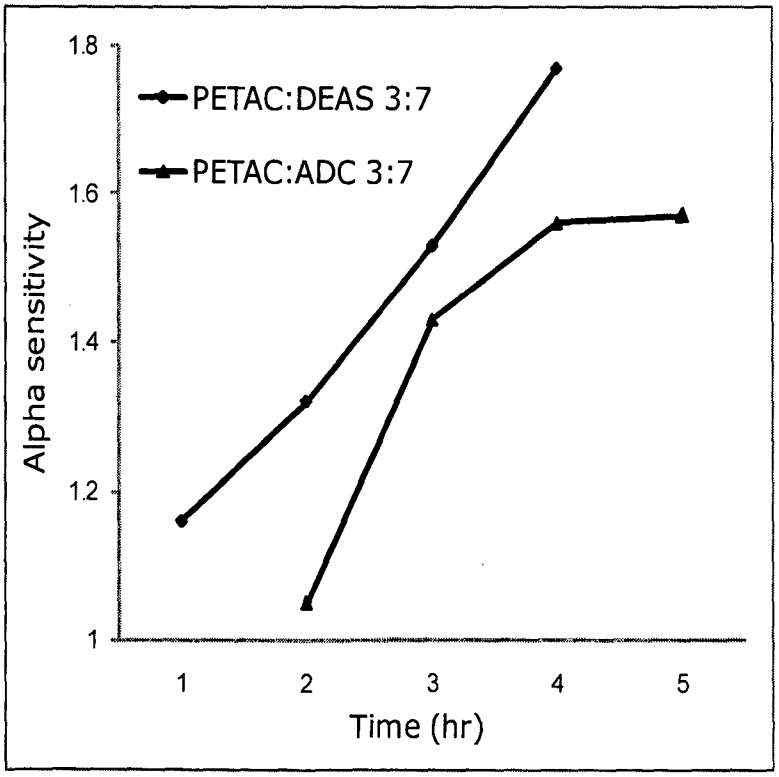

Figure 3.22: Variation of alpha sensitivity of PETAC:ADC 3:7 w/w and PETAC:DEAS 3:7 w/w copolymers.

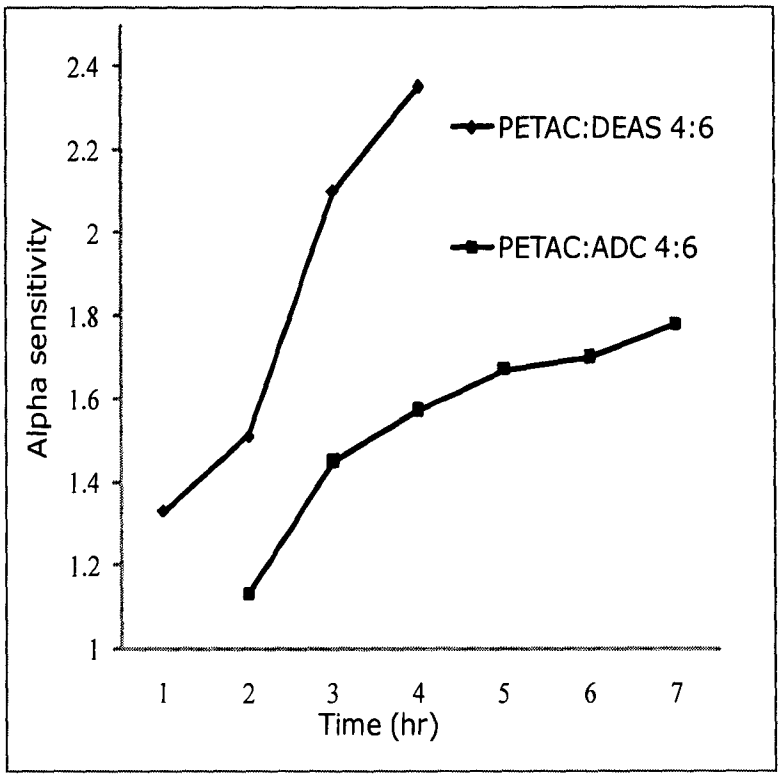

Figure 3.23: Variation of alpha sensitivity of PETAC:ADC and PETAC:DEAS 4:6 copolymers.

The maximum alpha sensitivity observed for the PETAC:DEAS 3:7 w/w copolymer film was 1.77 in 4 hr as compared to 1.57 of PETAC:ADC 3:7 w/w copolymer film in same time. The PETAC:DEAS 3:7 w/w copolymer films turned opaque after 3 hr of chemical etching.

It was observed that the copolymer PETAC:DEAS 4:6 w/w has a maximum sensitivity of 2.35 as compared to 2.03 and 1.77 of PETAC:DEAS 1:1 w/w and 3:7 w/w respectively. Thus, one can see that the introduction of the sulfonate group not only increases the sensitivity of the polymer but it also decreases the time required to develop tracks. The copolymers have higher sensitivity than their polycarbonate counterparts. The variation in track size of alpha and fission during sensitivity measurements of the co-

polymers is given in Table 3.36.

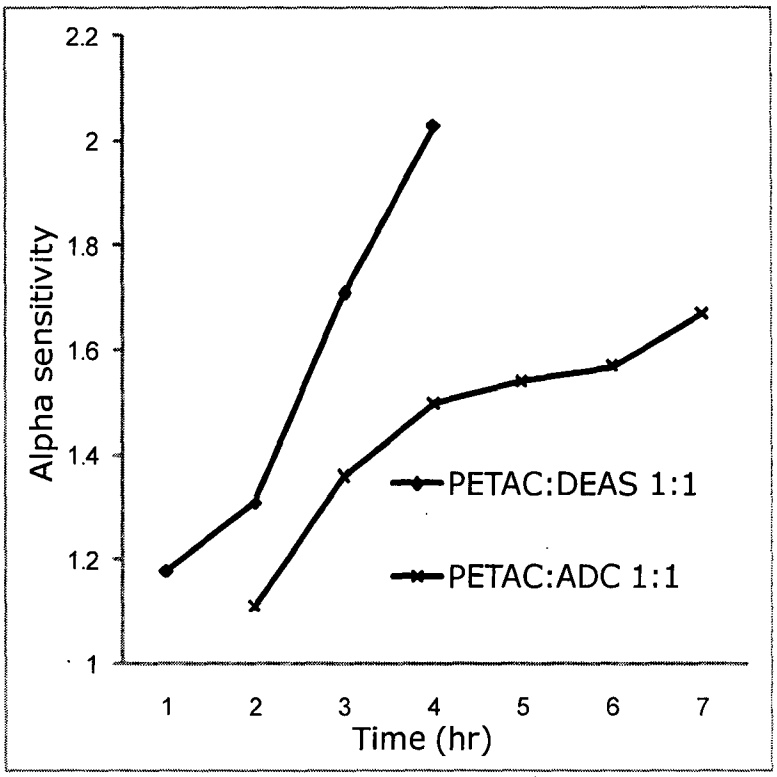

Figure 3.24: Variation of sensitivity of PETAC:ADC and PETAC:DEAS 1:1 copolymers.

Composition of PETAC:DEAS w/w	Alpha track diameter in μm after etching.			
	1 hr	2 hr	3 hr	4 hr
3:7	0.03	0.10	0.22	0.38
4:6	0.03	0.09	0.25	0.40
1:1	0.02	0.07	0.20	0.35

Table 3.36: Variation of alpha track size in different PETAC:DEAS copolymers.

Composition of PETAC:DEAS w/w	Fission track diameter in μm after etching.			
	1 hr	2 hr	3 hr	4 hr
3:7	0.11	0.27	0.48	0.72
4:6	0.08	0.20	0.42	0.63
1:1	0.07	0.19	0.39	0.60

Table 3.37: Variation of fission track size in different PETAC:DEAS copolymers.

The track growth rate increases with the increase in the concentration of DEAS in the copolymer. The sensitivity of the copolymers can be measured for only 4 hours as the tracks are lost due to removal of bulk surface. The detectors have good optical properties and can be used as track detectors.

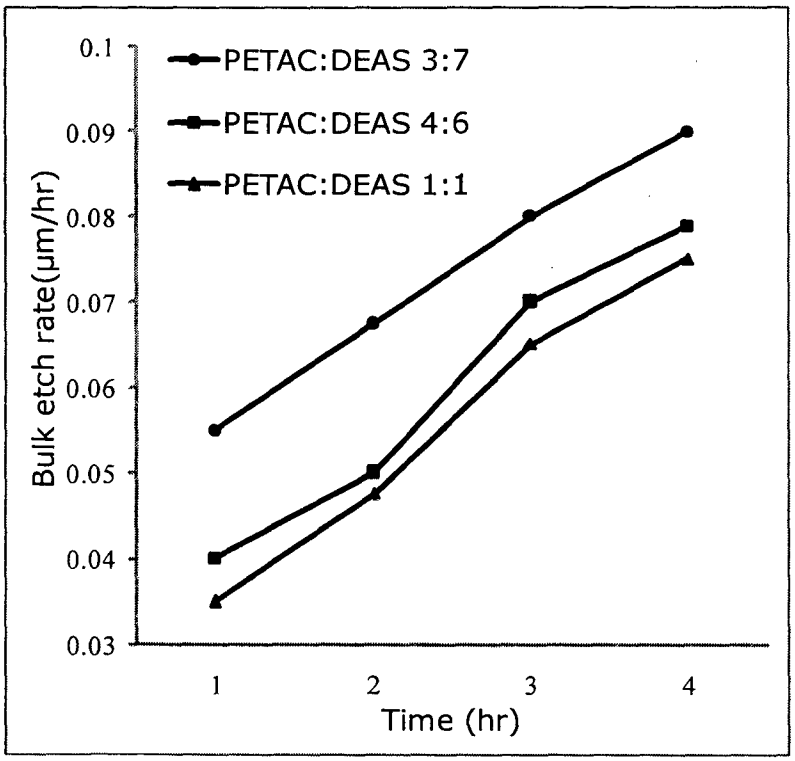

Figure 3.25: Bulk etch rate of different copolymers of PETAC and DEAS.

The bulk etch rate increases with the increase (Figure 3.25) in the concentration of DEAS monomer.

3.5.5 A ternary copolymer of ADC:DEAS:PETAC 3:3:4 w/w/w: Introduction of monomer containing more labile groups in ADC monomer increases the alpha sensitivity of the copolymer prepared. For *e.g.* the copolymer DEAS:ADC 3:7 w/w has a maximum alha sensitivity of 2.54 which is almost double than that obtained for PADC. As discussed earlier the higher sensitivity is due to the presence of more labile functional groups in the polymer matrix. We have earlier seen that the extent of the 3-D network in PADC polymer matrix increases when the monomer is copolymerized with a octafunctional monomer like PETAC. The maximum alpha sensitivity of PETAC:ADC 4:6 w/w copolymer was higher than PADC (CR-39™) polymer.

Thus, we thought of preparing a ternary copolymer containing ADC monomer, DEAS monomer and PETAC monomer. The PETAC should provide 3D network and DEAS a labile functional group. By combining 3 parts each of ADC and DEAS monomers instead of 6 parts of ADC alone as in PETAC:ADC 4:6 w/w copolymer. This should possibly give a polymer with much higher sensitivity. Thus, ADC:DEAS:PETAC 3:3:4 w/w/w a ternary copolymer was prepared by mixing the monomers in their respective weight compositions. IPP initiator 4 % and 1 % DOP was added to the monomer mixture. A heating profile derived for PETAC:ADC 1:1 w/w polymerization was used to polymerize the monomer. A film of size 624 ± 5 μm obtained was cut into pieces of 2 x 2 cm^2 and exposed to charged particles. The film on chemical etching in 6N NaOH at 70 °C, revealed alpha tracks in 15 minutes and alpha autoradiograph in 30 minutes.

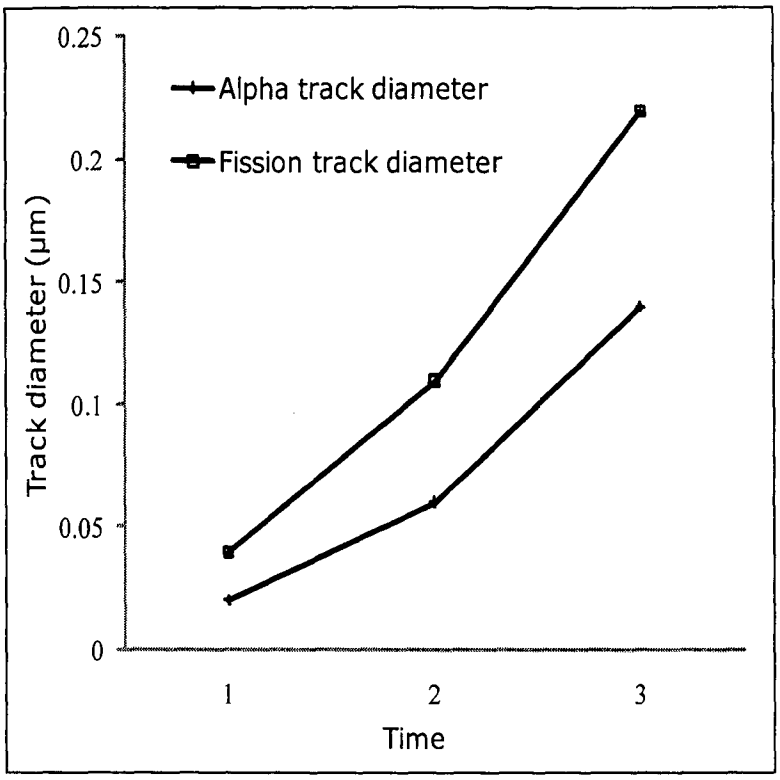

Figure 3.26: Alpha and fission track growth in ternary copolymer.

The polymer however turned opaque on etching for more than 3 hr. The alpha sensitivity for the polymer was determined. The growth of alpha and fission particle tracks is shown in Figure 3.26 above. The tracks were not visible after 3 hr of etching as the film turned opaque. Figure 3.27 gives the variation in the bulk etch rate of the ternary copolymer in comparison with PADC. The bulk etch rate of the ternary copolymer was more than PADC homopolymer. The bulk etch rate also increases with the etching time. From Figure 3.28 (see next page) below it is clear that the ternary copolymer PETAC:ADC:DEAS 4:3:3 w/w/w has a high alpha sensitivity of 2.44 and the value is achieved in just 3 hr of chemical etching. The rate of increase in track size is also less than the PETAC:DEAS 4:6 w/w copolymer which shows alpha sensitivity of 2.35 in 4 hr.

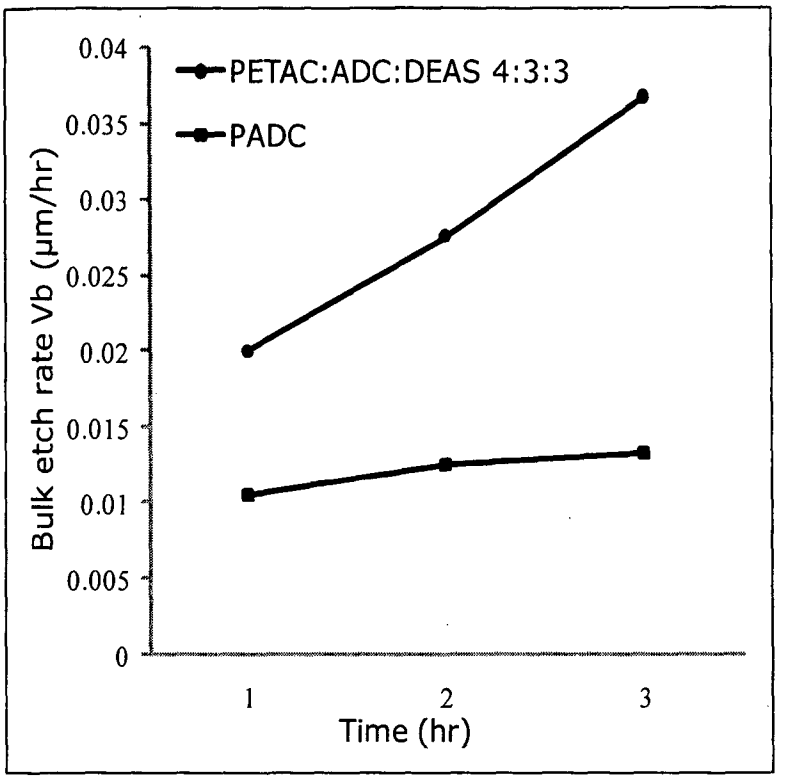

Figure 3.27: Variation of bulk etch rate in PETAC:DEAS:ADC 4:3:3 w/w/w copolymer.

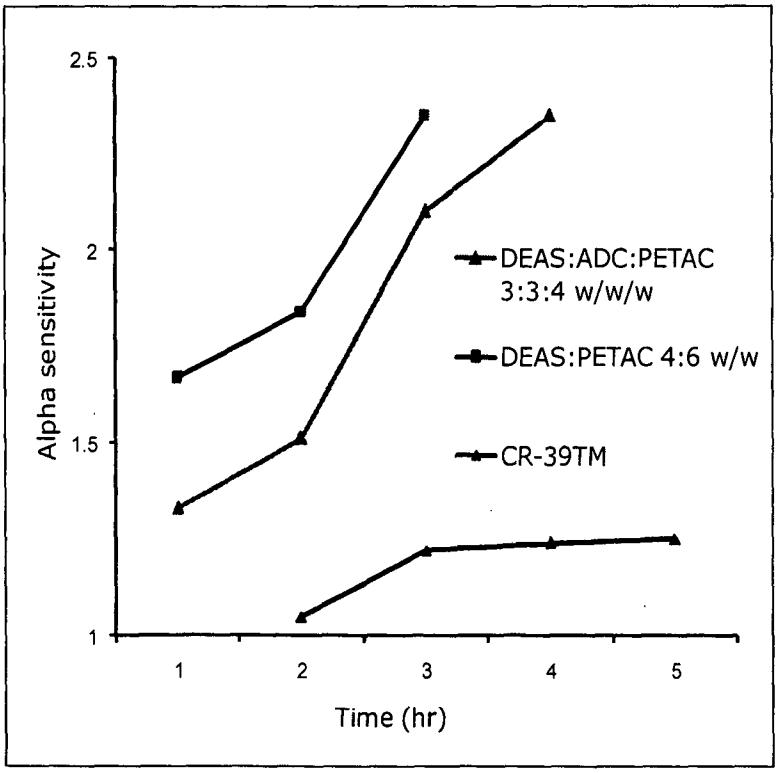

Figure 3.28: Comparative study of variation of sensitivity in different polymers.

3.5.6 Optimization of DAS, ADS, DAC and ADS copolymer composition: We have already studied the highly sensitive sulfonate group as a radiation sensitive group in different copolymer combinations. The copolymers prepared *e.g.* DEAS:ADC 3:7 w/w had higher alpha sensitivity than indegenous SR-86(20) *i.e.* DEAS:ADC 2:8 w/w . The higher alpha sensitivity of these polymers was attributed to the presence of more labile sulfonate group. It may be seen that sulfonate ($-SO_2-O-$) and sulfites -O-SO-O- are isomeric/ structurally related groups. The DAS monomer is the simplest biallylic monomer that can be prepared for polymerization and having a sulphite moiety. Sulfite -O-SO-O- is analogous to carbonates -O-CO-O- and can be seen as a radiation sensitive group. The monomer synthesis was performed by reacting thionyl chloride and allyl alcohol. ADS monomer was also synthesized susequently by reacting diallyl sulfite and diethylene glycol.

The thermal studies of the monomers, initiator mixture revealed that at temperatures above 50 °C the monomers forms a dark colored gel. Thus the monomer might react with the initiaor to cause some side reactions and thus consumes a part of it making the polymer film soft due to incomplete polymerization. Hence, the monomers should be polymerized at a constant temperature of 45 °C using IPP as initiator. In other variations tried to get a hard film, the initiator concentration was increased. The monomers were also copolymerized with DAC and ADC monomers in different weight ratios and at different initiator concentrations at a constant temperature of 45 °C to obtain a hard copolymer film. The physical properties of various sulfite containing polymers prepared are given in Table 3.38 (see next page).

Sr. No.	Composition of polymer(w/w)	% w/w Initiator	Thickness (μm)	Nature of the Polymer formed
1	DAS	8	----	Brown , very soft
2	ADS	8	----	Dark brown, very soft
3	DAS:DAC 1:1	4	635 ± 5	Hard, Light brown
4	DAS:DAC 1:1	8	688 ± 5	Light brown, hard
5	ADC:DAS 1:1	6	----	Very soft, brown film
6	ADC:DAS:DAC 1:1:1	6	715 ± 5	Light brown, hard
7	ADC:DAS 8:2	6	624 ± 5	Light brown, hard
8	ADC:ADS 1:1	4	----	Very soft, brown film
9	ADC:ADS 9:1	8	624 ± 5	Light brown, hard
10	ADC:ADS 9:1	15	626 ± 5	Light brown, hard
11	ADC:ADS 8:2	8	694 ± 5	Moderately hard film
12	ADC:ADS 7:3	8	633 ± 5	Soft polymer film

Table 3.38: Physical properties of different homopolymers of ADS, DAS and copolymers with ADC and DAC.

The homopolymers of ADS and DAS were completely soft polymers with a dark brown color. The DAS copolymer with ADC, having concentration of DAS higher than 20 % w/w were found to be soft polymer and cannot be used as track detectors. The DAC:DAS 1:1 w/w copolymer is a hard film and can be used as a track detector. A 1:1:1 w/w/w copolymer of DAS:ADC:DAC was also a hard polymer and can be used as a track detector. The ADS monomer was copolymerized with only ADC monomer. The copolymer ADC:ADS 7:3 w/w was a very soft polymer and cannot be used as

track detector. The 2:8 w/w and 1:9 w/w copolymers of ADS:ADC were hard and can be used as track detectors.

The hard copolymers were exposed to alpha and fission particles from respective sources in close contact. The films were etched with 6N NaOH at 70 °C. The track revelation properties of the polymers are summarized in the Table 3.39.

Composition of polymer w/w	Time to reveal (min)		Bulk etch rate (μm/hr)
	^{239}Pu alpha	^{252}Cf fission	
DAS:DAC 1:1	----	15	2.86
ADC:DAS:DAC 1:1:1	----	15	2.07
ADC:DAS 8:2	20	10	2.25
ADC:ADS 9:1	15	5	2.12
ADC:ADS 8:2	15	5	2.38

Table 3.39: Track revelation studies of different copolymers of DAS and ADS.

From the Table 3.39 above one can conclude that the polymers can be used for rapid analysis of charged particle tracks. The track detector can rapidly reveal the alpha and fission tracks. The fission fragment tracks are observed in 5 minutes in ADS:ADC copolymers. The DAS copolymers require 10-15 minutes etching to reveal tracks. The films remain clear during the first 10-15 minutes of chemical etching. A clear impression of the ^{239}Pu alpha autoradiograph is seen in just 15-20 minutes in polymers. Under an optical microscope the individual tracks are not much clear and

could not be counted due to the opaque nature of the film. The polymers with higher concentration of DAS do not reveal alpha autoradiograph as the film becomes opaque very fast.

3.5.6 Optimization of PBCBS and ADC copolymer composition: We had earlier synthesized a octafunctional monomer PETAC which had a higher sensitivity than PADC. It is also clear from the results obtained that the polymers containing sulfonate moieties are also more sensitive. We thought of preparing a monomer PBCBS as it would have both a higher functionality and also a sulfonate group. The monomer was copolymerised with ADC and its track detection studies were found.

Composition of PBCBS:ADC	Time required (min) to observe	
	Fission tracks	Alpha autoradiograph
2:8	30	90
2.5:7.5	30	90
3:7	30	60
4:6	30	60
CR-39™	60	120

Table 3.40: Track detection charecteristics of different polymers of PBCBS and ADC.

As expected, the copolymers had good track recording properties (Table 3.40). However, the white solid monomer was was found to decompose due to intramolecular reactions and hence further studies pertaining to this monomer were stoped.

3.6 Optimization of initiator concentration: The properties of particular polymer largely depend on the type and the concentra-

tion of initiator used. Both the T_g and radiation sensitivity increases with increase in initiator concentration up to a maximum level and decreases gradually as the initiator concentration is increased further.[92] The bulk etch rate also decreases accordingly to a minimum and then increases as the concentration increases further. The increase in density of crosslink's also increases the sensitivity of the detector material. At higher initiator concentration, the residual unsaturation is almost negligible. This is because of the possibility of formation of lower molecular weight polymer chains which decreases the extent of 3-D network. Thus, the optimum initiator concentration is important as the detector under study attains maximum sensitivity. To determine this optimum initiator concentration for maximum sensitivity a series of polymers with increasing initiator concentration are prepared and subjected to sensitivity analysis.

The alpha sensitivity of various polymers is determined by fission track diameter method and initiator concentration where the alpha sensitivity reaches a maximum for a given polymer is determined. The previously mentioned copolymers, best performing with reference to alpha sensitivity are also prepared using various initiator concentrations and variation of alpha sensitivity as a function of initiator concentration is noted to optimize initiator concentration. All these polymerizations are carried out by calculated heating profiles for the respective homopolymer or copolymer. In case of polymers where heating profiles are not calculated using Dial's method, the polymerizations are either carried out at a constant temperature or using a heating profile developed for corresponding structurally similar carbonate monomer was used. For polymer compositions where polymer turns opaque during etching

no sensitivity study was done.

3.6.1 Optimization of initiator concentration for DEAS:ADC 3:7 w/w copolymer: The optimization of monomer concentration studies revealed that the DEAS:ADC 3:7 w/w copolymer has a maximum sensitivity in the series of copolymers prepared of DEAS and ADC. As we had tested the copolymer with 4 % w/w of IPP initiator other polymerizations with IPP initiator concentration of 2, 3, 5, 6 % w/w were carried out. The DOP concentration in all the copolymers was 1 % w/w. The physical properties of all the polymers prepared are given in Table 3.41.

% w/w of IPP	Thickness (μm)	Hardness	Track detection properties
2	693 ± 10	Soft polymer	Alpha and fission
3	692 ± 10	Slightly hard	Alpha and fission
5	723 ± 10	Hard polymer	Alpha and fission
6	702 ± 10	Hard polymer	Alpha and fission

Table 3.41: Physical properties of DEAS:ADC 3:7 w/w copolymers prepared using different concentration of IPP initiator.

The polymers prepared using 3 - 6 % w/w initiator concentrations are hard and are suitable as track detectors. Alpha sensitivity studies were performed for these copolymers. The variation of alpha and fission track diameter in the polymers is depicted in the Figures 3.29 and 3.30 respectively (see next page). The film with 2 and 3 % IPP initiator becomes very soft after etching for more than 3 hr. The increase in the alpha track size was also not regular in case of these polymers. This might be due to incomplete polymerization in the polymer matrix.

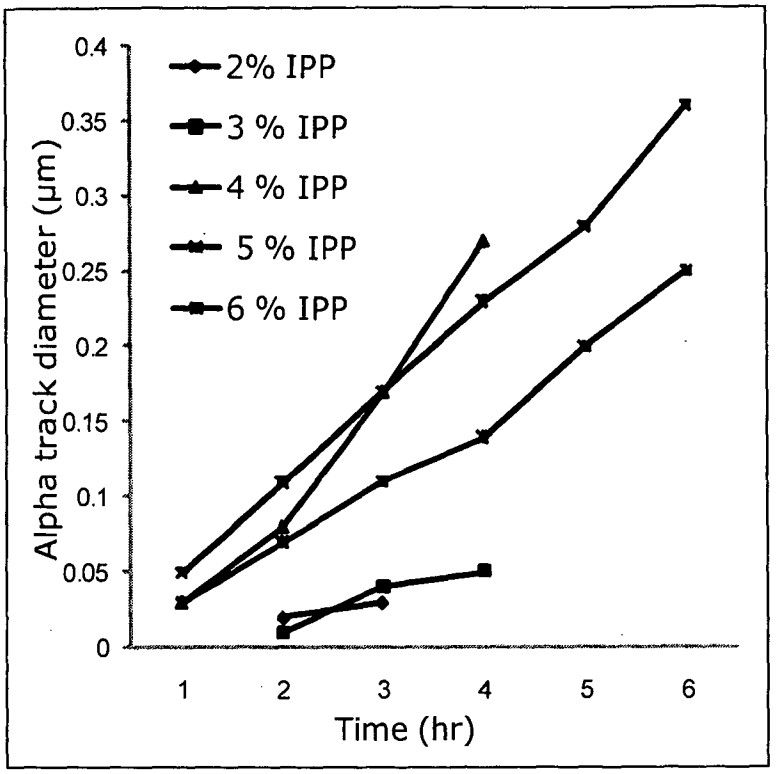

Figure 3.29: Variation in alpha track diameter in polymers.

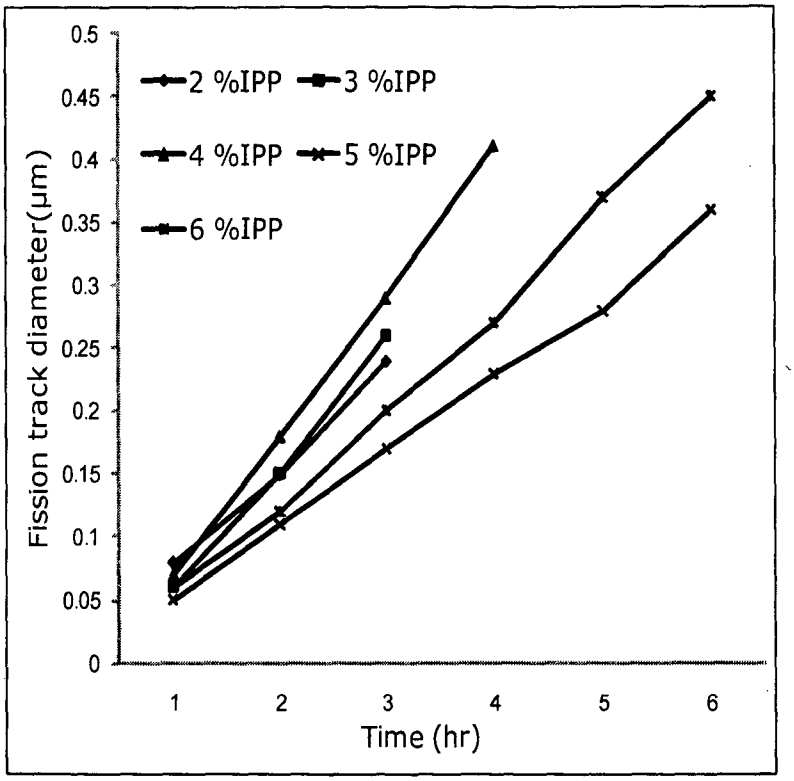

Figure 3.30: Variation in fission track diameter in polymers.

The rate of increase in the track sizes in the film with 5 % IPP was regular and the film also did not turn soft throughout the entire etching experiment. The film with 6 % initiator concentration had a steady increase in track diameter. The alpha sensitivity of the polymers prepared using different initiator concentration was determined using the variation of the track diameters measured. The variation of alpha sensitivity in different polymers prepared using different concentrations of innitiator is shown in Figure 3.31.

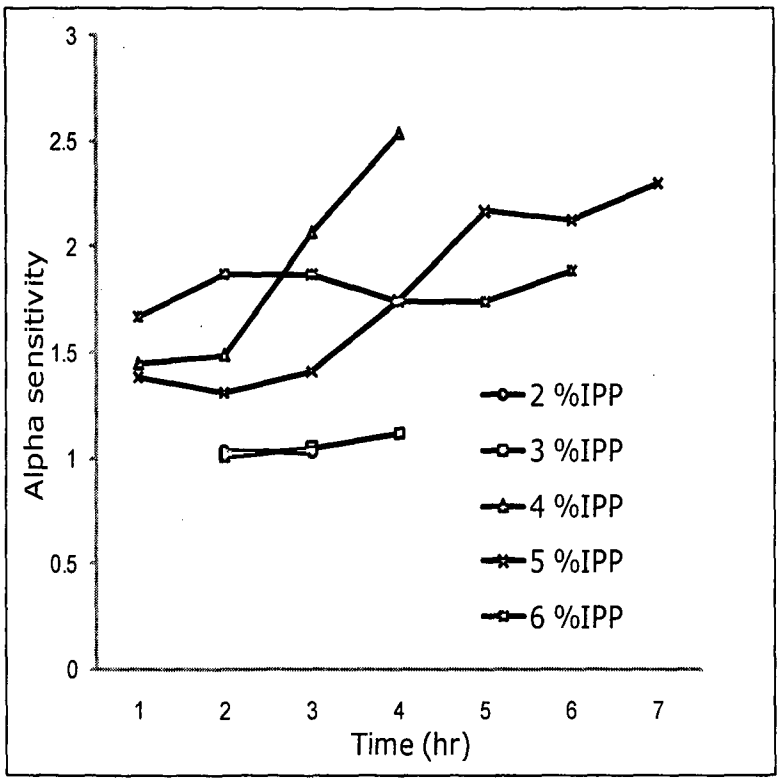

Figure 3.31: Variation of alpha sensitivity in different polymers.

The alpha sensitivity varied largely in different polymers. The films with 2 and 3 % w/w IPP concentration were soft and were least sensitive material. The film with 4 % w/w IPP initiator had a maximum sensitivity of 2.54 in 4 hrs and was the most sensitive copolymer. The polymer with 5 % w/w initiator concentration had a maximum sensitivity of 2.3 and required 6 - 7 hr of etching time.

The film with 6 % initiator had a maximum sensitivity of 1.87. The maximum alpha sensitivity obtained for different polymers is given in Table 3.42.

Sr. No.	% w/w of IPP	Maximum alpha sensitivity	Time to attain maximum sensitivity
1	2	1.04	2
2	3	1.12	4
3	4	2.54	4
4	5	2.30	7
5	6	1.87	3

Table 3.42: Maximum alpha sensitivity observed for polymers.

3.6.2 Optimization of initiator concentration for PETAC homopolymer and PETAC:ADC 4: 6 copolymer: The PETAC monomer and the copolymers of PETAC with ADC were initially polymerized using 6 % w/w of IPP initiator. PETAC:ADC 4:6 w/w copolymer had the maximum sensitivity in the copolymer series. However, the concentration of the initiator should be optimized so as to obtain the polymer with higher alpha sensitivity.

Sr. No.i	% w/w IPP nitiator	Thickness (μm)	% residual unsaturation
1	2	614 ± 5	7.22
2	3	624 ± 5	6.63
3	4	668 ± 5	6.01
4	5	683 ± 5	5.86
5	6	593 ± 5	6.23

Table 3.43: Physical properties of PETAC homopolymers.

The polymerization of PETAC homopolymer and PETAC:ADC 4:6 w/w copolymers was performed using IPP initiator with 2, 3, 4 and 5 % initiator concentrations. The physical properties of the polymers are given in Table 3.43 and Table 3.44 respectively.

Sr. No.	% w/w IPP initiator	Thickness (μm)	% residual unsaturation
1	2	674±5	24.21
2	3	705±5	8.39
3	4	645±5	5.81
4	5	685±5	5.47
5	6	635±5	5.34

Table 3.44: Physical properties of PETAC:ADC 4:6 w/w copolymer prepared using different initiator concentration.

PETAC homopolymer films prepared using different initiator concentrations were etched using 1 N NaOH at 70 °C. The film turned slightly opaque after etching for more than 15 hrs. This was later found to be due to the impure PETAC monomer obtained in some cases. Once the monomer was purifies using the silica gel column chromatography with *n*-hexanes/ethyl acatate as eluent no such problems were encountered in further studies. Figure 3.32 and 3.33 below (see next page) gives the variation of alpha and fission track diameters respectively. As the etching conditions used were milder the increase in the track size was very slow. Furthermore, the alpha tracks of measurable track diameter were observed only after 6 - 7 hr of chemical etching.

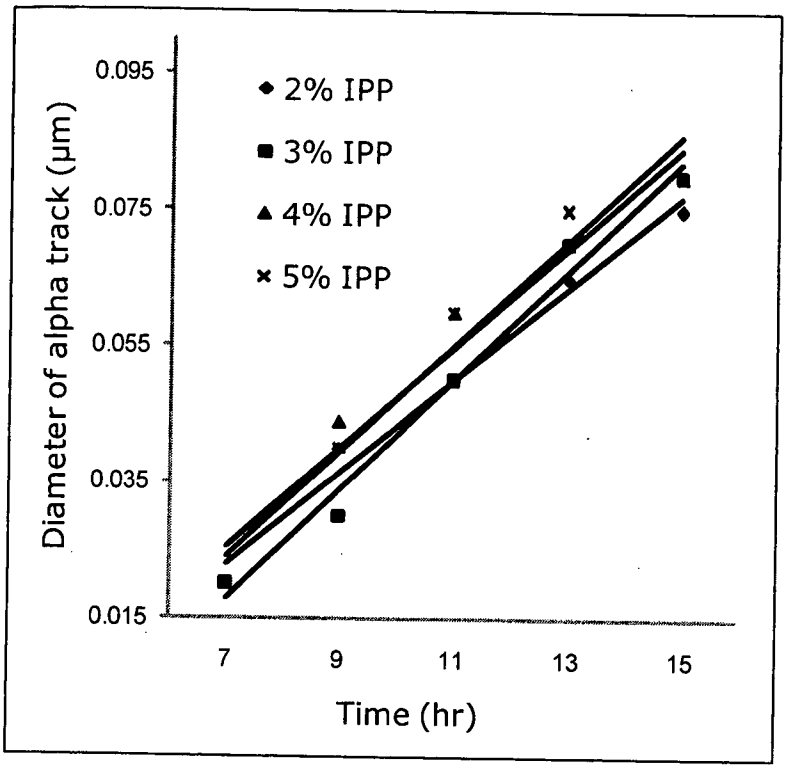

Figure 3.32: Variation of alpha track diameter in PETAC homopolymers prepared using different initiator concentration..

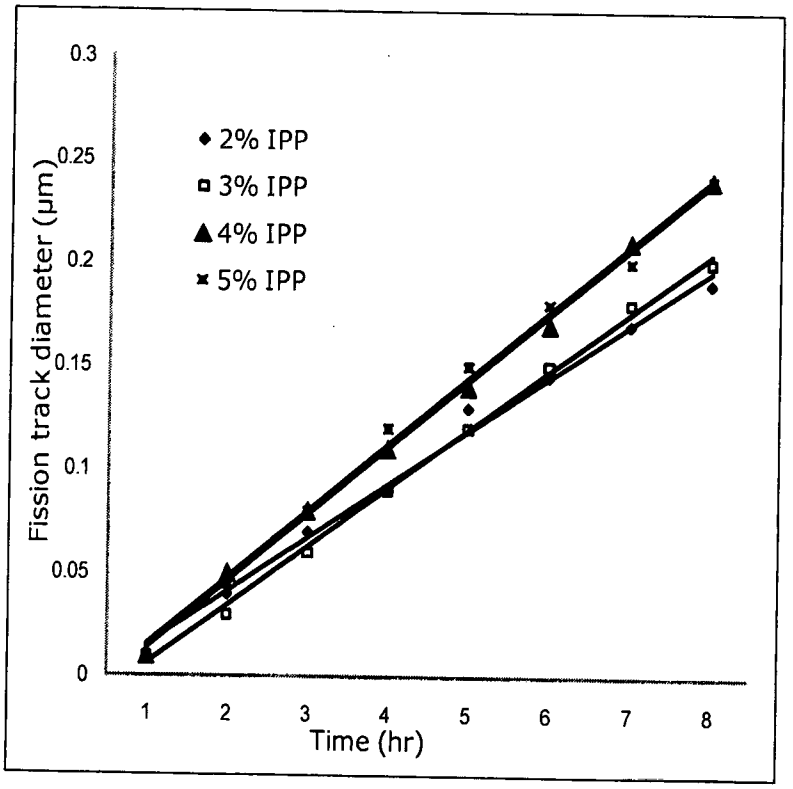

Figure 3.33: Variation of fission track diameter in PETAC homopolymers prepared using different initiator concentration.

The PETAC:ADC 4:6 w/w copolymer films prepared with different initiator concentrations were etched under the etching conditions of 4 N NaOH at 70 °C. The variation of alpha and fission track diameter is given in figures 3.34 and Figure 3.35 (see next page) respectively. Under the etching conditions utilized the polymer did not turn opaque even after etching for 15 hr.

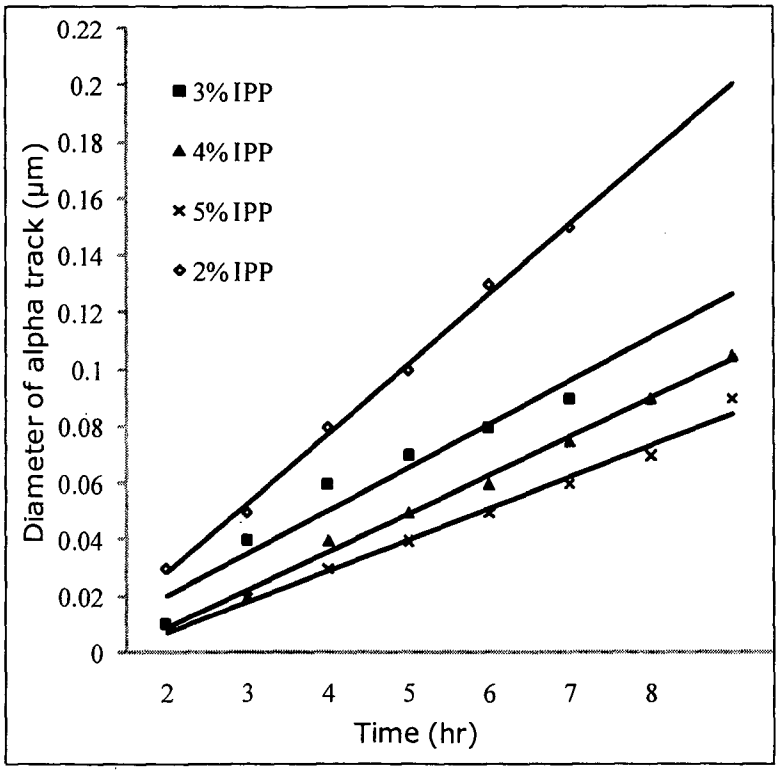

Figure 3.34: Variation in alpha track diameter in PETAC:ADC 4:6 w/w copolymers prepared using different initiator con centration.

The sizes of both alpha and fission tracks in the polymer prepared using 2 % w/w IPP initiator concentration increases very rapidly. This might be due to the higher track etch rate due to incomplete polymerization. The polymers prepared using 4 and 5 % IPP concentration were having a reduced rate of increase in

track diameter. The higher initiator concentration allows maximum polymerization and decreases the bulk etch rate.

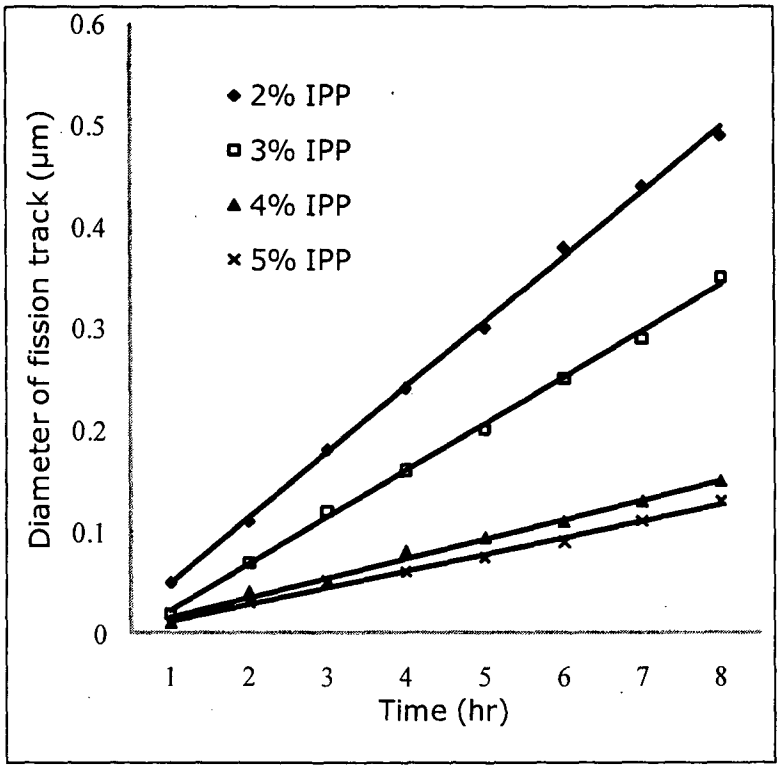

Figure 3.35: Variation in fission track diameter in PETAC:ADC 4:6 w/w copolymers prepared using different initiator con centration.

The alpha sensitivity for these polymers was calculated from the diameter of the alpha and fission tracks. Variation of the alpha sensitivity in PETAC homopolymers prepared using different initiator concentration is shown in Figure 3.36 (see next page). The alpha sensitivity of the polymer PETAC homopolymer prepared using 3 % w/w IPP initiator has a maximum value ofs 1.38 in 15 hrs of chemical etching. Thus, 3 % w/w of IPP initiator concentration can be used as optimum initiator concentration for polymerization of PETAC homopolymer.

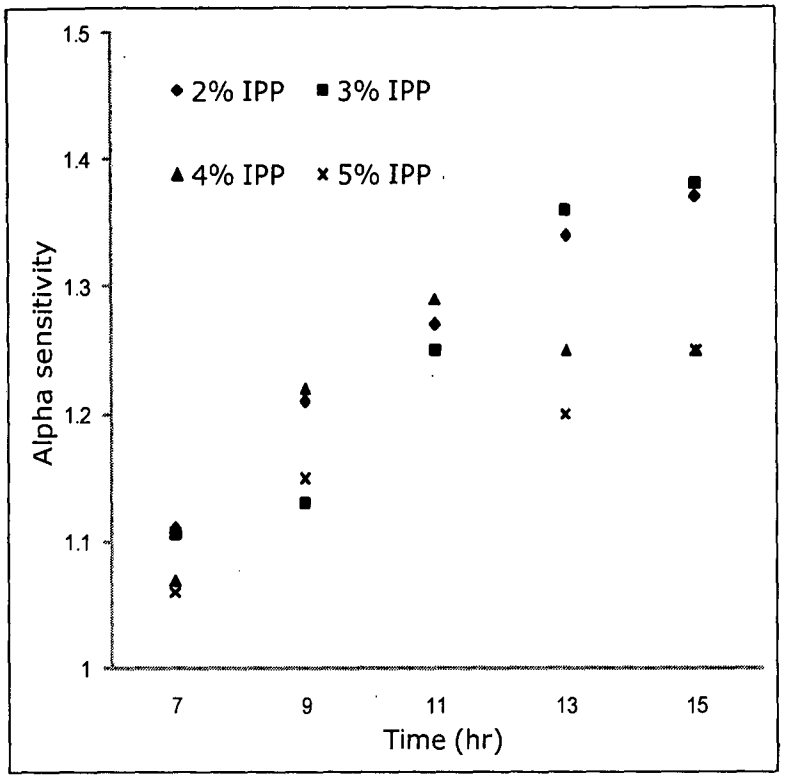

Figure 3.36: Variation of alpha sensitivity in PETAC homopolymers prepared using different initiator concentration.

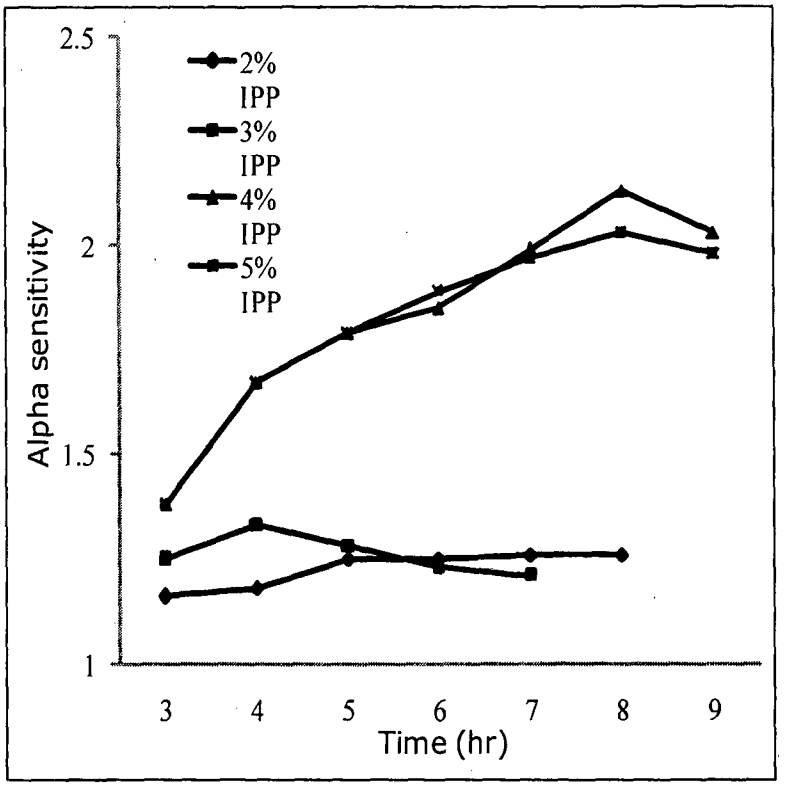

Figure 3.37: Alpha sensitivity variation in PETAC:ADC 4:6 w/w co-polymers prepared using different initiator concentration.

Variation in the alpha sensitivity of the polymers PETAC:ADC 4:6 w/w is shown in Figure 3.37. It is observed that the polymer prepared with 4 % initiator concentration shows the maximum sensitivity of 2.13. The maximum value of sensitivity is obtained after etching the film for 8 hr. The polymer prepared by using 5 % w/w IPP initiator concentration also shows a comparable sensitivity of 2.03 also in 8 hr. The polymers prepared using 2 and 3 % w/w initiator had a very low sensitivity. The sensitivity value is higher than CR-39™ and PETAC homopolymers. The variation in the bulk etch rate (Figure 3.38) of PETAC homopolymers was calculated using fission track diameter.

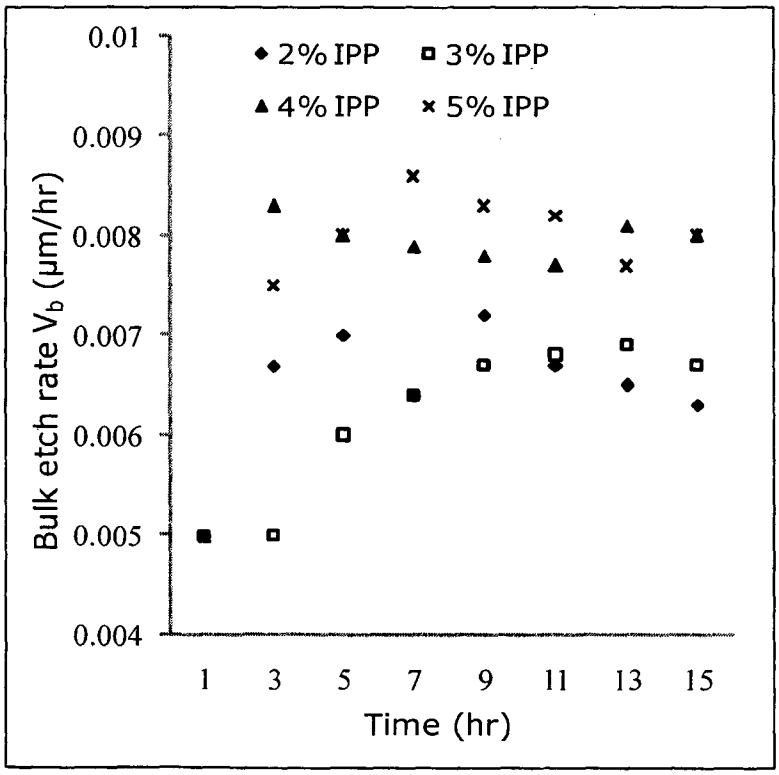

Figure 3.38: Variation of bulk etch rate in PETAC homopoly mers prepared using different initiator concentration.

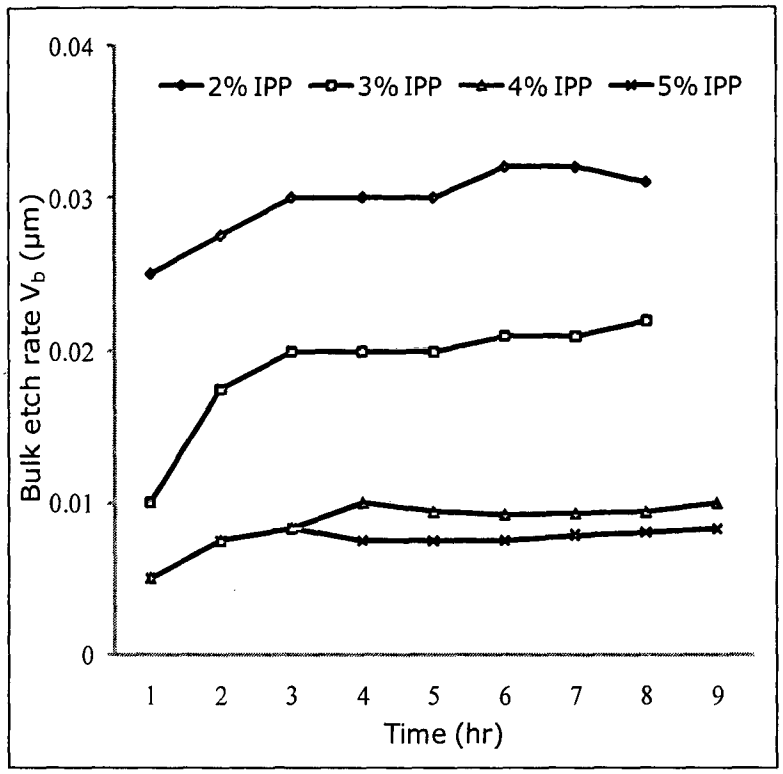

Figure 3.39: Variation of bulk etch rate in PETAC:ADC 4:6 w/w copolymers prepared using different initiator concentration.

The variation of bulk etch rate in PETAC:ADC 4:6 w/w co-polymers prepared with different initiator concentration can be seen in Figure 3.39. The homopolymers prepared with 2 and 3 % w/w IPP initiator concentration has a higher bulk etch rate as compared to other homopolymers. The bulk etch rate of polymers prepared using higher initiator concentration was low as compared to the other copolymers. The increased initiator concentration increases the amount of cross linking in the polymer matrix thereby hinder-ing the rapid chemical attack. Thus, the etching of the surface or the track becomes slow.

3.6.3 Optimization of initiator concentration for PETAC:DEAS copolymer: The PETAC:DEAS 4:6 w/w copolymer showed a max-

imum sensitivity in all the copolymers prepared in this series. The mixture was polymerized using 4 % w/w of BP initiator. The polymerization of the copolymer was performed using 3, 4, 5 and 6 % w/w BP initiator. The physical properties of the polymers obtained are given in Table 3.45.

% w/w BP initiator	Film thickness (μm)	Hardness
3	666 ± 5	Moderate
4	599 ± 5	Hard film
5	640 ± 5	Hard film
6	583 ± 5	Hard film

Table 3.45: Physical properties of DEAS:PETAC 6:4 w/w copolymers prepared using different initiator concentration.

All the copolymers prepared using different initiator concentration detected alpha and fission fragment tracks in less than 1 hr. The variation in the alpha and fission track size for different polymers is given in Figure 3.40 and 3.41 (see next page) respectively. The increase in size of alpha tracks was not uniform in the polymer prepared using 3 % w/w BP initiator. However, all the other polymers had a uniform increase in the track size. The fission track diameter variation was continuous in all the polymers prepared. It can be seen that at lower initiator concentration the rate of increase of track size is more.

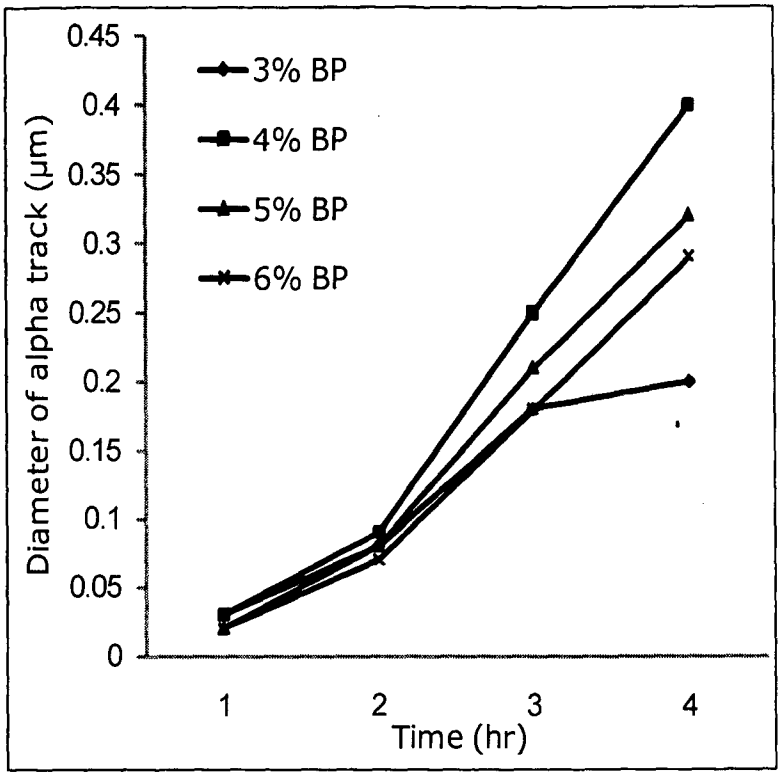

Figure 3.40: Alpha track diameter variation in copolymers of DEAS:PETAC 6:4 prepared with different initiator concentration.

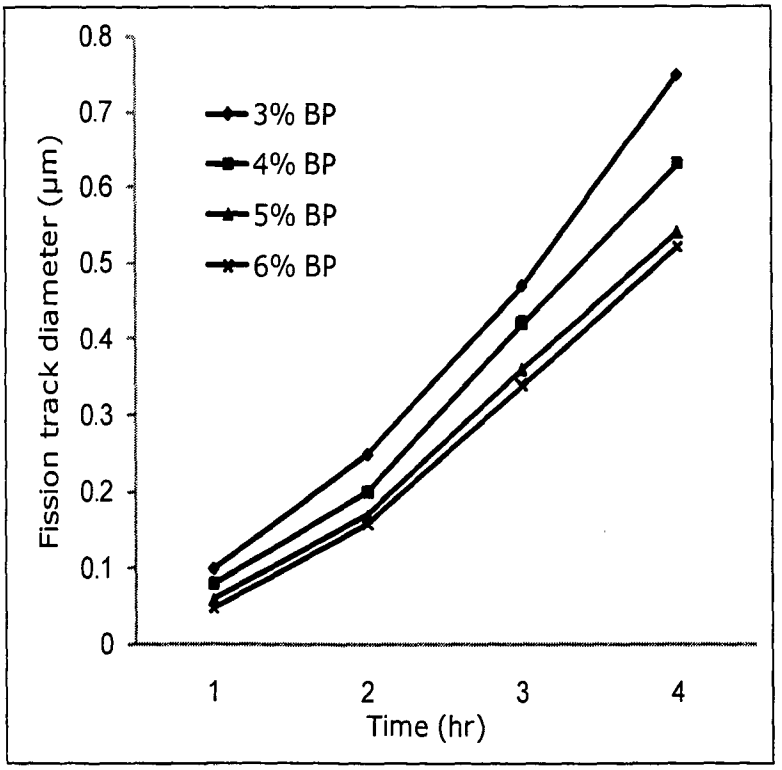

Figure 3.41: Variation in fission track diameter in copolymers of DEAS:PETAC 6:4 prepared with different initiator concentration.

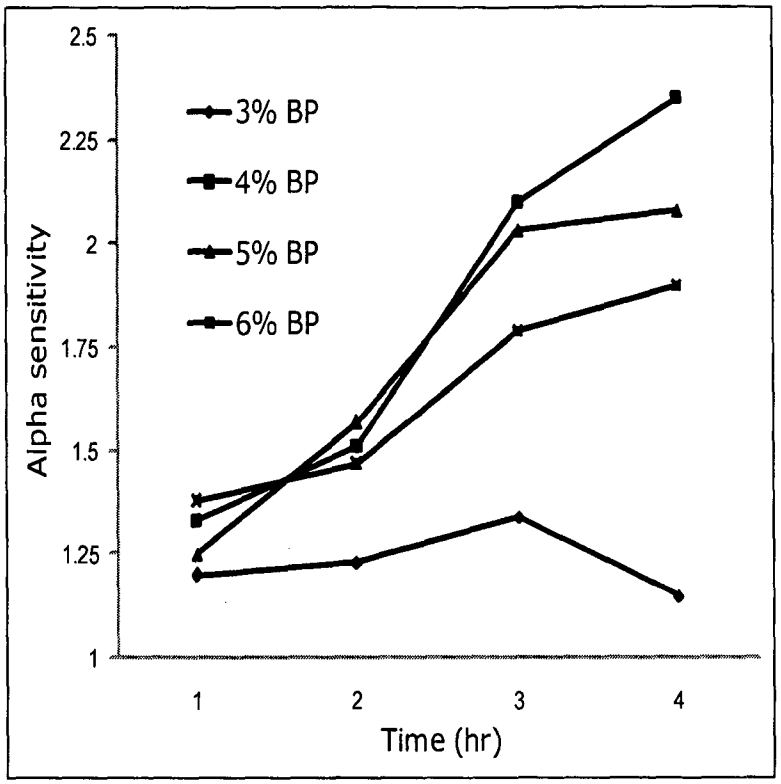

Figure 3.42: Variation in alpha sensitivity in different copolymers of DEAS:PETAC 6:4 prepared with different initiator concentration.

Figure 3.42 represents variation in alpha sensitivity of PETAC:DEAS 4:6 w/w copolymers prepared using different concentrations of initiator. The copolymer prepared using 4 % BP initiator shows a maximum sensitivity. The variation in the sensitivity of the polymer prepared using 3 % initiator was very less. Figure 3.43 (see next page) shows variation in bulk etch rate for DEAS:PETAC 6:4 w/w copolymers prepared using different initiator concentration. The polymer prepared with 3 % initiator shows a maximum bulk etch rate in the series and it decreases as the concentration of the initiator is increased. The polymers prepared with 5 and 6 % initiator concentration have almost comparable bulk etch rates.

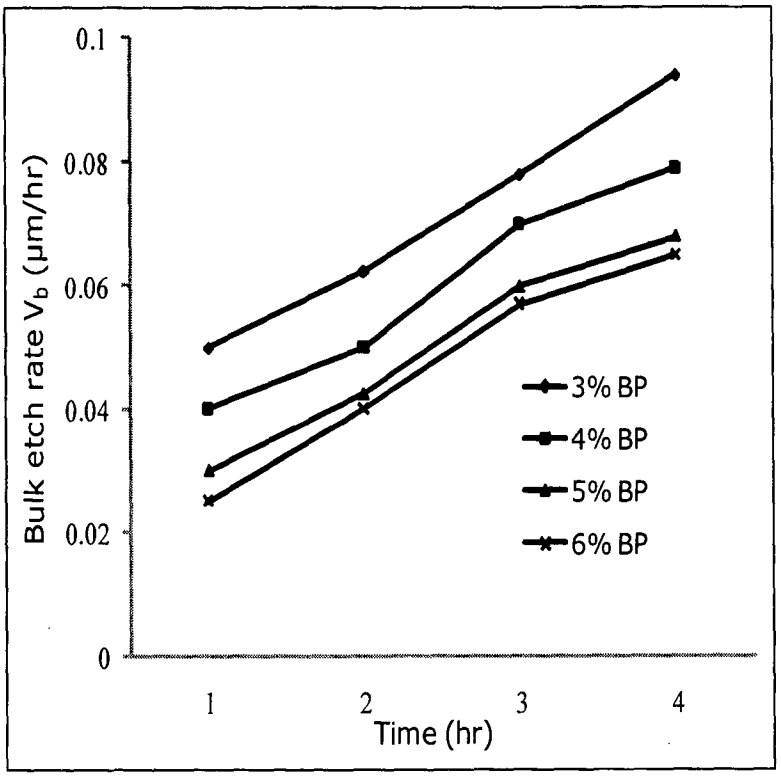

Figure 3.43: Variation in bulk etch rate of DEAS:PETAC 6:4 copolymers prepared using different initiator concentration.

w/w % IPP initiator	Maximum alpha sensitivity	Time to attain maximum sensitivity
3	1.34	4
4	2.35	4
5	2.08	4
6	1.79	3

Table 3.46: Maximum alpha sensitivity values for PETAC:ADC 4:6 w/w copolymers prepared using different initiator concentration.

The time required to attain maximum sensitivity in polymer is shown in Table 3.46 above. The polymer prepared with 4 % initiator shows the highest sensitivity of 2.35 in 4 hr.

3.6.4 Optimization of initiator concentration for ternary copolymer PETAC:DEAS:ADC 4:3:3 w/w/w copolymer: The ternary copolymer PETAC:DEAS:ADC 4:3:3 w/w/w was prepared initially using 4 % of IPP initiator. To optimize the initiator concentration polymerization of ternary copolymer was performed using different concentrations of IPP initiator. Physical properties of the polymers obtained are given in Table 3.47. Residual unsaturation could not be determined in this case as DEAS is involved.

Sr. No.	% w/w BP initiator	Film thickness (μm)	Hardness
1	3	----	Soft film
2	4	624 ± 5	Hard film
3	5	712 ± 5	Hard film
4	6	656 ± 5	Hard film

Table 3.47: Physical properties of ternary polymers prepared using different initiator concentration.

The polymer prepared using 3 % w/w initiator was soft and was not used for further studies. The polymers were tested for their alpha sensitivity using the track diameter method. The variation in the alpha and fission track diameters were determined as a function of time for PETAC:DEAS:ADC 4:3:3 w/w/w copolymers. The variation of alpha and fission track diameters is shown in figures 3.44 and 3.45 (see next page) respectively. The films were chemically etched in 6 N NaOH at 70 °C.

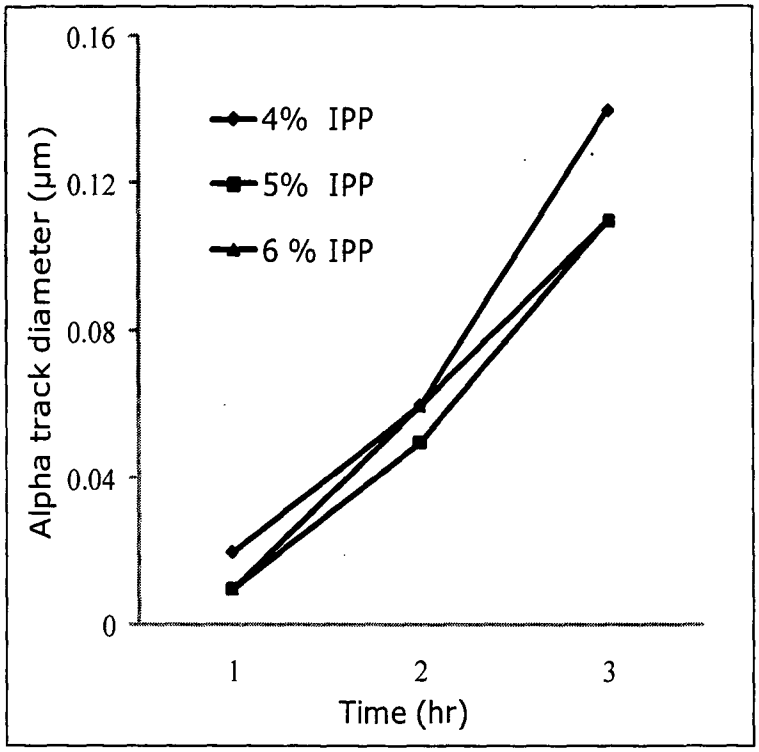

Figure 3.44: Variation of alpha track diameter in ternary copolymers prepared using different initiator concentration.

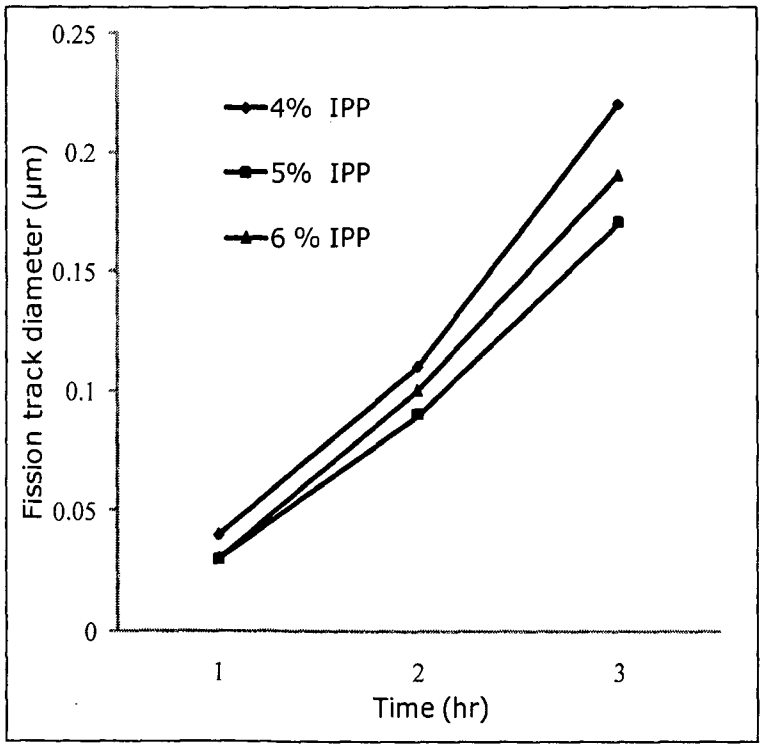

Figure 3.45: Variation of fission diameter in ternary copolymers prepared using different initiator concentration.

The polymeres with higher initiator concentration had lower track increase rate. The ternary copolymer prepared using 3 % IPP initiator very soft and was not used in this study. The bulk etch rate of the polymers was calculated using the fission track diameter. The variation in the bulk etch rate of the ternary copolymers is shown in Figure 3.46.

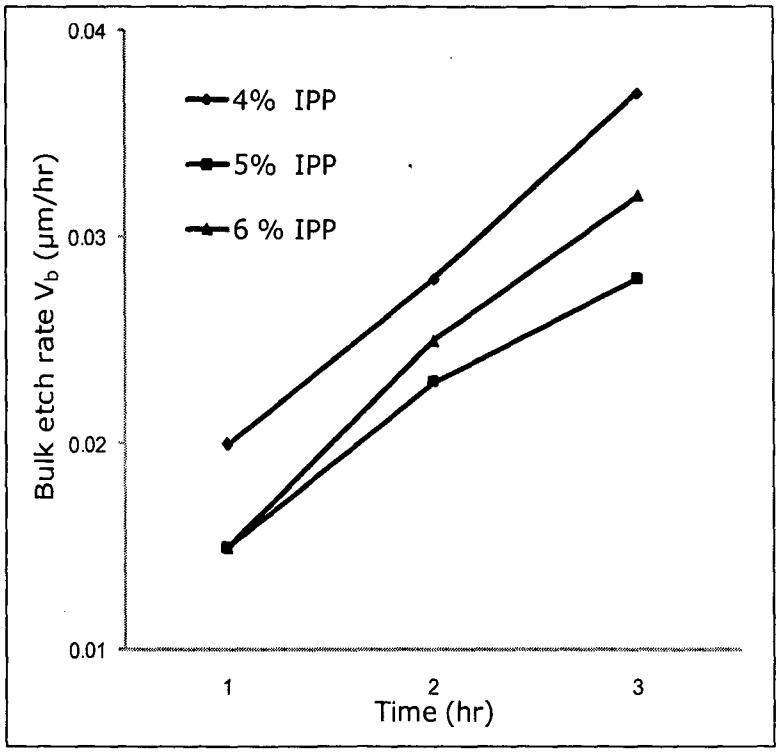

Figure 3.46: Variation in bulk etch rate of ternary polymers prepared using different initiator concentration.

The bulk etch rate is more in the polymer prepared using 4 % IPP initiator was found to be more as compared to the polymers prepared with 5 and 6 % initiator. The polymers however were etchable only for maximum 3 hr as further etching turned the polmers opaque under the etching conditions used. Thus the alpha sensitivity values for the polymers were determined for maximum

3 hr. The variation in the alpha sensitivity for the polymers was calculated by using the track diameter method and is shown in Figure 3.47.

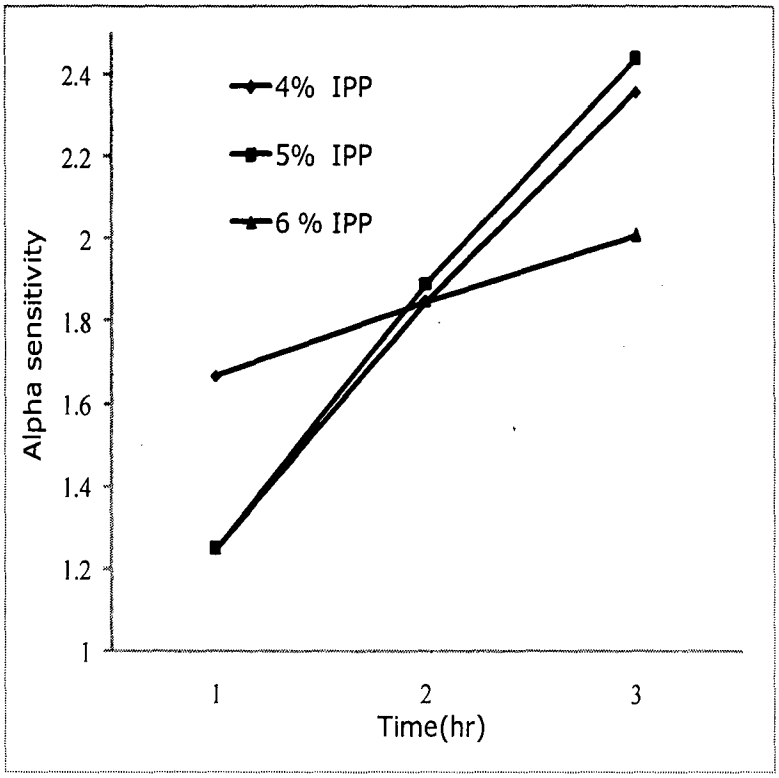

Figure 3.47: Variation in the alpha sensitivity of ternary polymers prepared using different initiator concentrations.

w/w % IPP initiator	Maximum alpha sensitivity	Time to attain maximum sensitivity
4	2.36	3
5	2.44	3
6	2.01	3

Table 3.48: Maximum alpha sensitivity values for PETAC:ADC:DEAS 4:3:3 w/w/w copolymers prepared with different initiator concentrations.

The polymer prepared using 5 % IPP initiator shows a maximum sensitivity. The time required for the polymers to attain maximum sensitivity is shown in Table 3.48 (see previous page). If the conditions of etching or polymerization are improved so as to delay the opaqueness which hinder sensitivity measurements the polymer with higher sensitivity can be obtained.

3.7 Optimization of etching conditions: It is well known that the conditions under which the plastic detectors are etched, profoundly affect the response of the plastic materials to the charged particles. The etching conditions alter many track detection characteristics of a nuclear track detector. The factors influenced by the etching conditions are

i) $V_t/V_b > 1$, the track development in a material is achieved by the realization of this condition and thus, it is necessary to follow the bulk etch rates as well as the track etch rates. Temperature and concentration of etchant is known to change the V_b.

ii) The track revelation times are also very important, since one of the practical requirements is the need for rapid track development to size that helps discrimination between tracks and background track like features.

iii) Consequently therefore, the change in etching conditions also changes the alpha sensitivity of the track detector.

iv) The surface characteristics of the films, since the films should be transparent upon etching in order to carry out the analysis under optical microscope.

The effect of variation in the etching conditions is pstudied by either varying the temperature at a constant concentration of the etchant or by varying the etchant concentration at a constant temperature. The bulk etch rate of the polymer film and post etch

surface appearance determines the utility of etching condition. In other words, the post etch surface of the detector should be clear with a moderate bulk etch rate. The detector film prepared using the optimized polymerization conditions as discussed above is cut into a sizes of 1 x 1 cm^2 and exposed to alpha particles from ^{239}Pu and fission fragment particles from ^{251}Cf source in close contact. The film is observed with respect to its track detection properties by varying the etching condition. The relative difference in bulk etch rate of the film and optical appearance is recorded.

3.7.1 Optimization of etching conditions for DAC and DAC:ADC 1:1 w/w polymer films: The DAC homopolymer can reveal only fission fragment tracks. The DAC:ADC 1:1 w/w copolymer can reveal both alpha and fission fragment tracks. However, the time required for development of alpha tracks with 6 N NaOH at 70 °C was 8-9 hr as compared to 3 hr required for PADC. The optimization of etching conditions of DAC homopolymer and DAC:ADC 1:1 w/w copolymer was carried out. The test films were etched in 5, 6 and 7 N NaOH at 70 and 80 °C. The variation in track revelation time is given in Table 3.49 below for DAC homopolymer.

Normality of NaOH	Temperature in °C	Post etch surface	Time (min) for fission tracks
5 N	70	Clear	50 - 60
	80	Clear	35 - 45
6 N	70	Clear	50 - 60
	80	Clear	35 - 45
7 N	70	Clear	45 - 55
	80	Clear	30 - 40

Table 3.49: Variation in the track revelation time for DAC:ADC 1:1 copolymer etched in 5, 6 and 7 N NaOH at 70 and 80 °C.

The track revelation studies indicate that there is no large drop in the track revelation time for fission fragments in DAC homopolymer etched under different etching conditions. The fission tracks were revealed in < 60 minutes at 70 °C and in < 45 minutes at 80 °C under all concentrations of etchants used. The films remain clear under all the etching conditions used. The other important factor to optimize the etching condition is the bulk etch rate of the polymer. The Bulk etch rate for the polymers was determined using the change in weight method. The variation in the bulk etch rate of the DAC homopolymer under different etching condition is shown in Figure 3.48.

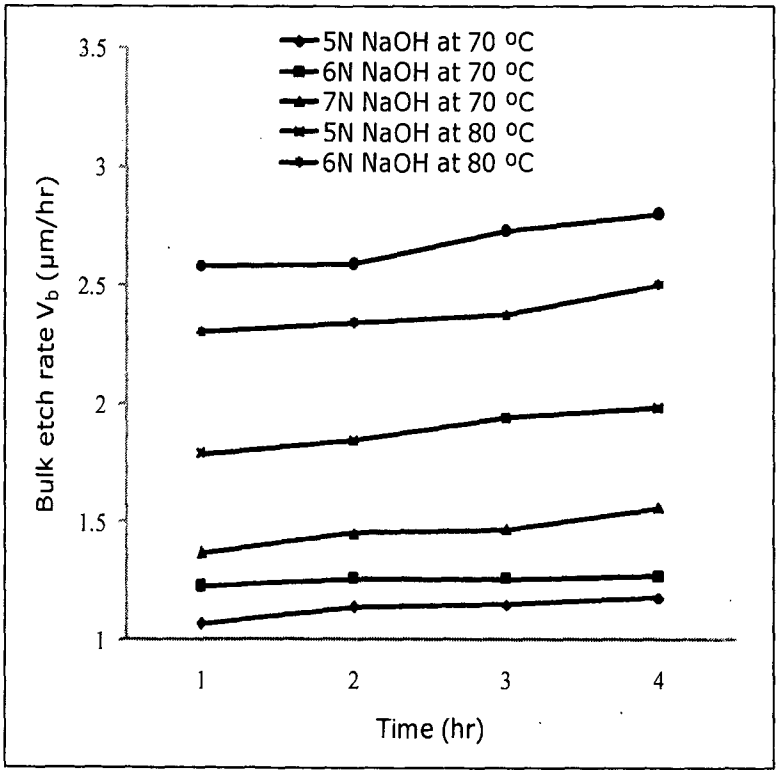

Figure 3.48: Variation in the bulk etch rate etched of DAC homopolymer in 5, 6 and 7 N NaOH at 70 °C and 80 °C.

From Figure 3.48 one can observe that at higher temperature of 80 °C and at 70 °C in 7 N NaOH the bulk etch rate is high.

The bulk etch rate at 70 °C in 6 N NaOH is low and is comparable to that of PADC. At still lower concentrations and temperatures the time required for track revelation would have been more. As the detector film detects only fission fragment tracks, 6 N NaOH at 70 °C may be considered as the optimum etching condition for etching the PDAC homopolymer.

Similar studies were performed on DAC:ADC 1:1 w/w copolymer and the track detection characteristics under different etching conditions were determined. Table 3.50 gives variation in track detection for DAC:ADC 1:1 w/w copolymer.

Normality of NaOH	Temperature in °C	Post etch surface	Time (min) to observe	
			fission	Alphas
5 N	70	Clear	50 - 60	460 - 480
	80	Clear	35 - 45	220 - 240
6 N	70	Clear	50 - 60	400 - 415
	80	Clear	35 - 45	220 - 240
7 N	70	Clear	45 - 55	280 - 300
	80	Clear	30 - 40	160 - 180

Table 3.50: Variation in the track revelation time for DAC:ADC 1:1 copolymer etched in 5, 6 and 7N NaOH at 70 and 80 °C.

The track revelation time for alpha autoradiograph has been reduced from 280 minutes to 220 minutes at the temperature of 80 °C in 6 N NaOH. The film also remains clear under all the etching conditions. The bulk etch rate variation at 70 and 80 °C is shown in Figure 3.48.

From the Figure 3.49 one can see that the bulk etch rate increases to around 2.25 μm/hr when etched in 6 N NaOH at 80 °C. However, the film remains clear even after chemical etching for 900 minutes. But at 7 N NaOH at 80 °C the film becomes slightly opaque when etched for more than 600 minutes. The bulk etch rate is also comparatively higher. Thus, the 6 N NaOH at 80 °C can be used as etching condition for further studies pertaining to DAC:ADC 1:1 w/w copolymer.

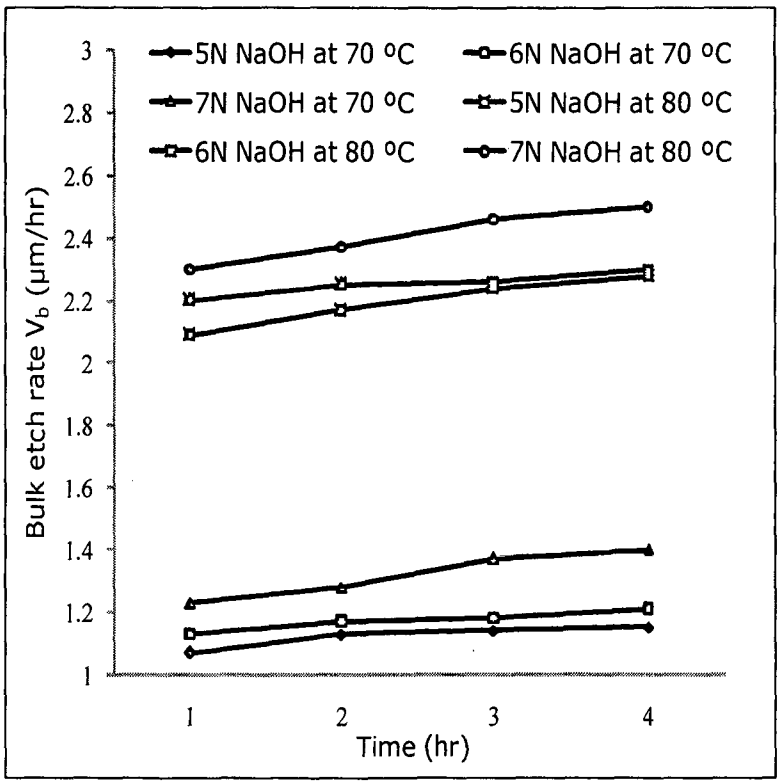

Figure 3.49: Variation in the bulk etch rate of DAC:ADC 1:1 w/w copolymer in 5, 6 and 7 N NaOH at 70 and 80 °C.

3.7.2 Optimization of etching conditions for DEAS:ADC 3:7 w/w copolymer films: The polymer sample films of size 1 x 1 cm^2 and were exposed to fission fragments and alpha particles from ^{252}Cf and ^{239}Pu source respectively in close contact (1 mm).

The films were then etched in 4 - 7 N NaOH solution and at temperatures between 60 °C to 80 °C. The bulk etch rate of the polymer, track development time and the physical appearance of the film were noted at different etching conditions. The time required to reveal tracks at different etching condition is given in the Table 3.51.

Etchant	Temperature	Time (min) to observe	
		Alpha tracks	Fission Fragments
4 N NaOH	60 °C	160 - 180	60 - 75
	70 °C	70 - 90	35- 45
	80 °C	50 - 60	25 - 30
5 N NaOH	60 °C	150 - 160	60 - 70
	70 °C	60 - 75	25 - 35
	80 °C	45 - 55	20 - 30
6 N NaOH	60 °C	110 - 130	50 - 60
	70 °C	50 - 60	20 - 30
	80°C	40 - 50	20 - 30
7 N NaOH	60 °C	100 - 120	50 - 60
	70 °C	50 - 60	20 - 30
	80 °C	40 - 50	15 - 30

Table 3.51: Time required at different temperatures for track development.

The films remain very clear when etched at 80 °C in 4 - 7 N NaOH, however, they become soft when etched for more than 120 minutes. It can be seen that the time required for track revelation at 60 °C was almost double than what is required at 70°C. The

bulk etch rate of the polymer under different etching conditions is graphically represented in Figures 3.49.

From the Figure 3.50, one can observe that the bulk etch rate increases with the increase in the concentration of the etchant as well as the etching temperature of the etchant solustion. The bulk etch rate at 60 °C is low but the time required to observe the tracks is more. At higher temperatures of 80 °C, the film becomes soft after etching for more than 2 hr. This is also reflected from the sudden increase in the bulk etch rate at 80 °C after 2 hr as evident from Figure 3.50.

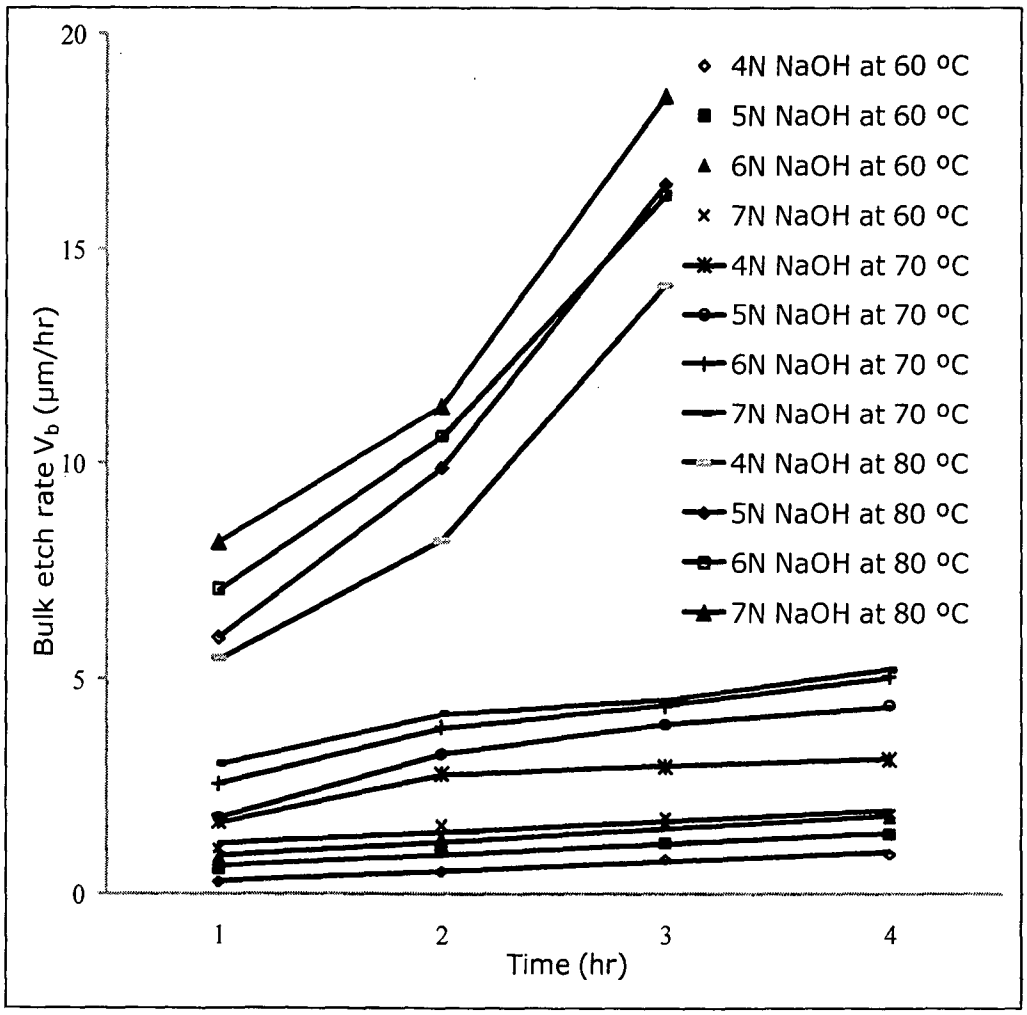

Figure 3.50: Variation in bulk etch rate of the DEAS:ADC 3:7 w/w copolymer at 60, 70 and 80 °C.

At 70 °C the time required to reveal tracks increases with the decrease in the etchant concentration but there is also not a large increase in the bulk etch rate. Thus, Like PADC therefore, etching of DEAS:ADC 3:7 w/w copolymer may be preferably done using 6 N NaOH at 70 °C. Alternatively, etching using 6 N NaOH at 60 °C may also be used. The sensitivity studies indicated that, maximum alpha sensitivity values are observed only after etching for 8 hr or more in 6 N NaOH at 60 °C. Thus etching under 6 N NaOH at 60 °C would be time consuming for alpha sensitivity measurements

3.7.3 Optimization of etching conditions for PETAC homopolymer and PETAC:ADC 4:6 w/w copolymer: Aqueous NaOH solutions with normality having concentrations ranging from 3 - 7 N was used for etching the detector films. The change in weight method was used to determine the bulk etch rate of the material. The polymer sample films of size 1 x 1 cm^2 were exposed to fission fragments and alpha particles from ^{252}Cf and ^{239}Pu source respectively in close contact (1 mm). The time required for track revelation and post etch appearance of the surface of the detector film was noted for PETAC homopolymer as well as PETAC:ADC 4:6 w/w copolymer.

Films developed small cracks when they were etched at higher temperatures of 80 °C. Furthermore, the films surface also turned foggy and its observation under an optical microscope also became difficult hence films were not etched at 80 °C at all etchant concentrations. The films were therefore etched at temperatures 50, 60 and 70 °C. Table 3.51 gives the track appearance time under different etching condition for PETAC homopolymer.

From the Table 3.52 below (see next page) it is observed

that the time required for track revelation is very less when the film was etched in 6 N NaOH at 70 °C. At 6 N NaOH at 60 °C the time required for track revelation was increased. The time required to observe alpha tracks when etched in at 3 N NaOH at 70 °C is nearly double than that required at 6 N NaOH concentration at 70 °C. The post etch surface appearence of the polymers was very clear under all the etching conditions used.

Etchant	Temperature	Time (min) to observe	
		Alpha tracks	Fission tracks
3 N NaOH	50 °C	340 - 360	100 - 120
	60 °C	220 - 240	70 - 90
	70 °C	175 - 180	50 - 60
4 N NaOH	50 °C	280 - 300	100 - 120
	60 °C	200 - 210	70 - 80
	70 °C	175 - 180	45 - 55
5 N NaOH	50 °C	220 - 240	75 - 90
	60 °C	140 - 150	50 - 60
	70 °C	110 - 120	40 - 50
6 N NaOH	50 °C	200 - 210	75 - 90
	60 °C	110 - 120	50 - 60
	70 °C	80 - 90	40 - 45

Table 3.52: Time required at different etching conditions for track development for PETAC homopolymer.

The bulk etch rate for the polymer was calculated using the wieght loss method. The variation in the bulk etch rate for PETAC

homopolymer under different etching conditions is given in Figure 3.51. As the bulk etch rate is very low at 50 °C, the change in weight of the film was very small and hence V_b was almost close to zero and hence the time required for track development was more. At 60 °C the bulk etch rate increases but remains lower than that of PADC. However, the track revelation time at 60 °C is comparable with that of PADC etched at 70 °C.

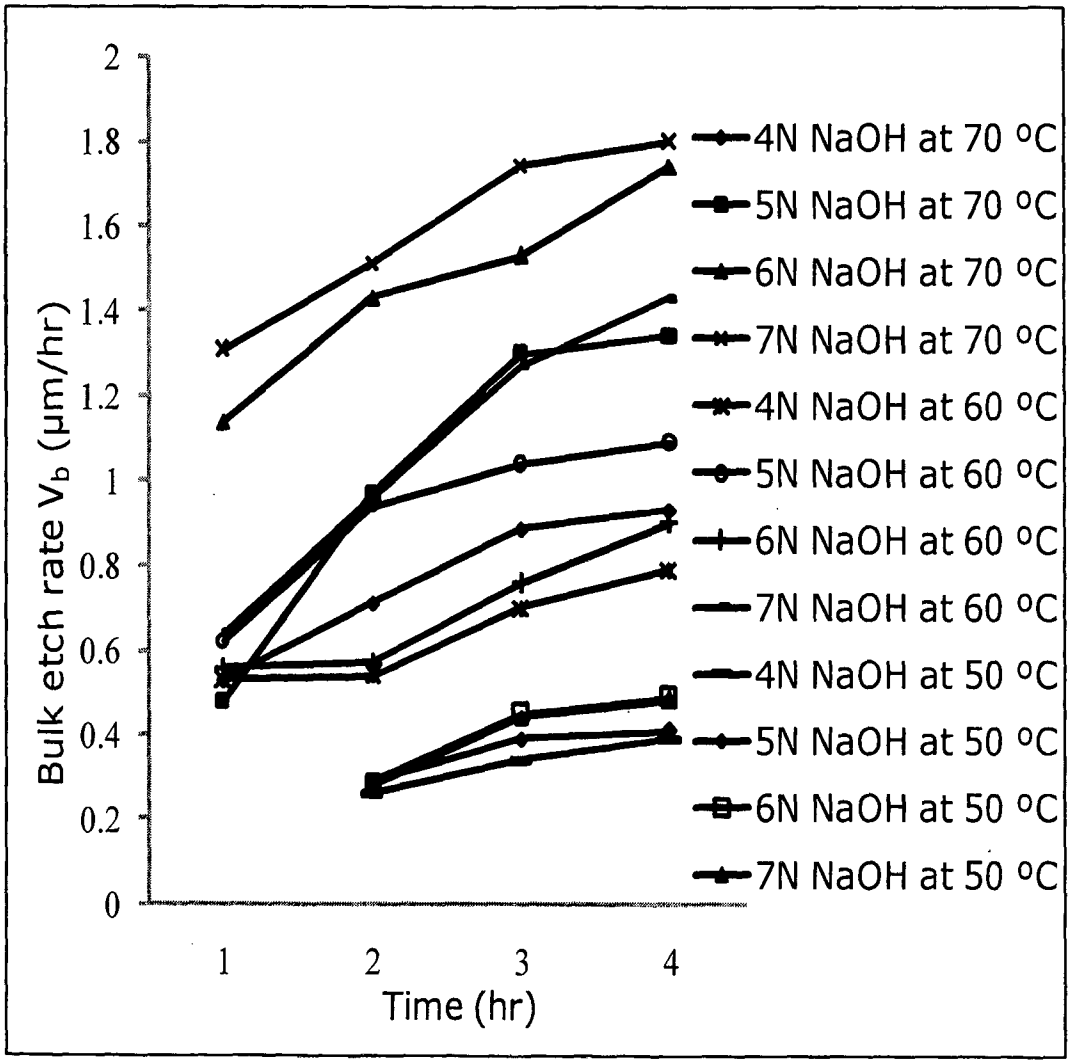

Figure 3.51: Variation in the bulk etch rate in PETAC homopolymer at 50, 60 and 70 °C under different etchant concentration.

The bulk etch rate of PPETAC at 70 °C in 6 N NaOH is comparable with that obtained of PADC under identical conditions but the track revelation time is reduced at this temperatures. At 70 °C, however, at lower etchant concentration the time for track development increases. Thus the 6 N NaOH at 70 °C can be used as optimum etching condition to etch the PPETAC homopolymer film.

Similar studies were performed on PETAC:ADC 4:6 w/w copolymer film and the time required to reveal the alpha and fission tracks under different etching conditions were found and is given in Table 3.53.

Etchant	Temperature	Time (min) to observe	
		Alpha tracks	Fission tracks
3 N NaOH	50 °C	280 - 300	100 - 120
	60 °C	170 - 180	60 - 70
	70 °C	140 - 150	50 - 60
4 N NaOH	50 °C	220 - 240	90 - 100
	60 °C	160 - 180	50 - 60
	70 °C	135 - 150	50 - 60
5 N NaOH	50 °C	160 - 180	70 - 80
	60 °C	110 - 120	45 - 50
	70 °C	75 - 90	35 - 45
6 N NaOH	50 °C	120-150	50 - 60
	60 °C	75 - 90	35 - 45
	70 °C	50 - 60	25 - 30

Table 3.53: Time required at different etching conditions for track development for PETAC:ADC 4:6 w/w copolymer.

The track detection studies reveal that the PETAC:ADC 4:6 w/w copolymer is more time efficient than PPETAC homopolymer and the CR-39™. The copolymer can reveal the alpha autoradiograph in just 60 minutes and the fission fragment tracks in 25-30 minutes when etched in 6 N NaOH at 70 °C. The track revelation times of PETAC:ADC 4:6 w/w copolymer etched in 6 N NaOH at 50 °C is ssimilar to CR-39™ etched in 6 N NaOH at 70 °C. The post etch surface of the copolymer films is clear under all the etching conditions used. The bulk etch variation is shown in Figure 3.52.

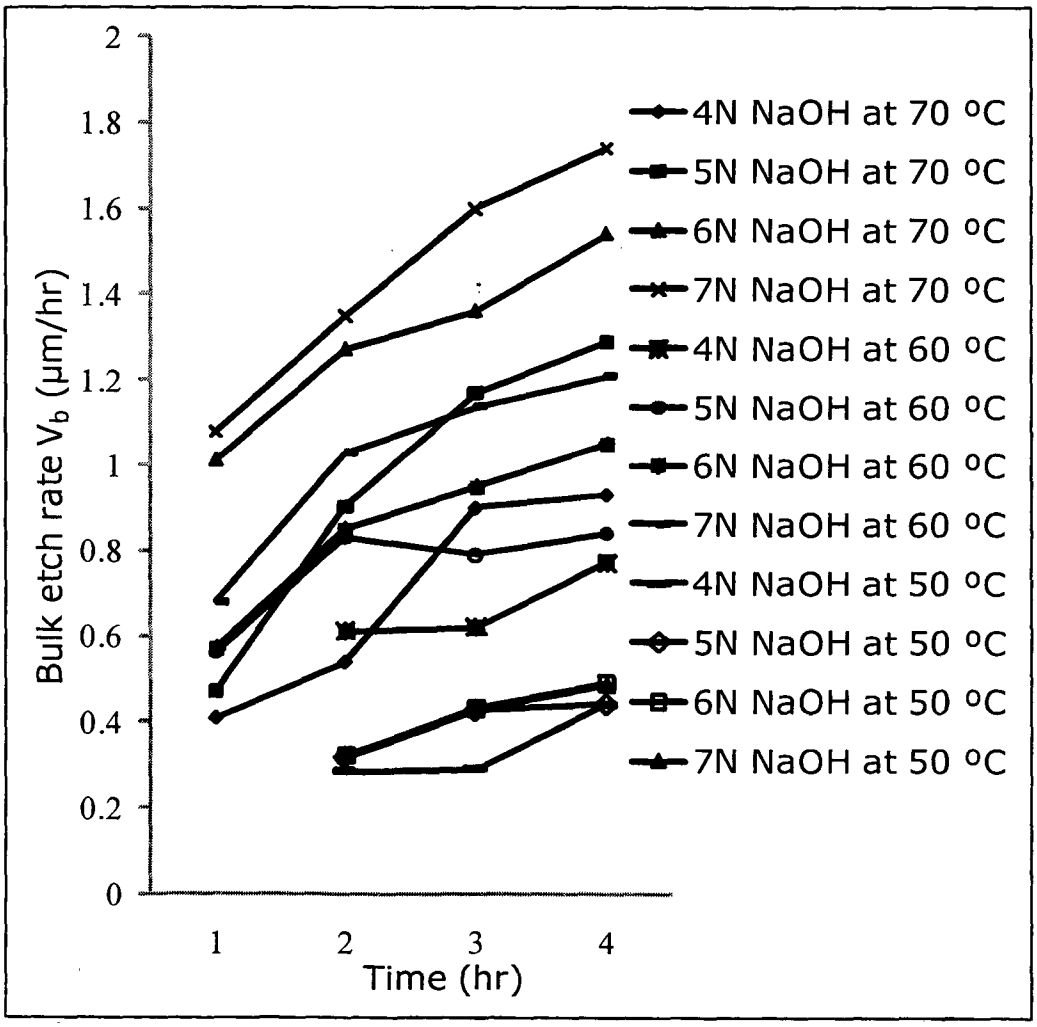

Figure 3.52: Variation in the bulk etch rate in PETAC:ADC 4:6 w/w copolymer at 50, 60 and 70 °C under different etchant concentration.

The films remained very clear during etching even in 6 N NaOH at 70 °C. However, at temperatures above 70 °C or NaOH concentrations more than 6N, detector films tend to develop cracks and become opaque. At lower temperatures and etchant concentration, track revelation time and the time required to obtain maximum sensitivity increases. In 6 N NaOH at 70 °C the bulk etch rate also does not increase more hence should be used as the optimum etching condition to etch the copolymer.

3.7.4 Optimization of etching conditions for PETAC:DEAS 4:6 w/w copolymer: The PETAC:DEAS 4:6 w/w copolymer was also studied for its variation in track revelation time and bulk etch rate studies at different etching conditions. The track revelation time at different etching conditions is given in Table 3.54.

Etchant	Temperature	Time (min) for		Post etch surface appearance
		Alpha	Fission	
4 N NaOH	60 °C	80 - 90	50 - 60	Clear hard film
	70 °C	50 - 60	45 - 50	Clear hard film
	80 °C	40 - 45	25 - 30	Film softens in 2 hr
5 N NaOH	60 °C	80 - 90	40 - 45	Clear hard film
	70 °C	50 - 60	30 - 35	Clear hard film
	80 °C	30 - 35	20 - 25	Film softens in 2hr
6 N NaOH	60 °C	65 - 75	30 - 35	Clear hard film
	70 °C	40 - 45	25 - 30	Clear hard film
	80 °C	25 - 30	15 - 20	Film softens in 2hr

Table 3.54: Track revelation time for PETAC:DEAS 4:6 w/w copolymer under different etching conditions.

It was observed that the film becomes very soft when it was etched at 80 °C for more than two hours. The track revelation time was however, less at this temperature. At 70 °C the film remains intact and the maximum sensitivity is observed after 3 - 4 hr of chemical etching under the conditions tried. At 60 °C the films remain clear but the track revelation time increases. The variation in the bulk etch rate for different polymers is given in Figures 3.53. From the Figures below it was observed that the films had a very high bulk etch rate at 80 °C. At 70 °C the values decreases and at 60 °C it decreases further.

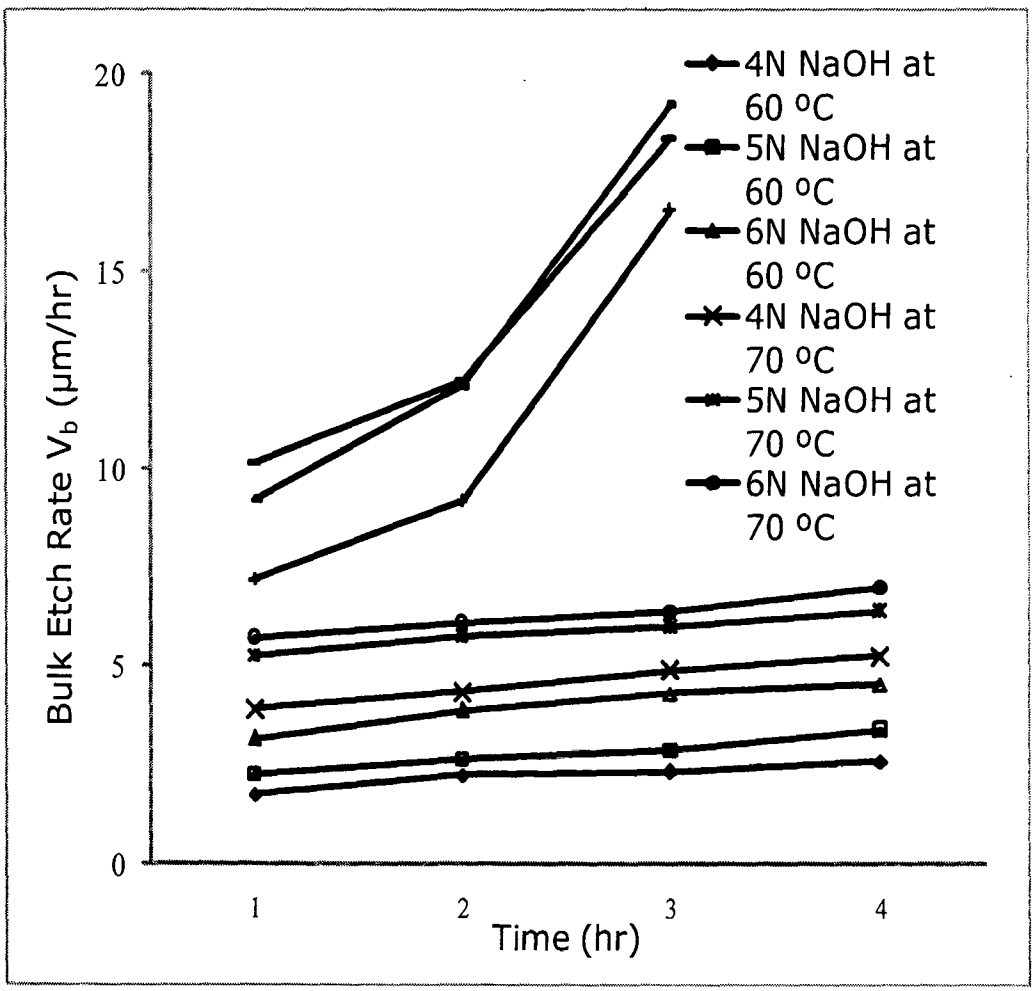

Figure 3.53: Variation in bulk etch rate of PETAC:DEAS under different etching condition.

Thus, for smooth etching of the PETAC:DEAS 4:6 w/w copolymer film 6 N NaOH at 60 °C appears to be good condition for etching. The polymer attains its maximum sensitivity in four hr. Furthermore, the sensitivity value increases from 2.13 in 9 hr for PETAC:ADC 4:6 w/w copolymer to 2.35 for PETAC:DEAS 4:6 w/w copolymer in just 4 hr in 6 N NaOH at 70 °C.

3.7.5 Optimization of etching conditions for PETAC:ADC:DEAS 4:3:3 w/w/w ternary copolymer: It was observed that the film becomes opaque when etched for more than 6 hr in 6 N NaOH at 70 °C, whereas, at 80 °C with 4-6 N NaOH the film become soft. Thus, if a suitable etching condition which can delay opaqueness and allow longer etching time, the alpha sensitivity may be higher. Table 3.55 below gives a maximum alpha sensitivity values, the time required and the post etch appearance of the film.

Etchant	Tempe-rature	Time (min) for		Post etch surface appearance	Alpha sensitivity
		Alpha	Fission		
4N NaOH	50°C	130-150	60 - 75	12 hr, opaque	1.73
	60°C	80 - 90	35 - 45	8 hr, opaque	1.96
	70°C	50 - 60	25 - 30	5 hr, opaque	2.13
5N NaOH	50°C	110-120	50 - 60	9 hr, opaque	1.87
	60°C	60 - 75	25 - 30	6 hr, opaque	2.01
	70°C	40 - 45	15 - 20	4 hr, opaque	2.30
6N NaOH	50°C	80 - 90	35 - 40	8 hr, opaque	1.97
	60°C	35 - 45	15 - 20	5 hr, opaque	2.24
	70°C	25 - 30	10 - 15	3 hr, opaque	2.36

Table 3.55: Maximum sensitivity values under different etching conditions used for ternary copolymer.

From the Table 3.55, one can observe that the alpha sensitivity is maximum when the film is etched at 70 °C. However, a comparable sensitivity values are obtained when the film is etched at 6 N NaOH at 60 °C and 5 N NaOH at 70 °C but the time required is longer. Thus 6 N NaOH at 70 °C appears to be a reasonable etching condition for the polymer.

3.7.6 Optimization of etching conditions for DAS:ADC 2:8 w/w copolymer: While both DAS:ADC 2:8 and ADS:ADC 1:9 w/w copolymers show an impression (alpha autoradiograph) of ^{239}Pu alpha particle source, clear image of alpha particle tracks and counting is possible only when exposure is carried out at around 3 cm distance from the source.

Etchant	Temperature	Time (min) to observe	
		Alpha tracks	Fission tracks
4 N NaOH	60 °C	80 - 90	25 - 30
	70 °C	50 - 60	15 - 20
	80 °C	40 - 45	8 - 10
5 N NaOH	60 °C	50 - 60	15 - 20
	70 °C	30 - 40	5 - 10
	80 °C	20 - 25	4 - 5
6 N NaOH	60 °C	30 - 40	7 - 10
	70 °C	25 - 30	5 - 10
	80 °C	15 - 20	3 - 5
7 N NaOH	60 °C	25 - 30	5 - 10
	70 °C	20 - 25	4 - 5
	80 °C	15 - 20	2 - 5

Table 3.56: Track revelation time under different etching conditions.

The polymer was etched in 4 - 7 N NaOH solution and at temperatures between 60 to 80 °C. The time required for track formation under different etching condition is given in the Table 3.56. It was observed that the fission fragment tracks can be seen within 10 minutes of etching. The tracks can be observed clearly under an optical microscope. The alpha autoradiograph however, requires longer time. But, Under all the etching conditions tried the film becomes foggy after chemical etching for more than 20 minutes. At higher temperatures of 80°C the foggy appearance is seen very rapidly. Thus 6N NaOH at 70°C can be used to etch the polymer.

3.7.7 Optimization of etching conditions for ADS:ADC 1:9 w/w copolymer: The optimization of etching conditions was also performed for ADS:ADC 1:9 w/w copolymer. The polymer had a similar etching chahacteristics to that of DAS:ADC 2:8w/w copolymer. The various etching conditions used to etch the films are enlisted in the Table 3.56(see next page). Apart from using normal alkaline solution many other etchants were tried such as barium hydroxide, potassium carbonate, alcoholic alkalies etc. The film got opaque under most of the conditions with a visual impression of alpha autoradiograph being seen. In the conditions under which the film remained clear, the film did not reveal any of the tracks. Thus, if polysulfite films are desired to be used for rapid fission fragment track analysis 2 - 3 N NaOH at 70 °C should be used as an etching condition.

Sr No	Etchant	Temp. °C	Time (min) for		Post etch nature of the film
			Fission	Alpha	
1	NaOH 10 N	70	1 - 2	5 - 10	Opaque in ~ 10 min
2	NaOH 9 N	70	1 - 2	5 - 10	Opaque in 10 min
3	NaOH 8 N	70	2 - 4	15 - 20	Opaque in 10-15 min
4	NaOH 7 N	70	2 - 5	15 - 20	Opaque in 10-15 min
5	NaOH 7 N	60	4 - 5	15 - 20	Opaque in 10-15 min
6	NaOH 6 N	90	2 - 3	5 - 10	Opaque in 5 min
7	NaOH 6 N	80	2 - 3	5 - 10	Opaque in ~10min
8	NaOH 6 N	70	3 - 5	20 - 25	Opaque in ~25 min
9	NaOH 6 N	60	3 - 5	25 - 30	Opaque in ~25 min
10	NaOH 6 N	50	8-10	no tracks	Opaque in 60 min
11	NaOH 5 N	70	5 - 10	30 - 40	Opaque in 30 min
12	NaOH 5 N	60	8- 10	no track	Opaque in 60 min
13	NaOH 5 N	50	8- 10	no track	Opaque in 60 min
14	NaOH 4 N	70	20	50 - 60	Opaque in ~60 min
15	NaOH 4 N	60	15 - 20	no tracks	Opaque in ~60 min
16	NaOH 3 N	70	8 - 10	50 - 60	Opaque in ~60 min
17	NaOH 2 N	70	10 - 20	60 - 70	Opaque in ~60 min
18	NaOH 1 N	80	8 - 10	80 - 90	Opaque in ~60 min
19	NaOH 4 N	70	10 - 20	60 - 70	Opaque in ~60 min
20	NaOH 0.5 N	70	120	No tracks	Blurring in 120 min
21	NaOH 0.2 N	70	120	No tracks	Blurring in 120 min
22	Sat.K_2CO_3	70	No tracks	No tracks	Blurring in 120 min
23	Sat.Na_2CO_3	70	No track s	No tracks	Blurring in 120 min
24	KOH 0.2 N in Sat.Na_2CO_3	70	120	No tracks	Blurring in 120 min
25	KOH 0.5 N in Sat.K_2CO_3	70	120	No tracks	Opaque in 120 min

26	Methanol	50	No tracks	No tracks	No blurring
27	Ethanol	50	No tracks	No tracks	No blurring
28	6N Metha-nolic KOH	50	No tracks	No tracks	Opaque in 4 min
29	Molten $Ba(OH)_2.8H_2O$	82	No tracks	No tracks	Opaque in 10 min

Table 3.57: Various etching conditions used for etching the ADS:ADC 1:9 w/w copolymer.

3.8 Sensitivity studies at the optimized etching conditions:

The polymers were cured using the heating profiles given at their optimized monomer concentration and initiator concentration given in the Table below. The initiator concentration for different polymers varied from 3 - 5 % w/w of initiator. Finally the etching was also performed under the etching conditions stated in the Table 3.58.

Homo/Co polymer w/w	Heating profile	% w/w IPP	Etching condition
DAC	As calculated for DAC	3.3	6 N NaOH 80 °C 6 N NaOH 70 °C
DAC:ADC 1:1	As calculated for DAC	3.3	6 N NaOH 80 °C
DEAS:ADC 3:7	Same as ADC/IPP	4	6N NaOH 70 °C 6N NaOH 60 °C
PETAC	As calculated for PETAC	3	6 N NaOH 70 °C
PETAC:ADC4:6	As calculated for PETAC:ADC	4	6 N NaOH 70 °C

PETAC:DEAS 4:6	Same as ADC/BP	4	6 N NaOH 70 °C
PETAC:ADC:DEAS 4:3:3	As calculated for PETAC:ADC	5	6 N NaOH, 70 °C
DAS:ADC 2:8	45 °C constant	8	2 - 3 N NaOH, 70 °C
ADS:ADC 1:9	45 °C constant	8	2-3 N NaOH,70 °C
PADC	ADC IPP	3.3	3-6 N NaOH, 70 °C

Table 3.58: Summary of optimized conditions for different polymers.

The etching conditions also varied from 6N NaOH at 60 °C to 6 N NaOH 80 °C. However, some of the polymers performed very well under two etching conditions and depending on the availability of time, either of the conditions can be used. The polymers were subjected to sensitivity study measurements under the optimized etching conditions. The alpha and the fission track diameters were measured over a time until a maximum sensitivity value is obtained for the polymer. The variation of alpha track diameter in different polymers prepared is shown in Figure 3.54(see next page).

As expected, the rate of increase in the alpha track diameter was maximum in the polymers with higher sulfonate groups. The DEAS:PETAC 6:4 w/w copolymer had the highest rate of alpha particle track growth. The track size growth for almost all carbonate containing polymers was nearly comparable. The variation in the fission track diameter for different polymers prepared and etched under optimum polymerization and etching conditions is shown in Figure 3.55(see next page).

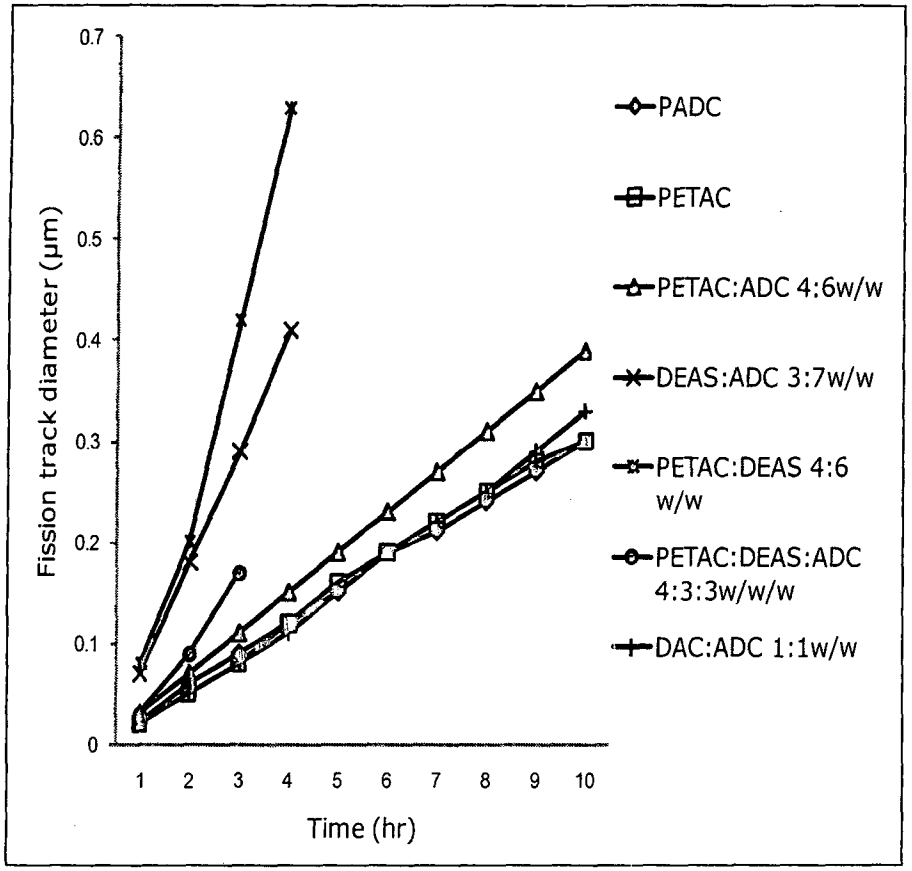

Figure 3.54: Variation in the alpha track diameter for different polymers prepared and etched under optimum polymerization and etching conditions.

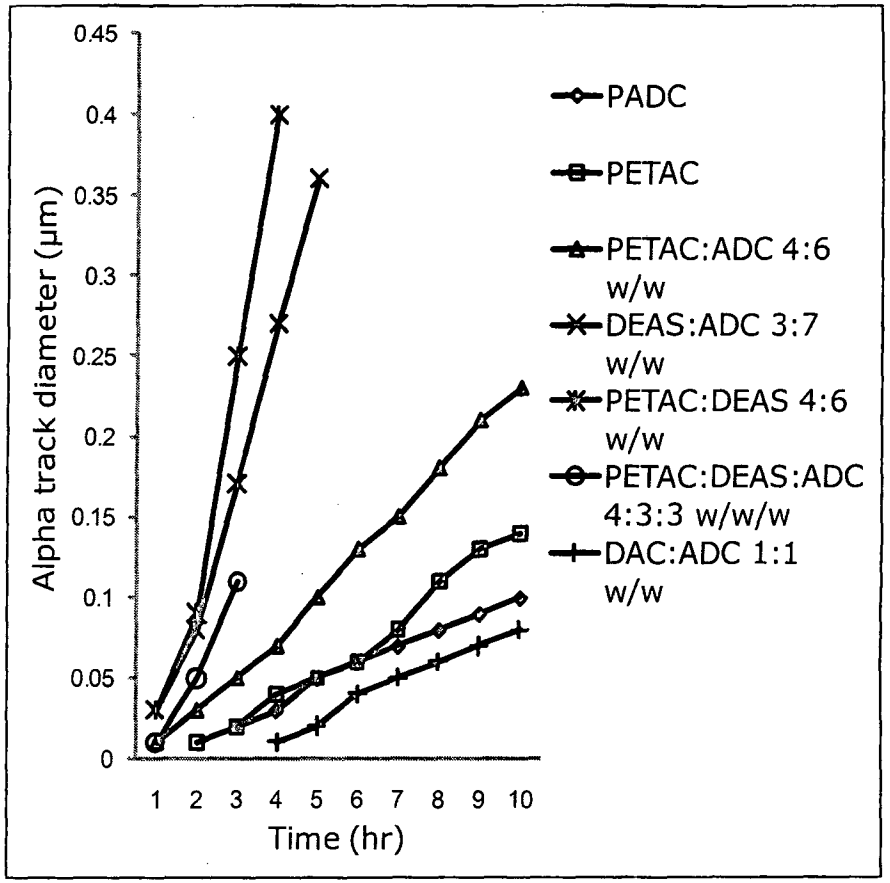

Figure 3.55: Variation in the fission track diameter for different polymers prepared and etched under optimum polymerization and etching conditions.

The fission track growth in case of polymers containing carbonate moieties was almost comparable with that of the alpha track growth. But the introduction of sulfonate groups enhances the track growth rate and reduces the time required to observe this tracks. Some of the sulfur containing polymers turn opaque after etching. The alpha and fission track diameters were used to calculate the variation in the sensitivity of the polymers and is represented in Figure 3.56.

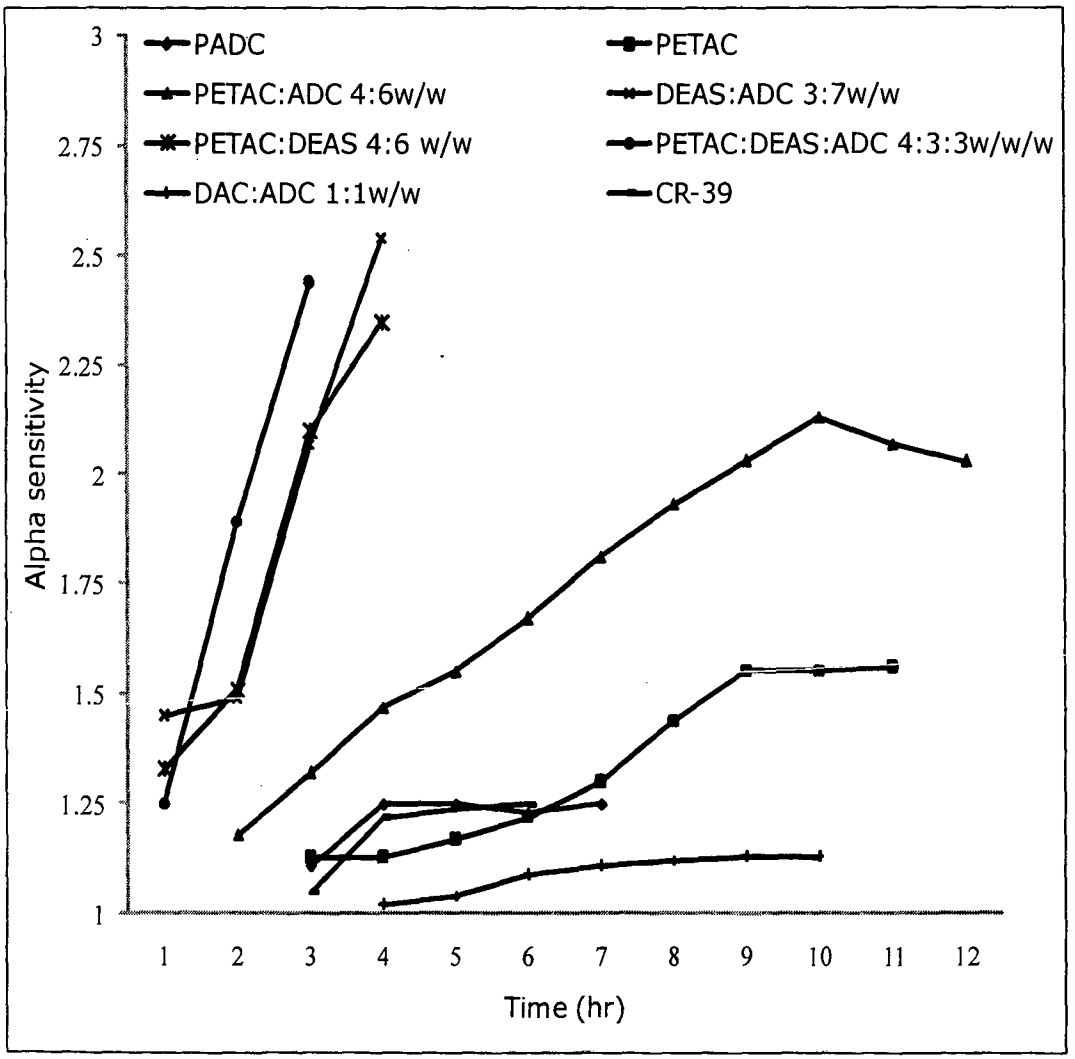

Figure 3.56: Variation in the alpha sensitivity for different polymers prepared and etched under optimum polymerization and etching conditions.

The ternary copolymer of DEAS:ADC:DEAS 4:3:3 w/w/w prepared with IPP initiator shows a maximum alpha sensitivity of 2.44 in just 3 hours. However, the copolymer becomes opaque thereby hindering further measurement of the track growth and inturn the alpha sensitivity. The DEAS:ADC 3:7 w/w copolymer prepared with 4 % IPP initiator has a alpha sensitivity of 2.54 as compared to 1.24 of PADC. The PETAC homopolymer and the PETAC:ADC 4:6 w/w copolymer were also having higher alpha sensitivity value than PADC.

Copolymer w/w	Time for track revelation in minutes in 6N NaOH at 70°C		Maximum alpha sensitivity, Time required (hr)
	Fission	Alphas	
DAC	60	Not observed	Not determined
DAC:ADC 1:1	60	480	1.18, 9 hr
DAS:ADC 2:8	10	20	Not determined
DAS:DAC 1:1	15	Not observed	Not determined
ADS:ADC 2:8	5	15	Not determined
ADC:ADS:DAC 1:1:1	10	Not observed	Not determined
DEAS	60	180	Not determined
DEAS:ADC 3:7	30	60	2.54, 4 hr
PETAC	45	90	1.54, 9 hr
PETAC:ADC 4:6	30	60	2.13, 10 hr
PETAC:DEAS 4:6	20	45	2.35, 4 hr
PETAC:ADC:DEAS 1:1:1	15	30	2.44, 3 hr
PADC (Indigenous)	60	120	1.24, 4 hr
CR-39™ (Imported)	60	120	1.28, 6 hr

Table 3.59: The variation in track revelation time and the alpha sensitivity of different copolymers etched under their optimized conditions.

The maximum alpha sensitivity of the polymers at optimum conditions and the alpha and fission track revelation time is given in Table 3.59 above.The variation in the bulk etch rate at their optimized conditions was determined using the fission track diameter method and is given in Figure 3.57.

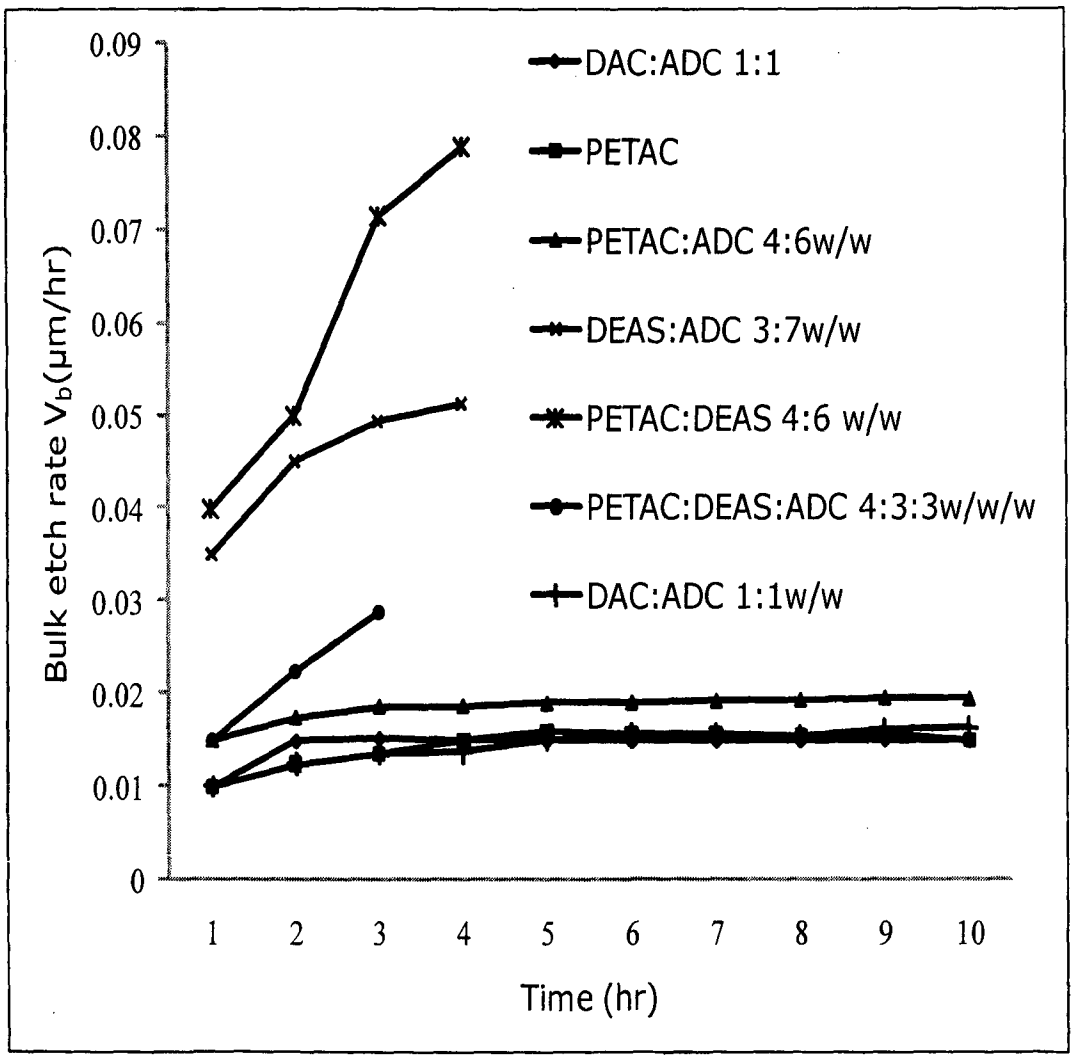

Figure 3.57: Variation in the bulk etch rate for different polymers prepared and etched under optimum polymerization and etching conditions.

The bulk etch rate of the detector increases with the increase in the sulfonate or sulphite concentration as a particular

sulfur containing groups in the polymer. The sulfonate, being more labile group, in higher concentration increases the rate of polymer hydrolysis thereby increasing the polymer degradation more rapidly. The sulphite is still more easily hydrolysed and hence bulk etch rate still increases to higher value. The polymers containing carbonate group has a lower bulk etch rate as the hydrolysis of carbonate is still more difficult.

3.9 Studies on variation of alpha track density with etching time: The alpha track detection efficiency for different polymers was determined by exposing the film to ^{239}Pu alpha source in 4π geometry at a distance of 3 cm. The tracks were counted after specific time intervals to get the optimum time, under the etching condition used, for etching of the film. The tracks were counted after different etching time intervals using an optical microscope till a constant value was obtained for a particular material under study. The maximum numbers of tracks seen at perticular time is optimum time to etch the detector film.

A blank film was also used in each case to find the number of background tracks. A 2 × 2 cm^2 film of the polymer was exposed to ^{239}Pu source for 5 minutes at a distance of 3 cm from source. The films were then etched and the tracks were counted. A total of 100 views were counted to find average track density (tracks/cm^2). The polymers containing sulphite moieties cannot be etched for long time. Hence, the number of tracks was counted by etching the film till it remains clear and tracks can be distinguished from the background. For the sulphite containing polymers track density relative to ADC were determined as the polymers become opaque if etched for long time. Table 3.60(see next page) gives the alpha track detection efficiency for different sulphite copolymers in comparison to PADC.

Detector	Number of alpha tracks	Track detection efficiency (%, relative to PADC)
PADC	19909	100
DAS:ADC 2:8 w/w	19127	96.07
ADS:ADC 1:9 w/w	19244	96.66

Table 3.60: Track detection efficiency for the sulphite containing polymers.

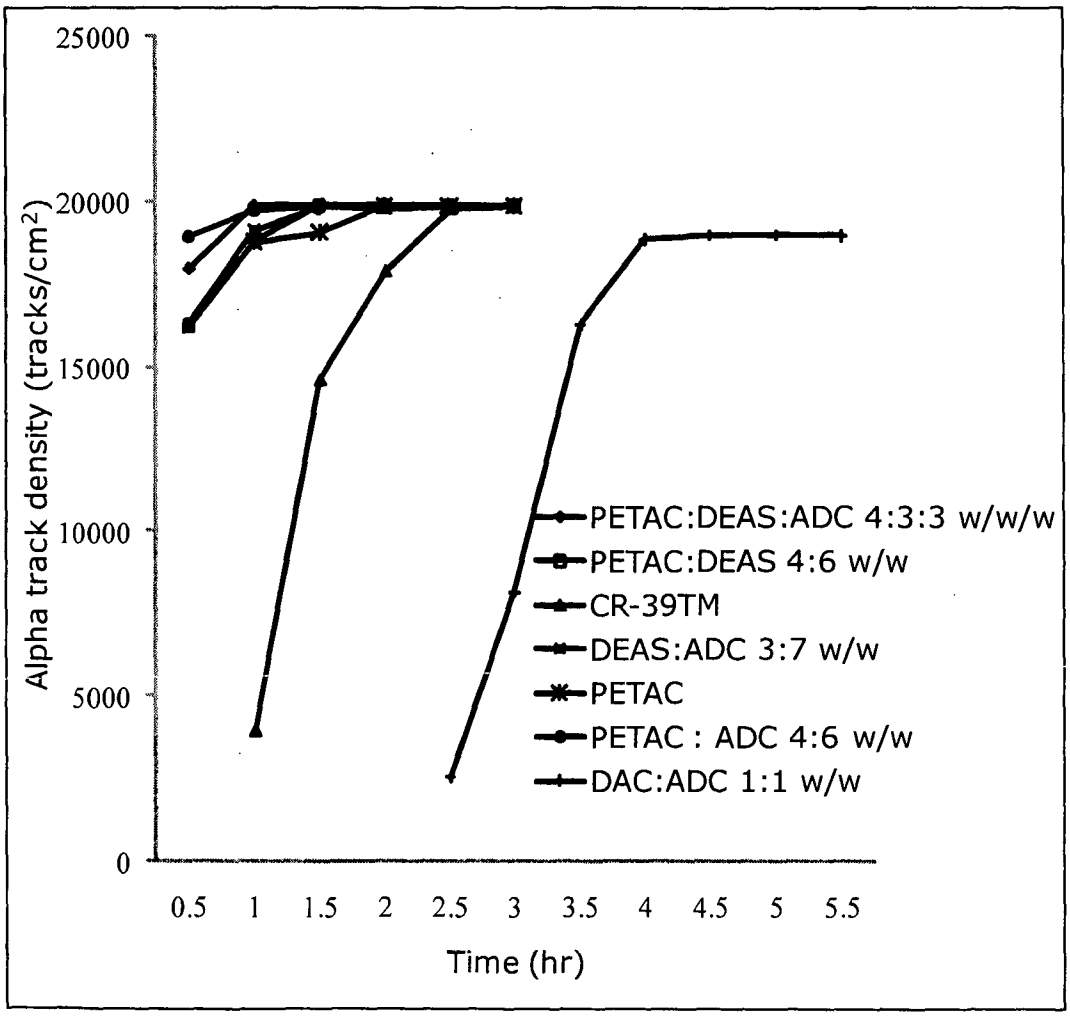

Figure 3.58: Variation in alpha track density in different copolymers exposed under identical conditions and etched using the optimized etching condition.

It can be seen that the maximum alpha track counting times vary considerably for different materials (Figure 3.58, See previous page). However, the maximum number of tracks obtained for different polymers is almost same. For DAC:ADC 1:1 w/w copolymer it is slightly less. From the data obtained, the etching time at which the maximum number of alpha tracks can be conveniently counted for different polymers are given in Table 3.61.

Detector film	Time to observe maximum density of alpha tracks (min)	Number of tracks/cm^2
CR-39™	180	19888
PETAC	150	19915
PETAC:ADC 4:6 w/w	120	19904
DEAS:ADC 3:7 w/w	90	19895
PETAC:ADC:DEAS 4:3:3 w/w/w	90	19924
DAS:ADC 2:8 w/w	20	19127
ADS:ADC 1:9 w/w	15	19244
DAC:ADC 1:1 w/w	300	19022
PETAC:DEAS 4:6w/w	150	19922

Table 3.61: Variation of time required for maximum alpha track density in different polymers.

3.10 Determination of background track like features: When a detector material is etched without exposure to radiation source, the material reveals structures similar to the track of a charged particle. These tracks may alter the end results of SSNTD applica-

tions if a blank film is not used. The density of the background track like features for different homopolymers and copolymers is given in Table 3.62.

Sr. No.	Detector film	Background track density (tracks/cm$^{2)}$
1	CR-39™	40-60
2	PADC indigenous	50-70
3	PETAC	120-140
4	PETAC:ADC 4:6 w/w	100-120
5	DEAS:ADC 3:7 w/w	130-150
6	PETAC:ADC:DEAS 4:3:3 w/w/w	160-180
7	DAS:ADC 2:8 w/w	270-290
8	ADS:ADC 1:9 w/w	170-190
9	DAC:ADC 1:1w/w	90-120

Table 3.62: Density of background track like features in various polymers.

3.11 Alpha to fission branching ratio: The fission tracks are observed in shorter time than required for alpha particles, and therefore, there is a considerable difference in the size and appearance time of the tracks in a given detector. Alpha and fission fragment tracks can be easily distinguished by sequential chemical etching method. The data obtained can be used for studies of half lives, alpha to fission fragment branching ratios and identification of radio nuclides using single detector.[135] The newly designed track detectors meets all the requirements and is time convenient as there is considerable difference in etching time and sizes of the

tracks formed as compared to CR-39™. The number of tracks found is comparable to CR-39™ track detector as can be seen in Table 3.63.

Homopolymer/ copolymer w/w	Fission tracks/cm^2	Alpha tracks/cm^2	Geometry for α/F.F.	
			2π	4π
CR-39™	4.09 x 10^2	64.41 x 10^2	15.75	30.82
DEAS: ADC 3:7	4.27 x 10^2	65.73 x 10^2	15.37	30.57
PETAC	4.15 x 10^2	65.48 x 10^2	15.77	30.96
PETAC:ADC 4:6	4.09 x 10^2	65.98 x 10^2	16.13	31.28
PETAC:DEAS 4:6	4.22 x 10^2	65.74 x 10^2	15.63	30.74
PETAC:DEAS:ADC 1:1:1 w/w/w	4.33 x 10^2	65.86 x 10^2	15.65	30.68

Table 3.63: Alpha to fission fragment branching ration in different polymeric track detectors.

Thus, the polymer can be used in to determine alpha to fission fragment branching ratio.

3.12 Neutron dosimetry studies: The suitability of some poly-carbonate detectors for the revelation of neutron tracks was checked. The experimental polymer sheets of PETAC homopoly-mer, PETAC:ADC 4:6 w/w and commercial CR-39™ of size 3 cm x 3 cm, along with polyethylene radiator were irradiated using 1 Ci, Am-Be neutron source with average neutron energy of 4.4 MeV to receive a dose equivalent to 340.4 mRem. The detectors were mounted on the ECE Cell and etched using 7 N KOH solution, in a incubator maintained at 60 °C, in two steps using the etching conditions generally used for commercial CR-39™. For the first

step - etching at low frequency of 100 Hz for 4 hours at 1250 volts peak to peak constant potential. This was followed by the second step - etching at high frequency of 3.5 kHz at 1250 volts for 40 min duration. A computer based image analysis system developed by Electronics Division; BARC was used for automatic counting of the ECE damage tracks. The PETAC:ADC 4:6 w/w copolymer was found to show good neutron sensitivity, comparable to that of CR-39™, whereas the PETAC homopolymer had feeble sensitivity towards neutrons. It was observed that, under the exposure and etching conditions mentioned above, both CR-39™ and PETAC: ADC 4:6 w/w copolymer detectors showed an average of 404 tracks/cm^2 while the PETAC homopolymer showed an average of 150 tracks/cm^2. It was also observed that size of tracks in the homopolymer was smaller than that in copolymer. Further studies in neutron dosimetry using these detectors are in progress.

Conclusions

1] A new monomer ADS has been prepared and cast polymerized for use as nuclear track detector. The monomer structure was characterized by using different spectroscopic techniques.

2] We have successfully designed, prepared and tested two homopolymers and more than six copolymer compositions for use in nuclear track detection. Some of the newly designed copolymers show remarkable track detection properties.

3] A series of copolymers of newly synthesized monomers with ADC was prepared to determine the optimum monomer concentration where the alpha sensitivity is maximum.

4] Successfully demonstrated the extension of Dial's kinetic model to study the polymerization kinetics of an octafunctional monomer like PETAC.

5] The kinetics of polymerization for DAC, PETAC homopolymers and PETAC:ADC 4:6 w/w copolymer is studied and heating profiles for polymerization is obtained using the Dial's methodology.

6] Some of the newly designed homopolymers/copolymers were found to have high alpha sensitivity, almost double than that of commercially available CR-39™ polymer. e.g. the DEAS:ADC 3:7 w/w copolymer shows an alpha sensitivity of 2.54; PETAC:DEAS 4:6 w/w copolymer has a maximum alpha sensitivity of 2.35 and a ternary copolymer of PETAC:DEAS:ADC 4:3:3 w/w/w has a maximum alpha sensitivity value of 2.44 in just 3 hours of chemical etching. The PETAC:ADC 4:6 w/w copolymer has a alpha sensitivity value of 2.13.

7] Some of the sulfur containing track detectors that can be

used for rapid fission track analysis were prepared. Use of the sulfite containing copolymers to reveal the fission fragment tracks in just 5-10 minutes has been demonstrated for the first time. The ternary copolymer can reveal the fission fragment tracks in 15 minutes and the alpha tracks in 30 minutes. Thus, the time required for track development has been reduced considerably (when compared with CR-39™).

8] We have successfully shown the effectiveness of dense 3D network on track detection parameters. Highly crosslinked polymer PETAC has a higher alpha sensitivity than CR-39™ polymer. Whereas, the PETAC:ADC 4:6 w/w copolymer was even more sensitive than PETAC homopolymer. This implies that the introduction of more crosslinking monomers is also important to improve the alpha sensitivity.

9] Successfully prepared DEAS:ADC copolymers having higher sensitivity than SR-86(20). DEAS copolymer with ADC 3:7 w/w was found to be a highly sensitive towards track detection. The polymer had alpha sensitivity almost double than that of commercially available CR-39™ polymer. The polymer also showed reduced track revelation time.

10] A new class of sulphur containing monomers/polymers i.e. polysulphites, was successfully introduced for the first time for use in nuclear track detection.

11] Some of the polymers can be used to reveal exclusively fission fragment tracks in presence of alpha particles. The DAC homopolymer can reveal only fission fragment tracks and is a commercially viable alternative to PADC for fission track analysis.

12] Some of the polymers appear to be promising for neutron

dosimetric studies, however this study is presently incomplete.

13] The effectiveness of the proposed protocol for development and testing of track detectors from allylic monomers was verified. While the protocol generally apeared to work fine some modifications of Dial's kinetic model for sulfur containing monomers was found to be a problen Hence, constant temperature polymerizaion was chosen as a alternative.

References

1] O. Glasser, *Dr. W. C. Röentgen.*, C. Charles. Thomas Publisher; Springfield, Illinosis 2nd edn., 1958.

2] H. Becquerel, *Compt. Rend.*, 1896, **122,** 420.

3] H. Becquerel, *Compt. Rend.*, 1896, **122**, 501.

4] P. Curie, Mme. S. Curie and G. Bemont, *Compt. Rend.*, 1898, **127,** 1215.

5] D. Gollnick, *Basic Radiation Protection Technology;* Pacific Radiation Press; 1983.

6] S. A. Durrani and R. K. Bull, *Solid State Nuclear Track Detection: Principles, Methods and Applications.*, Pergamon Press, 1987.

7] D. A. Young, *Nature.*, 1958, **182,** 375.

8] E. C. H. Silk and R. S. Barnes, *Philos. Mag.*, 1959, **4,** 970.

9] R. L. Fleischer, P. B. Price and R. M. Walker, *Annu. Rev. Nucl. Sci.*, 1965, **15,** 1.

10] B. G. Cartwright, E. K. Shirk and P. B. Price, Nucl. Instrum. Methods., 1978, 153, 457.

11] P. C. Kalsi, A. Ramaswami, V. K. Manchanda, *BARC Newsletter.*, 2005, **257,** 6.

12] A. G. Chmielewski, J. Michalick, M. Buczkowski and D. K. Chmielewska, *Nucl. Instrum. Methods Phys. Res. B.*, 2005, **236,** 329

13] C. Hepburn and A. H. Windle, *J. Mater. Sci.*, 1980, **15,** 279.

14] A. M. Bhagwat, *Solid State Nuclear Track detection: Theory and Applications,* Indian Society of Radiation Physics, Kalpakkam, 1993.

15] G. Somogyi and A. S. Szalay, *Nucl. Instrum. Methods.*, 1973, **109,** 211.

16] P. B. Price and R. M. Walker, *J. Appl. Phys.*, 1962, **33,** 3407.

17] K. N. Yu and D. Nikezic, *Mater. Sci. Eng.*, 2004, **R46**, 51.

18] R. L. Fliescher, P. B. Price, R. M. Walker and E. L. Hubbard, *Phys. Rev.*, 1964, **133,** 1443.

19] R. L. Fliescher, P. B. Price, R. M. Walker and E. L. Hubbard, *Phys. Rev.*, 1967, **156,** 353.

20] E. V. Benton, Charged particle tracks in polymers, No.4., USNRDL-TR-67-80, 1967

21] H. G. Paretzke, *Radiat. Eff. Defects.*, 1977, **34,** 3.

22] R. Katz and E. J. Kobetich, *Phys. Rev.*, 1968, **170,** 391.

23] M. Monin, *PNCF.*, 1968, **68,** RI-9.

24] F. Desauer, *Z. Physik.*, 1968, **38,** 107.

25] R. L. Fliescher and P. B. Price, *J. Geophys.Res.*, 1964, **69,** 331.

26] R. L. Fliescher, P. B. Price and R. M. Walker, *J. Appl. Phys.*, 1965, **36,** 3645.

27] W. H. Huang and R. M. Walker, *Science.*, 1967, **155,** 1103.

28] D. S. Burnett, C. Hohenberg, M. Maurette, M. Monin, R. Walker and D. Woolum, *Apollo 16 Preliminary Science Report, NASA Pub.*, 1972, **315,** 19.

29] R. M. Walker, Z. Zinner and M. Maurette, *Apollo 17 Preliminary Science Report, NASA Pub.*, 1973, **330,** 2.

30] A. A. Miller, E. J. Lawton and J. S. Bafwitt, *J. Polymer Sci.*, 1959, **14,** 503.

31] P. Y. Apel, I. V. Blonskaya, A. Y. Didyk, S. N. Dmitriev, O. L. Orelovitch, D. Root, L. I. Samoilova and V. A. Vutsadakis, *Nucl. Instrum. Methods B.*, 2001, **179(1),** 55.

32] L. Tommassino, *Electrochemical Etching of Damaged Track Detectors by H. V. Pulse and Sinusoidal Waveform,* Internal Repot- Lab. Dosdimetria e Standardizzaaione, CNEN Casaccia,

Rome, 1970.

33] T. A. Gruhn, W. K. Li, E. V. Benton, R. M. Cassou and C. S. Johnson, *Proceedings of the 10th Conference on Solid State Nuclear Track Detectors,* Lyon, 1979

34] C. W. Y. Yip, J. P. Y. Ho, V. S. Y. Koo, D. Nikezic and K. N. Yu, *Radiat. Meas.,* 2003, **37,** 197.

35] T. Portwood, D. L. Henshaw and J. Stejny, *Nucl. Tracks. Radiat. Meas.*, 1986, **12(1-6),** 109.

36] M. Siems, K. Freyer, H. C. Treutler, G. Jonsson and W. Enge, *Radiat. Meas.,* 2001, **34,** 81.

37] F. Abu-Jarad, A. M. Hala, M. Farhat and M. Islam, *Radiat. Meas.,* 1997, **28,** 111.

38] D. Sinha, S. Ghosh, A. Srivastava, V.G. Dedgaonkar, K.K. Dwiwedi, *Radiat. Meas.,* 1997, **28,** 145.

39] Reimar Spohr, *European Research Training Network EuNITT*, Report M 2.1., 2001 3

40] P. Apel, *Track Membranes, Contribution to IAEA Consultant's Meeting,* JAERI, Takasaki, 1999.

41] R. L. Fleischer, P. B. Price and R. M. Walker, *Nuclear Tracks in Solids. Principles and Applications.*, University of California Press, California, 1975.

42] Berkeley, 1975, pp.1-605, direct communication: Pavel Yu. Apel, Joint Institute of Nuclear Reactions, 141980 Dubna, Russia

43] J. A. Morley, *Trans. Am. Nucl. Soc.,* 1972, **15,** 120.

44] Kodak-Pathe, *Instructions for the Use of CA80-15 Film and LR-115 Film*, type I and type IL.

45] M. Varnagy, I. Szabo, S. Juhasz and I. Csikai, *Nucl. Instr. Meth.,* 1973, **106,** 301.

46] G. P. Dixon and J. G. Williams, *Nucl. Instr. Meth.*, 1976, **135,** 293.

47] M. G. Seitz, R. M.Walker and B. S. Carpenter, *J. AppI. Phys.*, 1973, **44,** 510.

48] *US Pat.* 3 501 636, 1970.

49] F. Geisler and P. R. Phillips, *Rev. Sci. Instrum.*, 1972, **43,** 283.

50] J. W. N. Tuyn, *Nucl. Appl.*, 1967, **3,** 372.

51] A. L Khovanivich, G. L. Pikalov and I. F. Kryvokrysenko, *At. Energy.*, 1970, **29,** 367.

52] H.A. Khan, *Radiation Eff. defects.*, 1971, **8,** 135.

53] G. Meesen and A. Poffin, *Radiat. Meas.*, 2001, **34,** 161.

54] J. Block, J. S. Humphrey and J. E. Nichols, *Rev. Sci. Instrum.*, 1969, **40,** 509.

55] R. L. Fleischer, P. B. Price and R. M. Walker, *Rev. Sci. Instrum.*, 1966, **37,** 525.

56] M. M. Monnin and G. E. Blanford, *Science.*, 1973, **181,** 743.

57] K. Becker, *Health Phys.*, 1966, **12,** 955.

58] R. H. Iyer, *Science Today.*, 1977, **37,** 8.

59] B. C. Christner, E. Mosley-Thompson, L. G. Thompson and J. N. Reeve, *Environ. Microbiol.*, 2001, **3,** 570.

60] P. B. Price, *Radiat. Meas.*, 2005, **40,** 146.

61] R. H. Iyer and K. K. Dwivedi, *Radiat. Meas.*, 2003, **36,** 63.

62] S. Biswas, N. Durgaprasad, J. Nivatia, V. S. Venkatavardhan, J. N. Goswami, U.B. Jayanhi, D. Lal and S. K. Matto, *Astrophys. Space Sci.*, 1975, **35,** 317.

63] S. Biswas and J. N. Goswami, *Curr. Sci.*, 1995, **69,** 721.

64] L. T. Chadderton, D. Fink, H. Mockel, K. K. Dwivedi and A. Hammoudi, *Radiat. Eff. Defect Solids.*, 1993, **127,** 163.

65] R. H. Iyer and N. K. Chaudhuri, *Radiat. Meas.*, 1997, **27,** 524.

66] V. S. Nadkarni, *Ph.D. Thesis*, University of Mumbai, 1996.

67] L. M. Kovalenko, L. N. Gaichenko, Ya. I. Lavrentovich and A. M. Kabakchi, *Atomnaya Energiya.*, 1971, **31(5),** 510.

68] K. Ogura, M. Asano, N. Yasuda and M. Yoshida, *Nucl. Instr. Meth. B.*, 2001, **185,** 222.

69] A. Schulz, G. Siegmon and W. Enge, *Nucl. tracks. Radiat. Meas., 1991, **19(1-4),** 117.*

70] M. Fujii, *Nucl. Instr. Meth. A.*, 1985, **236,** 183,

71] T. Tsuruta, *Radiat. Meas.*, 2000, **32,** 289.

72] V. V. Shirkowa and S. P. Tretyakova, *Radiat. Meas.*, 2001, **34,** 177.

73] A. A. A. Mascarenhas, *Ph.D. Thesis*, Goa University, 2007.

74] M. Fujii, R. Yokota and Y. Atarashi, *Nucl. Tracks. Radiat. Meas.*, 1990, **17(1),** 19.

75] M. Fujii and R. Yokota, *Nucl. Tracks.*, 1986, **12 (1-6),** 55.

76] M. Fujii and J. Nishimura, *Nucl. Instr. Meth.*, 1984, **226,** 496.

77] J. Stejny and T. Portwood, *Nucl. Tracks.*, 1986, **12 (1-6),** 59.

78] A. Mascarenhas, R. V. Kolekar, P. C. Kalsi, A. Ramaswami, V. B. Joshi, S. G. Tilve and V. S. Nadkarni, *Radiat. Meas.*, 2006, **41(1),** 22.

79] Y. Komaki, N. Ishikawa, N. Morishita and S. Takamura, *Radiat. Meas.*, 1996, **26(1),** 123.

80] T.L. Cottrell, *The Strengths of Chemical Bonds.*, Butterworths, London, 2nd edn., 1958.

81] S.W. Benson, *J. Chem. Educ.*, 1965, **42,** 502.

82] A. Laville, J. Perez-Peraza, D. Lopez, M. Balcazar-Garcia and A. Lopez, *Rev. Mexicana Astron. Astrof.*, 1987, **14,** 776.

83] P. B. Price, D. O'Sullivan, *P. H. Fowler and V. M. Clapham edition SSNTDs.*, Pergamon Press, Oxford. 1982 929

84] J. M. G. Cowie, *Polymers: chemistry and physics of modern materials*, International Textbook Company Limited, Aylesburry, 1973.

85] W. R. Dial, W. E. Bissinger, B. J. Dewitt and F.Strain, *Ind. Eng. Chem.*, 1955, **47,** 2447.

86] P. H. Fowler, V. M. Clapham, D. L. Henshaw, D. O'Sullivan and A. Thompson, *Proceedings of the 10th International Conference on Solid State Nuclear Track Detectors.*, Lyon, 1979

87] C. E. Schildknecht, *Allyl compounds and their polymer*, Wiley-Interscience, New York, 1973

88] D. L. Henshaw, N. Griffiths, O. A. L. Lender and E.V. Benton, *Nucl. Instrum. Meth.*, 1881, **180,** 65.

89] K. Kinoshita and P. B. Price, *Rev. Sci. Instrum.*, 1980, 51, 32.

90] V. S. Nadkarni, S. G. Tilve and A. A. A. Mascarenhas, *Des. Monomers polym.*, 2003, **8(2),** 177

91] A. A. A. Mascarenhas, V. K. Mandrekar, P. C. Kalsi, S. G. Tilve, V. S. Nadkarni, Radiat. Meas., 2009, 44(1), 50.

92] S. Ahmad and J. Stejny, *Nucl. tracks Radiat. Meas.*, 1991, **19 (1-4),** 11.

93] H. S. Kaufman, J. J. Falcetta, *Introduction to polymer science and technology: an SPE textbook*, Wiley-Interscience Publi cation, New York, 1977.

94] R. C. Laible, *Chem. Rev.*, 1958, **58 (5),** 807.

95] *US Pat.* 2 597696, 1952.

96] D. S. Breslow and G. E. Hulse, *J. Am. Chem. Soc.*, 1954, **76,** 6399.

97] R. Hart and R. Janssen, *Makromol. Chem.*, 1961 **43,** 242.

98] E.J. Goethals, J. Bomberke and E. De Witte, *Makromol. Chem.*, 1959, **108,** 312.

99] G. Gerlish, *Ann.* 1875, **178,** 85.

100] *US Pat.* 2 462 433, 1963.

101] H. L. Wheeler and G. S. Jamieson, *J. Am. Chem. Soc.*, 1903, **25,** 719.

102] O. Hecht, *Ber.* 1890, **23,** 287.

103] H. Rheinboldth and O. Diepenbruck, *Ber.* 1926, **59,** 1311.

104] *US Pat.* 3 072 616, 1963.

105] L. N. Lewin, *J. Prakt. Chem.*, 1930, **127(1),** 77.

106] A. H. Ford-moore, *J. Chem. Soc.*, 1949, 2433.

107] *US Pat.* 2 958 679, 1960.

108] *US Pat.* 2 849 330, 1958.

109] J. Bassett, R. C. Denney, G. H. Jeffery and J. Mendham, *Vogel's Textbook of Quantitative Inorganic Analysis*, 4th edn., English Language Book Society/Longman, 1978.

110] K. Nozaki, *Ind. Engg. anal. ed.* 1946, **18(9)**, 583.

111] V. K. Mandrekar, S. G. Tilve and V. S.Nadkarni, *Radiat. Phys. Chem.*, 2008, **77(9),** 1027

112] Z. S. Kocsis, K. K. Dwivedi and R. Brandt, *Radiat. Meas.*, 1997, **28,** 177.

113] V. S. Nadkarni, *Indian J. Phys.*, 2009, **83(6),** 805.

114] L. Pasquato, G. Modena, L. Cotarca, P. Delogue and S. Mantovani, *J. Org. Chem.*, 2000, **65,** 8224.

115] *US Pat.* 2 592 058, 1952.

116] *IP Pat.* 196 627.

117] J. Otera, *Chem. Rev.*, 1993, **93,** 1449.

118] V. K. Mandrekar, S. G. Tilve and V. S. Nadkarni, *NSRP-2007*, Chennai, Jan 29-31, 2007.

119] H. F. Van Woerden, *Chem. Rev.,* 1963, **63(6),** 557.

120] F. G. Bordwill and P. Landis, *J. Am. Chem. Soc.*, 1958, **80(23)** 6379

121] W. Bissinger, F. Kung, *J. Am. Chem. Soc.*, 1947, **69,** 2158.

122] V. K. Mandrekar, S. G. Tilve and V. S. Nadkarni, *Proceedings of the Trombay Symposium of Radiation and Photochemistry,* Trombay. 2007.

123] V. K. Mandrekar, S. G. Tilve and V. S. Nadkarni. *Proceedings of the 23rd International Conference of Nuclear Track Society,* Beizing, 2006.

124] S. Karsh, D. Freitag, p. Schwab and P. Metz, *Synthesis.*, 2004, **10,** 1696.

125] V. S. Nadkarni, *Proceedings of the 15th SSNTD-15*, Tehry, Jun 21-23, 2007

126] V. K. Mandrekar, S. G.Tilve and V. S. Nadkarni, *Proceedings of the 15th SSNTD-15*, Tehry, Jun 21-23, 2007

127] V. K. Mandrekar, S. G.Tilve, V. S. Nadkarni, *Proceedings of the 23rd International Conference of Nuclear Track Society*, Beizing, 2006.

128] V. K. mandrekar, G. Chourasiya, P.C. Kalsi, S.G. Tilve, V.S. Nadkarni, *Nucl. Instrum. Meth. B.,* 2010, **268(5),** 537.

129] F. Strain, W. E. Bissinger, W. R. Dial, H. Rudoff, B. J. DeWitt, H. C. Stevens and J. H. Langston, *J. Am. Chem. Soc.,* 1950, **72,** 1254.

130] C.H. Issidorides and R. Gulen, *Org. Synth., Coll. Vol.*, 1963, **4,** 679. *Coll. Vol.* 1958, **38,** 65.

131] B. R. Srinivasan, V. S.Nadkarni, V. Mandrekar and P. Raghavaiah, *Acta Cryst.*, 2007, **E63,** 4166.

132] A. Bondi, *J. Phys. Chem. B.*, 1964, **68,** 441.

133] C. Chatgilialoglu, *J. Org. Chem.*, 1986, **51,** 2871.

134] S. Patai and Z. Rappoport, *The chemistry of sulphonic acids, esters and their derivatives*, John Wiley & Sons, New York, 1991.

135] A. K. Pandey, R. C. Sharma, P. C. Kalsi and R. H. Iyer, *Nucl. Instrum. Meth. B.*, 1993, **82,** 151.

List of Publications

International peer revieved journal publications

1) Nuclear Track Detection using Thermoset Polycarbonates Derived from Pentaerythritol
Vinod K. Mandrekar, G. Chourasiya, P. C. Kalsi, S. G. Tilve and V. S. Nadkarni
Nuclear Instruments and Method in Physics Research B., 2010, **268,** 537

2) First Report of Preparation of poly(nitro-carbonate) Thermoset Polymers for Nuclear Track Detection
A.A.A. Mascharenhas, V. K. Mandrekar, S.G.Tilve and V. S. Nadkarni
Radiation Measurements., 2009, **44,** 50.

3) Novel Polysulfonates & Poly(sulfonate-co-carbonate) Polymers for Nuclear Track Detection
Vinod K. Mandrekar, S. G.Tilve, V. S. Nadkarni,
Radiation Physics and Chemistry., 2008 **77** 1027.

4) 3-Oxapentane-1,5-diyl bis(allylsulfonate)
B. R. Srinivasan, V. S. Nadkarni, V. Mandrekar and P. Raghavaiah
Ac266ta Crystallographica 2007 **E 63** o4166

Papers accepted at international symposia

1] Poly(Nitro-carbonate) thermoset polymers for Nuclear Track Detection,
23rd International Conference of Nuclear Track Society, Beizing-2006, Sep11-15, 2006

2] Pentaerythritol based thermoset polymers for nuclear track detection
23rd International Conference of Nuclear Track Society, Beizing-2006, Sep11-15, 2006

3] Development of Novel Poly (sulphite-carbonate) Materials for Solid State Nuclear Track Detection
23rd International Conference of Nuclear Track Society, Beizing-2006, Sep11-15, 2006

4] High Sensitivity Nuclear Track Detector
MACRO-2008, Taipei, June 29 to July 4, 2008

Papers presented at National symposia

1] Designing novel poly(nitro-carbonate) type materials for track detection,
The 14th National Symposium on Solid State Nuclear Track Detectors, Aligarh, SSNTDs-14, Nov10-12, 2005.

2] Designing polymers for nuclear track detection,
Indian Society of Chemists and Allied Scientists, Goa, ISCAS-2005, Dec-2005

3] Develpment of novel poly(sulphite-carbonate) materials for solid state nuclear track detection
Trombay Symposium on Radiation and Photochemistry, Trombay, TSRP-2007, Jan5-9, 2006

4] Diallyl carbonate based polymers for charged particle detection,
National Symposium on Radiation and Photochemistry, Chennai, NSRP-2007, Jan29-31, 2007

5] Development of novel polysulphonate and poly(sulphonate-carbonate) materials for nuclear track detection,
The 15th National Symposium on Solid State Nuclear Track Detectors, Tehry, SSNTD-15, Jun 21-23, 2007

6] New polymer materials for nuclear track detection
Royal Society of Chemistry-West India Section Students Symposium-2007, Goa, RSC-West-2007, Oct 19-20, 2007

7] Novel High Sensitivity Poly(Sulphonate-Carbonate) Nuclear Track Detector-I: Poly(PECS-co-ADC)
Nuclear and Radiochemistry Symposium, Mumbai, NUCAR-2009, Jan 7-10, 2009

8] Novel Polymeric Materials for Nuclear Track Detection
The 16th National Symposium on Solid State Nuclear Track Detectors, Amritsar, SSNTD-16, Jun 21-23, 2010